FUNCTIONAL CHIRAL HYDROGEN-BONDED ASSEMBLIES

Functional Chiral Hydrogen-Bonded Assemblies

Miguel Angel Mateos Timoneda

Thesis University of Twente, Enschede, The Netherlands

ISBN 90-365-2180-7

Publisher:

Print Partners Ipskamp, Postbus 33, 7500 AH Enschede, The Netherlands

http://www.ppi.nl

FUNCTIONAL CHIRAL HYDROGEN-BONDED ASSEMBLIES

PROEFSCHRIFT

ter verkrijging van
de graad van doctor aan de Universiteit Twente,
op gezag van de rector magnificus,
prof. dr. W.H.M. Zijm,
volgens besluit van het College voor Promoties
in het openbaar te verdedigen
op vrijdag 22 april 2005 om 13.15 uur

door

Miguel Angel Mateos Timoneda

geboren op 26 december 1976

te Almería, Spanje

Dit proefschrift is goedgekeurd door:

Promotor: Prof. dr. ir. D. N. Reinhoudt

Assistent-promotor: Dr. M. Crego Calama

A mis padres

Contents

Chapter 1

General introduction

Supramolecular chemistry focuses quite literally on going "beyond" molecular chemistry.[1] It can be described as the study of systems which contain more than one molecule that are held together via noncovalent interactions, and it aims to understand the structure, function, and properties of these assemblies. Interest in supramolecular chemistry arose when chemistry became a relatively mature discipline and the synthesis and properties of molecular compounds had become well understood, leading to the synthesis of very complex molecules such as vitamine B_{12}.[2] The domain of supramolecular chemistry was recognized as such when Donald J. Cram,[3] Jean-Marie Lehn,[4] and Charles J. Pedersen[5] were jointly awarded the Nobel Prize for Chemistry in 1987 for their work on "host-guest" assemblies (in which a host molecule recognizes and selectively binds a certain guest).

Inspired by Nature,[6] the supramolecular chemists focused their attention on the design and synthesis of molecules that will recognize each other via *self-assembly*, in order to create new functional materials and devices. One of the main advantages of the self-assembly is that the assembled structures are generally formed under thermodynamically controlled conditions, allowing the error-correction of mismatched structures, often giving rise to quantitative yields of the product.[7]

One of the major goals of supramolecular chemistry is the synthesis of supramolecular assemblies with novel functions that are not found in the single molecules or ions. The properties of the supramolecular devices can be as diverse as magnetic

properties, catalytic activity, fluorescence, redox properties, as well as supramolecular chirality. The control over these properties of the systems is of crucial importance for their application in the fields of separations, sensing, catalysis, and material science. Supramolecular chemistry is intimately related, and especially self-assembly, to *bottom-up* approach in nanotechnology as many nanotech devices will be based on the principles of supramolecular chemistry.

In this Thesis the noncovalent synthesis of assemblies based on hydrogen bonding is described. The presented studies are focused on the amplification of chirality in these self-assembled structures, as well as on the (chiral) molecular recognition properties of these assemblies acting as receptors. Finally, the problem of kinetic limitations in noncovalent synthesis, using biological concepts, for the enantioselective noncovalent synthesis of large hydrogen-bonded assemblies is addressed.

In Chapter 2 an overview of supramolecular chirality in self-assembled systems is given. The concepts and principles that have recently emerged are discussed and examples are given that illustrate the control over these systems reached in the last years.

Chapters 3 and 4 describe the amplification of chirality in hydrogen-bonded double and tetrarosette assemblies, respectively. Theses studies have been carried out using "sergeants-and-soldiers" experiments under thermodynamically controlled conditions and theoretical models have been developed to obtain the thermodynamic and kinetic parameters of the chiral amplification.

Chapters 5 and 6 describe the ability of double and tetrarosettes to complex neutral molecules. Chapter 5 reports the enantioselective recognition of saccharide derivatives by tetrarosette assemblies. The encapsulation was studied by ^{1}H NMR and CD spectroscopy. In Chapter 6 the ability of double and tetrarosette assemblies to act as receptors for multiple neutral guest molecules is described. The double rosette assemblies function as an *endo-exo* receptor while the tetrarosette assemblies are *endo-endo-endo* receptors for different guest molecules.

Finally, in Chapter 7 the chaperone effect used in nature for the correct folding of proteins is used for the formation of cyanurate-based tetrarosette assemblies. The barbiturate molecules act as chaperone and inhibit or correct non-productive interactions between the cyanurate and tetramelamine building blocks. The kinetics of the self-

assembly process was studied by ^{1}H NMR and CD spectroscopy. Subsequently, this concept was used to form enantiopure assemblies and kinetic studies were used to determine the half-life time of assembly racemization.

References

[1] Lehn, J.-M. *Supramolecular Chemistry: Concepts and Perspectives*, VCH, Weinheim, **1995**.

[2] Nicolau, K. C.; Sorensen, E. J. *Classics in Total Synthesis: Targets, Strategies, Methods*, VCH, Weinheim, **1996**.

[3] Cram, D. J. *Angew. Chem. Int. Ed. Engl.* **1988**, *27*,1009-1020.

[4] Lehn, J.-M. *Angew. Chem. Int. Ed. Engl.* **1988**, *27*, 89-112.

[5] Pedersen, C.-J. *Angew. Chem. Int. Ed. Engl.* **1988**, *27*, 1021-1027.

[6] Reinhoudt, D. N.; Crego-Calama, M. *Science* **2002**, *295*, 2403-2407.

[7] Whitesides, G. M.; Mathias, J. P.; Seto. C. *Science* **1991**, *254*, 1212-1319.

Chapter 2

Supramolecular chirality of self-assembled systems in solution*

Self-assembly plays an important role in the formation of many (chiral) biological structures, such as DNA, α-helices or β-sheets of proteins. This process, which is the main tool of Supramolecular Chemistry (i.e. the chemistry of the molecular assemblies and of the intermolecular bonds), starts to play a significant role in nanotechnology for the construction of functional synthetic structures of nanometer size. The control of chirality in synthetic self-assembled systems is very important for applications of these systems e.g. in molecular recognition or mimicking of the catalytic activity of enzymes. In this chapter the most representative contributions in the field of supramolecular chirality in finite systems are described.

* Part of this chapter has been published: Mateos-Timoneda, M. A.; Crego-Calama, M.; Reinhoudt, D. N. *Chem. Soc. Rev.* **2004**, *33*, 363-372.

2.1. Self-assembly and chirality

The *general* term of *self-assembly* has been defined as the autonomous organization of components into patterns or structures without human intervention.[1] Self-assembly is of vital importance in biological processes such as the transfer and storage of genetic information in nucleic acids and the organization of proteins into efficient molecular machines. Therefore, the use of self-assembly is a very powerful tool to mimic biological functions.[2] Self-assembly is also regarded as the most efficient way in the *bottom-up* approach in nanotechnology for the fabrication of complex 'supermolecules' and structures.[3,4] Their spatial disposition is transferred from one or more chiral centers[5] to the molecules that form these supramolecules or macromolecular aggregates, and consequently to the nanoscopic dimension. The control over the spatial disposition of atoms and molecules is very important because it can have dramatic consequences in chemical systems. For example, some enzymes only catalyze the reaction of one enantiomer of the substrate leaving the other enantiomer unchanged.[6] Also in materials science, chirality has great effects. The use of one enantiomer instead of the racemic mixture (mixture of equal amounts of a pair of enantiomers) increases the second-order nonlinear optical (NLO) susceptibility about 30 times.[7] The initial study and control of the supramolecular chirality in solution should also aim to translate the chirality into two-dimensional structures because any kind of a working device will probably need to be confined to a surface.[3,8] There are already a few examples dealing with the concept of chirality on surfaces ("two-dimensional chirality").[3,9] Nevertheless, they are still concerned with very simple concepts of chirality without much stereocontrol. On the contrary, the field of supramolecular chirality in solution starts nowadays to master the control over almost all aspects of chirality.

Self-assembly has also been used in the synthesis of dynamic supramolecules such as catenanes and rotaxanes. These structures are not self-assembled systems in a strict sense (they are not under thermodynamic equilibrium), so they are not enclosed here. Nevertheless, they display an interesting case of supramolecular chirality, *i.e.* topological or dynamic chirality.[10,11]

2.2. Supramolecular chirality: concepts

It is well know that chirality at the *molecular level* is displayed when the atoms of a molecule are arranged in one unique manner in space. This different arrangement is due to the presence of a chiral centre or the absence of planes of symmetry. Isomers that contain chiral centres are called stereoisomers and they are divided in two categories: enantiomers (stereoisomers whose molecules are nonsuperposable mirror images of each other) and diastereomers (stereoisomers whose molecules are not mirror images of each other). Similarly, chirality is also expressed at the *supramolecular level*. Supramolecular chirality involves the nonsymmetric arrangement of molecules in a noncovalent assembly. This can be initiated by the properties of the components, i.e. one or more of the components are asymmetric or the achiral components associate in such a way that the assembly has no elements of symmetry (Figure 2.1).[12] Therefore, noncovalent synthesis allows the preparation of supermolecules in a diastereomeric or enantiomeric form.

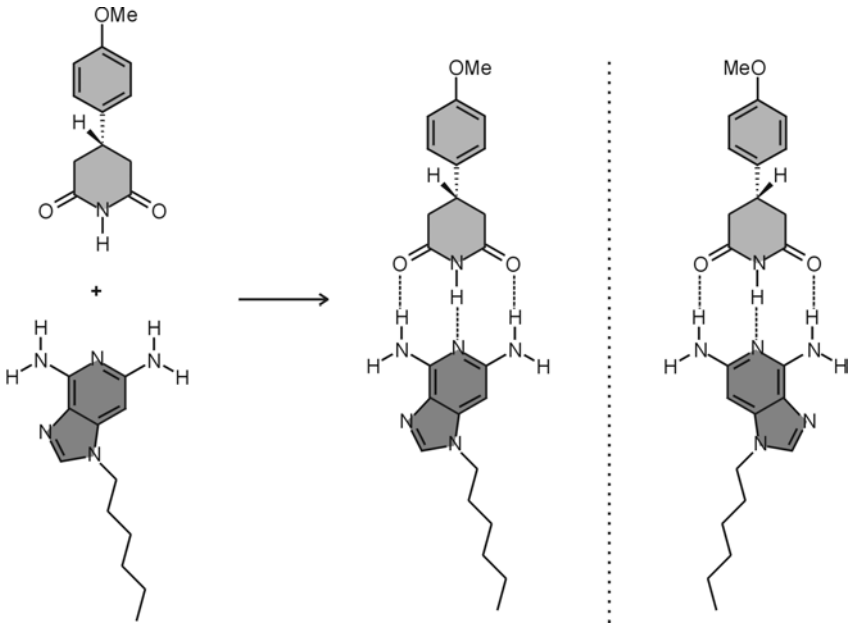

Figure 2.1. Assembly process of two achiral molecules leading to a chiral supermolecule due to the perpendicularity of the symmetry planes of the molecular components.

2.2.1. Supramolecular chirality in molecular recognition

Molecular recognition is defined by the selective recognition of substrate molecules (guests) by synthetic receptors (hosts).[13] This binding process can lead to the formation of chiral supermolecules if the substrate and/or the receptor are chiral or the binding process occurs in an asymmetric fashion.[14] The field of supramolecular chemistry in the area of molecular recognition has reached such a level of control that the complexation of biologically interesting chiral molecules such as carnitine,[15] cytochrome c,[16] and many others has been achieved. Even though there are some examples of selective chiral molecular recognition, the control over this process remains elusive. A beautiful example has been reported by Morán and coworkers.[17] They studied the recognition of a (*S*)-lactic acid derivative with a chromenone-benzoxazole derivative receptor (Figure 2.2). The chiral recognition in these systems arises from strong steric hindrance, so that the association constant for the two enantiomeric hosts differs by a factor of nine.

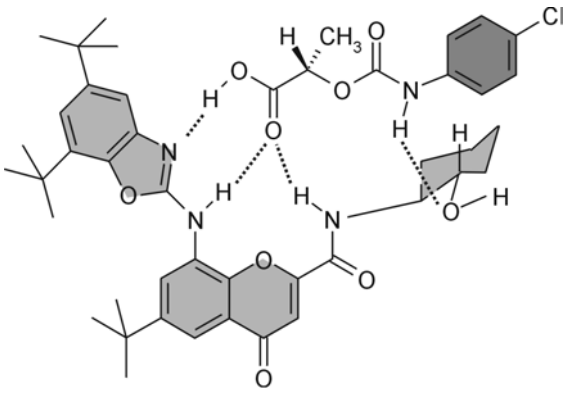

Figure 2.2. Proposed structure for the complex of chromenone-benzoxazole receptor and (S)-lactic acid derivative.

The stereoselective recognition of amino acids has been intensively studied for its implications in the understanding of many biological processes. Morán et al. reported the synthesis and the enantioselective recognition of different amino acid derivatives by trans-benzoxanthene derivatives,[18] observing chiral recognitions up to 20 (the chiral

recognition is defined as the ratio between the association constants of the different enantiomers of the receptor and the amino acid derivative).

A well studied system is the bisporphyrin based system.[19] As a result of the control reached over the parameters that govern the induction of supramolecular chirality in this system, it is possible to use this bisporphyrin system as an effective chirality sensor for the determination of absolute configuration of amino acid and "simple" amines and alcohols (Figure 2.3).[20-22]

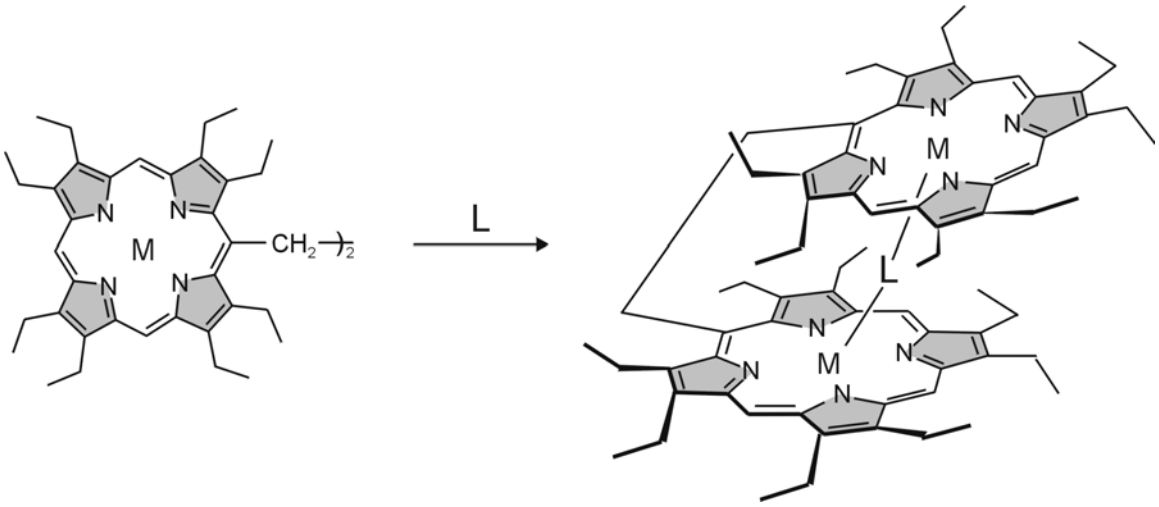

Figure 2.3. Schematic representation of the bisporphyrin system and formation of the tweezer conformation upon chiral recognition of guest molecules (L).

Aida et al. studied the resolution of racemic mixtures of helical oligopeptides through stereoselective helix bundling by using a cyclodimeric zinc porphyrins host bearing a guest binding chiral cavity with two helical peptidic units.[23] The stereoselective process comes from the recognition of the helical structures of the guest by the host, rather than the point chiralities (amino acid residues) in their chain, upon binding in the confined cavity, leading to a difference of ~ 5 between the association constants of the two different enantiomers of the guest.

Due to the commercial applications of caffeine (it is one of the most widely used drugs in the world), its recognition by, specially, biomolecular receptors has been widely investigated.[24] Waldvogel et al. studied the enantiofacial differentiation of caffeine by chiral modified supramolecular receptors based on triphenylene ketals.[25] This

discrimination (up to 9 to 1 of the two different diastereomers) arises from repulsive interactions, which can be modulated by steric modifications of the cavity.

Recently, the use of self-assembled receptors has attracted much attention due to the many advantages of this *noncovalent* approach.[4] The potential of self-assembled receptors depends on the identification of noncovalent structural motifs whose enthalpic driving force for self-assembly is sufficient to overcome the unfavorable entropic price associated with the aggregation of several components into a single supramolecular entity. On the other hand, the use of self-assembly for the formation of molecular receptors has many advantages (see section 2.2.2), such as the possibility to use dynamic combinatorial libraries in the fast development of new synthetic receptors, as well as the amplification of the best receptor of the generated library.

Reinhoudt et al. used the tetrarosette assemblies for the recognition of saccharide molecules. These assemblies are able to complex saccharides in an enantioselective fashion, allowing the amplification of the best receptor from a racemic mixture of the self-assembled receptors.[26]

The enantioselective binding of amino acids and amino alcohols has also been studied in self-assembled chiral basket-shaped receptors.[27] The chiral host formed aggregates in aqueous environment. This aggregates showed binding of aromatic amino acids with discrimination between amino acid enantiomers.

The chiral molecular recognition process has also been named induction of supramolecular chirality.[28] This type of chiral recognition has been the object of many reviews.[29-31]

2.2.2. Self-assembly of finite chiral superstructures

The term *molecular self-assembly* can be defined as the spontaneous association of two or more molecules under thermodynamic equilibrium resulting in the generation of well-defined aggregates (strict self-assembly) or of extended polymolecular assemblies (self-organization) by means of noncovalent interactions such as hydrogen bonds, metal-coordination or π–π interactions.[4,12] The use of noncovalent bonds has the advantage that they are formed spontaneously and reversibly under thermodynamic equilibrium, with the

possibility of error correction and without undesired side products. For these reasons, self-assembly is a valuable tool for the noncovalent synthesis of nanostructures such as helicates, grids,[32] capsules,[33] etc. To achieve this, kinetically labile reactants capable of suitable exchange reactions in solution are required, but this allows rapid racemization to occur. Consequently, the majority of the supramolecular architectures are formed by a racemic mixture, but for functional supramolecules[10,34] the control over the stereoselectivity in the self-assembly process is very important.

2.2.2.a. Diastereoselective noncovalent synthesis

As it has been pointed out above, all the assemblies that have an asymmetric arrangement of their building blocks are chiral. The general method to control the supramolecular chirality is the introduction of chiral centers in the building blocks (asymmetric induction).[35] In this way, the resulting chiral assemblies exist as two different species that have a diastereomeric relationship. This approach is called induction of chirality or diastereoselective noncovalent synthesis.

Using noncovalent synthesis, diastereomeric relations can be induced in self-assembled aggregates, ranging from hydrogen-bonded rosette assemblies[36] to hydrogen-bonded[37] or metal-coordinated capsules.[33]

Nice examples of diastereoselective noncovalent synthesis of double rosette assemblies have been described by Reinhoudt et al. (Figure 2.4). Double rosettes are formed upon mixing calix[4]arene dimelamines and barbituric or cyanuric acid derivatives in a ratio of 3:6 in apolar solvents such as chloroform, toluene, or benzene.[38] These hydrogen-bonded assemblies can exist in three different conformations with D_3-, C_{3h}-, or C_s-symmetry (Figure 2.4a). In the D_3-conformer the two melamine fragments of the calix[4]arene component adopt an antiparallel (staggered) orientation (Figure 2.4b), which renders the assembly chiral. The chirality of these assemblies arises from the two melamine rings attached to the calix[4]arene that can adopt either a clockwise (*P*) or counterclockwise (*M*) configuration.

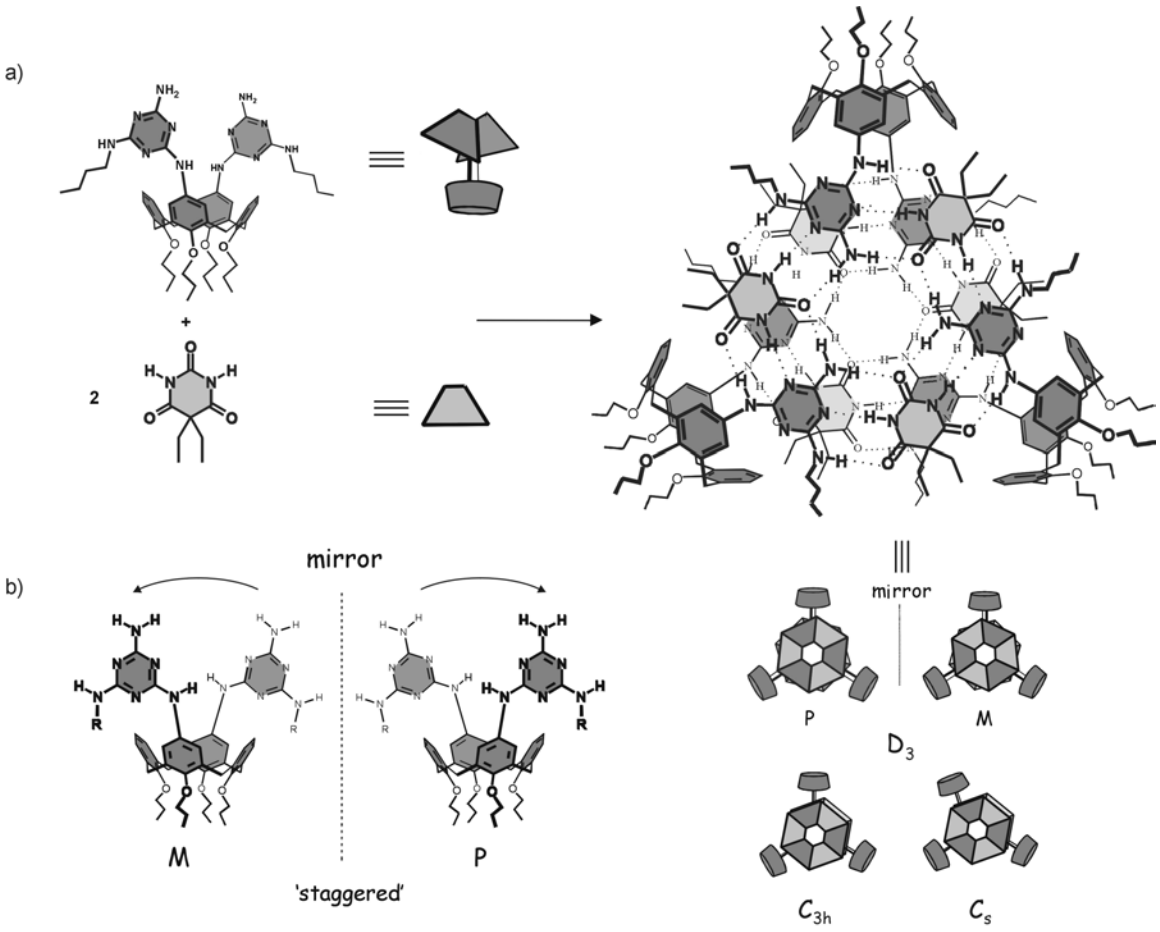

Figure 2.4. a) Formation of the double rosette assemblies and schematic representation of the building blocks and the different possible constitutional isomers with D_3-, C_{3h}-, and C_s-symmetry. b) Representation of the two staggered conformations of the dimelamine fragments of the calix[4]arene components.

The complete noncovalent diastereomeric synthesis (formation of only one handedness of the possible two (*P*) or (*M*), see figure 2.4) has been achieved in two different ways. Firstly, via the introduction of chiral centers in one of the components, either the calix[4]arene dimelamine or barbituric/cyanuric acid derivative (Figure 2.5a). This results in the presence of six chiral centers in close proximity to the core of the assembly.[39] Secondly, via complexation of chiral acids or diacids by a racemic mixture of amino-substituted double rosette assemblies (Figure 2.5b).[40,41] The first methodology leads to assemblies with a diastereomeric excess (d.e.) of 96%. The second case gives assemblies in which the d.e. is ~90%.

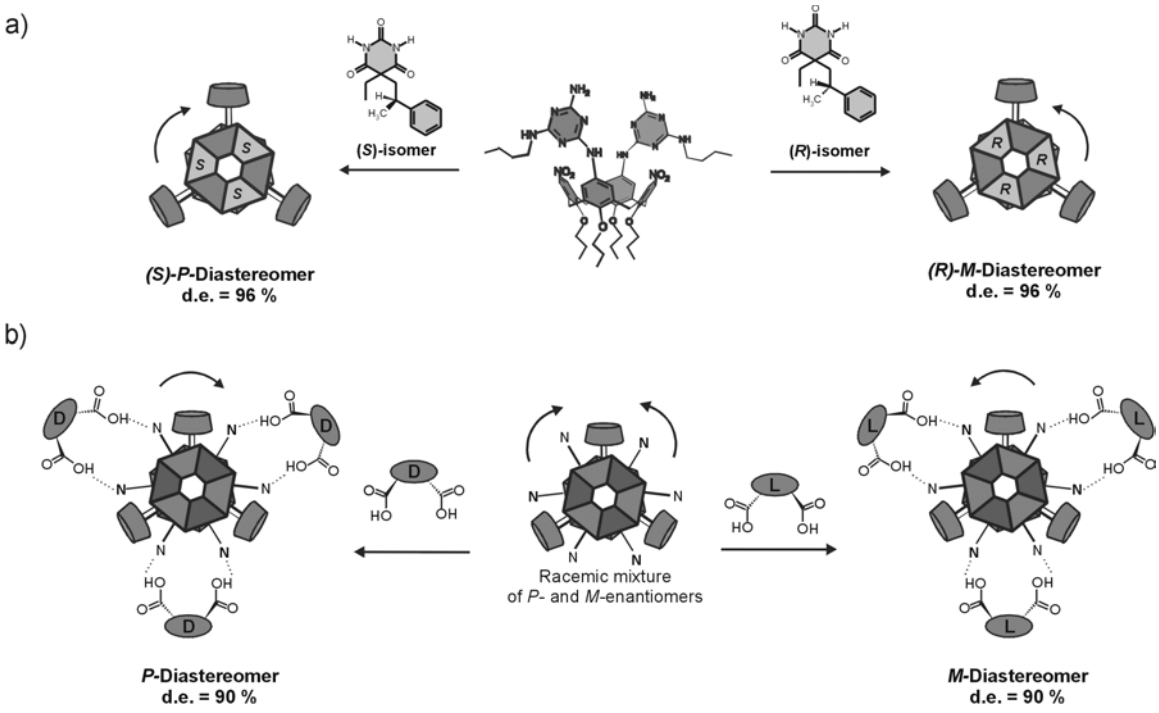

Figure 2.5. Diastereoselective synthesis of double rosette assemblies via a) introduction of chiral centers in the assembly using a chiral barbiturate and b) complexation of chiral carboxylic diacids.

Fenniri et al. exploited the heterobicyclic base **G**^**C** for the self-assembly of rosettes with functionalities in the periphery of the assembly (Figure 2.6).[42] At high concentrations, **G**^**C** undergoes hierarchical self-assembly to generate rosette nanotubes and addition of chiral amino acids, that bind to the crown ether moiety via electrostatic interactions, promotes the transition from racemic to chiral rosette nanotubes with predefined helicities.[43]

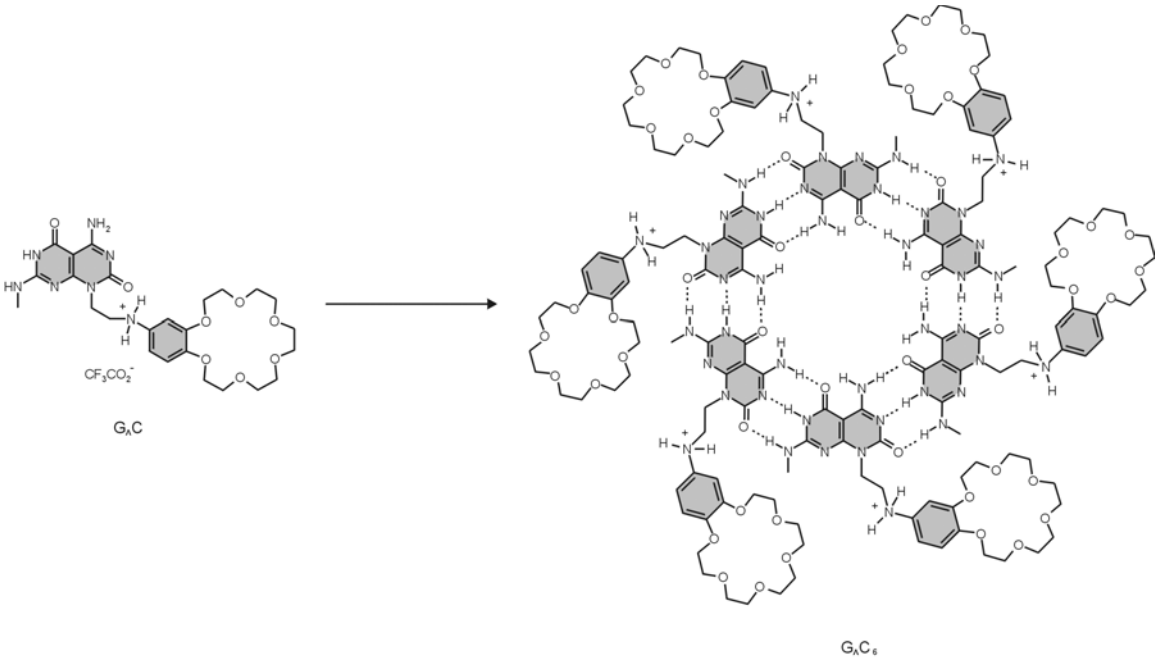

Figure 2.6. Hierarchical self-assembly of rosettes from module **G^C**.

Complete diastereoselectivity, *i.e.* formation of only one diastereomer, has been achieved by Gottarelli and Davis with guanosine octamers, templated by K^+ ions, due to the presence of eight sugar moieties (Figure 2.7a).[44] Rebek et al. demonstrated that certain symmetric molecules, possessing groups able to form and accept hydrogen bonds, dimerize to form molecular capsules with dissymmetrical cavities in the presence of a chiral template. These capsules preferentially form one of the two possible diastereomeric complexes (Figure 2.7b). This leads to a diastereomeric excess up to ~35%.[45]

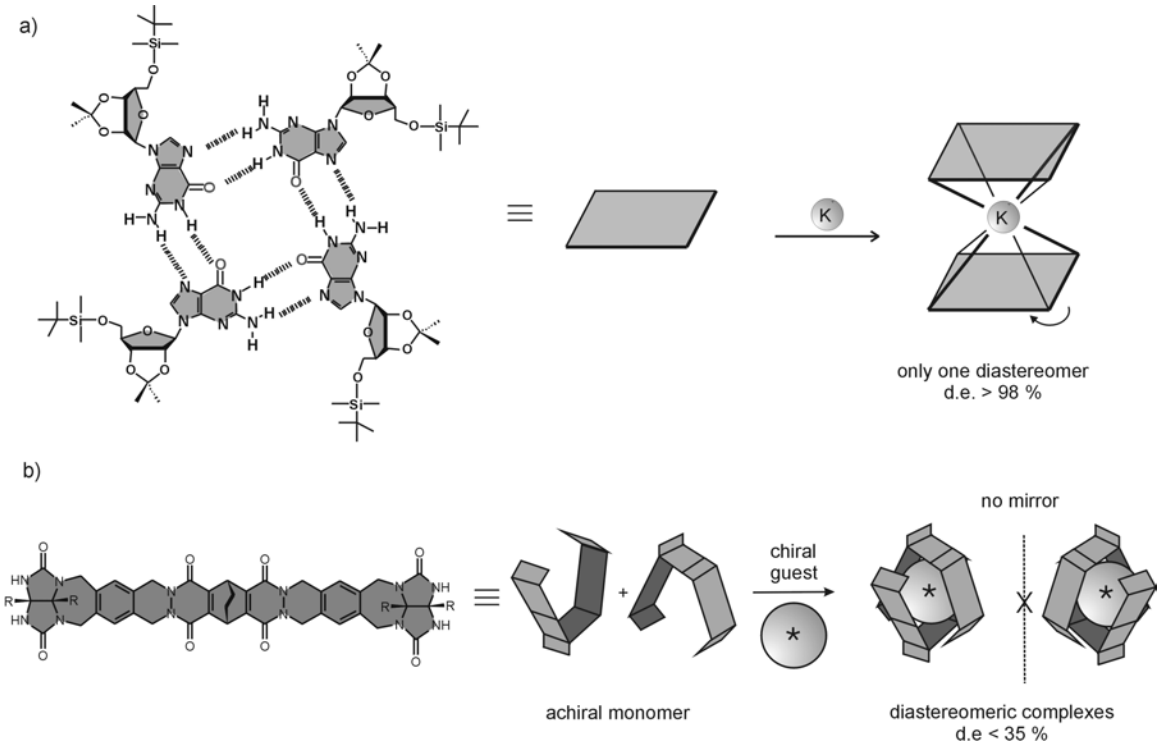

Figure 2.7. Diastereoselective noncovalent synthesis of a) guanosine octamers templated by K^+ ions and b) molecular capsule upon guest complexation.

Fujita et al. reported the induction of chirality in the self-assembly of catenane structures through reversible metal coordination.[46] The coordination ring derived from a pentakis(*m*-phenylene) derivative is reversibly catenated through efficient aromatic stacking (Figure 2.8a). The catenaned structure is characterized by the helical chirality and by the ancillary chiral unit on the metal ion. The supramolecular chirality is only observed if the coordinated rings are catenated.

The encapsulation of one or more chiral guests (in odd number) in cylindrical capsules leads to the formation of a new class of diastereomeric complexes (*diastereomeric constellations*) due to the restricted exchange of positions of the different guest molecules.[47] Thus, the encapsulation of three chiral propylene sulfide molecules (e.e. up to 88%) results in the formation of six different encapsulated (*R*)- and (*S*)-propylene sulfide. The capsules in which two guests of similar stereochemistry are present exist as a diastereomeric constellation due to the constrained movement of the guest (Figure 2.8b).[48]

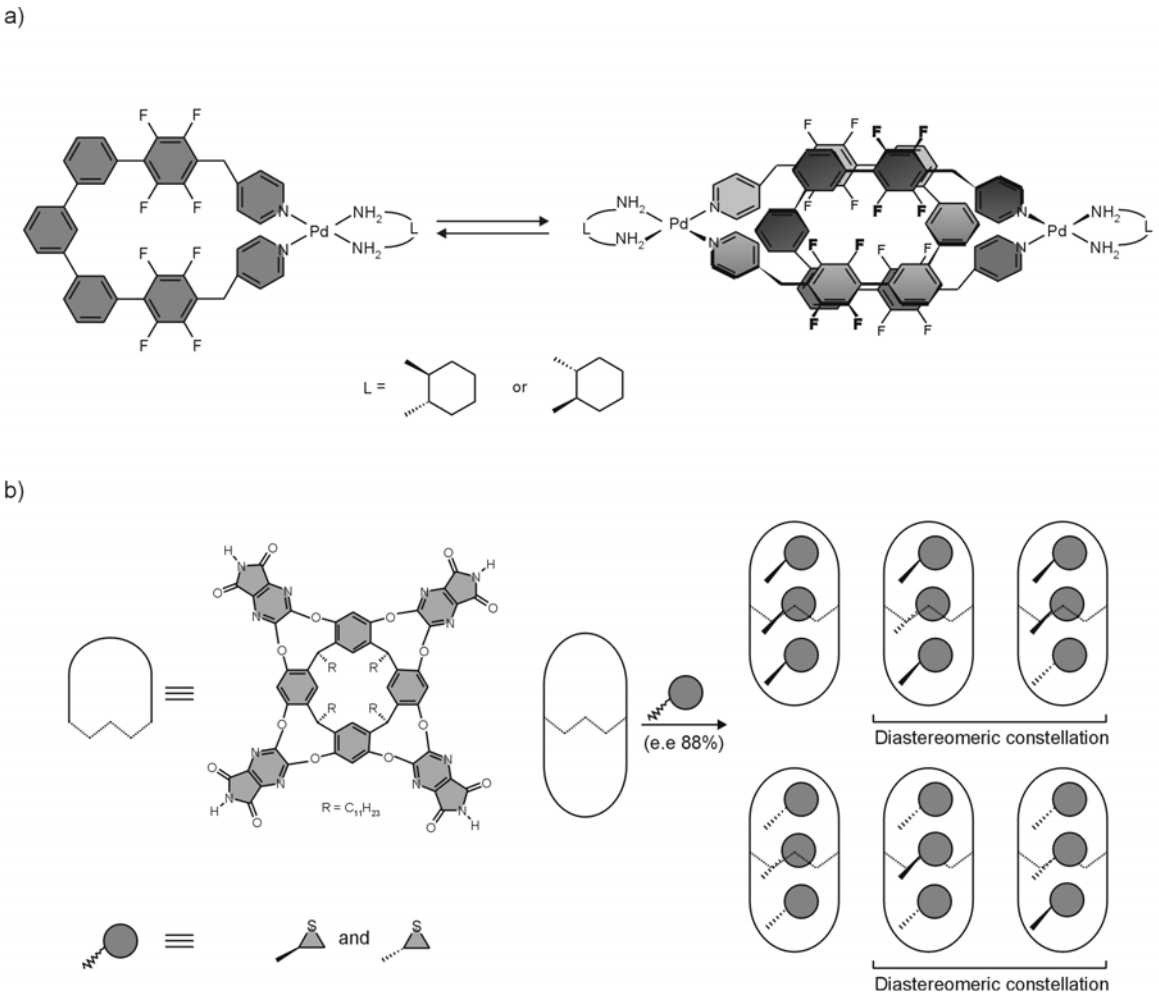

Figure 2.8. a) Self-assembly of the helical [2]catenanes and the components of the rings. b) Schematic representation of the resorcin[4]arene and propylene sulfide, and the six different constellations of encapsulated (*R*)- and (*S*)-propylene sulfide.

The two different approaches used for the diastereomeric noncovalent synthesis in hydrogen-bonded assemblies have been also used for the diastereoselective formation of self-assembled structures based on metal coordination, *e.g.* metal helicates,[49,50] and porphyrinate double deckers (Figure 2.9).[51] However, when chiral ligands are introduced in metal helicates (discrete linear polynuclear oligomers formed by one or more organic ligands coordinating a series of metal ions) three forms of chirality must be distinguished. Firstly, the chirality given by the optically active carbon (*R*/*S*), secondly, the coordination environment around the metal centers (Δ/Λ), and thirdly the overall *P* or *M* sense of the helix (Figure 2.9a).[52]

In general, for metal-coordinated assemblies the control over the chirality is somewhat different due to their higher kinetic stability when compared to the hydrogen-bonded assemblies. In this regard, chiral metal-coordinated assemblies resemble more their analogous synthesized by reversible covalent bonds.

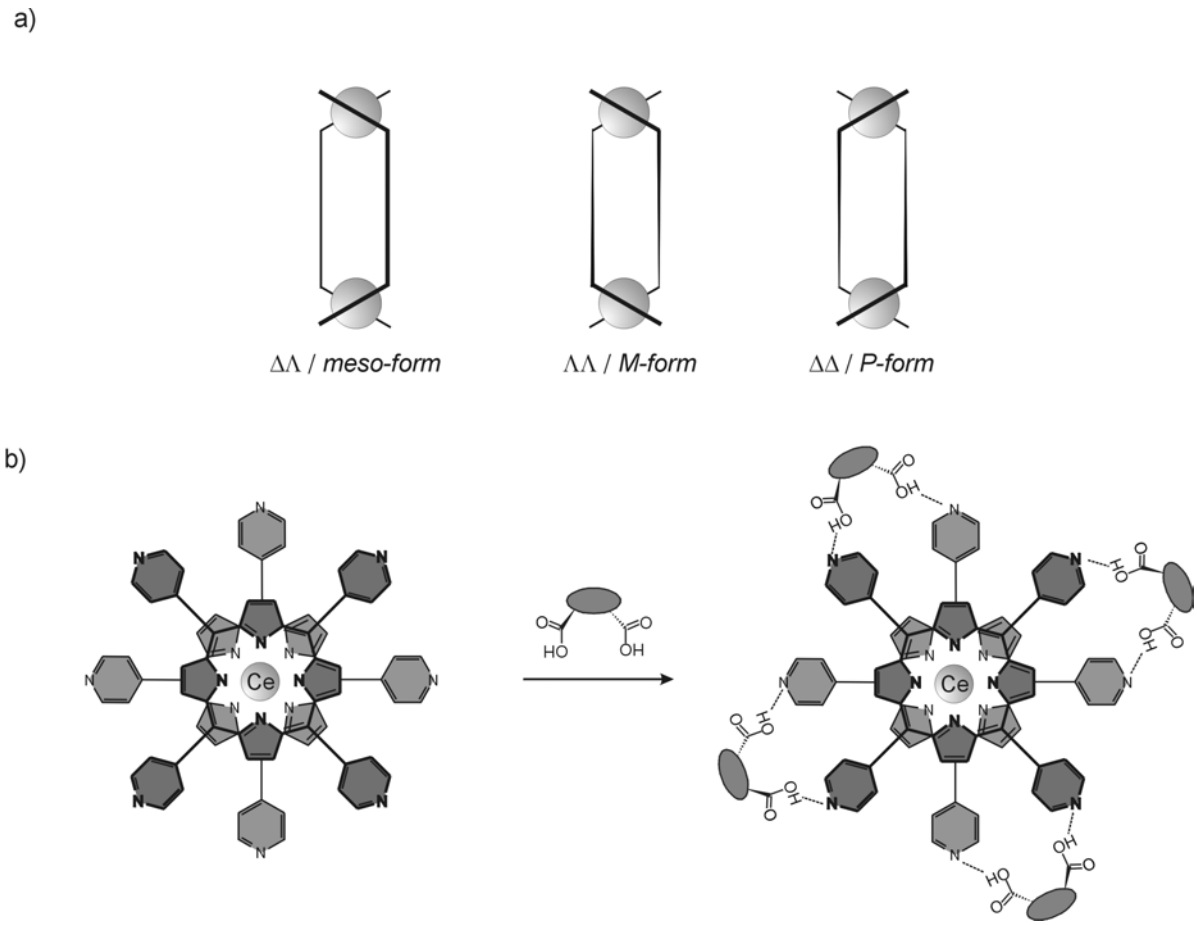

Figure 2.9. Schematic illustration of a) chirality for metal helicates and b) diastereoselective synthesis of porphyrinate double-deckers.

Albrecht and coworkers used chiral ligands to induce the formation of only one handedness in metal helicates. The use of *L*-tartaric acid derivative ligands leads to the diastereoselective formation of right-handed triple-stranded helicates with iron(III) or gallium(III) ion.[53] Moreover, these helicates are able to bind lithium with high specificity. Another way to achieve the diastereoselective noncovalent synthesis of charged helicates is the use of chiral counterions (Pheiffer effect).[54] This strategy has lead to the formation of chiral dinuclear triple helicates with d.e. up to 82% upon complexation with chiral

counteranions (Figure 2.10a).[55] The chiral counterions have also been used for the discrimination of enantiomers of propeller-like cobalt complexes[56] and for the determination of the enantiomeric excess of planar chiral cations.[57] The use of chiral templates has also been reported in the diastereoselective synthesis of double metal helicates. Enantiopure binaphtalene template was substituted with strands of pyridine-containing arylene ethynylene capable of assembling through metal coordination, resulting in the total transfer of the molecular chirality of the template to the double stranded helicate (Figure 2.10b).[58]

Raymond et al. reported the encapsulation of organometallic complexes, into a chiral, well defined cavity of a metal-ligand assembly.[59] Moreover, they have studied the catalytical activity of the encapsulated species in the C-H bond activation with aldehydes.[60] The C-H bond activation of aldehydes proceeds with highly specific size and shape selectivity, as well as modest diastereoselectivity (up to 70%).

One problem in the diastereoselective synthesis of metal helicates is the formation of *meso*-helicates, *i.e.* an achiral supramolecular architecture that bears two oppositely configured chiral units.[61] Albrecht et al. synthesized several dicatechol ligands with different spacers (stereocontrolling units) and studied their dinuclear metal complexes (Figure 2.10c).[62] It was found that an odd number of methylene units gives rise to *meso*-helicates.

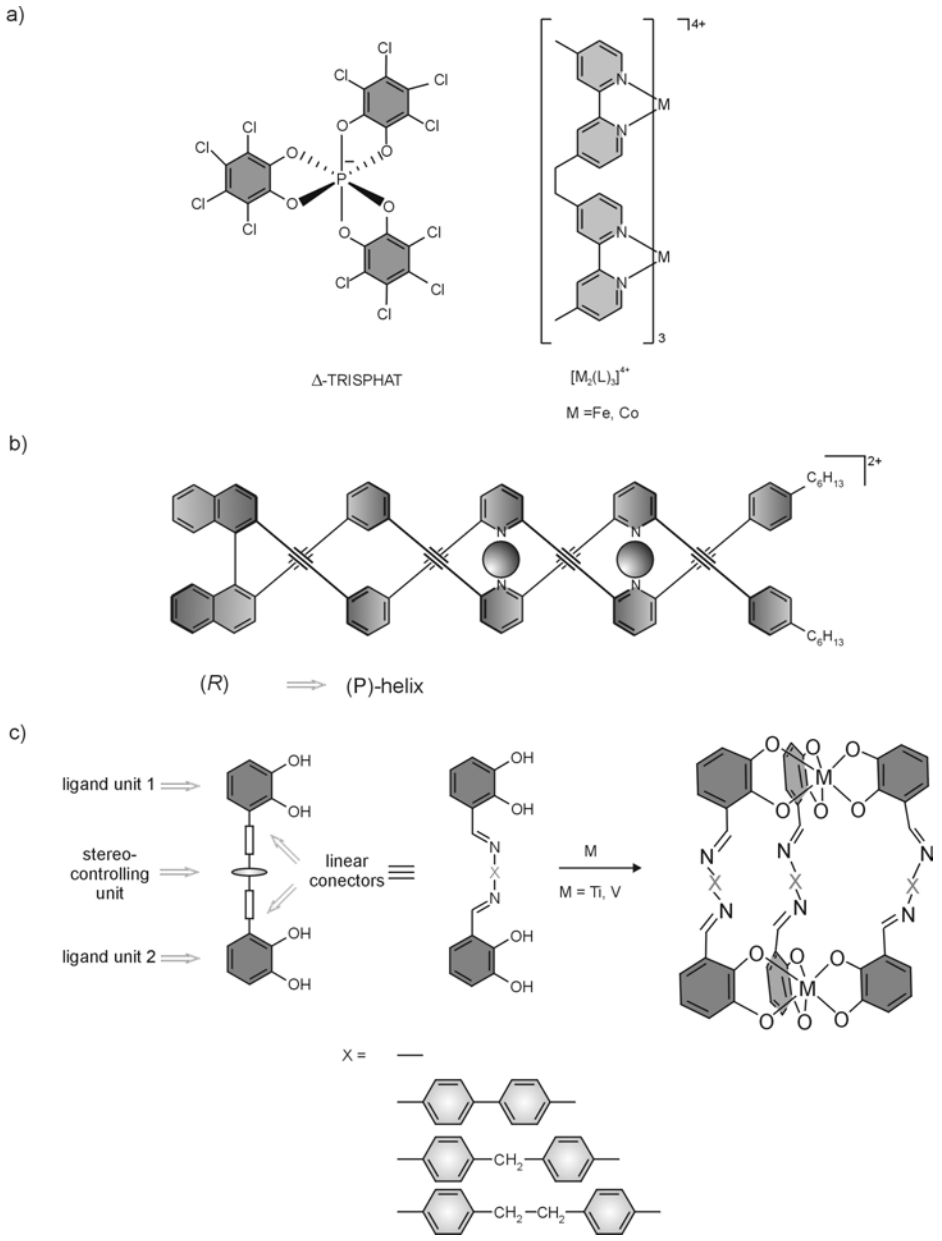

Figure 2.10. a) Chemical representation of the cationic dinuclear metal helicates and the chiral counteranion, b) schematic representation of the template synthesis of diastereomeric double stranded helicates, and c) schematic and chemical representation of dicatechol ligands possessing rigid connectors and small central stereo-controlling alkyl units, and formation of triple stranded helicates.

Salvadori and coworkers studied the ligand lability and chirality inversion in ytterbium complexes as a key step in the catalytic activity of these kind of complexes.[63] Upon addition of the same ligand with different stereochemistry to the diastereomeric ytterbium complex, ligand exchange leads to the formation of a small quantity of

heterochiral complexes. However, upon addition of a molar excess of ligand, complete chirality inversion is observed.

2.2.2.b. Enantioselective noncovalent synthesis

By definition, enantiomers have equal thermodynamic stabilities. Therefore, the formation or isolation of pure enantiomers is a challenging task. In general, in covalent synthesis there are two ways to obtain pure enantiomers, either via resolution of racemic mixtures by crystallization (self-resolution) or chiral chromatography, or by means of enantioselective synthesis. In principle, these strategies are also applicable in noncovalent synthesis. Enantiomerically pure metal-ligand complexes (Figure 2.11) and porphyrinate double-deckers have been obtained via chiral column chromatography.[64-66] In general, the enantioselective noncovalent synthesis of self-assembled structures is more challenging due to the inherently low kinetic stability of these assemblies.

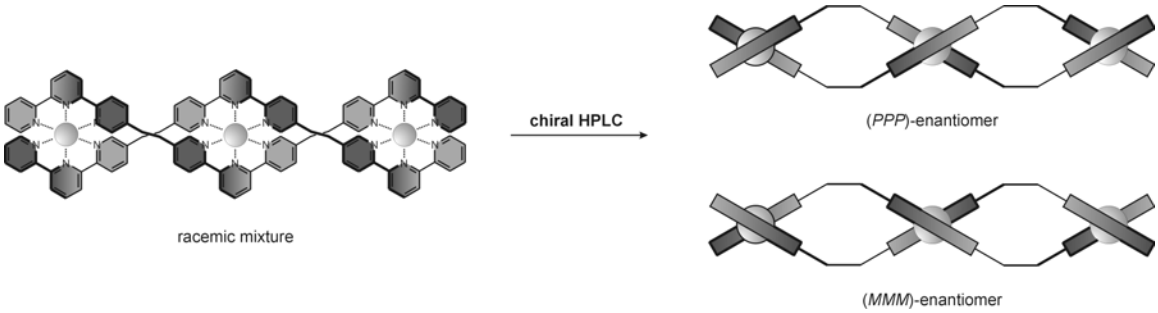

Figure 2.11. Chromatographic resolution of metal helicates.

2.2.2.b.1. Self-resolution

Self-resolution or enantioselective self-assembly has been defined as the spontaneous selection of components with the same chirality from an enantiomeric mixture that leads to the formation of homochiral assemblies. This is a characteristic phenomenon in the solid state (Figure 2.12)[67,68] but it still is a rare event in solution, in liquid crystals or in self-assembled monolayers.[9,69]

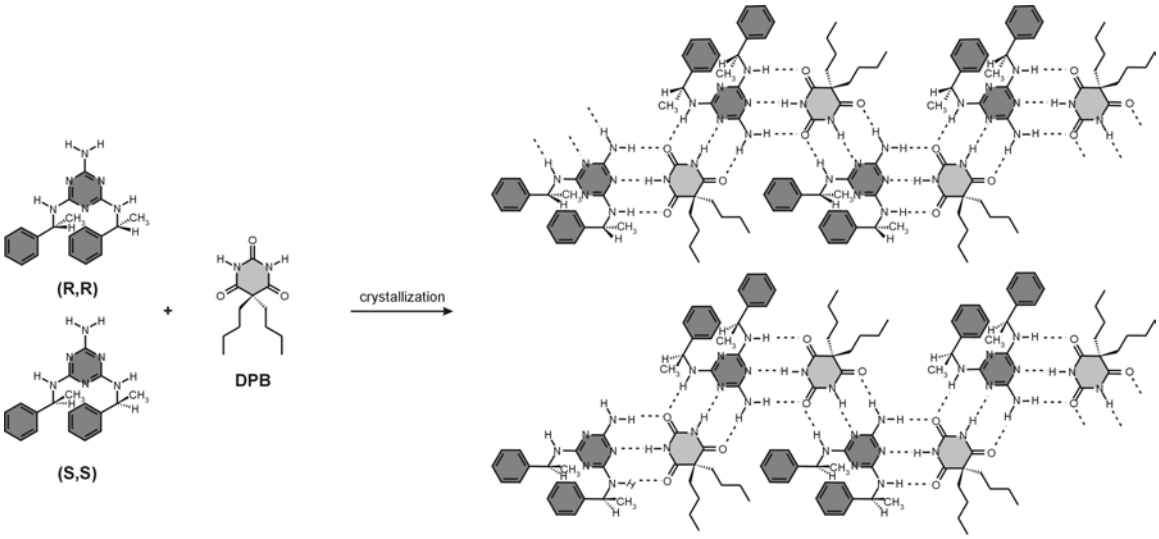

Figure 2.12. Stereoselective self-assembly of chiral dimelamines and DPB (5,5-dipropyl-barbiturate) giving the two homochiral 'crinkled' tapes.

In their studies of molecular recognition of aromatic substrates by self-assembled metallomacrocycles Harding et al. reported ligand self-resolution in the assembly of [2 + 2] metallomacrocycles.[73] The addition of zinc(II) to racemic molecular clefts resulted in the formation of [2 + 2] metallomacrocycles in which the stereoisomeric ligands underwent self-recognition to form a pair of enantiomeric metallomacrocycles. Self-resolution has also been observed in the self-assembled complex of 4,4'-biquinazoline and ruthenium.[74] This complex consist of atropisomeric[75] (Δλ/Λδ) and (Δδ/Λλ) pairs of enantiomers (Figure 2.13). Upon crystallization, spontaneous resolution of the major Δλ/Λδ pair occurs to give Δλ/Λδ crystals. This process has been studied in other kinds of atropisomeric molecules.[76]

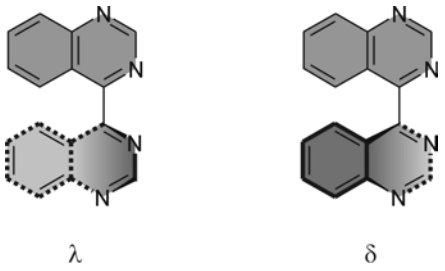

Figure 2.13. Schematic representation of the atropisomeric ligand, which can adopt a λ or δ configuration in the complex.

Some examples of self-resolution have been reported in solution. The cyclization of racemic 2-ureido-4[1H]-pyrimidinone (Upy) derivatives in chloroform solutions leads to the selective formation of the homochiral cyclic dimers of Upy derivatives (Figure 2.14).[70]

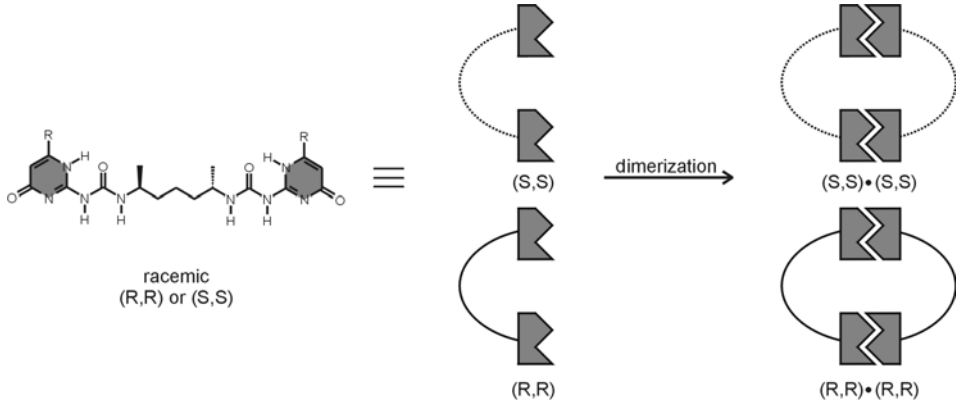

Figure 2.14. Schematic representation of the dimerization process of the racemic Upy units.

Also double rosette assemblies display complete enantioselective self-resolution. Mixing of building blocks with opposite handedness or chirality does not lead to the formation of heterochiral assemblies (Figure 2.15).[39] Surprisingly, for assemblies comprising nonchiral calix[4]arene dimelamine components the formation of heteromeric or heterotopic (i.e. assemblies comprising structurally different building blocks) double rosette assemblies is possible.[71,72]

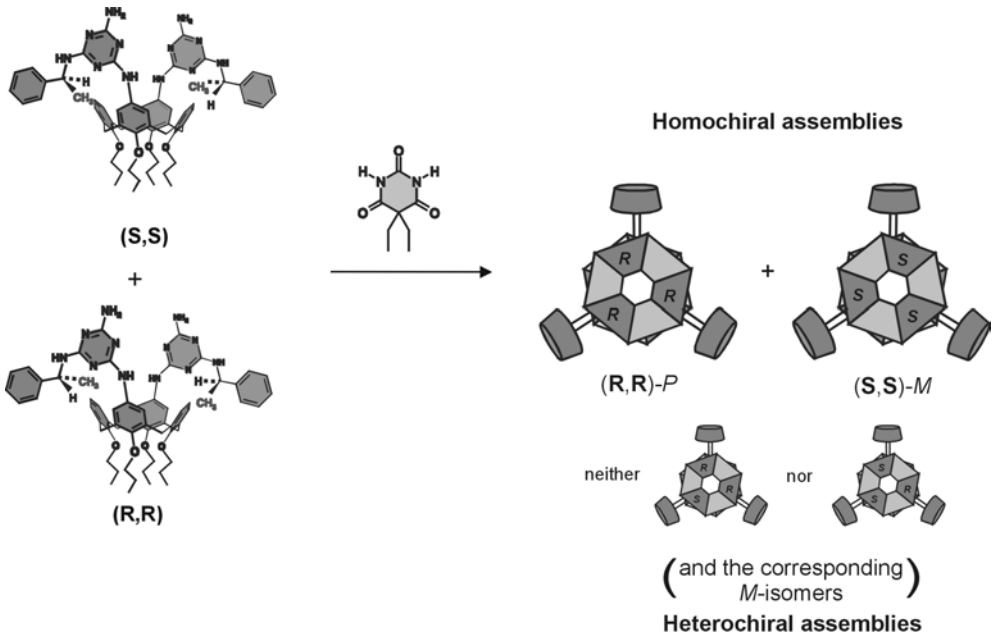

Figure 2.15. Enantioselective self-resolution in double rosette assemblies from a mixture of enantiomeric building blocks.

One attractive option for the formation of metal helicates is the noncovalent synthesis of the ligand strands. Kuroda et al. studied the self-assembly of dinuclear double-stranded helicates formed by noncovalent ligands strands.[77] The helicates self-assembly from eight simple components and this self-assembly process exhibits remarkable stereoselectivity, where only homochiral ligand sets are observed.

2.2.2.b.2. Chiral memory

The synthesis of enantiopure self-assembled aggregates from achiral components has been achieved using the "chiral memory" concept previously reported by the group of Yashima for the enantioselective synthesis of covalent *P*- or *M*-helical polymers.[78] The *chiral memory* concept implies the use of a chiral auxiliary that interacts stereoselectively in a noncovalent manner to give preferentially one of the two possible enantiomeric forms. Subsequently, the additive is removed or replaced by an achiral analogue while the induced chirality is preserved. This replacement of the chiral "additive" is the crucial step in this strategy. The resulting structure is still optically active, although none of its

components are chiral. This strategy has been used to synthesize enantiomerically enriched self-assembled double rosette assemblies with an enantiomeric excess (*e.e.*) of 90 to 96%.[41,79] This enantioselective noncovalent synthesis of the double rosette assemblies (Figure 2.16a,b) has been accomplished in two different ways: formation of a diastereomeric assembly using chiral building blocks that are later replaced by achiral ones leading to an enantiopure system, or complexation of chiral diacids by amino-substituted double rosette assemblies and subsequent removal of the acids. In the first case, the use of a chiral barbiturate compound leads to the formation of a diastereomeric assembly with a d.e. of 96 %. The subsequent exchange of the chiral barbiturate for an achiral cyanurate gave an enantiopure assembly with a e.e. of 96 % (Figure 2.16a). This exchange of the barbiturate for a cyanurate is possible because of the formation of stronger hydrogen bonds between the melamine-cyanurate pair than between the melamine-barbiturate pair due to the higher acidity of the cyanurate. In the second way, the formation of only one diastereomer with a d.e. up to 90 % is induced by complexation with chiral dicarboxylic acids. The removal of the diacids by precipitation of the salt upon the addition of amine leads also to the formation of the enantiopure assemblies (Figure 2.16b). Similarly, noncovalent H-bonded capsules have been synthesized with 50% e.e. (Figure 2.16c) by Rebek et al.[80] The crucial step is the exchange of the guest without racemization of the assembly. This step proceeds through windows of the capsule that form without disrupting the entire hydrogen-bonded seam of the capsule.

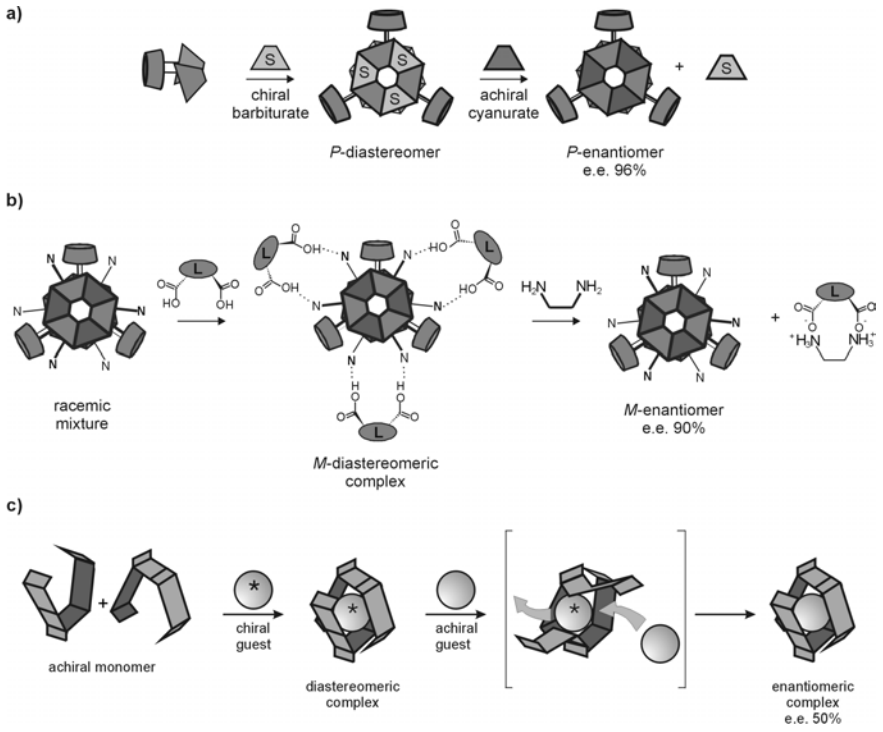

Figure 2.16. Schematic representation of the noncovalent enantioselective synthesis of double rosette assemblies via introduction of chiral barbiturate and posterior exchange by achiral cyanurate (a) or via complexation of chiral dicarboxylic acids (b) and of H-bonded capsules using the concept of chiral memory showing the nondissociative exchange of the guest (c).

The memory of chirality has been also reported for the enantioselective synthesis of the more kinetically stable metal complexes and porphyrinate double deckers. Raymond et al. reported the enantioselective formation of tetrahedral metal complexes of tris(catecholate)gallium (III). These complexes encapsulate ammonium cations. In the presence of an achiral guest, they exist as a mixture of enantiomers (ΛΛΛΛ or ΔΔΔΔ). The encapsulation of a chiral ammonium cation leads to the formation of only one of the two possible diastereomers. Subsequent exchange of the chiral ammonium for an achiral one results in a formation of an enantiopure complex that retains its enantiopurity for at least eight months.[81] Moreover, the complex retains its chirality even after exchange of the ligands that form the complex (Figure 2.17).[82]

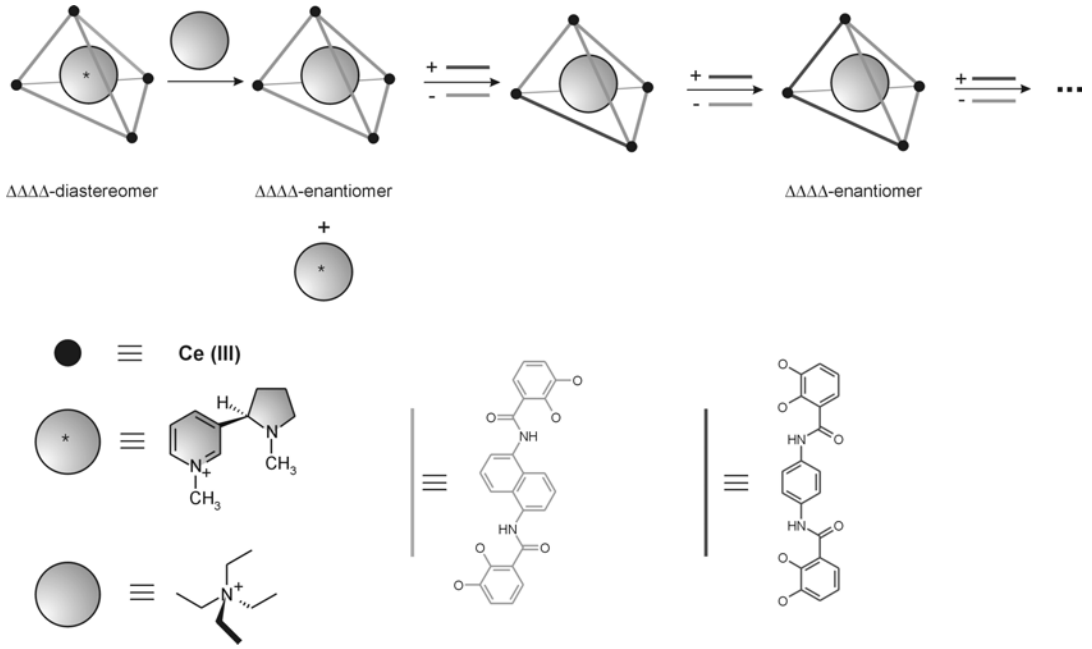

Figure 2.17. Schematic representation of the replacement of the chiral ammonium cation for an achiral and posterior exchange of the ligand. In both steps the chirality of the metal complex is preserved.

Recently, the same group has also reported the resolution of the same kind of compounds using enantiopure ferric complexes and posterior exchange by gallium, retaining the stereochemistry of the complex.[83] This phenomenon has also been observed in the self-aggregation of oppositely charged achiral porphyrins in the presence of chiral aggregates of aromatic amino acids.[84]

2.2.2.b.3. Other cases

A nice example of enantioselective synthesis arises from the encapsulation of alkanes (*n*-$C_{10}H_{22}$ to *n*-$C_{14}H_{30}$) by a self-assembled synthetic capsule formed by two resorcinarene-based tretraimide (for chemical structure of the synthetic capsule, see Figure 2.8b).[85] This is a special case because helical structures are not encountered as conformation of naturally occurring hydrocarbons. On the other hand, the straight-chain hydrocarbons are forced to adopt a helical (chiral) conformation to fit in the cavity and to maximize CH/π interactions with the aromatic walls of the self-assembled receptor during the encapsulation process, and therefore they exist as a mixture of enantiomers in

the interior of the self-assembled capsule. However, the helix-helix interconversion (racemization) occurs rapidly on the NMR time scale.

2.2.2.c. Amplification of chirality: The 'sergeants-and-soldiers' principle

Amplification of chirality occurs in systems in which a small initial amount of chiral bias induces a high diastereomeric or enantiomeric excess.[34] Green and coworkers reported few years ago for the first time the amplification of chirality in polyisocyantes having a stiff helical backbone.[86] They found that polymers containing small percentage of the chiral monomers still expressed a strong chiroptical activity. The reason for this amplification is that the achiral units are forced to follow the helicity induced for the chiral units. This is commonly referred to as the 'sergeants-and-soldiers' principle. This phenomenon has been also studied in noncovalent polymeric structures by Meijer et al.[87]

The amplification of chirality in well-defined systems has been investigated in double rosette assemblies using the 'sergeants-and-soldiers' principle.[88] For this purpose, solutions of chiral and racemic assemblies in benzene were mixed in ratios varying between 90:10 and 10:90 at room temperature. Interestingly, the CD-intensities increase in time as a result of the formation of the heteromeric assemblies (Figure 2.18).[71] A plot of the thermodynamic value against the ratio of chiral rosette used shows the typical nonlinear behavior of the 'sergeants-and-soldiers' experiments (Figure 2.18).

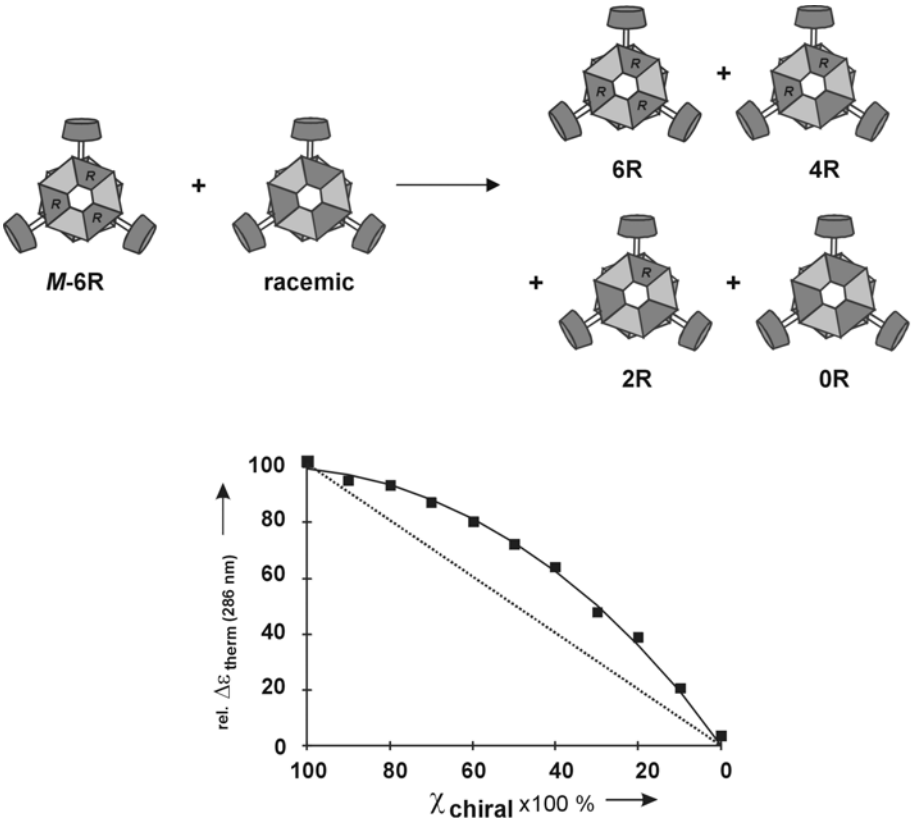

Figure 2.18. Schematic representation of the formation of the heteromeric assemblies (top), and plot of the relative CD-intensities at the thermodynamic equilibrium for different mole fractions of the chiral component (bottom). The dotted line represents the values in absence of chiral amplification.

Purello and coworkers combine the use of chiral memory and amplification of chirality in the self-aggregation of opposite charged porphyrins.[84] The addition of equimolar amounts of oppositely charged porphyrins to solutions of imprinted assemblies (assemblies in which the chirality has been memorized) resulted in a linear growth of the optical activity of the aggregates increasing the porphyrins concentration, showing a 100% enantiospecific chiral growth.

Amplification of chirality has been also reported in the formation of homochiral oligopeptides from amino acids of low enantiomeric excess.[89,90]

2.2.3. Chirality in liquid crystals and other macromolecular aggregates

A liquid crystal may be defined as an ordered fluid that is intermediate between the three dimensionally ordered crystal phase and the disordered liquid phase.[91] This is referred as a mesophase and its components as mesogens. These mesophases are classified upon their symmetry, distinguishing three major classes: nematic, cholesteric (also denominated chiral nematic[92]) and smectic. Due to their symmetries, the three mesophasic structures can be chiral, leading to materials with interesting properties for practical applications such as materials for processing and displaying color information, and optical filters and reflectors.[92,93] Chirality in these systems can be introduced via the chiral centers of the mesogen molecules and via the use of achiral bent-core molecules ('bow' or 'banana' shape molecules[94]). This kind of molecules can form chiral liquid crystal phases due to the spontaneous chiral supramolecular organization of the achiral molecules. Furthermore, the use of self-assembled systems based on metal coordination and H-bonding interactions has been found to be a versatile tool to obtain liquid crystals with controlled supramolecular chirality.[95-97] In this context, the formation of diastereomeric species,[98] the observation of self-resolution[99] and the amplification of chirality ('sergeants-and-soldiers' principle) has been reported.[94,96,97]

Using chiral mesogens it is possible to create chiral liquid crystals of different mesophases.[100] Kato and coworkers used this strategy to create chiral thermotropic liquid crystals using folic acid derivatives upon addition of achiral ions (Figure 2.19).[101] The formation of helical (chiral) structures in liquid crystalline materials using metal-organic complexes has also been studied employing chiral mesogens.[102]

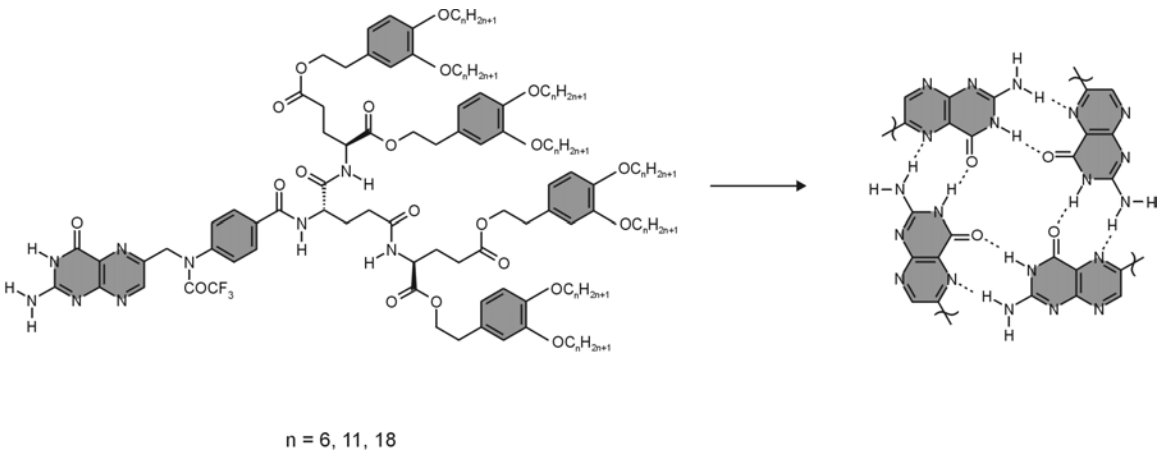

Figure 2.19. Molecular structures of folic acid derivatives and their self-assembly in hydrogen-bonded tetramers.

Supramolecular polymers may be defined as the polymers based on monomeric units held together with directional and reversible secondary interactions, such as hydrogen bonding, metal coordination, or π-π stacking.[103] Supramolecular polymers have received a lot of attention for their possible applications in the field of material science.[104] This kind of polymers display supramolecular chirality, usually, forming helical structures. The formation of diastereomeric helices is based in the introduction of chiral centers in the building blocks (Figure 2.20) (asymmetric induction).[103,105] Numerous cases of amplification of chirality for these structures have been reported.[87,106]

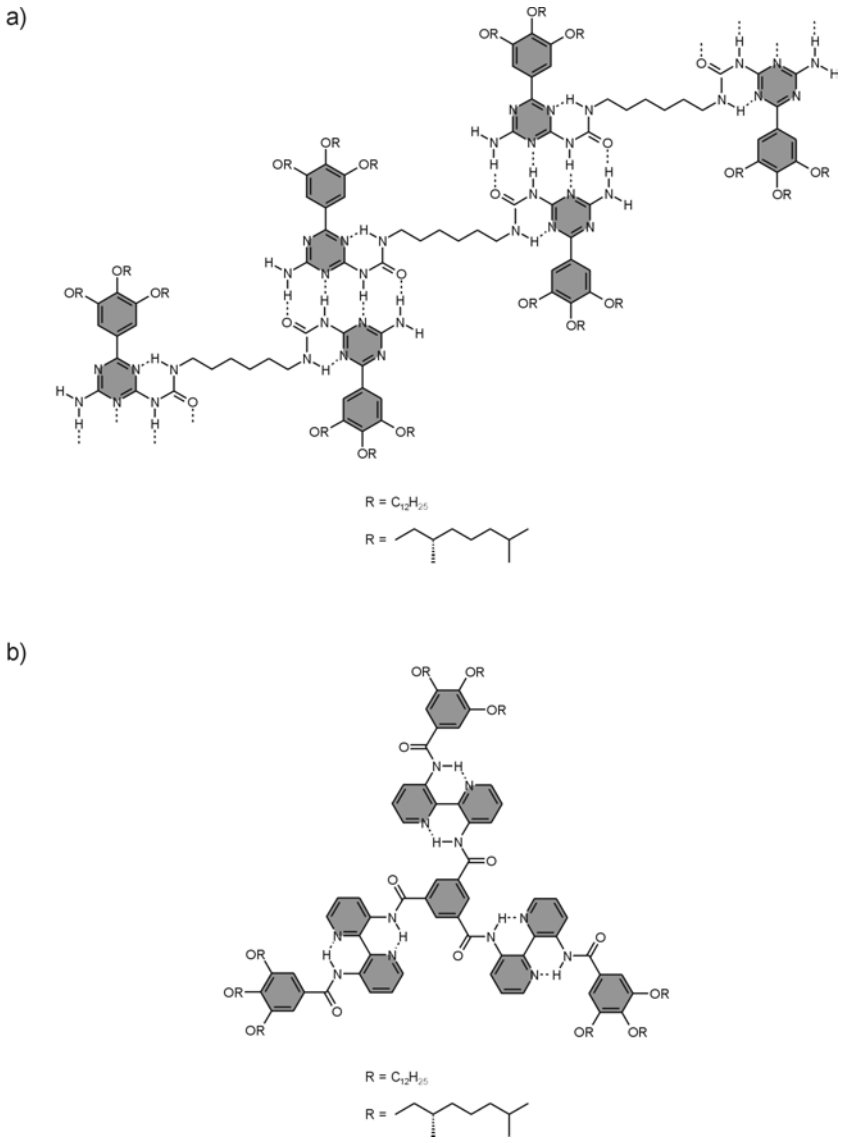

Figure 2.20. Supramolecular polymers based on a) bifunctional ureidotriazines with achiral and chiral side-chains, and b) C_3-symmetrical disc-shaped molecules with achiral and chiral side-chains.

Meijer et al. have studied the formation of chiral supramolecular polymers using different systems, such us oligo(p-phenylenevinylene)s (OPV),[107] hydrogen bonded dimers of OPVs,[108] hydrogen bonded assemblies of OPVs and perylene dyes,[109] OPVs rosettes,[110] ureidopyrimidinone derivatives (Upy),[111] ureidotriazines (UTr),[112] and 1,3,5-tricarboxamide derivatives (Figure 2.21).[113] The introduction of chiral groups in the periphery of these systems leads to the formation of only one of the two possible helix-senses. Moreover, the addition of chiral components to the assemblies of achiral

components biases the helicity of the assemblies in a supramolecular form of the 'sergeants and soldiers' principle.[86] The group of van Gestel has developed several theoretical methods to explain the 'sergeants and soldiers' principle in supramolecular polymers.[114,115]

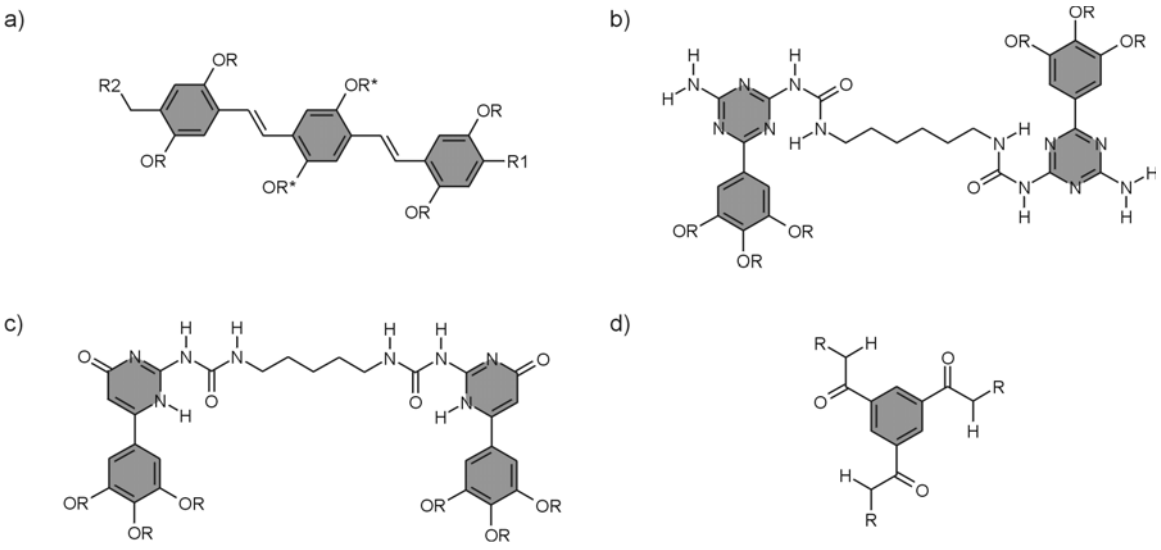

Figure 2.21. Chemical structure of a) generic oligo(p-phenylenevinylene)s (OPV), b) ureidotriazines (UTr), c) ureidopyrimidinone derivatives (Upy), and d) 1,3,5-tricarboxamide derivatives.

Yashima et al. have studied the induction of macromolecular helicity and the memory of this helicity in poly(phenylacetylene) polymers through noncovalent interactions.[116] These polymeric systems have been used for detection and amplification of chirality for a wide range of chiral molecules.[117]

Recently, the induction of chirality through recognition of saccharides in hydrogen-bonding oligomers and oligohydrazide foldamers has been reported.[118,119]

2.3. Conclusion and outlook

For more than a century, chemists have been concerned about the synthesis of new molecules via disruption and construction of covalent bonds. In covalent synthesis, the preparation of pure chiral molecules is still a major topic of interest especially because of its implication in the development of new drugs and catalysts. In noncovalent

synthesis the formation of chiral self-assembled aggregates is still in its infancy due to the highly dynamic character of noncovalent interactions. Nevertheless, in this chapter it has been shown that there are examples of noncovalent systems in which the process of self-assembly can be fully controlled, resulting in the stereoselective synthesis of diastereomeric and enantiomeric assemblies. Control over the processes of chiral memory and chiral amplification has very promising consequences. It is clear that control over supramolecular chirality of increasingly complex synthetic assemblies will be of crucial importance to their application in the field of molecular recognition, catalysis, material sciences, and specially nanotechnology.

The research described in this thesis covers different aspects of supramolecular chirality in hydrogen-bonded assemblies, such as amplification of chirality, enantioselective formation of tetrarosette assemblies using a '*catalytic chaperon effect*' and chiral molecular recognition using double and tetrarosette assemblies as receptor molecules.

2.4. References

[1] Whitesides, G. M.; Grzybowski, B. *Science* **2002**, *295*, 2418-2421.

[2] Fiammengo, R.; Crego-Calama, M.; Reinhoudt, D. N. *Curr. Opin. Chem. Biol.* **2001**, *5*, 660-673.

[3] De Feyter, S.; De Schryver, F. C. *Chem. Soc. Rev.* **2003**, *32*, 139-150.

[4] Philp, D.; Stoddart, J. F. *Angew. Chem. Int. Ed. Engl.* **1996**, *35*, 1154-1196.

[5] The term "chirality center" is the most recently IUPAC-approved name (*Pure Appl. Chem.* **1996**, *vol. 8*, p 293). At various times it has been called a stereogenic center, a stereocentre, a chiral center, and an asymmetric carbon.

[6] Bruice, P. Y. *Organic Chemistry*, Prentince Hall, NJ, USA, 3rd edn., **2001**.

[7] Verbiest, T.; van Elshocht, S.; Kauranen, M.; Hellemans, L.; Snauwaert, J.; Nuckolls, C.; Katz, T. J.; Persoons, A. *Science* **1998**, *282*, 913-915.

[8] Pease, A. R.; Jeppesen, J. O.; Stoddart, J. F.; Luo, Y.; Collier, C. P.; Heath, J. R. *Acc. Chem. Res.* **2001**, *34*, 433-444.

[9] Pérez-García, L.; Amabilino, D. B. *Chem. Soc. Rev.* **2002**, *31*, 342-356.

[10] Schalley, C. A.; Beizai, K.; Vögtle, F. *Acc. Chem. Res.* **2001**, *34*, 465-476.

[11] Tseng, H.-R.; Vignon, S. A.; Celestre, P. C.; Stoddart, J. F.; White, A. J. P.; Williams, D. J. *Chem. Eur. J.* **2003**, *9*, 543-556.

[12] Lehn, J.-M. *Supramolecular Chemistry: Concepts and Perspectives*, VCH, Weinheim, **1995**.

[13] Reinhoudt, D. N.; Crego-Calama, M. *Science* **2002**, *295*, 2403-2407.

[14] Topiol, S.; Sabio, M. *Enantiomer* **1996**, *1*, 251-265.

[15] Ballester, P.; Shivanyuk, A.; Rafai, A.; Rebek, J. Jr. *J. Am. Chem. Soc.* **2002**, *124*, 14014-14016.

[16] Hamuro, Y.; Crego-Calama, M.; Park, H. S.; Hamilton, A. D. *Angew. Chem. Int. Ed.* **1997**, *36*, 2680-2683.

[17] Almaraz, M.; Raposo, C.; Martín, M.; Caballero, M. C.; Morán, J. R. *J. Am. Chem. Soc.* **1998**, *120*, 3516-3517.

[18] Oliva, A. I.; Simón, L.; Muñiz, F. M.; Sanz, F.; Morán, J. R. *Chem. Commun.* **2004**, 426-427.

[19] Borovkov, V. V.; Hembury, G. A.; Inoue, Y. *Acc. Chem. Res.* **2004**, *37*, 449-459.

[20] Borovkov, V. V.; Lintuluoto, J. M.; Sugiura, M.; Inoue, Y.; Kuroda, R. *J. Am. Chem. Soc.* **2002**, *124*, 11282-11283.

[21] Borovkov, V. V.; Hembury, G. A.; Inoue, Y. *Angew. Chem. Int. Ed.* **2003**, *42*, 5310-5314.

[22] Proni, G.; Pescitelli, G.; Huang, X.; Quraishi, N. Q.; Nakanishi, K.; Berova, N. *Chem. Commun.* **2002**, 1590-1591.

[23] Guo, Y.-M.; Oike, H.; Saeki, N.; Aida, T. *Angew. Chem. Int. Ed.* **2004**, *43*, 4915-4918.

[24] a) Fiammengo, R.; Crego-Calama, M.; Timmerman, P.; Reinhoudt, D. N. *Chem. Eur. J.* **2003**, *9*, 784-792; b) Waldvogel, S. R.; Fröhlich, R.; Schalley, C. A. *Angew. Chem. Int. Ed.* **2000**, *39*, 2472-2475.

[25] Schopohl, M. C.; Siering, C.; Kataeva, O.; Waldvogel, S. R. *Angew. Chem. Int. Ed.* **2003**, *42*, 2620-2623.

[26] Ishi-i, T.; Mateos-Timoneda, M. A.; Timmerman, P.; Crego-Calama, M.; Reinhoudt, D. N.; Shinkai, S. *Angew. Chem. Int. Ed.* **2003**, *42*, 2300-2305.

[27] Escuder, B.; Rowan, A. E.; Feiters, M. C.; Nolte, R. J. M. *Tetrahedron* **2004**, *60*, 291-300.

[28] Borovkov, V. V.; Harada, T.; Inoue, Y.; Kuroda, R. *Angew. Chem. Int. Ed.* **2002**, *41*, 1378-1381.

[29] Webb, T. H.; Wilcox, C. S. *Chem. Soc. Rev.* **1993**, *22*, 383-395.

[30] Chen, H.; Weiner, W. S.; Hamilton, A. D. *Curr. Opin. Chem. Biol.* **1997**, *1*, 458-466.

[31] Fitzmaurice, R. J.; Kyne, G. M.; Douheret, D.; Kilburn, J. D. *J. Chem. Soc.*, *Perkin Trans. 1* **2002**, 841-864.

[32] Swiegers, G. F.; Malefetse, *T. J. Chem. Rev.* **2000**, *100*, 3483-3538.

[33] Hof, F.; Craig, S. L.; Nuckolls, C., Rebek, J. Jr. *Angew. Chem. Int. Ed.* **2002**, *41*, 1488-1508.

[34] Feringa, B. L.; van Delden, R. A. *Angew. Chem. Int. Ed.* **1999**, *38*, 3418-3438.

[35] a) Schalley, C. A.; Lützen, A.; Albrecht, M. *Chem. Eur. J.* **2004**, *10*, 1072-1080; b) Hamann, C.; von Zelewsky, A.; Neels, A.; Stoeckli-Evans, H. *Dalton Trans.* **2004**, 402-406.

[36] Simanek, E. E.; Qiao, S.; Choi, I. S.; Whitesides, G. M. *J. Org. Chem.* **1997**, *62*, 2619-2621.

[37] Prins, L. J.; Timmerman, P.; Reinhoudt, D. N. *Angew. Chem. Int. Ed.* **2001**, *40*, 2382-2426.

[38] Timmerman, P.; Vreekamp, R. H.; Hulst, R.; Verboom, W.; Reinhoudt, D. N.; Rissanen, K.; Udachin, K. A.; Ripmeester, J. *Chem. Eur. J.* **1997**, *3*, 1823-1832.

[39] Prins, L. J.; Huskens, J.; de Jong, F.; Timmerman, P.; Reinhoudt, D. N. *Nature* **1999**, *398*, 498-502.

[40] Ishi-i, T.; Crego-Calama, M.; Timmerman, P.; Reinhoudt, D. N.; Shinkai, S. *Angew. Chem. Int. Ed.* **2002**, *41*, 1924-1929.

[41] Ishi-i, T.; Crego-Calama, M.; Timmerman, P.; Reinhoudt, D. N.; Shinkai, S. *J. Am. Chem. Soc.* **2002**, *124*, 14631-14641.

[42] Fenniri, H.; Mathivanan, P.; Vidale, K. L.; Sherman, D. M.; Hallenga, K.; Wood, K. V.; Stowell, J. G. *J. Am. Chem. Soc.* **2001**, *123*, 3854-3855.

[43] Fenniri, H.; Deng, B.-L.; Ribbe, A. E. *J. Am. Chem. Soc.* **2002**, *124*, 11064-11072.

[44] Marlow, A. L.; Mezzina, E.; Spada, G. P.; Masiero, S.; Davis, J. T.; Gottarelli, G. J. *J. Org. Chem.* **1999**, *64*, 5116-5123.

[45] Rivera, J. M.; Martín, T.; Rebek, J. Jr. *Science* **1998**, *279*, 1021-1023.

[46] Hori, A.; Akasaka, A.; Biradha, K.; Sakamoto, S.; Yamaguchi, K. Fujita, M. *Angew. Chem. Int. Ed.* **2002**, *41*, 3269-3272.

[47] a) Shivanyuk, A.; Rebek, J. Jr. *J. Am. Chem. Soc.* **2002**, *124*, 12074-12075; b) Scarso, A.; Shivanyuk, A.; Rebek, J. Jr. *J. Am. Chem. Soc.* **2003**, *125*, 13981-13983.

[48] Yamanaka, M.; Rebek, J. Jr. *Chem. Commun.* **2004**, 1690-1691.

[49] Albrecht, M. *Chem. Rev.* **2001**, *101*, 3457-3498.

[50] Piguet, C.; Bernardinelli, G.; Hopfgarther, G. *Chem. Rev.* **1997**, *97*, 2005-2062.

[51] Takeuchi, M.; Imada, T.; Shinkai, S. *Angew. Chem. Int. Ed.* **1998**, *37*, 2096-2099.

[52] Prabaharan, R.; Fletcher, N. C.; Nieuwenhuyzen, M. *J. Chem. Soc., Dalton Trans.* **2002**, 602-608.

[53] Albrecht, M.; Schmid, S.; deGroot M.; Weis, P.; Fröhlich, R. *Chem. Commun.* **2003**, 2526-2527.

[54] Pfeiffer, P.; Quehl, K. *Chem. Ber.* **1931**, *64*, 2667-2671.

[55] Lacour, J.; Jodry, J. J.; Monchaud, D. *Chem. Commun.* **2001**, 2302-2303.

[56] Amouri, H.; Thouvenot, R.; Gruselle, M.; Malézieux, B.; Vaissermann, J. *Organometallics* **2001**, *20*, 1904-1906.

[57] Gruselle, M.; Thouvenot, R.; Malézieux, B.; Train, C.; Gredin, P.; Demeschik, T. V.; Troitskaya, L. L.; Sokolov, V. I. *Chem. Eur. J.* **2004**, *10*, 4763-4769.

[58] Orita, A.; Nakano, T.; An, D. L.; Tanikawa, K.; Wakamatsu, K.; Otera, J. *J. Am. Chem. Soc.* **2004**, *126*, 10389-10396.

[59] Fiedler, D.; Leung, D. H.; Bergman, R. G.; Raymond, K. N. *J. Am. Chem. Soc.* **2004**, *126*, 3674-3675.

[60] Leung, D. H.; Fiedler, D.; Bergman, R. G.; Raymond, K. N. *Angew. Chem. Int. Ed.* **2004**, *43*, 963-966.

[61] Albrecht, M. *Chem. Eur. J.* **2000**, *6*, 3485-3489.

[62] Albrecht, M.; Janser, I.; Houjou, H.; Frölich, R. *Chem. Eur. J.* **2004**, *10*, 2839-2850.

[63] Di Bari, L.; Lelli, M.; Salvadori, P. *Chem. Eur. J.* **2004**, *10*, 4594-4598.

[64] Hasenknopf, B.; Lehn, J.-M. *Helv. Chim. Acta* **1996**, *79*, 1643-1650.

[65] Werner, A.; Michels, M.; Zander, L.; Lex, J.; Vogel, E. *Angew. Chem. Int. Ed.* **1999**, *38*, 3650-3653.

[66] Tashiro, K.; Konishi, K.; Aida, T.; *Angew. Chem. Int. Ed. Engl.* **1997**, *36*, 856-858.

[67] Russel, K. C.; Lehn, J.-M.; Kyritsakas, N.; DeCian, A.; Fischer, J. *New. J. Chem.* **1998**, *22*, 123-128.

[68] Bowyer, P. K.; Cook, V. C.; Gharib-Naseri, N.; Gugger, P. A.; Rae, A. D.; Swiegers, G. F.; Willis, A. C.; Zank, J.; Wild, S. B. *Proc. Natl. Acad. Sci. U.S.A.* **2002**, *99*, 4877-4882.

[69] Yue, W. M.; Bishop, R.; Scudder, M. L.; Craig, D. C. *Chem. Lett.* **1998**, 803-804.

[70] ten Cate, A. T.; Dankers, P. Y. W.; Kooijman, H.; Spek, A. L.; Sijbesma, R. P.; Meijer, E. W. *J. Am. Chem. Soc.* **2003**, *125*, 6860-6861.

[71] Crego-Calama, M.; Hulst, R.; Fokkens, R.; Nibbering, N. M. M.; Timmerman, P.; Reinhoudt, D. N. *Chem. Commun.* **1998**, 1021-1022.

[72] Crego-Calama, M.; Timmerman, P.; Reinhoudt, D. N. *Angew. Chem. Int. Ed.* **2000**, *39*, 755-758.

[73] Anderberg, P. I.; Turner, J. J.; Evans, K. J.; Hutchins, L. M.; Harding, M. M. *Dalton Trans.* **2004**, 1708-1714.

[74] Ademi, L.; Constable, E. C.; Housecroft, C. E.; Neuburger, M.; Schaffner, S. *Dalton Trans.* **2003**, 4565-4567.

[75] For a definition of atropisomers see: Eliel, E. L.; Wilen, S. H.; Mander, L. N. *Stereochemistry of Organic Compounds*, John Wiley, New York, **1994**.

[76] Jayanti, S.; Radhakrishnan, T. P. *Chem. Eur. J.* **2004**, *10*, 2661-2667.

[77] Telfer, S. G.; Sato, T.; Kuroda, R. *Angew. Chem. Int. Ed.* **2004**, *43*, 581-584.

[78] Yashima, E.; Maeda, K.; Okamoto, Y. *Nature* **1999**, *399*, 449-451.

[79] Prins, L. J.; de Jong, F.; Timmerman, P.; Reinhoudt, D. N. *Nature* **2000**, *408*, 181-184.

[80] Rivera, J. M.; Craig, S. L.; Martín, T.; Rebek, J. Jr. *Angew. Chem. Int. Ed.* **2000**, *39*, 2130-2132.

[81] Terpin, A. J.; Ziegler, M.; Johnson, D. W.; Raymond, K. N. *Angew. Chem. Int. Ed.* **2001**, *40*, 157-160.

[82] Ziegler, M.; Davis, A. V.; Johnson, D. W.; Raymond, K. N. *Angew. Chem. Int. Ed.* **2003**, *42*, 665-668.

[83] Brumaghim, J. L.; Raymond, K. N. *J. Am. Chem. Soc.* **2003**, *125*, 12066-12067.

[84] Lauceri, R.; Raudino, A.; Scolaro, L. M.; Micali, N.; Purrello, R. *J. Am. Chem. Soc.* **2002**, *124*, 894-895.

[85] a) Scarso, A.; Trembleau, L.; Rebek, J. Jr. *Angew. Chem. Int. Ed.* **2003**, *42*, 5499-5502; b) Scarso, A.; Trembleau, L.; Rebek, J. Jr. *J. Am. Chem. Soc.* **2004**, *126*, 13512-13518.

[86] Green, M. M.; Rediy, M. P.; Johnson, R. J.; Darling, G.; O'Leary, D. J.; Willson, G. J. *J. Am. Chem. Soc.* **1989**, *111*, 6452-6454.

[87] Palmans, A. R. A.; Vekemans, J. A. J. M.; Havinga, E. E.; Meijer, E. W. *Angew. Chem. Int. Ed. Engl.* **1997**, *36*, 2648-2651.

[88] Prins, L. J.; Timmerman, P.; Reinhoudt, D. N. *J. Am. Chem. Soc.* **2001**, *123*, 10153-10163.

[89] Saghatelian, A.; Yokobayashi, Y.; Soltani, K.; Ghadiri, M. R. *Nature* **2001**, *409*, 797-801.

[90] Cintas, P. *Angew. Chem. Int. Ed.* **2002**, *41*, 1139-1145.

[91] Demus, D.; Goodby, J.; Gray, G. W.; Spiess, H.-W., Vill, V. *Handbook of Liquid Crystals*, Wiley-VCH, Weinheim, *volume 1*, **1998**.

[92] Tamaoki, N. *Adv. Mater.* **2001**, *13*, 1135-1147.

[93] Chen, H. P.; Katsis, D.; Mastrangelo, J. C.; Chen, S. H.; Jacobs, S. D.; Hood, P. J. *Adv. Mater.* **2000**, *12*, 1283-1286.

[94] Link, D. R.; Natale, G.; Saho, R.; Maclennan, J. E.; Clark, N. A.; Körblova, E.; Walba, D. M. *Science* **1997**, *278*, 1924-1927.

[95] Kato, T. *Science* **2002**, *295*, 2414-2418.

[96] Trzaska, S. T.; Hsu, H.-F.; Swager, T. M. *J. Am. Chem. Soc.* **1999**, *121*, 4518-4519.

[97] Barberá, J.; Cavero, E.; Lehmann, M.; Serrano, J.-L.; Sierra, T.; Vázquez, J. T. *J. Am. Chem. Soc.* **2003**, *125*, 4527-4533.

[98] Walba, D. M.; Körblova, E.; Shao, E.; Maclennan, J. E.; Link, D. R.; Glaser, M. A.; Clark, N. A. *J. Phys. Org. Chem.* **2000**, *13*, 830-836.

[99] Tsiourvas, D.; Paleos, C. M.; Skoulios, A. *Chem. Eur. J.* **2003**, *9*, 5250-5258.

[100] Kitzerow, H. S.; Bahr, C. *Chirality in Liquid Crystals*, Springer, New York, **2001**.

[101] Kato, T.; Matsuoka, T.; Nishii, M.; Kamikawa, Y.; Kanie, K.; Nishimura, T.; Yashima, E.; Ujiie, S. *Angew. Chem. Int. Ed.* **2004**, *43*, 1969-1972.

[102] Serrano, J. L.; Sierra, T. *Coord. Chem. Rev.* **2003**, *242*, 73-85.

[103] a) A. Ciferri, *Supramolecular Polymers*, Marcel Dekker, New York, **2000**; b) Brunsveld, L.; Folmer, B. J. B.; Meijer, E. W.; Sijbesma, R. P. *Chem. Rev.* **2001**, *101*, 4071-4098.

[104] Percec, V.; Glodde, M.; Bera, T. K.; Miura, Y.; Shiyanovskaya, I.; Singer, K. D.; Balagurusamy, V. S. K.; Heiney, P. A.; Schnell, I.; Rapp, A.; Spiess, H. W.; Hudson, S. D.; Duan, H. *Nature* **2002**, *419*, 384-387.

[105] Cornelissen, J. J. L. M.; Rowan, A. E.; Nolte, R. J. M.; Sommerdijk, N. A. J. M. *Chem. Rev.* **2001**, *101*, 4039-4070.

[106] a) Brunsveld, L.; Schenning, A. P. H. J.; Broeren, M. A. C.; Janssen, H. M.; Vekemans, J. A. J. M.; Meijer, E. W. *Chem. Lett.* **2000**, 292-293; b) Brunsveld, L.; Lohmeijer, B. G. G.; Vekemans, J. A. J. M.; Meijer, E. W. *Chem. Commun.* **2000**, 2305-2306; c) Schenning, A. P. H. J.; Jonkheijm, P.; Peeters, E.; Meijer, E. W. *J. Am. Chem. Soc.* **2001**, *123*, 409-416; d) Brunsveld, L.; Meijer, E. W.; Prince, R. B.; Moore, J. S. *J. Am. Chem. Soc.* **2001**, *123*, 7978-7984.

[107] George, S. J.; Ajayaghosh, A.; Jonkheijm, P.; Schenning, A. P. H. J.; Meijer, E. W. *Angew. Chem. Int. Ed.* **2004**, *43*, 3422-3425.

[108] Jonkheijm, P.; Hoeben, F. J. M.; Kleppinger, R.; van Herrikhuyzen, J.; Schenning, A. P. H. J.; Meijer, E. W. *J. Am. Chem. Soc.* **2003**, *125*, 15941-15949.

[109] Würthner, F.; Chen, Z.; Hoeben, F. J. M.; Osswald, P.; You, C.-C.; Jonkheijm, P.; van Herrikhuyzen, J.; Schenning, A. P. H. J.; van der Schoot, P. P. A. M.; Meijer, E. W.; Beckers, E. H. A.; Meskers, S. C. J.; Janssen, R. A. J. *J. Am. Chem. Soc.* **2004**, *126*, 10611-10618.

[110] Jonkheijm, P.; Miura, A.; Zdanowska, M.; Hoeben, F. J. M.; De Feyter, S.; Schenning, A. P. H. J.; De Schryver, F.; Meijer, E. W. *Angew. Chem. Int. Ed.* **2004**, *43*, 74-78.

[111] Hirschberg, J. H. K. K.; Koevoets, R. A.; Sijbesma, R. P.; Meijer, E. W. *Chem. Eur. J.* **2003**, *9*, 4222-4231.

[112] Hirschberg, J. H. K. K.; Ramzi, A.; Sijbesma, R. P.; Meijer, E. W. *Macromolecules* **2003**, *36*, 1429-1432.

[113] Masuda, M.; Jonkheijm, P.; Sijbesma, R. P.; Meijer, E. W. *J. Am. Chem. Soc.* **2003**, *125*, 15935-15940.

[114] van Gestel, J.; van der Schoot, P.; Michels, M A. J. *Macromolecules* **2003**, *36*, 6668-6673.

[115] van Gestel, J. *Macromolecules* **2004**, *37*, 3894-3898.

[116] a) Ishikawa, M.; Maeda, K.; Mitsutsuji, Y.; Yashima, E. *J. Am. Chem. Soc.* **2004**, *126*, 732-733; b) Maeda, K.; Morino, K.; Okamoto, Y.; Sato, T.; Yashima, E. *J. Am. Chem. Soc.* **2004**, *126*, 4329-4342; c) Onouchi, H.; Kashiwagi, D.; Hayashi, K.; Maeda, K.; Yashima, E. *Macromolecules* **2004**, *37*, 5495-5503; d) Nonokawa, R.; Oobo, M.; Yashima, E. *Macromolecules* **2003**, *36*, 6599-6606; e) Nishimura, T.; Ohsawa, S.; Maeda, K.; Yashima, E. *Chem. Commun.* **2004**, 646-647; f) Nishimura, T.; Tsuchiya, K.; Ohsawa, S.; Maeda, K.; Yashima, E.; Nakamura, Y.; Nishimura, J. *J. Am. Chem. Soc.* **2004**, *126*, 11711-11717.

[117] a) Nonokawa, R.; Yashima, E. *J. Am. Chem. Soc.* **2003**, *125*, 1278-1283; b) Morino, K.; Watase, N.; Maeda, K.; Yashima, E. *Chem. Eur. J.* **2004**, *10*, 4703-4707; c) Yashima, E.; Maeda, K.; Nishimura, T. *Chem. Eur. J.* **2004**, *10*, 42-51.

[118] Inouye, M.; Waki, M.; Abe, H. *J. Am. Chem. Soc.* **2004**, *126*, 2022-2027.

[119] Hou, J.-L.; Shao, X.-B.; Chen, G.-J.; Zhou, Y.-X.; Jiang, X.-K.; Li, Z.-T. *J. Am. Chem. Soc.* **2004**, *126*, 12386-12394.

Chapter 3

Controlling the amplification of chirality in double rosette assemblies*

In this chapter the amplification of chirality (a high enantiomeric or diastereomeric excess induced by a small initial amount of chiral bias) in double rosette hydrogen-bonded assemblies has been studied using 'sergeants-and-soldiers' experiments under thermodynamically controlled conditions. Here, it is shown that different substitutions and structural variations in the building blocks that form these self-assembled systems can be used to control the extent of the chiral amplification.

* This work has been published: Mateos-Timoneda, M. A.; Crego-Calama, M.; Reinhoudt, D. N. *Supramol. Chem.* **2005,** *17*, 67-79.

3.1. Introduction

Amplification of chirality is the process from which a high enantiomeric or diastereomeric excess (*e.e.* or *d.e.*, respectively) is induced by a small initial amount of chiral bias.[1] Chiral amplification is a widely study process due to its implication for the origin of life and in enantioselective autocatalytic processes.[1-5] Green and co-workers first reported the amplification of chirality in polyisocyanate polymers possessing a stiff helical backbone. The helicity of this backbone can be controlled via the insertion of chiral centres in the peripheral groups. The optical activity of the polymer remains constant even when the percentage of chiral units is lowered to 5%. This phenomenon is referred as 'sergeants-and-soldiers' principle:[6] the achiral units are forced to follow the helicity induced by the chiral units. This phenomenon has been widely studied in covalent and noncovalent polymers.[7-14] A nice example has been reported by Meijer et al. who have used 'sergeants-and-soldiers' experiments to study the assembly of helical columns of supramolecular hydrogen-bonded polymers.[15] Additionally, several theoretical models have been developed to fit the *amplified* experimental data and to obtain the parameters that govern the amplification of chirality in polymeric structures.[16-20] Recently, chiral amplification has been also studied in the formation of solid polymer films,[21] in the recognition of chiral amines and amino alcohols by optically inactive polyacetylenes[22,23] and other supramolecular assemblies,[24,25] in the cyclodimerization of saddle-shape porphyrins upon interaction with mandelic acid,[26] and in the formation of chiral liquid crystalline phases.[27-30]

Previously, our group showed for the first time, that the 'sergeants-and-soldiers' principle also applies to dynamic hydrogen-bonded assemblies of well-defined (finite) molecular composition.[31] It was found that the optical activity of a 50:50 mixture of chiral:achiral assemblies increases from the expected 50%, in the absence of chiral amplification, to the observed 97%. In this study, it was also shown that the dissociation rate of the dimelamine components influences the thermodynamics of chiral amplification, *i.e.* a decrease of the dissociation rate constant causes a larger amplification of chirality. Furthermore, model simulations showed that it would be possible to achieve high chiral amplification (*d.e.* > 99%) in these dynamic systems even when only 0.1% of the components are chiral. This chapter describes a more extensive study on the amplification of chirality in double rosette hydrogen-bonded assemblies under thermodynamically controlled conditions.

A large variety of systems comprising chiral and racemic structurally closely related assemblies $\mathbf{1}_3$•$(CYA)_6$ were studied in order to determine which parameters govern the extent of amplification of chirality for this type of hydrogen-bonded assemblies.

3.2. Formation of double rosette assemblies

Earlier studies have shown that hydrogen-bonded double rosettes assemblies $\mathbf{1}_3$•$(BA/CYA)_6$ are spontaneously formed by mixing calix[4]arene dimelamines **1** with 2 equivalents of barbiturates (BA) or cyanurates (CYA) in apolar solvents, such as chloroform, benzene and toluene (Figure 3.1).[32,33] The assembly formation is driven by the formation of 36 complementary hydrogen-bonds between the donor-acceptor-donor (DAD) array of the calix[4]arene dimelamine and acceptor-donor-acceptor (ADA) array of the barbiturate/cyanurate building blocks.

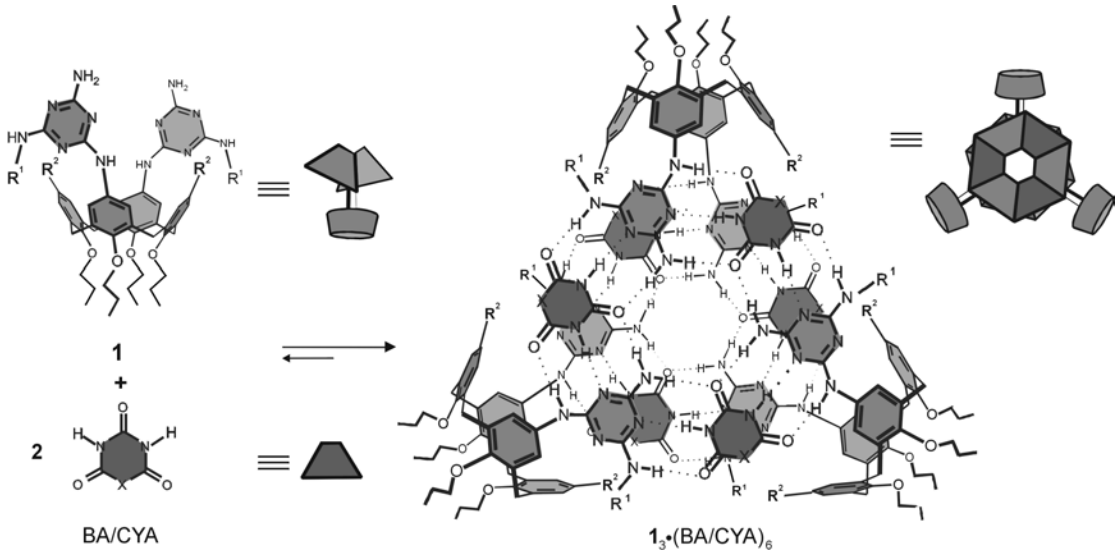

Figure 3.1. Schematic representation of the molecular building blocks and their self-assembly into double rosettes $\mathbf{1}_3$•$(BA/CYA)_6$.

These assemblies can exist in three different isomeric forms with D_3-, C_{3h}- and C_s-symmetry (Figure 3.2).[34] The assemblies with D_3-symmetry, which is the predominant isomer, are chiral due to the staggered (antiparallel) orientation of the two melamine fragments, leading to a twist of the two different rosette planes, which can either adopt a clockwise ((*P*)-isomer) or counterclockwise ((*M*)-isomer) conformation. In both C_{3h}- and C_s-isomers, the two melamine fragments adopt an

eclipsed (parallel) orientation and are therefore achiral. The difference between these isomers is the 180° rotation of one of the calix[4]arene dimelamines in the case of the C_s-isomer.

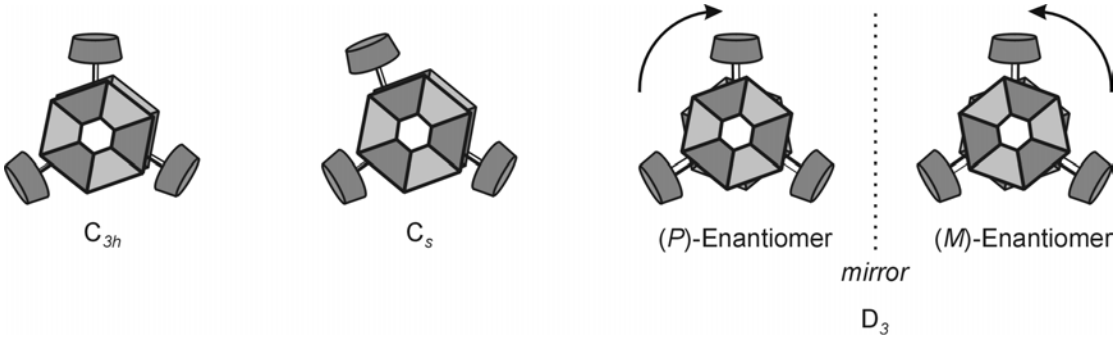

Figure 3.2. Schematic representation of the possible isomers with C_{3h}-, C_s-, and D_3-symmetry. Both the (*P*)- and (*M*)-enantiomers of the D_3-symmetrical isomer are depicted.

3.3 Characterization of double rosette assemblies

Double rosette assemblies can conveniently be characterized by ^{1}H NMR spectroscopy.[33] Titration experiments have proven the 1:2 stoichiometry and the strong cooperativity of the assembly process. Upon formation of the assembly the diagnostic signals of the imide NH protons of BA/CYA are observed between δ = 13 and 16 ppm. The number of signals in this region indicates the isomeric form of the assembly. For the D_3- and C_{3h}-isomers only two different signals are observed, while six different signals are observed for the assembly with C_s-symmetry.

The D_3-isomer is the most common one, and in the absence of any centre of chirality, it is formed as a racemic mixture of both (*P*)- and (*M*)-enantiomers. However, upon introduction of chiral centres in one of the molecular components of the assembly (calix[4]arene dimelamines or barbiturate/cyanurate), only one of the two possible diastereoisomers is formed with a diastereomeric excess (*d.e.*) up to 96%.[35,36] When chiral cyanurates are used the sense of the twist of the melamine fragments is dictated by the stereochemistry of the chiral centre in the cyanurates, *i.e.* a cyanurate bearing a chiral centre with (*R*)-stereochemistry leads only to the formation of, for example the (*P*)-diastereomer, while the (*S*)-isomer then leads only to (*M*)-diastereomer. These chiral (*P*)- and (*M*)-assemblies are highly circular-dichroism (CD) active due to the dissymmetric arrangement of the different

chromophores within the rigid structure and therefore this characterization technique is of tremendous value.

Another characterization technique is MALDI-TOF mass spectrometry after Ag^+ labelling.[37,38] This is an extremely mild technique and provides a nondestructive way to generate charged assemblies based on the high affinity of Ag^+ for (two) cooperative π-donors, cyano or crown-ether functionalities.

Finally, X-ray crystallography provides evidence for the existence of double rosette assemblies in the solid state. The crystal structure of **1b**$_3$•(DEB)$_6$ (see Chart 3.1) shows that the two single rosette planes are neatly stacked on top of each other, with an interatomic distance of 3.2-3.5 Å (Figure 3.3). Furthermore, it shows that the calix[4]arene units are fixed in a *pinched* cone conformation, the only conformation that allows simultaneous participation of the calix[4]arene units in both the upper and the lower rosette motifs.

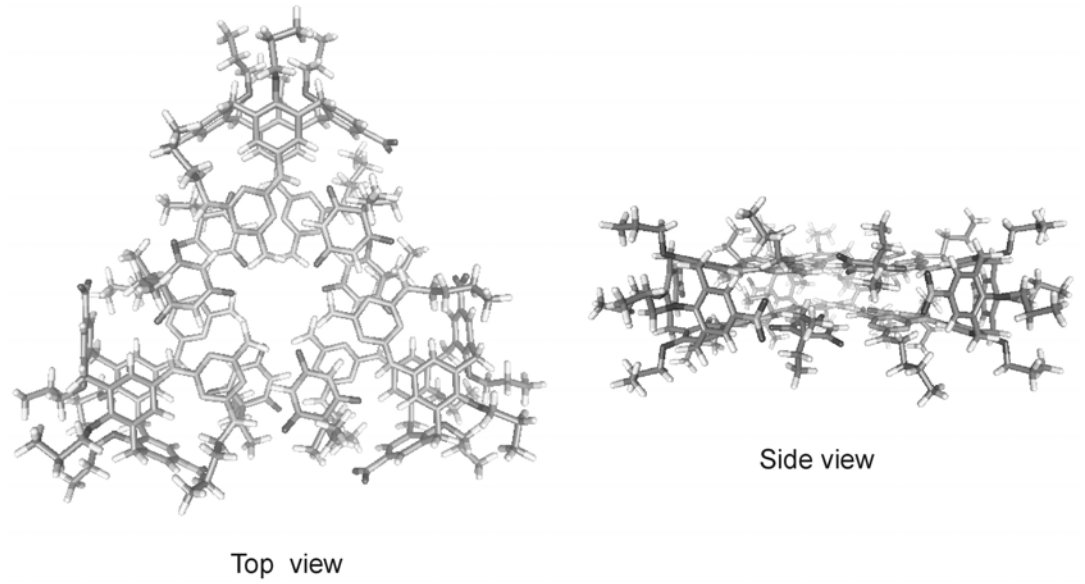

Figure 3.3. Top and side view of the X-ray crystal structure of assembly **1b**$_3$•(DEB)$_6$.

3.4. Results and discussion

With the aim of controlling the degree of chiral amplification in double rosette hydrogen-bonded assemblies, structural variations within the building blocks have been introduced in three different positions, *i.e.* in the two melamine moieties and the calix[4]arene skeleton (**1**), and the chiral cyanurate (*CYA) (see Figure 3.1). For this purpose, different calix[4]arene dimelamines bearing different groups in R^1 position

(**1a**, **1d**, **1f-h**), R^2 position (**1b-c**, **1e**) as well as different chiral ((*R*)-MePheCYA, (*R*)-MePropCYA, (*L*)-PhealaCYA, (*L*)-ValCYA and (*S*)-2-MeBuCYA) and achiral (BuCYA and BenCYA) cyanurates were synthesized (Chart 3.1). Subsequently, the amplification of chirality of different systems formed with these assemblies, was determined.

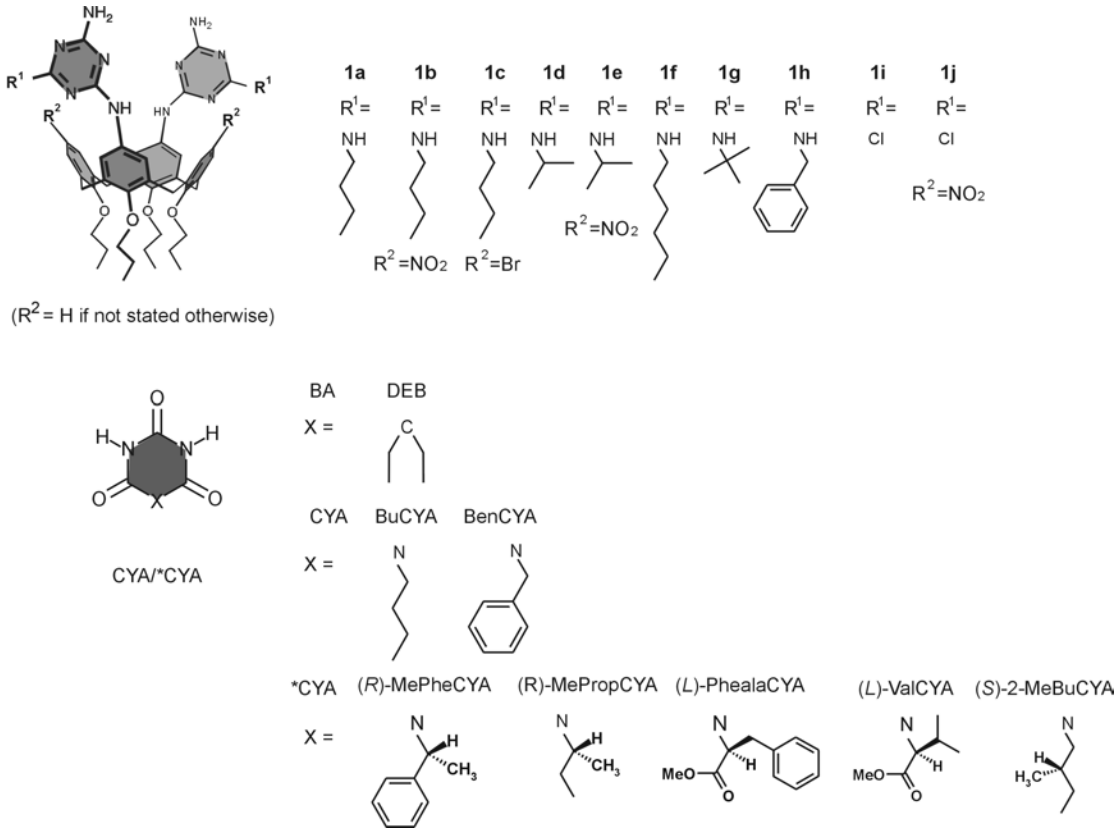

Chart 3.1. Molecular structures of dimelamines **1** and BA/CYA derivatives

3.4.1. Synthesis

Calix[4]arene dimelamines **1a-c**, **1h** and bis(chlorotriazine) calix[4]arene derivatives **1i-j** (chart 3.1) were synthesized following literature procedures.[33] Calix[4]arene dimelamines **1d-g** were synthesized by reaction of the corresponding bis(chlorotriazine) calix[4]arene **1i,j** with an excess of the corresponding amine, i.e. *i*-propylamine (**1d**,**e**), hexylamine (**1f**) or *t*-butylamine (**1g**) in THF. Cyanurates BuCYA, BenCYA, (*R*)-MePheCYA, (*L*)-PhealaCYA and (*L*)-ValCYA were prepared following literature procedures.[36] Cyanurates (*R*)-MePropCYA and (*S*)-2-MeBuCYA were synthesized in one step via ring closure of the corresponding amine with N-

chlorocarbonylisocyanate in THF under extremely dry conditions (see experimental section).

3.4.2. Amplification of chirality in assemblies ***1***$_3$*•(CYA/*CYA)*$_6$

Solutions of the assembly (*P*)-**1b**$_3$•((*R*)-MePheCYA)$_6$ and racemic **1b**$_3$•(BenCYA)$_6$ in benzene (1 mM) were mixed in ratios ranging from 90:10 to 10:90 and the CD intensity at 308 nm was measured as a function of time at 70 ^{o}C. The thermodynamic equilibrium is reached almost immediately after the mixing process (specially for the higher ratios of chiral assembly). From these measurements, the relative CD intensities were related to a calculated 100% value based on the ratio (*P*)-**1b**$_3$•((*R*)-MePheCYA)$_6$/(*P*)-**1b**$_3$•(BenCYA)$_6$ and plotted as a function of time (Figure 3.4a).[39] It was assumed that all the assemblies present in solution after the mixing process have the same $\Delta\varepsilon_\lambda$ (CD intensity at the wavelength of maximum absorbance), which seems reasonable regarding their very similar molecular structure and the number of chromophores.[40] For the high ratio values of (*P*)-**1b**$_3$•((*R*)-MePheCYA)$_6$, the CD intensities at t=0 do not correspond to the initial mol fraction of (*P*)-**1b**$_3$•((*R*)-MePheCYA)$_6$, because immediately after mixing the thermodynamic value for $\Delta\varepsilon_\lambda$ is reached (Figure 3.4a). In the rest of the text, these thermodynamic values will be referred to as relative $\Delta\varepsilon_{therm}$. When there would be no amplification of the chirality in the system, the CD-intensity of the mixtures would increase linearly with the molar fraction of chiral assembly present, *i.e.* a mixture with 50% of chiral assembly will display a CD-intensity corresponding to this 50% of chiral assembly component. However, a plot of the relative $\Delta\varepsilon_{therm}$ as a function of the ratio chiral:non-chiral rosette assemblies shows the typical non-linear behavior of the 'sergeants-and-soldiers' principle (Figure 3.4b), the CD intensities of the mixtures increase non-linearly with the percentage of chiral assembly present.[31] For example, when a 70:30 mixture of **1b**$_3$•(BenCYA)$_6$ and (*P*)-**1b**$_3$•((*R*)-MePheCYA)$_6$ reaches the thermodynamic equilibrium, the relative CD-intensity has increased from 30% (expected in the case where there is no chiral amplification) to 75%.

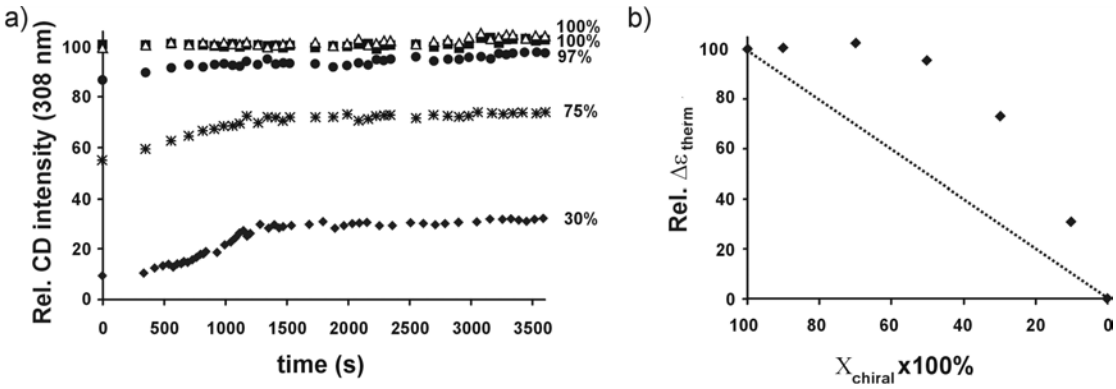

Figure 3.4. a) Plot of the relative CD intensity at 308 nm, versus the time for a mixture of (*P*)-**1b**$_3$•((*R*)-MePheCYA)$_6$ and **1b**$_3$•(BenCYA)$_6$ with different initial mole fractions of **1b**$_3$•((*R*)-MePheCYA)$_6$ (♦: 10%; *: 30%; ●: 50%; ■: 70%; Δ: 90%) (the % in the graphic represents the relative CD-intensity reached at the thermodynamic equilibrium). b) Plot of the relative CD-intensities at the thermodynamic equilibrium for different mole fractions of chiral component. The dotted line represents the expected CD-intensity when there is no amplification of chirality.

The non-linear increase of the CD intensity is due to the exchange between the chiral and nonchiral cyanurates within the assemblies, that is to say, to the presence of the heteromeric assemblies **1b**$_3$•(BenCYA)$_n$((*R*)-MePheCYA)$_{6-n}$ (n = 1-5) (Figure 3.5). The ^{1}H NMR spectrum clearly shows the presence of numerous signals in the region of 15-14 ppm due to the formation of these heteromeric assemblies (Figure 3.5).[41] The presence of 1 to 5 chiral centers ((*R*)-MePhe) in these assemblies leads to the preferential formation of (*P*)-diastereomer. Thus, these assemblies exhibit a higher diastereomeric excess (*d.e.*) than the expected statistical 16% per chiral center in the absence of chiral amplification. This increase of the *d.e.* of the heteromeric assemblies is related to the introduction of a difference in the free energy between the (*P*)- and (*M*)-diastereomers by the chiral centers. Even assembly **1b**$_3$•(BenCYA)$_6$, which does not contain any chiral center, exists in the mixture mainly as the (*P*)-enantiomer due to the exchange process between BenCYA and (*R*)-MePheCYA and the chiral memory effect.[42,43]

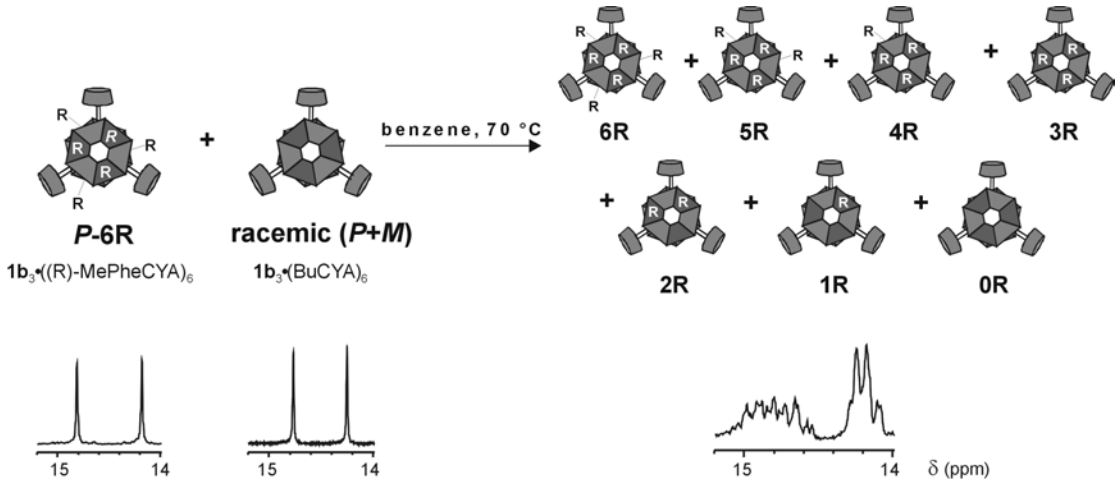

Figure 3.5. Schematic representation of the mixing process and formation of the heteromeric assemblies $\mathbf{1b}_3$•(BenCYA)$_n$((*R*)-MePheCYA)$_{6-n}$ (n = 1-5) from the homomeric assemblies $\mathbf{1b}_3$•((*R*)-MePheCYA)$_6$ (***P*-6R**, where R denotes the chiral group (*R*)-MePhe) and $\mathbf{1b}_3$•(BenCYA)$_6$ (racemic) (top) and part of their ^{1}H NMR spectra (bottom). The ^{1}H NMR spectrum of the mixture corresponds to a 1:1 mixture of $\mathbf{1b}_3$•((*R*)-MePheCYA)$_6$ and $\mathbf{1b}_3$•(BenCYA)$_6$ recorded 30 minutes after mixing. All spectra were recorded in benzene-d$_6$ at room temperature.

3.4.3. Thermodynamic model

The curve of amplification of chirality (Figure 3.4b) was fitted to a thermodynamic model based on the difference in free energy between the (*P*)- and (*M*)-diastereomers of the homo/heteromeric assemblies $\mathbf{1}_3$•(CYA)$_n$(*CYA)$_{6-n}$ (n= 0-6) at thermodynamic equilibrium. All the equilibria accounted in the model are depicted in Figure 3.6. The formation of the rosette is considered to take place in one step from the different building blocks. The influence of the dissociation rate constant is not included in the model, however, from previous studies it is well-known to affect the extent of chiral amplification.[31] Cooperativity is also not included in the model and therefore, ΔG^o is assumed to increase linearly with the number of chiral components present. Each chiral substituent present in the unfavorable (*M*)-diastereomer[44] induces a free energy difference $\Delta G^o_{M/P}$, which results in a decrease of the equilibrium constant (K) between the (*M*)-isomer and the free components with a factor of $f_m = e^{\frac{-\Delta G^o_{M/P}}{RT}}$. For example, for an assembly containing three chiral centers, the equilibrium constant is decreased by a factor of f_m^3. The equilibrium constant is assumed to be the same for every assembly. Statistical factors are included in the

model accounting for the statistically different possibilities of formation of each assembly. The model only takes the cyanurate components into account and not the calix[4]arene dimelamine moieties because the chirality in the assemblies is introduced by the chiral centers on the cyanurates. Thus, least square fit of the CD data for the system formed from $\mathbf{1b}_3$•(BenCYA)$_6$ and (*P*)-$\mathbf{1b}_3$•((*R*)-MePheCYA)$_6$ (Figure 3.4b) using the model resulted in $\Delta G^{o}_{M/P}$ (343 K) = 4.2 kJ mol^{-1} per chiral substituent. This corresponds to a total free energy difference ΔG^{o}_{tot} (343 K) = 25.2 kJ mol^{-1} between the favored (*P*)- and the unfavored (*M*)-diastereomers of assembly $\mathbf{1b}_3$•((*R*)-MePheCYA)$_6$ containing six chiral centers.

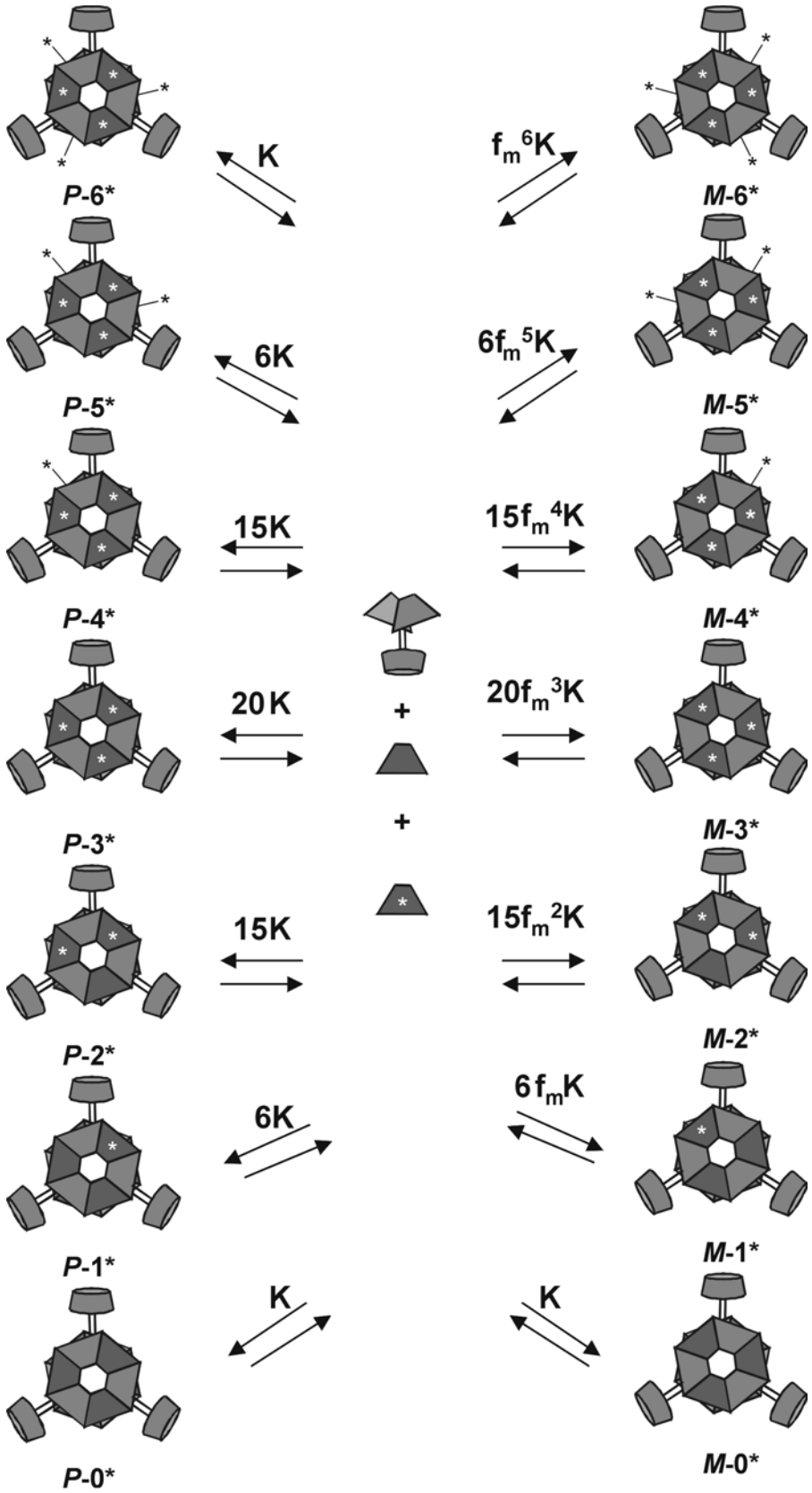

Figure 3.6. Thermodynamic model. Each chiral substituent in assemblies $\mathbf{1}_3$•$(CYA)_n(*CYA)_{6-n}$ (n= 0-6) lowers the equilibrium constant of the unfavored (*M*)-isomer by a factor $f_m = e^{\frac{-\Delta G^o_{M/P}}{RT}}$. (* denotes the chiral components of the assembly).

3.4.4. Influence of the calix[4]arene dimelamine substituents (R^1 and R^2) on the amplification of chirality

The extent of the chiral amplification using the thermodynamic model mentioned above was studied for a variety of systems in which the substituent R^1 (Figure 3.1) of the dimelamine becomes gradually bulkier. The influence of the substituent was studied using the systems comprising the dimelamines **1a**, **1d**, **1f**, **1g**, and **1h**, bearing butyl-, *i*-propyl-, hexyl-, *t*-butyl-, and benzyl-amino functionalities, respectively. (*R*)-MePheCYA was chosen as the chiral cyanurate and BenCYA as nonchiral cyanurate because both have the same chromophore (phenyl groups) ensuring the same maximum $\Delta\varepsilon_\lambda$ in all the assemblies.

Mixtures of assemblies (*P*)-**1x**$_3$•((*R*)-MePheCYA)$_6$ and **1x**$_3$•(BenCYA)$_6$ (**x= a, d, f-h)** in ratios varying between 90:10 and 10:90 were prepared and the CD intensity at 300 nm was measured as a function of time at 70 ^oC in benzene. After 30 minutes the $\Delta\varepsilon_{therm}$ is reached, and it is plotted versus the molar ratio of chiral assembly. In all the cases, the CD intensities are significantly higher than the sum of the CD intensities of the individual assemblies ('sergeants-and-soldiers' behavior). The results for these systems are summarized in Figure 3.7 and Table 3.1.

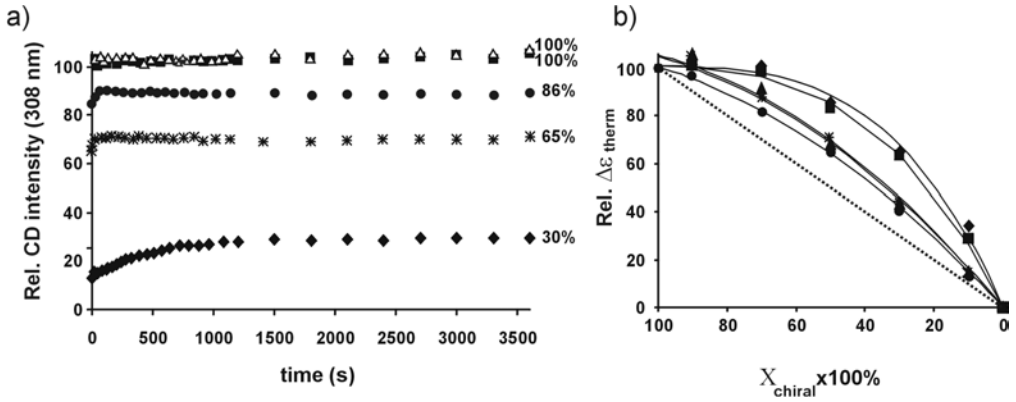

Figure 3.7. a) Plot of the relative CD-intensity measured at 300 nm versus the time for a mixture of (*P*)-**1a**$_3$•((*R*)-MePheCYA)$_6$ and **1a**$_3$•(BenCYA)$_6$ with different initial mole fractions of (*P*)-**1a**$_3$•((*R*)-MePheCYA)$_6$ (♦: 10%; *: 30%; ●: 50%; ■: 70%; Δ: 90%) (the % in the graphic represents the relative CD-intensity reached at the thermodynamic equilibrium). b) Plot of the relative CD-intensities at the thermodynamic equilibrium for different mole ratios of chiral component for different systems (**1a**: ♦; **1d**: ■; **1f**: ∗; **1g**: ▲; **1h**: ●). The solid lines represent the calculated best fit using the thermodynamic model. The dotted line represents the expected CD-intensity in absence of amplification of chirality.

Table 3.1: Difference in free energy between the (*P*)- and (*M*)-diastereomers of assemblies $\mathbf{1x}_3$•((*R*)-MePheCYA)$_6$ as a result of the presence of chiral centres in the assembly calculated using the thermodynamic model.[a]

1x	$\Delta G^o_{M/P}$ (kJ mol^{-1})[b]	ΔG^o_{tot} (kJ mol^{-1})[c]
1a	3.5	21.0
1d	3.0	18.0
1f	1.4	8.4
1g	1.4	8.4
1h	1.3	7.8

[a] [(*P*)-$\mathbf{1x}_3$•((*R*)-MePheCYA)$_6$] = [$\mathbf{1x}_3$•(BenCYA)$_6$] = 1.0 mM, 343 K, benzene. [b] Difference of free energy per chiral center. [c] Total free energy difference between (*P*)- and (*M*)-diastereomers of assemblies $\mathbf{1x}_3$•((*R*)-MePheCYA)$_6$.

Fitting the experimental data to the thermodynamic model gave the ΔG^o between the different diastereomers of the assemblies. The analysis of the data shows that increasing the size of the substituents of the melamine moieties results on a decrease of the difference in free energy between the (P)- and (M)-diastereomers ($\Delta G^o_{M/P}$), *e.g.* for a ratio 70:30 achiral:chiral assembly for the system formed with calix[4]dimelamine **1a** (R^1 = butyl), the thermodynamic relative CD-intensity increases to 65% (from the expected 30% without amplification), while for the system formed with calix[4]arene dimelamine **1h** (R^1 = benzyl), the thermodynamic value only increases to 44%. These values are related to a difference in the $\Delta G^o_{M/P}$, decreasing from 3.5 kJ mol^{-1} to 1.3 kJ mol^{-1} per chiral centre for the systems bearing butyl and benzyl substituents in the calix[4]arene dimelamine ring, respectively, which correspond to a ΔG^o_{tot} of 21.0 kJ mol^{-1} and 7.8 kJ mol^{-1} for assemblies (*P*)-$\mathbf{1a}_3$•((*R*)-MePheCYA)$_6$ and (*P*)-$\mathbf{1h}_3$•((*R*)-MePheCYA)$_6$ containing each 6 chiral substituents.

Upon introduction of bulky substituents on the calix[4]arene dimelamine building block an increase of $\Delta G^o_{M/P}$, and therefore an enhanced amplification of chirality (smaller ratio of chiral assembly needed to obtain 100% of relative CD-intensity in mixtures achiral:chiral assemblies) was expected. The observed decrease in the $\Delta G^o_{M/P}$ when bulky substituents are present in the assembly might come from a decrease of the thermodynamic stability of the system.[45] To prove this hypothesis, ^{1}H NMR studies of the mixtures after the amplification experiments were performed. The

study for the systems (*P*)-**1f**$_3$•((*R*)-MePheCYA)$_6$/**1f**$_3$•(BenCYA)$_6$ (**1f** = hexyl substituents) and (*P*)-**1g**$_3$•((*R*)-MePheCYA)$_6$/**1g**$_3$•(BenCYA)$_6$ (**1g** = *t*-butyl substituents) showed that after the mixing, the rosettes in the mixture are not formed for 100%, as it can be deduced by integration of the CH_2- bridged proton resonances of the calix moiety and the hydrogen-bonded NH-proton resonances of the cyanurates. One possible explanation for the thermodynamic destabilization can be extracted from the molecular modelling studies (Quanta 97, CHARMm 24.0). The introduction of steric hindrance in the dimelamine moiety induces a twist of the two melamine fragments, and therefore a decrease of the planarity of the rosette *floors*. This will result in a weaker hydrogen-bond array and a decrease of the stability of the assemblies (Figure 3.8).

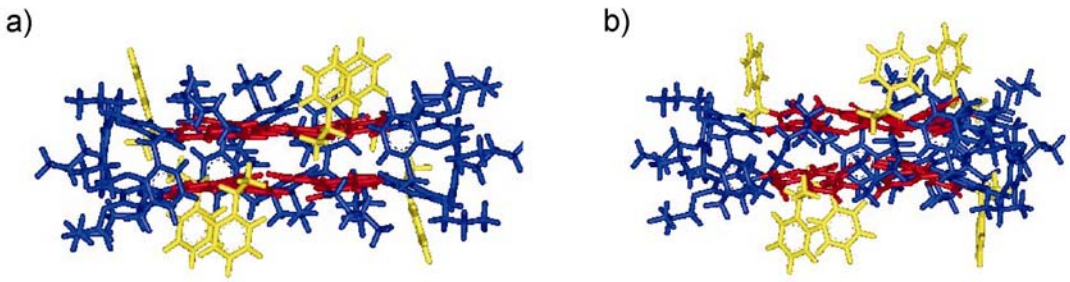

Figure 3.8. Gas-phase minimized structures of assemblies a) **1a**$_3$•(*R*)-MePheCYA$_6$ and b) **1g**$_3$•(*R*)-MePheCYA$_6$ bearing butyl and t-butyl chains in the dimelamine moiety, respectively. The calix[4]arene moieties are depicted in blue, the rosette motifs in red and the (*R*)-MePhe chiral groups of the cyanurate compounds in yellow.

The effect on the amplification of chirality upon the introduction of substituents in the calix[4]arene skeleton (R^2, Chart 3.1) was also studied. For this purpose, calix[4]arene dimelamines substituted with butyl groups in the melamine rings and different substitutions (R^2) (hydrogen (**1a**), nitro (**1b**), and bromide (**1c**) groups) in the calix[4]arene skeleton were synthesized. Mixtures of assemblies (*P*)-**1x**$_3$•((*R*)-MePheCYA)$_6$ and **1x**$_3$•(BenCYA)$_6$ (**x = a-c)** in ratios varying between 90:10 and 10:90 (nonchiral:chiral rosette assemblies) were prepared and the CD intensity at 308 nm was measured as a function of time at 70 ^oC in benzene (Figure 3.9a). The $\Delta\varepsilon_{therm}$ reached after 30 minutes was plotted versus the mole ratio of chiral component (Figure 3.9a). Also for these systems the CD-intensities deviate from linearity, showing the typical 'sergeants-and-soldiers' behavior (Figure 3.9b).

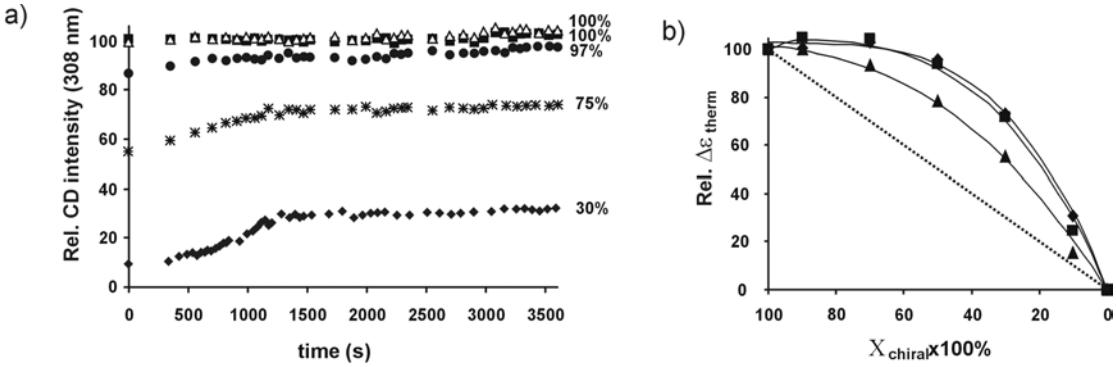

Figure 3.9. a) Plot of the Rel. CD intensity (at 308 nm) against the time for a mixture of (*P*)-**1b**$_3$•((*R*)-MePheCYA)$_6$ and **1b**$_3$•(BenCYA)$_6$ with different initial mole fractions of **1b**$_3$•((*R*)-MePheCYA)$_6$ (♦: 10%, *: 30%, ●: 50%, ■: 70%, Δ: 90%) (the % in the graphic represents the relative CD-intensity reached at the thermodynamic equilibrium). b) Plot of the relative CD-intensities at the thermodynamic equilibrium for different mole ratios of chiral component (**1a**: ■, **1b**: ♦, **1c**: ▲). The solid lines represent the calculated best fit using the thermodynamic model previously described. The dotted line represents the expected CD-intensity in absence of amplification of chirality.

The data (Figure 3.9 and Table 3.2) clearly show that the introduction of groups in the calix[4]arene skeleton has a great influence on the amplification of chirality for these systems. The presence of the nitro substituents ($R^2 = NO_2$) on the calix[4]arene skeleton (**1b**) increases the value of $\Delta G^o_{M/P}$ compared with the one lacking substituents in this position (4.2 kJ mol^{-1} and 3.5 kJ mol^{-1} respectively), while the presence of the bromide substituents induces a decrease of $\Delta G^o_{M/P}$ to 2.0 kJ mol^{-1}. The cause of these large differences is not clear but the big influence exerted by these functional groups could be due to either steric (bulkiness of the groups) and/or electronic factors (electrostatic repulsion/attraction) introduced by the substituents in the calix[4]arene skeleton. These factors could influence the conformation of the calix[4]arene skeleton and the strength of the hydrogen bonds and, consequently the planarity and stability of the rosettes. The introduction of the nitro substituents in the calix[4]arene skeleton (**1b**) slows down the kinetics of the process compared to the introduction of the bromo substituents (**1c**).[44,46] This can be seen by looking at the time before the amplification of chirality starts.

Table 3.2: Difference in free energy calculated using the thermodynamic model between the (*P*)- and (*M*)-diastereomers of assemblies $\mathbf{1x}_3$•((*R*)-MePheCYA)$_6$ as a result of the presence of chiral centres in the assembly.[a]

1x	$\Delta G^o_{M/P}$ (kJ mol^{-1})[b]	ΔG^o_{tot} (kJ mol^{-1})[c]
1a	3.5	21.0
1b	4.3	25.8
1c	2.0	12.0

[a] [(*P*)-$\mathbf{1x}_3$•((*R*)-MePheCYA)$_6$] = [$\mathbf{1x}_3$•(BenCYA)$_6$] = 1.0 mM, 343 K, benzene. [b] Difference of free energy per chiral center. [c] Total free energy difference between (*P*)- and (*M*)-diastereomers of assemblies $\mathbf{1x}_3$•((*R*)-MePheCYA)$_6$.

The presence of nitro groups in the calix[4]arene skeleton has a large effect on the extent of the amplification of chirality in these dynamic assemblies, leading to systems displaying a large amplification of chirality. For this reason, the influence of the substituent in the dimelamine moiety (R^1) was investigated when the nitro group is present in the calix[4]arene skeleton (R^2 =NO_2). For this purpose, the assemblies formed with the dimelamines **1b** and **1e** bearing butyl and *i*-propyl substituents, respectively and nitro substituents in the calix[4]arene skeleton, and the cyanurates (*R*)-MePheCYA and BenCYA were studied. The results obtained are displayed in Table 3.3.

Table 3.3: Differences in free energy calculated using the thermodynamic model between the (*P*)- and (*M*)-diastereomers of assemblies $\mathbf{1x}_3$•((*R*)-MePheCYA)$_6$.[a]

1x	$\Delta G_{M/P}$ (KJ mol^{-1}) [b]	ΔG_{tot} (KJ mol^{-1}) [c]
1b	4.3	25.8
1e	4.2	25.2

[a] [(*P*)-$\mathbf{1x}_3$•((*R*)-MePheCYA)$_6$] = [$\mathbf{1x}_3$•(BenCYA)$_6$] = 1.0 mM, at 343 K, benzene. [b] Difference of free energy per chiral center. [c] Total free energy difference between (*P*)- and (*M*)-diastereomers of assemblies $\mathbf{1x}_3$•((*R*)-MePheCYA)$_6$.

Surprisingly the presence of sterically demanding substituents in the dimelamine rings of **1e** (*i*-propyl groups) does not influence the degree of amplification of the system when the nitro substituents are present in the calix[4]arene skeleton. The $\Delta G^o_{M/P}$ for **1e** only decreases by 0.1 kJ mol^{-1} when compared with the melamine **1b** (butyl groups). When the substituents are hydrogens instead of nitro

groups the introduction of *i*-propyl groups (**1d**) induces a decrease of the $\Delta G = 0.5$ kJ mol^{-1} when compared with calix[4]arene dimelamines containing butyl groups (**1a**) (see table 3.1). As it was explained above, the presence of the nitro groups in the calix[4]arene skeleton slows down the exchange of the dimelamine moieties (see figure 3.9a). As shown before,[31] this decrease of the dissociation rate constant results in an increase of the chiral amplification.

3.4.5. Influence of the cyanurate substituent (X) on the amplification of chirality

The amplification of chirality was also studied for systems with different chiral cyanurates (*CYA = (*R*)-MePropCYA, (*R)*-MePheCYA, (*L*)-PhealaCYA, and (*L*)-ValCYA), in which the N-substituent gradually increases in size. All these cyanurates have the chiral center in the α-position relative to the nitrogen. Furthermore, the amplification of chirality with (*S*)-2-MeBuCYA with the chiral center in β-position was also studied.

Mixtures of assemblies (*P*)-**1a**$_3$•(*CYA)$_6$ and **1a**$_3$•(CYA)$_6$ (*CYA = (*R*)-MePropCYA,[47] (*R*)-MePheCYA, (*L*)-PhealaCYA, and (*L*)-ValCYA; CYA = BenCYA and BuCYA**)** in ratios varying between 90:10 and 10:90 were prepared and the CD intensity at 300 nm was measured as a function of time at 70 ^{o}C in benzene. Immediately the $\Delta\varepsilon_{therm}$ was reached, and it was plotted versus the molar ratio of chiral assembly (Table 3.4 and Figure 3.10).

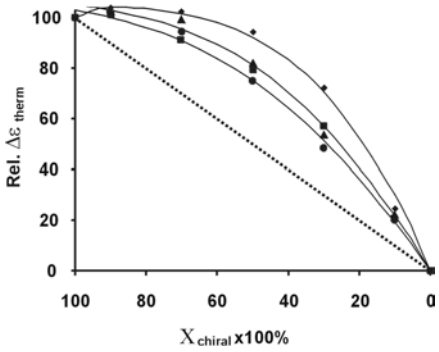

Figure 3.10. Plot of the relative CD-intensities at the thermodynamic equilibrium for different mole ratios of chiral component (*P*)-**1a**$_3$•(*CYA)$_6$ for systems formed with (*P*)-**1a**$_3$•(*CYA)$_6$ and **1a**$_3$•(CYA)$_6$ (♦: (*R*)-MePheCYA/BenCYA; ●: (*R*)-MePropCYA/BuCYA; ■: (*L*)-PhealaCYA/BenCYA; ▲: (*L*)-ValCYA/BuCYA). The solid lines represent the calculated best fit using the thermodynamic model described above. The dotted line represents the expected CD-intensity in absence of amplification of chirality.

As it can be deduced from the data and contrary to what happens with the substitution in the calix[4]arene dimelamine building blocks, the introduction of substituents in the cyanurate component which are less sterically demanding decreases the difference in free energy between the (*P*)- and (*M*)-diastereomers. For example, the difference in the free energy introduced by one chiral center for (*R*)-MePheCYA is 3.5 kJ mol^{-1}, while this difference drops to 1.9 kJ mol^{-1} with the less bulky cyanurate (*R*)-MePropCYA. The introduction of bulky amino acids as chiral residues in cyanurates (*L*)-PhealaCYA and (*L*)-ValCYA also decreases the degree of the chiral amplification. For all these systems, the decrease of the chiral amplification might come from the decrease on the rigidity of the assemblies.

Table 3.4: Differences in free energy calculated between the (*P*)- and (*M*)-diastereomers of assemblies **1a**$_3$•(*CYA)$_6$ as a result of the presence of chiral centres in the assembly.[a]

*CYA	$\Delta G^o_{M/P}$ (KJ mol^{-1}) [b]	ΔG^o_{tot} (KJ mol^{-1}) [c]
(*R*)-MePheCYA	3.5	21.0
(*L*)-PhealaCYA	2.3	13.8
(*L*)-ValCYA	2.3	13.8
(*R*)-MePropCYA	1.9	11.4
(*S*)-2-MeBuCYA	-	-

[a] [(*P*)-**1a**$_3$•(*CYA)$_6$] = [**1a**$_3$•(CYA)$_6$] = 1.0 mM, 343 K, benzene. [b] Difference of free energy per chiral center. [c] Total free energy difference between (*P*)- and (*M*)-diastereomers of assemblies **1a**$_3$•(*CYA)$_6$.

The amplification of chirality in systems in which the chirality center is further away from the core of the assembly was also studied. For that purpose, the cyanurate ((*S*)-2-MeBuCYA) in which the chiral center is in the β-position with respect to the nitrogen atom was synthesized. However, the ^{1}H NMR spectrum of the assembly **1a**$_3$•((*S*)-2-MeBuCYA)$_6$ exhibits two sets of two sharp signals with different intensity in the region where the hydrogen-bonded NH-protons of the cyanurate are expected (δ = 15-13 ppm) (Figure 3.11). The unequal intensity of the signals rules out the possible presence of an isomer with C_{3h}-symmetry.[48] Therefore, these signals can only be explained by the presence of both (*M*)- and (*P*)-diastereomers. Consequently, the system formed with this cyanurate is not suitable to carry out the experiments of amplification of chirality because of the lack of total diastereomeric induction.

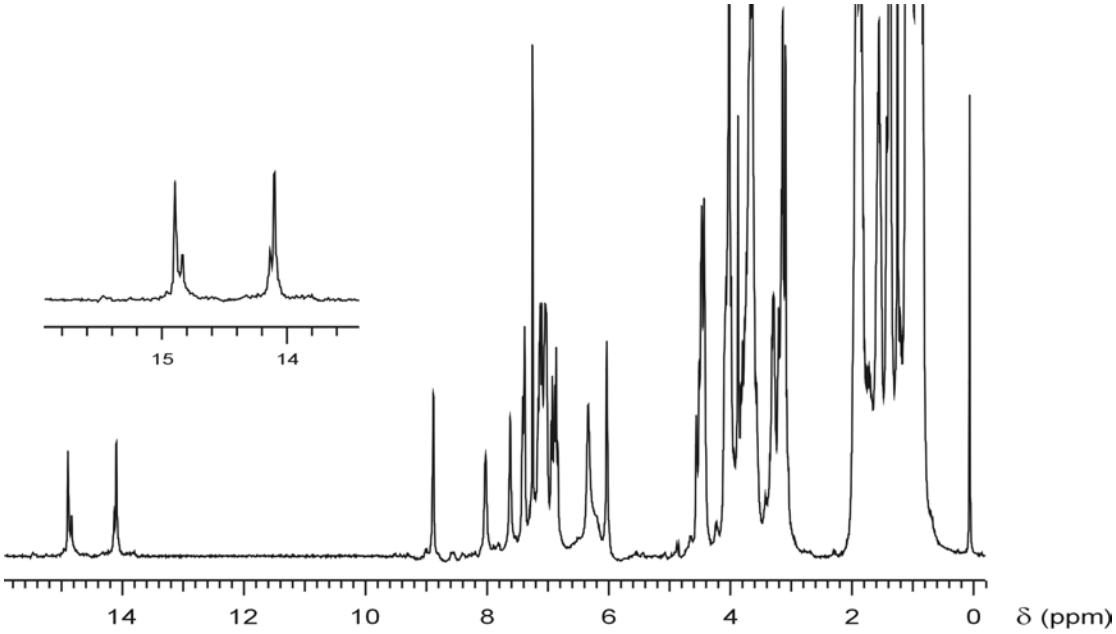

Figure 3.11. ^{1}H NMR spectrum **1a**$_3$•((*S*)-2-MeBuCYA)$_6$ (1.0 mM). The inset shows the presence of the two different sets of signals of different intensity in the region δ = 15-13 ppm. The spectrum was recorded in benzene-d_6 at 298 K.

3.5. Conclusions

The experiments and the thermodynamic model presented in this chapter provide a new insight in the amplification of chirality in hydrogen-bonded assemblies. It has been shown that the amplification of chirality in these noncovalent assemblies can be modulated via the introduction of different substituents in the building blocks, i.e. calix[4]arene dimelamines or cyanurate derivatives. The introduction of sterically demanding substituents in the melamine moieties (R^1 substituents) decreases the amplification of chirality. Furthermore, the amplification of chirality is highly influenced by the presence of functional groups directly attached to the calix[4]arene skeleton (R^2 substituents). This influence might be due to the geometric constrains induced by these substituents in the assembly and/or electronic factors. Contrary, the presence of bulky substituents in the cyanurate components leads to a large free energy difference (ΔG^o) between the diastereomers, and, therefore, to a large amplification of chirality. The introduction of nitro substituents in the calix[4]arene skeleton seems to influence the chiral amplification in the hydrogen-bonded assemblies the most, probably due to a decrease in the kinetics of the mixing process,

leading to systems with a higher degree of chiral amplification. Therefore, in the next chapter, the study of assemblies with a lower rate of dissociation of the dimelamine component of the assembly (a slow mixing process) will be discussed. The rate decrease could also be achieved by increasing the number of the hydrogen bonds that held the components together. The candidates for this purpose are the tetrarosette assemblies in which the components are held together via the formation of 72 cooperative hydrogen bonds.

3.6. Experimental section

THF was freshly distilled from Na/benzophenone, and CH_2Cl_2 from $CaCl_2$. All chemicals were of reagent grade and used without further purification. NMR spectra were recorded on a Varian Unity 300 (^{1}H NMR 300 MHz) using tetramethylsilane (TMS) or the corresponding residual solvent signal as internal standard. FAB-MS spectra were recorded on a Finningan MAT 90 spectrometer with *m*-nitrobenzyl alcohol (NBA) as a matrix. CD spectra were recorded on a JASCO J-715 spectropolarimeter. Flash column chromatography was performed using silica gel (SiO_2, E. Merck, 0.040-0.063 mm, 230-400 mesh)

Synthesis. The synthese of compounds **1a-1c**, **1h-1j**, BuCYA, BenCYA, (*R*)-MePheCYA, (*L*)-PhealaCYA, and (*L*)-ValCYA have been reported previously.[33,36]

General procedure for the synthesis of calix[4]arene dimelamines 1d, 1f, 1g and 1e.

A solution of bis(chlorotriazine) **1i/1j (1i** for **1d**, **1f** and **1g**; **1j** for **1e**), diisopropylethylamine (12 equiv.) and the corresponding amine (36 equiv.) in THF was refluxed for 1 week. The mixture was evaporated to dryness. The residue was dissolved in CH_2Cl_2, washed with water and brine, and the organic layer dried over Na_2SO_4. Evaporation of the organic solvent gave the corresponding calix[4]arene dimelamine **1** as a crude product, which was purified by column chromatography (SiO_2, CH_2Cl_2/MeOH/NH_4OH = 90/9.5/0.5%).

5,17-N,N'-Bis[4-amino-6-(2-methylethylamino)-1,3,5-triazin-2yl]diamino-25,26,27,28-tetrapropoxycalix[4]arene (1d). Compound **1d** was prepared from calix[4]arene bis(chlorotriazine) **1i** (0.15 g, 0.16 mmol) and *i*-propylamine (0.5 ml) and was obtained as a white solid (74%). R_f = 0.5 (CH_2Cl_2/MeOH/NH_4OH 90:9:1); ^{1}H NMR (300 MHz, DMSO-d_6) δ 6.9-6.7 (br m, 6 H, Ar*H*), 6.6-6-2 (br m, 8H, *o*-N*H*ArH + N*H* + NHAr*H*), 5.0-4.8 (br m, 4H, NH_2), 4.43, 3.10 (ABq, 8 H, ^{2}J(H,H) = 13.5 Hz, ArCH_2Ar), 4.01 (q, 2 H, ^{3}J(H,H) = 6.6 Hz, NHC*H*$(CH_3)_2$), 3.93 (t, 4H, ^{3}J(H,H) = 6.6 Hz, OCH_2), 3.68 (t, 4 H, ^{3}J(H,H) = 6.6 Hz, OCH_2), 2.0-1.8 (m, 8H, OCH_2CH_2), 1.15 (d, 12 H, ^{3}J(H,H) = 6.6 Hz, NHCH(CH_3)$_2$), 1.03 (t, 6H, ^{3}J(H,H) = 7.5 Hz, O$(CH_2)_2CH_3$), 1.0-0.8 (t, 6H, ^{3}J(H,H) = 7.5 Hz, O$(CH_2)_2CH_3$). MS (FAB): m/z = 925.5 (100) ([M+H$^+$], calcd 925.5). $C_{52}H_{68}N_{12}O_4$: calcd C 67.51, N 18.17, H 7.41; found: C 67.33, N 18.02, H 7.46.

5,17-N,N'-Bis[4-amino-6-(2-methylethylamino)-1,3,5-triazin-2yl]diamino-11,23-dinitro-25,26,27,28-tetrapropoxycalix[4]arene (1e). Compound **1e** was prepared from calix[4]arene bis(chlorotriazine) **1j** (0.10 g, 0.10 mmol) and *i*-propylamine (0.3 ml) and was obtained as a white solid (65%). R_f = 0.5 (CH_2Cl_2/MeOH/NH_4OH 90:9:1); ^{1}H NMR (300 MHz, DMSO-d_6) δ 7.7 (br s, 4H, *o*-NO_2Ar*H*), 6.7-6.2 (m, 8H, *o*-N*H*ArH + N*H* + NHAr*H*), 5.0-4.9 (m, 4H, NH_2), 4.35, 3.18 (ABq, 8H, 2J(H,H) = 13.0 Hz, ArCH_2Ar), 3.98 (q, 2 H, ^{3}J(H,H) = 6.6 Hz, NHC*H*$(CH_3)_2$), 3.95 (t, 4H, ^{3}J(H,H) = 6.6 Hz, OCH_2), 3.72 (t, 4 H, ^{3}J(H,H) = 6.6 Hz, OCH_2), 2.0-1.8 (m, 8H, OCH_2CH_2), 1.15 (d, 12 H, ^{3}J(H,H) = 6.6 Hz, NHCH(CH_3)$_2$), 1.03 (t, 6H, ^{3}J(H,H) = 7.5 Hz, O$(CH_2)_2CH_3$), 1.0-0.8 (t, 6H, ^{3}J(H,H) = 7.5 Hz, O$(CH_2)_2CH_3$). MS (FAB): m/z = 1015.3 (100) ([M+H$^+$], calcd 1015.5). $C_{52}H_{66}N_{14}O_8$: calcd C 61.52, N 19.32, H 6.55; found: C 61.33, N 19.24, H 6.51.

5,17-N,N'-Bis[4-amino-6-(hexylamino)-1,3,5-triazin-2yl]diamino-25,26,27,28-tetrapropoxycalix[4]arene (1f). Compound **1f** was prepared from calix[4]arene bis(chlorotriazine) **1i** (0.11 g, 0.12 mmol) and hexylamine (1.0 ml) and was obtained as a white solid (65%). R_f = 0.6 (CH_2Cl_2/MeOH/NH_4OH 90:9:1); ^{1}H NMR (300 MHz, DMSO-d_6) δ 7.0–6.7 (br m, 6H, Ar*H*), 6.6-6.2 (br m, 8H, *o*-N*H*ArH + N*H* + NHAr*H*), 4.43, 3.10 (ABq, 8 H, ^{2}J(H,H) = 13.5 Hz, ArCH_2Ar), 3.93 (t, 4H, ^{3}J(H,H) = 6.6 Hz, OCH_2), 3.68 (t, 4 H, ^{3}J(H,H) = 6.6 Hz, OCH_2), 3.31 (q, 4 H, ^{3}J(H,H) = 6.3 Hz,

NHCH_2) 2.0-1.8 (m, 8H, OCH_2CH_2), 1.9 (m, 8H, $NHCH_2CH_2CH_2(CH_2)_2CH_3$), 1.6-1.3 (m, 8H, $NHCH_2CH_2CH_2(CH_2)_2CH_3$) 1.15 (t, 6 H, ^{3}J(H,H) = 7.4 Hz, $O(CH_2)_2CH_3$), 1.0-0.8 (m, 12H, $NH(CH_2)_5CH_3$ + $O(CH_2)_2CH_3$). MS (FAB): m/z = 1009.7 (100) ([M+H$^+$], calcd 1009.2). $C_{58}H_{80}N_{12}O_4$: calcd C 68.89, N 16.58, H 8.01; found: C 68.53, N 16.42, H 8.46.

5,17-N,N'-Bis[4-amino-6-(2,2-dimethylethylamino)-1,3,5-triazin-2yl]diamino-25,26,27,28-tetrapropoxycalix[4]arene (1g). Compound **1g** was prepared from calix[4]arene bis(chlorotriazine) **1i** (0.15 g, 0.16 mmol) and *t*-butylamine (0.6 ml) and was obtained as a white solid (76%). R_f = 0.6 (CH_2Cl_2/MeOH/NH_4OH 90:9:1); ^{1}H NMR (300 MHz, DMSO-d_6) δ 7.4–7.1 (br m, 6H, Ar*H*), 6.6-6.2 (br m, 8H, *o*-N*H*ArH + N*H* + NHAr*H*), 4.35, 3. 05 (ABq, 8 H, ^{2}J(H,H) = 13.5 Hz, $ArCH_2Ar$), 3.86 (t, 4H, ^{3}J(H,H) = 6.6 Hz, OCH_2), 3.62 (t, 4 H, ^{3}J(H,H) = 6.6 Hz, OCH_2), 2.0-1.8 (m, 8H, OCH_2CH_2), 1.58 (s, 18H, $NC(CH_3)_3$), 1.15 (t, 6 H, ^{3}J(H,H) = 7.4 Hz, $O(CH_2)_2CH_3$), 1.0-0.8 (m, 6H, $O(CH_2)_2CH_3$). MS (FAB): m/z = 953.6 (100) ([M+H$^+$], calcd 953.5). $C_{54}H_{72}N_{12}O_4$: calcd C 68.04, N 17.63, H 7.61; found: C 67.89, N 17.88, H 7.69.

General procedure for the synthesis of the cyanurates (*R*)-MePropCYA and (*S*)-2-MeBuCYA.[49]

The reaction is performed under flame-dried conditions and a continuous flow of argon. The argon was led through water in order to trap formed phosgene before leaving the reaction system. The corresponding amine was suspended in THF and N-chlorocarbonylisocyanate (2 equiv.) was added slowly. After stirring at room temperature for 2 hours, the reaction mixture was refluxed for 2 days. After evaporation of the solvent, the residue was redissolved in CH_2Cl_2, washed with water, dried over Na_2SO_4 and purified by column chromatography (SiO_2, CH_2Cl_2/MeOH/NH_4OH : 90/9.5/0.5).

N-((*R*)-1-methylpropyl)-1,3,5-triazine-2,4,6(1H, 3H, 5H)-trione (= (*R*)-MePropCYA). Compound (*R*)-MePropCYA was prepared from (*R*)-sec-butylamine (0.5 ml, 5 mmol) and N-chlorocarbonylisocyanate (0.8 ml, 10 mmol) and was obtained as a white solid (34%). R_f = 0.4 (CH_2Cl_2/MeOH/NH_4OH 90:9:1); ^{1}H NMR (300 MHz, DMSO-d_6) δ 11.32 (s, 2H, N*H*), 4.44-4.58 (m, 1H, N*C*H), 1.82-1.99 (m,

1H, C*H*$_2$CH$_3$), 1.57-1.73 (m, 1H, C*H*$_2$CH$_3$), 1.31 (d, 3H, 3J (H,H) = 7.0 Hz, *CHC*H*$_3$), 0.79 (m, 3H, CH$_2$C*H*$_3$). MS (FAB): m/z = 184.0 (100) ([M-H$^+$], calcd 184.1). $C_7H_{11}N_3O_3$: calcd C 45.40, N 22.69, H 5.99; found: C 45.66, N 22.49, H 5.78.

N-((*S*)-2-methylbutyl)-1,3,5-triazine-2,4,6(1H, 3H, 5H)-trione (= (*S*)-2-MeBuCYA). Compound (*S*)-2-MeBuCYA was prepared from (*S*)-2-methylbutylamine (0.6 ml, 5 mmol) and N-chlorocarbonylisocyanate (0.8 ml, 10 mmol) and was obtained as a white solid (20%). R_f = 0.4 (CH_2Cl_2/MeOH/NH_4OH 90:9:1); ^{1}H NMR (300 MHz, DMSO-*d*$_6$) δ 11.38 (s, 2H, N*H*), 3.53 (m, 2H, ^{3}J (H,H) = 5.4 Hz, NC*H*$_2$), 1.74 (d, 2H, ^{3}J (H,H) = 5.4 Hz, CHC*H*$_3$), 1.32 (m, 1H, NCH$_2$CHCH$_3$CH*H*), 1.08 (m, 1H, NCH$_2$CHCH$_3$C*H*H), 0.80 (m, 3H, CH$_2$C*H*$_3$). ^{13}C NMR (75 MHz, DMSO-*d*$_6$), d 150.1, 45.8, 32.6, 26.3, 16.4, 10.9. MS (FAB): m/z = 200.1 (100) ([M+H$^+$], calcd 200.1). $C_8H_{13}N_3O_3$: calcd C 48.23, N 21.09, H 6.58; found: C 48.29, N 21.00, H 6.65.

Assembly formation. Assemblies were formed by dissolving the calix[4]arene dimelamines **1** and the corresponding cyanurate (CYA/*CYA) in a 1:2 molar ratio in THF, after which the solvent was evaporated under high vacuum. After being dried under high vacuum, the assemblies were ready for use.

CD titration studies. Assembly solution (1.0 mM) of the homomeric assemblies were mixed in ratios 90:10 to 10:90 at room temperature and injected into a thermostated cell (0.01 cm width) immediately after mixing. The CD intensities were monitored in time at constant temperature. The resulting plots were treated as described in the text.

Thermodynamic model. The model was implemented in MicroMath® Scientist® for Windows, Version 2.01. Text file of the model is provided in the appendix.

Molecular mechanics calculations. Initial structures, created by manual modification of the X-ray structure of a double rosette assembly,[33] and by observed NOE connectivities used as distance constraints, as well as visualizations were carried

out with Quanta 97.[50] The MD calculations were run with CHARMm, version 24.0.[51] Parameters were taken from Quanta 97, and point charges were assigned with the charge template option in Quanta/CHARMm; excess charge was smoothened, rendering overall neutral residues. A distance-dependent dielectric constant was applied with $\varepsilon = 1$. No cut-offs on the nonbonded interactions were used. Energy-minimized were performed with the Steepest Descent and Adopted Basis Newton-Raphson methods until the root mean square of the energy gradient was <0.001 kcal mol^{-1} $Å^{-1}$.

3.7. References and Notes

[1] Feringa, B. L.; van Delden, R. A. *Angew. Chem. Int. Ed.* **1999**, *38*, 3418-3438.

[2] Shibata, T.; Yamamoto, J.; Matsumoto, N.; Yonekubo, S.; Onsanai, S.; Soai, K. *J. Am. Chem. Soc.* **1998**, *120*, 12157-12158.

[3] Sato, T.; Urabe, H.; Ishiguro, S.; Shibata, T.; Soai, K. *Angew. Chem. Int. Ed.* **2003**, *42*, 315-317.

[4] Kitamura, M.; Suga, S.; Oka, H.; Noyori, R. *J. Am. Chem. Soc.* **1998**, *120*, 9800-9809.

[5] Girard, C.; Kagan, H. *Angew. Chem. Int. Ed. Engl.* **1998**, *37*, 2952-2959.

[6] Green, M. M.; Rediy, M. P.; Johnson, R. J.; Darling, G.; O'Leary, D. J.; Wilson, G. J. *J. Am. Chem. Soc.* **1989**, *111*, 6452-6454.

[7] Green, M. M.; Peterson, N. C.; Sato, T.; Teramoto, A.; Cook, R.; Lifson, S. *Science* **1995**, *268*, 1860-1866.

[8] Green, M. M.; Park, J.-W.; Sato, T.; Teramoto, A.; Lifson, S.; Selinger, R. L.; Selinger, J. W. *Angew. Chem. Int. Ed.* **1999**, *38*, 3138-3154.

[9] Green, M. M.; Cheon, K.-S.; Yang, S.-Y.; Park, J.-W.; Swansburg, S.; Liu, W. *Acc. Chem. Res.* **2001**, *34*, 672-680.

[10] Palmans, A. R. A.; Vekemans, J. A. J. M.; Havinga, E. E.; Meijer, E. W. *Angew. Chem. Int. Ed. Engl.* **1997**, *36*, 2648-2651.

[11] Brunsveld, L.; Schenning, A. P. H. J.; Broeren, M. A. C.; Janssen, H. M.; Vekemans, J. A. J. M.; Meijer, E. W. *Chem. Lett.* **2000**, 292-293.

[12] Brunsveld, L.; Lohmeijer, B. G. G.; Vekemans, J. A. J. M.; Meijer, E. W. *Chem. Commun.* **2000**, 2305-2306.

[13] Schenning, A. P. H. J.; Jonkheijm, P.; Peeters, E.; Meijer, E. W. *J. Am. Chem. Soc.* **2001**, *123*, 409-416.

[14] Brunsveld, L.; Meijer, E. W.; Prince, R. B.; Moore, J. S. *J. Am. Chem. Soc.* **2001**, *123*, 7978-7984.

[15] Masuda, M.; Jonkheijm, P.; Sijbesma, R. P.; Meijer, E. W. *J. Am. Chem. Soc.* **2003**, *125*, 15935-15940.

[16] van Gestel, J.; van der Schoot, P.; Michels, M. A. J. *Macromolecules* **2003**, *36*, 6668-6673.

[17] Teramoto, A. *Prog. Polym. Sci.* **2001**, *26*, 667-720.

[18] Selinger, J. V.; Selinger, R. L. B. *Phys. Rev. E* **1997**, *55*, 1728-1731.

[19] Gu, H.; Sato, T.; Teramoto, A.; Varichon, L.; Green, M. M. *Polym. J.* **1997**, *29*, 77-84.

[20] Lifson, S.; Andreola, C.; Peterson, N. C.; Green, M. M. *J. Am. Chem. Soc.* **1989**, *111*, 8850-8858.

[21] Saxena, A.; Guo, G.; Fujiki, M.; Yang, Y.; Ohira, A.; Okoshi, K.; Naito, M. *Macromolecules* **2004**, *37*, 3081-3082.

[22] Yashima, E.; Matsushima, T.; Okamoto, Y. *J. Am. Chem. Soc.* **1997**, *119*, 6345-6359.

[23] Yashima, E.; Maeda, K.; Nishimura, T. *Chem. Eur. J.* **2004**, *10*, 42-51.

[24] Ishi-i, T.; Crego-Calama, M.; Timmerman, P.; Reinhoudt, D. N.; Shinkai, S. *J. Am. Chem. Soc.* **2002**, *124*, 14631-14641.

[25] Fenniri, H.; Deng, B.-L.; Ribbe, A. E. *J. Am. Chem. Soc.* **2002**, *124*, 11064-11072.

[26] Mizuno, Y.; Aida, T. *Chem. Commun.* **2003**, 20-21.

[27] Oda, M.; Nothofer, H.-G.; Lieser, G.; Schref, U.; Meskers, S. C. J.; Neher, D. *Adv. Mater.* **2000**, *12*, 362-365.

[28] Link, D. R.; Natale, G.; Saho, R.; Maclennan, J. E.; Clark, N. A.; Körblova, E.; Walba, D. M. *Science* **1997**, *278*, 1924-1927.

[29] Trzaska, S. T.; Hsu, H.-F.; Swager, T. M. *J. Am. Chem. Soc.* **1999**, *121*, 4518-4519.

[30] Barberá, J.; Cavero, E.; Lehmann, M.; Serrano, J.-L.; Sierra, T.; Vázquez, J. T. *J. Am. Chem. Soc.* **2003**, *125*, 4527-4533.

[31] Prins, L. J.; Timmerman, P.; Reinhoudt, D. N. *J. Am. Chem. Soc.* **2001**, *123*, 10153-10163.

[32] Vreekamp, R. H.; van Duynhoven, J. P. M.; Hubert, M.; Verboom, W.; Reinhoudt, D. N. *Angew. Chem. Int. Ed. Engl.* **1996**, *35*, 1215-1218.

[33] Timmerman, P.; Vreekamp, R. H.; Hulst, R.; Verboom, W.; Reinhoudt, D. N.; Rissanen, K.; Udachin, K. A.; Ripmeester, J. *Chem. Eur. J.* **1997**, *3*, 1823-1832.

[34] Prins, L. J.; Jolliffe, K. A.; Hulst, R.; Timmerman, P.; Reinhoudt, D. N. *J. Am. Chem. Soc.* **2000**, *122*, 3617-3627.

[35] Prins, L. J.; Huskens, J.; de Jong, F.; Timmerman, P.; Reinhoudt, D. N. *Nature* **1999**, *398*, 498-502.

[36] Prins, L. J.; Hulst, R.; Timmerman, P.; Reinhoudt, D. N. *Chem. Eur. J.* **2002**, *8*, 2288-2301.

[37] Jolliffe, K.; Crego-Calama, M.; Fokkens, R.; Nibbering, N. M. M.; Timmerman, P.; Reinhoudt, D. N. *Angew. Chem. Int. Ed.* **1998**, *37*, 1247-1251.

[38] Timmerman, P.; Jolliffe, K. A.; Crego-Calama, M.; Weidmann, J.-L.; Prins, L. J.; Cardullo, F.; Snellink-Ruël, B. H. M.; Fokkens, R.; Nibbering, N. M. M.; Shinkai, S.; Reinhoudt, D. N.; *Chem. Eur. J.* **2000**, *6*, 4104-4115.

[39] Assembly (*P*)-**1b**$_3$•(BenCYA)$_6$ which is formed using an enantioselective process (substitution of a chiral barbiturate derivative for the nonchiral BenCYA)[42] has a slightly lower Δε than assembly (*P*)-**1b**$_3$•((*R*)-MePheCYA)$_6$. For this reason, the relative CD intensities were related to the ratio (*P*)-**1b**$_3$•((*R*)-MePheCYA)$_6$/(*P*)-**1b**$_3$•(BenCYA)$_6$.

[40] Previous studies have shown that assemblies containing similar chromophores exhibit similar CD intensities.[35]

[41] The presence of two signals in the region of 15-14 ppm, where the hydrogen-bonded imide NH protons of the cyanurate component appear in the ^{1}H NMR spectrum, is characteristic for the formation of homomeric hydrogen-bonded double rosette assemblies **1**$_3$•(CYA/*CYA)$_6$. When heteromeric assemblies are formed, the NH protons are not magnetically equivalent, consequently giving rise to a far more complicated ^{1}H NMR spectrum.

[42] Prins, L. J.; de Jong, F.; Timmerman, P.; Reinhoudt, D. N. *Nature* **2000**, *408*, 181-184.

[43] Prins, L. J.; Verhage, J. J.; de Jong, F.; Timmerman, P.; Reinhoudt, D. N. *Chem. Eur. J.* **2002**, *8*, 2302-2313.

[44] When the chiral centers are in the cyanurate building blocks, a center with (*R*)-stereochemistry induced generally the formation of assemblies with (*P*)-helicity. Thus, when (*R*)-MePheCYA is present the formation of the (*M*)-diastereomer is unfavorable. A special case are the cyanurate formed with amino acid residues. All the (*L*)-amino acid base cyanurate ((*S*)-stereochemistry) induce (*P*)-helicity in the corresponding assemblies.

[45] The thermodynamic stability of **1a**$_3$•((*R*)-MePheCYA)$_6$ and **1g**$_3$•((*R*)-MePheCYA)$_6$ in polar solvents has been also studied. The χ (χ = percentage of polar solvent at which 50% of the assembly is still intact) in MeOH for assemblies **1a**$_3$•((*R*)-MePheCYA)$_6$ (butyl chain), and **1g**$_3$•((*R*)-MePheCYA)$_6$ (*t*-butyl chain) shows a decrease from 60% to 7.5%, suggesting a decrease of thermodynamic stability of the assemblies upon increase of the bulkiness of the substituents.

[46] The kinetics of the system formed with dimelamine **1b** are slower than the kinetics of the systems formed with **1c** as can be judged comparing figures 3.9 and 3.7 respectively. However, it is not possible to determine the kinetic parameters of both chiral amplification processes.

[47] For the systems formed with (*R*)-MePropCYA and (*L*)-ValCYA, the achiral cyanurate BuCYA was chosen.

[48] Based on symmetry arguments, the isomer with D_3-symmetry bearing chiral centres should have two signals in the ^{1}H NMR spectrum because the two different protons involved in the hydrogen-bonding network reside in a chemically different environment within the assembly. On the other hand, the isomer with C_{3h}-symmetry should have four signals of equal intensity in the ^{1}H NMR spectrum.

[49] Kimizuka, N.; Kawasaki, T.; Hirata, K.; Kunitake, T. *J. Am. Chem. Soc.* **1998**, *120*, 4094-4104.

[50] Quanta97, *Molecular Simulations*, Waltham, MA, **1997**.

[51] a) Brooks, B. R.; Bruccoleri, R. E.; Olafsen, B. D.; States, D. J.; Swaminathan, S.; Karplus, M. *J. Comput. Chem*. **1983**, *4*, 187-217; b) Momany, F. A.; Klimkowski, V. J.; Schäfer, L. *J. Comput. Chem*. **1990**, *11*, 654-662; c) Momany, F. A.; Rone, R.; Kunz, H.; Frey, R. F.; Newton, S. Q.; Schäfer, L. *J. Mol. Struct*. **1993**, *286*, 1-18.

APPENDIX TO CHAPTER 3

This model is implemented in MicroMath® Scientis® for Windows, Version 2.01.

Thermodynamic Model

```
// MicroMath Scientist Model File
IndVars: RTOT
DepVars: S, R, B, PR6, MR6, PR5B1, MR5B1, PR4B2, MR4B2, PR3B3, MR3B3,
PR2B4, MR2B4, PR1B5, MR1B5, PB6, MB6
Params: SF, KROS, fm
PR6=KROS*R^6
MR6=fm^6*KROS*R^6
PR5B1=6*KROS*R^5*B
MR5B1=6*fm^5*KROS*R^5*B
PR4B2=15*KROS*R^4*B^2
MR4B2=15*fm^4*KROS*R^4*B^2
PR3B3=20*KROS*R^3*B^3
MR3B3=20*fm^3*KROS*R^3*B^3
PR2B4=15*KROS*R^2*B^4
MR2B4=15*fm^2*KROS*R^2*B^4
PR1B5=6*KROS*R*B^5
MR1B5=6*fm*KROS*R*B^5
PB6=KROS*B^6
MB6=KROS*B^6

RROS=6*PR6+5*PR5B1+4*PR4B2+3*PR3B3+2*PR2B4+PR1B5+6*MR6+5*MR5B1
+4*MR4B2+3*MR3B3+2*MR2B4+MR1B5
R=RTOT-RROS
```

BROS=6*PB6+5*PR1B5+4*PR2B4+3*PR3B3+2*PR4B2+PR5B1+6*MB6+5*MR1B5
+4*MR2B4+3*MR3B3+2*MR4B2+MR5B1
B=6-RTOT-BROS

P=PR6+PR5B1+PR4B2+PR3B3+PR2B4+PR1B5+PB6
M=MR6+MR5B1+MR4B2+MR3B3+MR2B4+MR1B5+MB6
S=SF*((P-M)/(P+M))
0.0<R<1
0.0<B<1
***

With RTOT = total concentration of chiral cyanurate ***CYA**; S = CD-intensity;
R = concentration of ***CYA**; B = concentration of **CYA**; SF = scaling factor;
$f_m = \exp -((\Delta G_{P/M}^0)/RT)$; KROS = 10^{10}. In this model the composition of the assemblies is given by the letters R and B (R for ***CYA** and B for **CYA**) and the chirality of the assembly by the letter M or P.

Chapter 4

Chiral amplification in tetrarosette assemblies

In this chapter, the amplification of chirality in tetrarosette assemblies under thermodynamic equilibrium is described. The extent of the chiral amplification obtained using 'sergeants-and-soldiers' experiments depends only on the structure of the spacer of the assembly and it is independent on the methodology used for the formation of the tetrarosette assemblies. The difference in free energy ($\Delta G^{o}_{M/P}$) between the M- and P-diastereomers for these assemblies is up to 40 times higher than for double rosette assemblies.

4.1. Introduction

Amplification of chirality (for definition see Chapter 3), generating homochiral molecules or architectures, has repeatedly been tackled by chemists.[1,2] The term 'sergeants-and-soldiers' and 'majority rule' were introduced by Green et al. in their studies on the chirality in stiff helical polymers such as polyisocyanates.[3,4] The 'sergeants-and-soldiers'effect is characterized by a (strong) nonlinear response of the optical properties of the (achiral) systems to the addition of a small amount of homochiral material.[3,5] Whereas the 'majority rule' represents a similar effect for chains consisting of both enantiomeric forms, one of which is present in (small) excess.[6,7] These phenomena have been reported for polymeric structures, both covalent and noncovalent,[8,9] as well as in other supramolecular systems such as in the recognition of chiral amines and acids by hydrogen-bonded assemblies and polymers.[10] The importance and precedents of chiral amplification have been outlined in Chapter 3 and will not be discussed here.

Previous studies in our group investigated the amplification of chirality in double rosette assemblies[11] and the parameters that govern this phenomenon. It was found that an important factor for the amplification of chirality in these hydrogen-bonded assemblies is the dissociation rate constant for the dimelamine components. A lower dissociation rate constant will lead to a higher degree of amplification of chirality, that it is to say a larger optical activity with lower amounts of chiral component. Moreover, it is theoretically possible to achieve a high degree of chiral amplification even when only 0.1% of the components are chiral. The conclusive studies of the chiral amplification with double rosettes, in particular the influence of the differently substituted building blocks, *i.e*. dimelamine and cyanurate, are described in Chapter 3.

In this chapter the amplification of chirality of tetrarosette assemblies[12,13] under thermodynamically controlled conditions is studied. These larger assemblies can be considered as two covalently linked double rosette assemblies (Scheme 4.1). The dissociation of one tetramelamine building block (**TM**) requires the disruption of 24 H-bonds and therefore a smaller dissociation rate constant with respect to double rosette assemblies (in which only 12 H-bonds have to be disrupted to dissociate one dimelamine (**DM**)) is predicted. Thus, according to our kinetic model previously developed,[11] a much

higher amplification of chirality is expected for the system formed with tetrarosette assemblies. Therefore, the chiral amplification of cyanurate-based tetrarosette assemblies was studied in detail, with particular attention to the procedure followed for the noncovalent synthesis of the assemblies and to the flexibility of the spacer (X) used to covalently link the two calix[4]arene dimelamines (Chart 4.1).

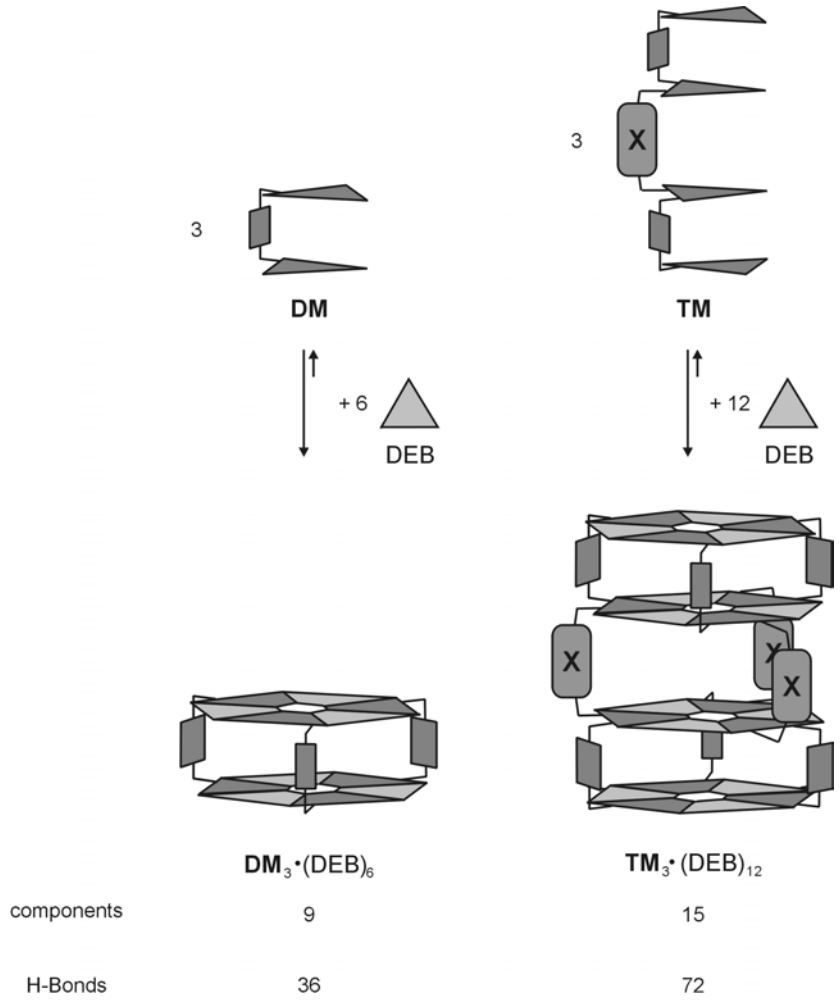

Scheme 4.1. General schematic representation of the formation of double and tetrarosette assemblies $\mathbf{DM}_3$•$(DEB)_6$ and $\mathbf{TM}_3$•$(DEB)_{12}$. The number of components and hydrogen bonds that held the assemblies together is shown. (**DM** = calix[4]arene dimelamine; **TM** = calix[4]arene tetramelamine, DEB = 5,5-diethylbarbituric acid).

4.2. Results and discussion

4.2.1 Synthesis and characterization

Tetramelamines (**TM**) **1a** and **1b** (Chart 4.1) have been synthesized following methods previously described.[12,13]

Similarly to double rosette assemblies (see Chapter 3), tetrarosette assemblies can conveniently be characterized by ^{1}H NMR spectroscopy.[12] Upon formation of the assembly **1a-b**$_3$•(DEB)$_{12}$, four singlets of equal intensity are observed in the region between δ = 13 and 16 ppm, characteristic of the hydrogen-bonded imide NH protons of DEB. Integration of the appropriate signals in the ^{1}H NMR spectrum confirmed the expected 1:4 stoichiometry for assemblies **1a-b**$_3$•(DEB)$_{12}$. Tetrarosette assemblies can adopt a large variety of different isomeric structures as result of the staggered (S) or eclipsed (E) orientation of the melamine rings in each rosette layer. Nevertheless, ^{1}H NMR (four signals for the NH protons of DEB) and gas-phase MM calculations have shown the formation of only the SSS-isomer.

This SSS-isomer exists as a mixture of enantiomers (*P*- and *M*-enantiomers) in the absence of any source of chirality due to the staggered orientation of the different melamine rings. However, the introduction of chiral centers in one of the building blocks of the assembly leads to the formation of only one of the two possible diastereomers. Therefore, these assemblies are also highly circular dichroism (CD) active.

MALDI-TOF mass spectrometry measurements after Ag^+ labelling provide additional evidence for the formation of tetrarosettes.[14] For example, assembly **1b**$_3$•(EPB)$_{12}$ (Chart 4.1) was mixed with 1.5 equivalents of $AgCF_3COO$ in $CHCl_3$ and the mass spectrum was measured.[15] The spectrum shows an intense signal at m/z = 8585.2 (calcd for $C_{468}H_{546}N_{96}O_{60}$•$^{107}Ag^+$ = 8583.1) for the corresponding monovalent Ag^+ complex (Figure 4.1). Signals corresponding to more highly charged or fragmented Ag-complexed assemblies were not observed.

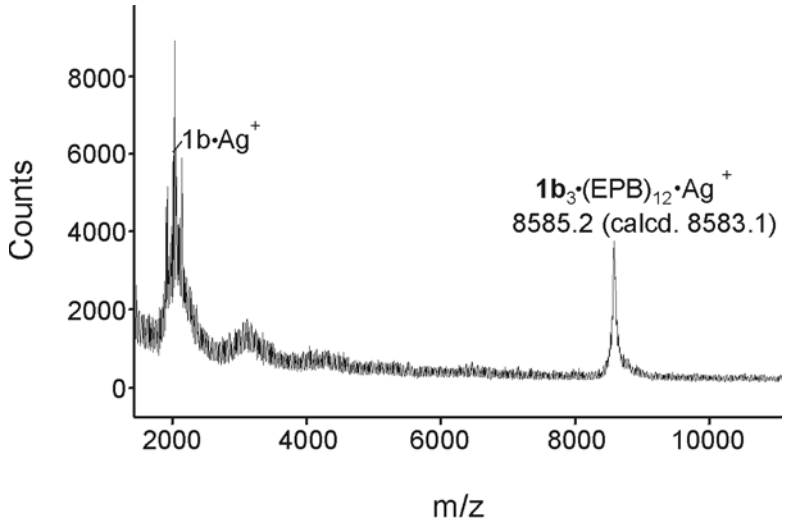

Figure 4.1. MALDI-TOF mass spectrum of the Ag^+ complex of assembly $\mathbf{1b}_3$•$(EPB)_{12}$.

4.2.2. Tetrarosette formation

Barbiturate-based tetrarosette assemblies $\mathbf{1}_3$•$(DEB)_{12}$ are spontaneously formed in apolar solvents, such as chloroform, benzene or toluene, when three equivalents of tetramelamine **1** (Chart 4.1) are mixed with twelve equivalents of 5,5-diethylbarbiturate (DEB) at room temperature. The driving force for the self-assembly of these nanostructures is the formation of 72 cooperative hydrogen bonds.[12] The self-assembling process brings together fifteen components leading to the formation of assemblies with high kinetic stability, with a dissociation rate constant for one tetramelamine of 2.8×10^{-5} s^{-1} (in $CHCl_3$ at 25 ^oC) and an activation energy of 98.7 kJ mol^{-1}, indicating the enormous enthalpy price that must be paid in order to dissociate one tetramelamine from the tetrarosette assembly, a process that involves the disruption of 24 H-bonds.

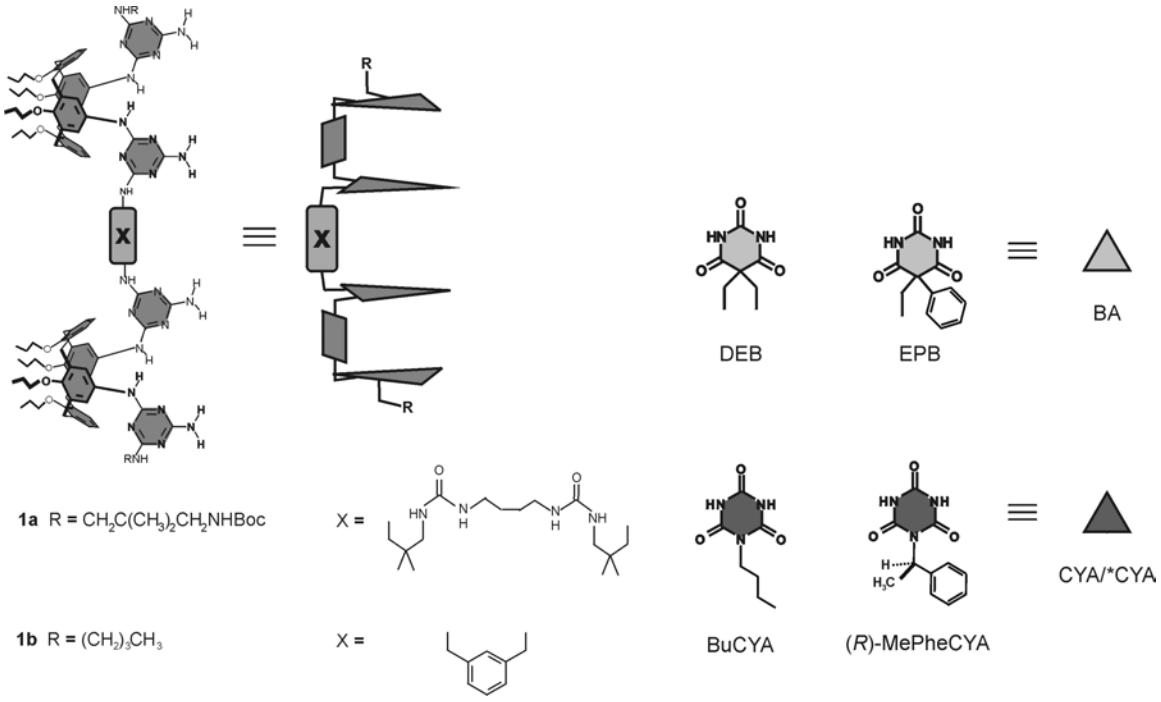

Chart 4.1. Chemical and schematic representation of tetramelamines **1a-b** and barbiturate (BA)/cyanurate (CYA/*CYA) building components.

However, similar assembly experiments with **1a-b** and cyanuric acid derivatives (BuCYA and (*R*)-MePheCYA) instead of DEB (Chart 4.1) gave completely different results.[16] For example, mixing tetramelamine **1a** with BuCYA (1:4 ratio) in chloroform at room temperature did not show the expected formation of the corresponding assembly $\mathbf{1a}_3$•$(\text{BuCYA})_{12}$. This mixing process leads to the formation of nondefined structures which display an extremely high kinetic stability (see Chapter 7 for discussion).

This problem in the noncovalent synthesis of tetrarosette assemblies can be overcome using two different approaches: (i) mixing the two building blocks (tetramelamine and cyanurate derivatives (1:4 ratio)) in toluene and heating the resulting solution at 100 ^{o}C for one week (*direct method*) (Figure 4.2a), and (ii) formation of the assembly using DEB and subsequent exchange by cyanuric acid derivatives (1:1 ratio DEB:cyanuric acid) (*exchange method*) (Figure 4.2b).[16] This method is based on the strategy previously exploited for the enantioselective formation of double rosette assemblies.[17]

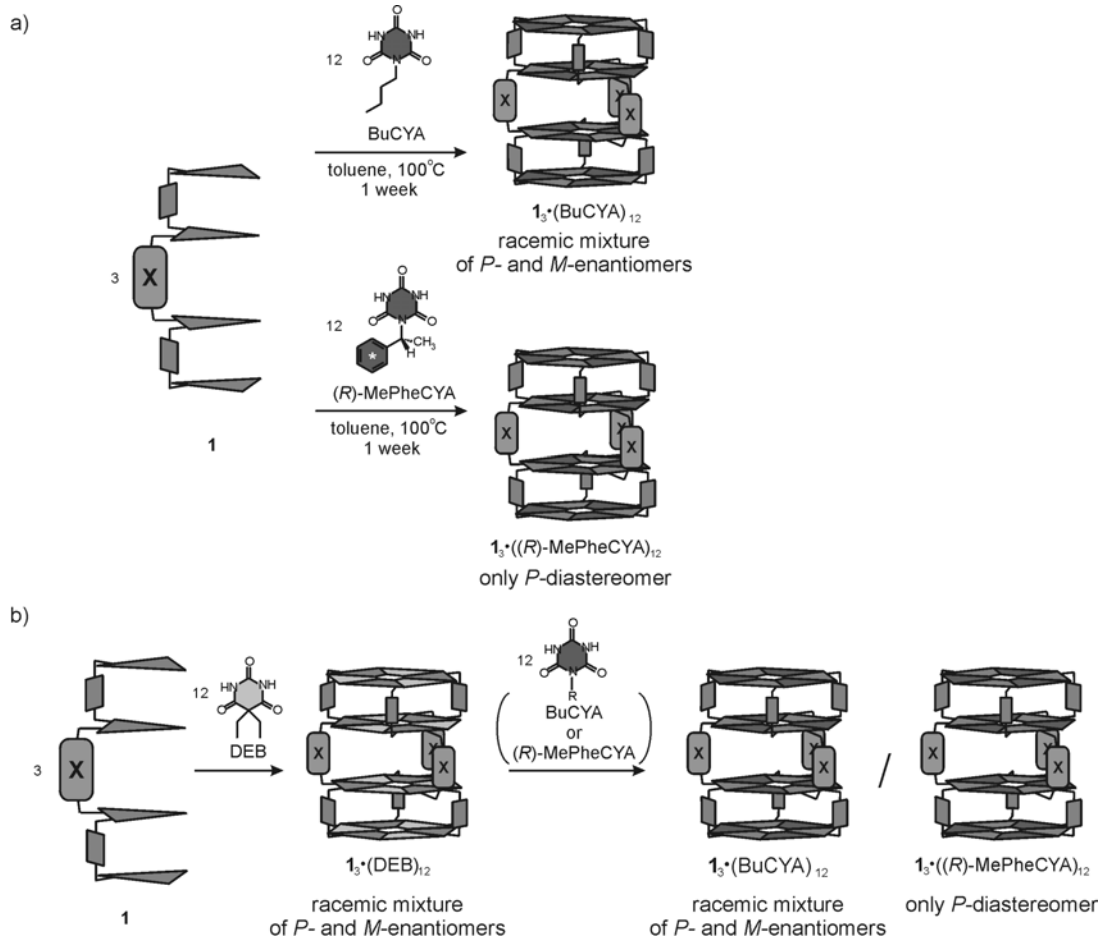

Figure 4.2. Schematic representation of a) *direct method* and b) *exchange method* for the formation of cyanurate-based tetrarosette assemblies. In the absence of chiral centers, the assemblies are present as a racemic mixture. However, upon introduction of chiral centers ((*R*)-MePhe) only the *P*-diastereomer is formed.

The formation of the tetrarosette assemblies by the two different methods was studied by ^{1}H NMR spectroscopy.

The ^{1}H NMR spectrum of a mixture of tetramelamine **1a** and cyanurate derivative in toluene-d_8 at room temperature shows a complicated set of signals (Figure 4.3a), suggesting the formation of a mixture of ill-defined assemblies. However, formation of tetetrarosette assembly **1a**$_3$•(BuCYA)$_{12}$ is observed upon heating at 100 ^{o}C for one week in toluene as can be judged from the appearance of four signals of equal intensity in the region δ =15-13 ppm in the ^{1}H NMR spectrum (1.0 mM in toluene-d_8), (*direct method*) (Figure 4.3b).

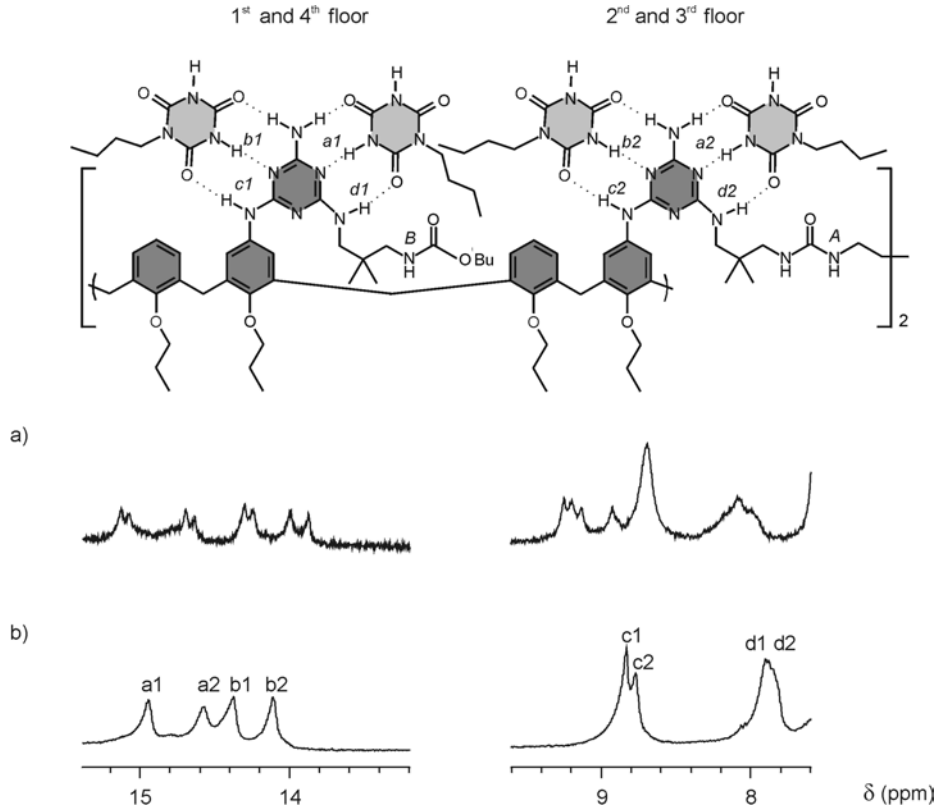

Figure 4.3. Parts of the ^{1}H NMR spectra of a 1:4 mixture of **1a** and BuCYA (a) immediately after mixing, and (b) after 1 week at 100 ^{o}C in toluene (**1a**$_3$•(BuCYA)$_{12}$). Both spectra were recorded in toluene-d_8 at room temperature.

The first step of tetrarosette formation using the second method (*exchange method*) is the noncovalent synthesis of the barbiturate-based assembly **1a**$_3$•(DEB)$_{12}$ (Figure 4.4). The ^{1}H NMR spectrum of this assembly (1.0 mM in toluene-d_8) shows four sharp signals in the region between δ = 15-13 ppm, characteristic of the formation of tetrarosette assemblies (Figure 4.4a). The second step is the exchange of DEB by cyanurate derivatives (BuCYA or (*R*)-MePheCYA), resulting in the exclusive formation of **1a**$_3$•(BuCYA)$_{12}$ or **1**$_3$•((*R*)-MePheCYA)$_{12}$. The ^{1}H NMR spectra of these assemblies (1.0 mM in toluene-d_8) show the disappearance of the signals of assembly **1a**$_3$•(DEB)$_{12}$ and the appearance of four new signals at lower magnetic field and a new broad signal at ~ 8.4 ppm corresponding to free DEB (Figures 4.4b and c). Thus, the ^{1}H NMR spectroscopy clearly indicates that the exchange of DEB by the cyanurate derivatives has taken place.[16] The replacement of the barbiturate by cyanurate derivatives is due to the

formation of stronger hydrogen bonds between the melamine-cyanurate than between melamine-barbiturate because of the higher acidity of the cyanurate derivative.[18]

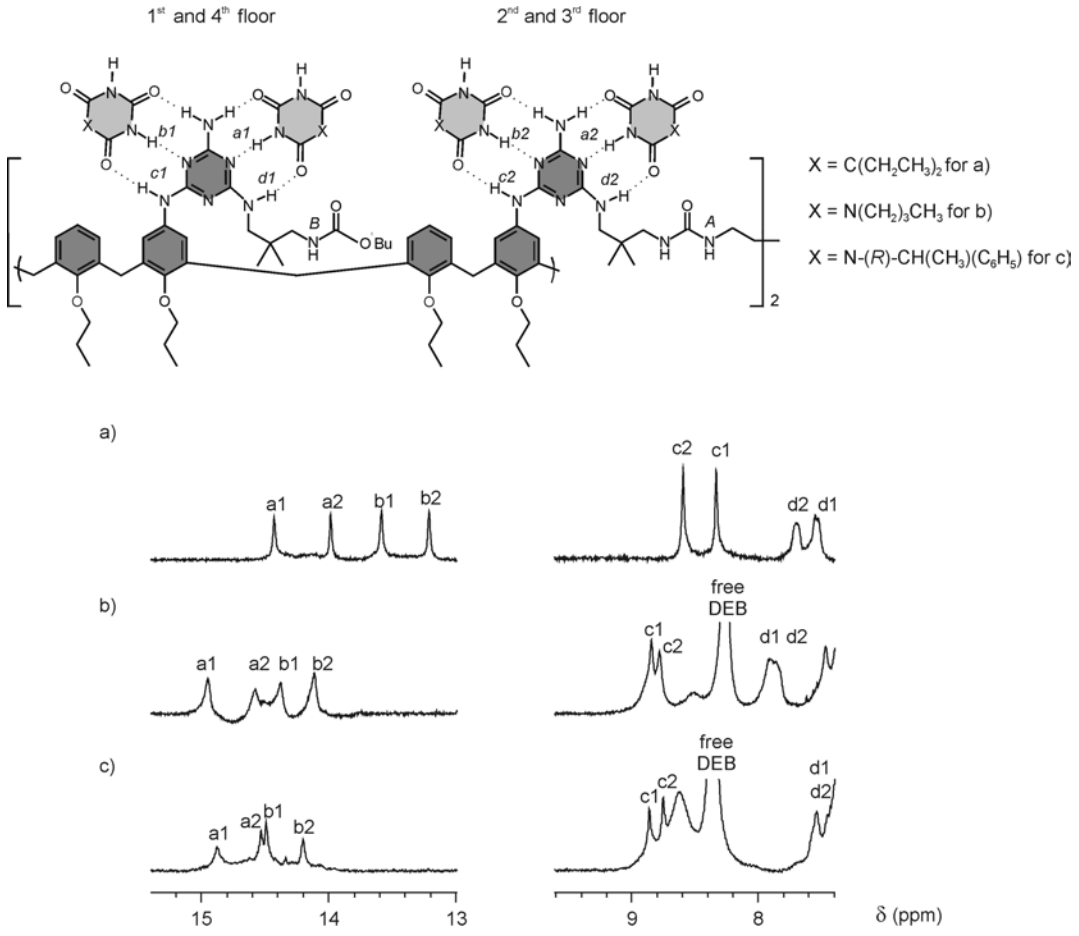

Figure 4.4. Parts of the ^{1}H NMR spectra of (a) **1a**$_3$•(DEB)$_{12}$, and after the addition of 12 equivalents (1:1 ratio DEB:cyanurate) of (b) BuCYA and (c) (*R*)-MePheCYA. All ^{1}H NMR spectra were recorded in toluene-d_8 (1.0 mM) at room temperature.

4.2.3. Amplification of chirality in tetrarosette assemblies ***1***$_3$*•(CYA/*CYA)*$_{12}$

Solutions of the assembly (*P*)-**1a**$_3$•((*R*)-MePheCYA)$_{12}$ and racemic **1a**$_3$•(BuCYA)$_{12}$ in toluene (1 mM) (formed using the *direct method*) were mixed in ratios ranging from 90:10 to 10:90 and introduced in a thermostated bath at 100 ^{o}C. Aliquots of these solutions were taken and the CD-spectra of these mixtures were measured every 24 hours over a period of two days (Figure 4.5). After this time the thermodynamic equilibrium is reached.

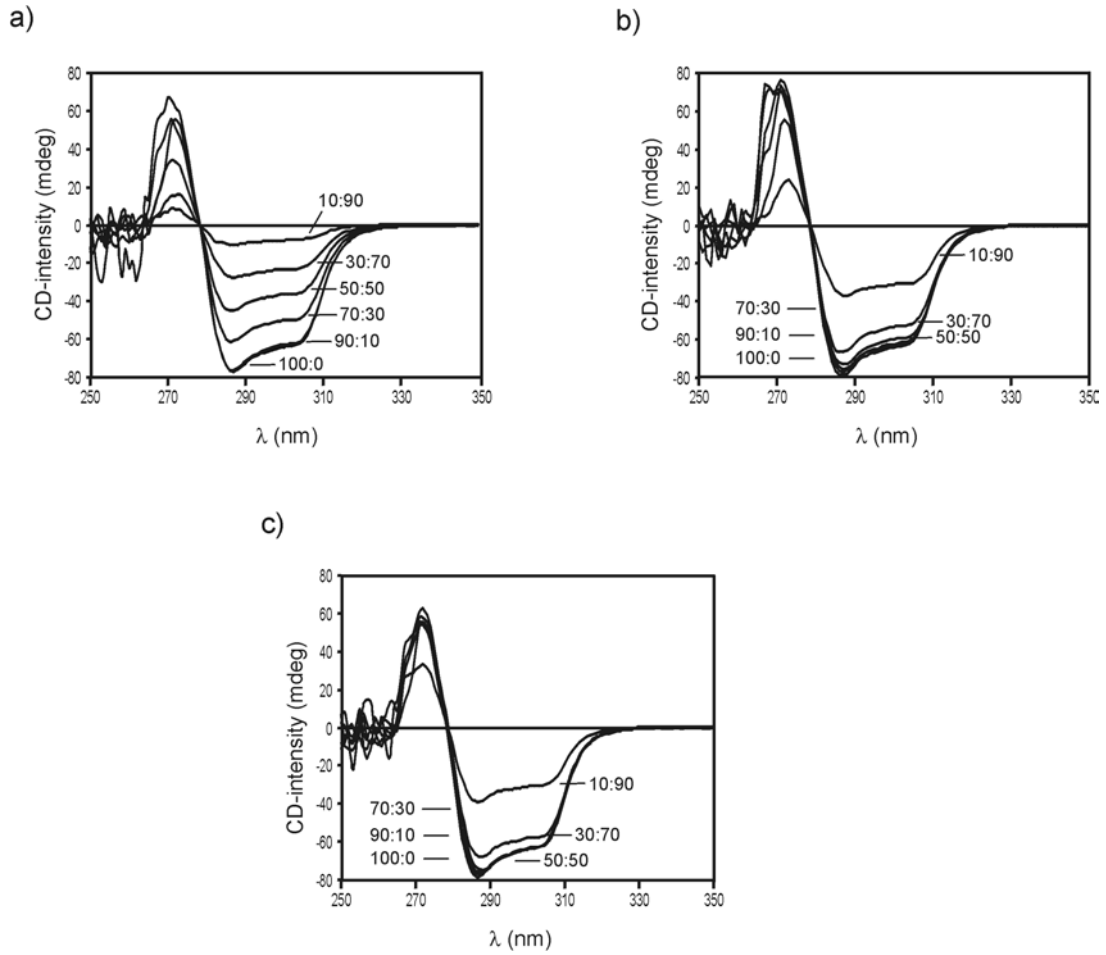

Figure 4.5. CD-spectra of mixtures of (*P*)-**1a**$_3$•((*R*)-MePheCYA)$_{12}$ and **1a**$_3$•(BuCYA)$_{12}$ a) immediately after mixing, and after (b) 24 hours at 100 ^{o}C and (c) 48 hours at 100 ^{o}C. Both tetrarosette assemblies were formed using the *direct method*.

The maximum CD-intensity of the mixtures of (*P*)-**1a**$_3$•((*R*)-MePheCYA)$_{12}$ and **1a**$_3$•(BuCYA)$_{12}$ immediately after mixing corresponds to the CD-intensity of the chiral assembly component; *i.e.* the mixture with 50% of chiral assembly displays a CD-intensity corresponding to the 50% of chiral assembly component (Figure 4.5a). Thus, immediately after mixing the 'sergeants-and-soldiers' phenomenon has not taken place. However, after 24 hours at 100 ^{o}C, the CD-intensity does no longer correspond to the percentage of chiral assembly in the mixture, showing the typical 'sergeants-and-soldiers' behavior (Figure 4.5b). After 48 hours at 100 ^{o}C, the CD-intensity of the different

mixtures of chiral:achiral assemblies does not increase anymore, indicating that the thermodynamic equilibrium has been reached (Figure 4.5c).

From these measurements, the relative CD intensities were related to a calculated value based on the ratio (*P*)-**1a**$_3$•((*R*)-MePheCYA)$_{12}$/(*P*)-**1a**$_3$•(BuCYA)$_{12}$ and plotted as a function of the molecular fraction of the chiral component (Figure 4.6).[19]

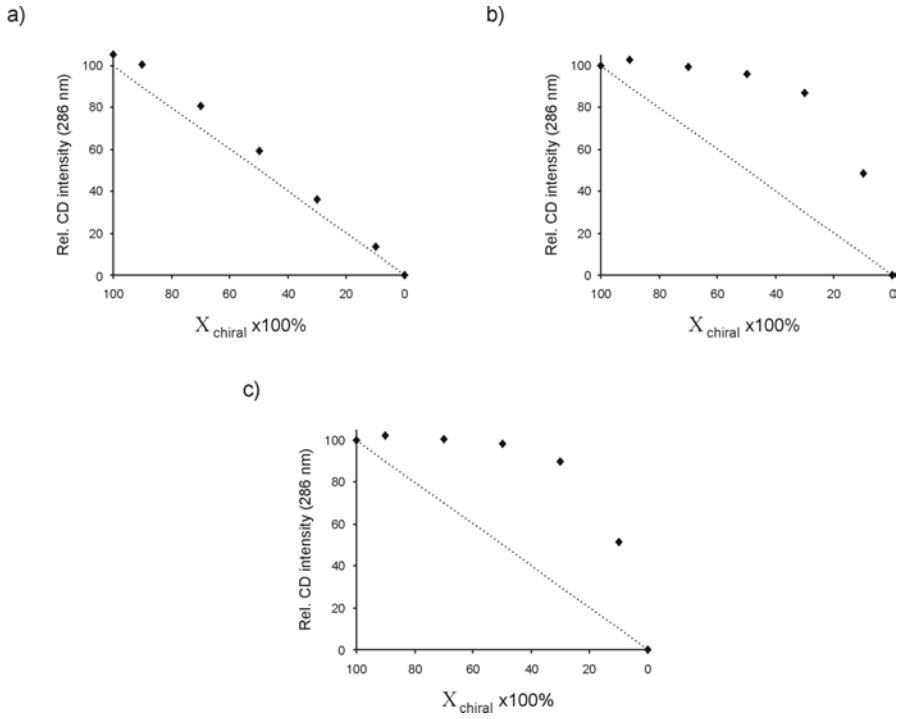

Figure 4.6. Plots of the relative CD intensity measured at 286 nm for the molar ratio of chiral assembly (*P*)-**1a**$_3$•((*R*)-MePheCYA)$_{12}$ (a) immediately after mixing, (b) after 24 hours at 100 ^{o}C and (c) after 48 hours at 100 ^{o}C. The assemblies were formed using the *direct method*. The dotted lines represent the expected CD intensity in absence of chiral amplification.

The plot of the relative CD intensity (measured at 286 nm) as a function of the molar ratio of chiral rosette assembly immediately after mixing (Figure 4.6a) shows clearly that the CD intensities of the mixtures do not increase with the percentage of chiral assembly present, indicating that chiral amplification has not taken place. However, the plots after 24 and 48 hours at 100 ^{o}C show a nonlinear increase of the CD intensities at different molar ratios of chiral assembly (Figure 4.6b and c, respectively), *i.e.* the typical nonlinear behavior resulting from the 'sergeants-and-soldiers' principle shows clearly the amplification of chirality. For example, when a 90:10 mixture of

1a$_3$•(BuCYA)$_{12}$ and (*P*)-**1a**$_3$•((*R*)-MePheCYA)$_{12}$ reaches the thermodynamic equilibrium, the relative CD intensity has increased from 10% (expected in the case where there is no chiral amplification) to 52%. The nonlinear increase of the CD intensity is due to the exchange between the chiral and nonchiral cyanurates within the assemblies, that is to say, to the presence of the heteromeric assemblies **1a**$_3$•(BuCYA)$_n$((*R*)-MePheCYA)$_{12-n}$ (n = 1-11), in which the presence of 1 to 11 chiral centers ((*R*)-MePhe) in these assemblies leads to the preferential formation of (*P*)-diastereomer (see Chapter 3 for a detailed description).

4.2.4. Thermodynamic model

The curve of the amplification of chirality for the system formed by mixing **1a**$_3$•(BuCYA)$_{12}$ and (*P*)-**1a**$_3$•((*R*)-MePheCYA)$_{12}$ after 48 hours at 100 ^{o}C (Figure 4.5c) was fitted to a thermodynamic model based on the difference in free energy between the (*P*)- and (*M*)- diastereomers of the homo/heteromeric assemblies **1a**$_3$•(BuCYA)$_n$((*R*)-MePheCYA)$_{12-n}$ (n = 0-12) at the thermodynamic equilibrium. All the equilibria accounted in the model are depicted in Figure 4.7. The formation of the tetrarosette assemblies is considered to take place in one step from the different building blocks. The influence of the dissociation rate constant is not included in the model. Cooperativity is also not included in the model and therefore, ΔG^o is assumed to increase linearly with the number of chiral components. Each chiral substituent present in the unfavorable (*M*)-diastereomer[20] induces a free energy difference $\Delta G^o_{M/P}$, which results in a decrease of the equilibrium constant (K) between the (*M*)-isomer and the free components with a factor of $f_m = e^{\frac{-\Delta G^o_{M/P}}{RT}}$. For example, for an assembly containing six chiral centers, the equilibrium constant is decreased by a factor of f_m^6. The equilibrium constant is assumed to be the same for every assembly. Statistical factors are included to account for the statistically different possibilities of formation of each assembly. Thus, least squares fit of the CD data for the system formed from **1a**$_3$•(BuCYA)$_{12}$ and (*P*)-**1a**$_3$•((*R*)-MePheCYA)$_{12}$ (Figure 4.6c) using the model described above resulted in $\Delta G^o_{M/P}$ = 119.4 ± 1.7 kJ mol^{-1} per chiral substituent. This corresponds to a total free energy difference ΔG^o_{tot} = 1432.8 ±

20.4 kJ mol^{-1} between the favored (*P*)- and the unfavored (*M*)-diastereomers of assembly (*P*)-**1a**$_3$•((*R*)-MePheCYA)$_{12}$ containing twelve chiral centers.

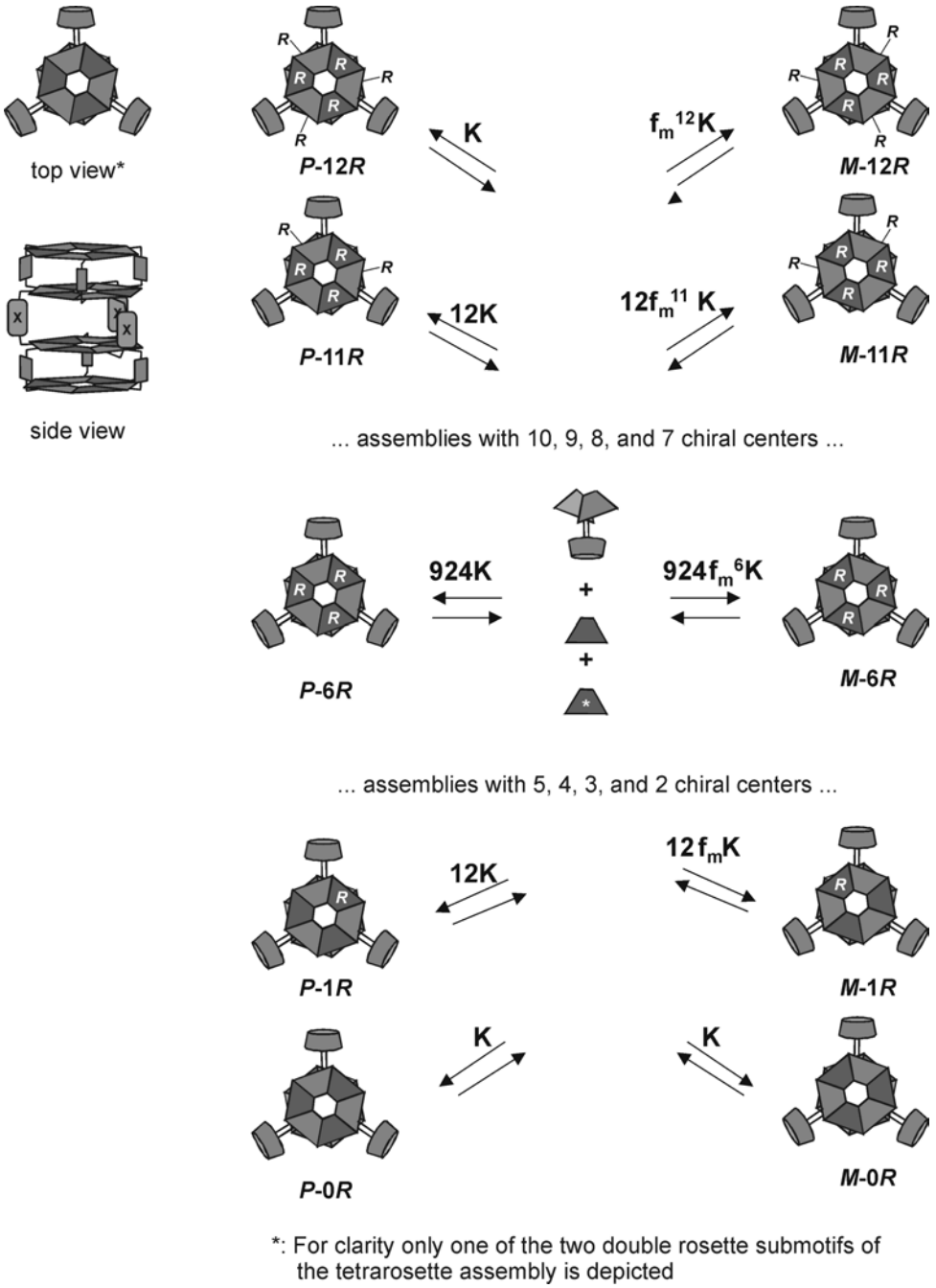

Figure 4.7. Thermodynamic model. Each chiral substituent in assemblies **1a**$_3$•(BuCYA)$_n$((*R*)-MePheCYA)$_{12-n}$ (n = 0-12) lowers the equilibrium constant of the unfavored (*M*)-isomer by a factor $f_m = e^{\frac{-\Delta G^{o}_{M/P}}{RT}}$. *R* denotes the chiral components of the assembly.

4.2.5. Influence of the noncovalent synthetic procedure on the amplification of chirality

The extent of the chiral amplification using the thermodynamic model mentioned in section 4.2.4 was studied for **1a**$_3$•(BuCYA)$_{12}$ and (*P*)-**1a**$_3$•((*R*)-MePheCYA)$_{12}$ prepared using the *exchange method* to asses the influence of the synthetic path followed in the formation of the tetrarosettes assemblies in the amplification of chirality.

Thus, similar "sergeants-and-soldiers" experiments were carried out with mixtures of assemblies **1a**$_3$•(BuCYA)$_{12}$ and (*P*)-**1a**$_3$•((*R*)-MePheCYA)$_{12}$ formed using the *exchange method*. The calculated difference in free energy between the favored *P*- and unfavored *M*-diastereomers of (*P*)-**1a**$_3$•((*R*)-MePheCYA)$_{12}$ was also $\Delta G^{o}_{M/P}$ = 119.4 ± 2.1 kJ mol^{-1}!

Comparison of the results obtained in the amplification of chirality for the system **1a**$_3$•(BuCYA)$_{12}$ and (*P*)-**1a**$_3$•((*R*)-MePheCYA)$_{12}$ formed using the *direct* and the *exchange method* showed no dependence of the method of formation of the assemblies in the extent of the chiral amplification under thermodynamically controlled conditions (Figure 4.8 and Table 4.1).

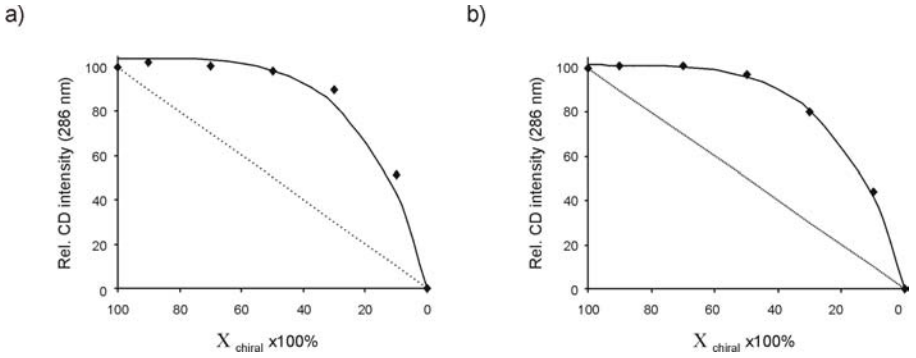

Figure 4.8. Plots of the relative CD intensity at measured at 286 nm against the molar ratio of chiral assembly (*P*)-**1a**$_3$•((*R*)-MePheCYA)$_{12}$ formed using a) the *direct method*, and b) *exchange method*.

Table 4.1: Difference in free energy between the (*P*)- and (*M*)-diastereomers of assemblies **1a**$_3$•((*R*)-MePheCYA)$_{12}$ as a result of the presence of chiral centers in the assembly calculated using the thermodynamic model.[a]

Method	$\Delta G^o_{M/P}$ (kJ mol^{-1})[b]	ΔG^o_{tot} (kJ mol^{-1})[c]
direct	119.4 ± 1.7	1432.8 ± 20.4
exchange	119.4 ± 2.1	1432.8 ± 25.2

[a] [(*P*)-**1a**$_3$•((*R*)-MePheCYA)$_{12}$] = [**1a**$_3$•(BuCYA)$_{12}$] = 1.0 mM, 343 K, benzene. [b] Difference of free energy per chiral centre. [c] Total free energy difference between (*P*)- and (*M*)-diastereomers of assemblies **1a**$_3$•((*R*)-MePheCYA)$_{12}$.

There is a large difference in free energy of the *P*- and *M*-diastereomers introduced in the assemblies per chiral center between double (see Chapter 3) and tetrarosettes. For the best case of chiral amplification in double rosette assemblies a $\Delta G^o_{M/P}$ of 4.3 kJ mol^{-1} was obtained. This difference in free energy for tetrarosette assemblies is $\Delta G^o_{M/P}$ = 119.4 kJ mol^{-1}. Kinetic studies on the amplification of chirality for double rosettes have shown the important role of the dissociation rate constant of the dimelamine components to obtain a high chiral amplification at the thermodynamic equilibrium.[11] Thus, a possible explanation for the difference in amplification of chirality between double and tetrarosettes assemblies might come from the decrease of the dissociation rate constant of the tetramelamine building blocks. This decrease is due to the increase in the number of hydrogen bonds that held the melamine together (12 and 24 H-bonds for double and tetrarosette assemblies, respectively).

To investigate the role of the dissociation rate constant in the amplification of chirality in tetrarosette assemblies, kinetic experiments were carried out with the system comprising assemblies **1a**$_3$•(BuCYA)$_{12}$ and (*P*)-**1a**$_3$•((*R*)-MePheCYA)$_{12}$, formed using the *direct method*. The CD intensity at 286 nm of mixtures **1a**$_3$•(BuCYA)$_{12}$ and (*P*)-**1a**$_3$•((*R*)-MePheCYA)$_{12}$ in benzene (1.0 mM) at 70 ^{o}C was measured as a function of time (Figure 4.9).

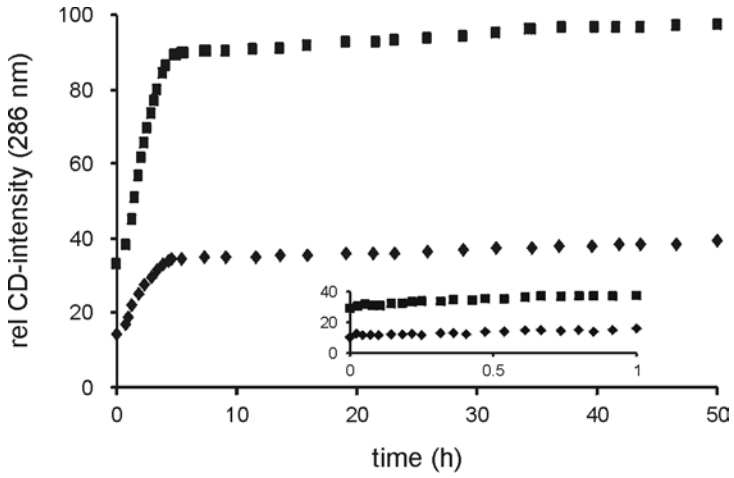

Figure 4.9. Increase of the relative CD intensity (at 286 nm) in time for mixtures of **1a**$_3$•(BuCYA)$_{12}$ and (*P*)-**1a**$_3$•((*R*)-MePheCYA)$_{12}$ with different initial mole fractions of **1a**$_3$•(BuCYA)$_{12}$ (♦: 10%; ■: 30%). The inset shows the increase of the relative CD intensity (at 286 nm) during the first hour. All spectra were recorded in benzene at 70 ^{o}C.

Figure 4.9 shows that the relative CD intensities at t = 0 corresponds to the initial mole fraction of (*P*)-**1a**$_3$•((*R*)-MePheCYA)$_{12}$. However, the relative CD intensity starts to change (t_{init}) after about 30 minutes and 15 minutes for mixtures of **1a**$_3$•(BuCYA)$_{12}$ and (*P*)-**1a**$_3$•((*R*)-MePheCYA)$_{12}$ of ratios 90:10 and 70:30, respectively. However, for double rosette assemblies, the CD intensities increase rapidly in time. Thus, from this difference in t_{init} for double and tetrarosettes it is possible to conclude that the dissociation rate of the tetramelamine moieties is smaller than the one of the dimelamine moieties and, therefore, a larger amplification of chirality is expected for the systems formed with tetrarosette assemblies. Moreover, simulations using the kinetic model developed for double rosettes showed that lowering the dissociation rate of the melamines results in an increase of t_{init} and the degree of chiral amplification.[11] Unfortunately, due to the complexity of the system (twelve chiral centers), the development of a kinetic model to fit the data and obtain an accurate value for the dissociation rate constant for tetrarosette assemblies was not successful.[21]

4.2.6. Influence of the spacer (X) of the tetramelamine on the amplification of chirality

The extent of the chiral amplification using the thermodynamic model mentioned earlier (see section 4.2.4) was also studied for systems in which the spacer X of the tetramelamine becomes less flexible (Chart 4.1). For this purpose, the amplification of chirality was studied in systems in which the bisureido spacer of tetramelamine **1a** was replaced by the rigid *m*-xylene spacer in **1b**.

Thus, mixtures of assemblies (*P*)-**1b**$_3$•((*R*)-MePheCYA)$_{12}$ and **1b**$_3$•(BuCYA)$_{12}$ in ratios varying between 90:10 and 10:90 prepared using the *direct* and the *exchange* methods were introduced in a thermostated bath at 100 ^{o}C for two days. Aliquots of these solutions were taken and their CD spectra were measured (every 24 hours) over a period of two days, period after which the thermodynamic equilibrium is reached. The plot of the relative CD intensity (at 286 nm) at the thermodynamic equilibrium shows, in all cases, that the CD intensities are significantly higher than the sum of the CD intensities of the individual assemblies ('sergeants-and-soldiers' behavior). Similar to assemblies formed with tetramelamine **1a**, the method of assembly formation with tetramelamine **1b** does not influence the amplification of chirality in these systems. In Figure 4.10 and Table 4.2 are summarized the results obtained for the systems formed with the flexible tetramelamine **1a** and the rigid tetramelamine **1b**.

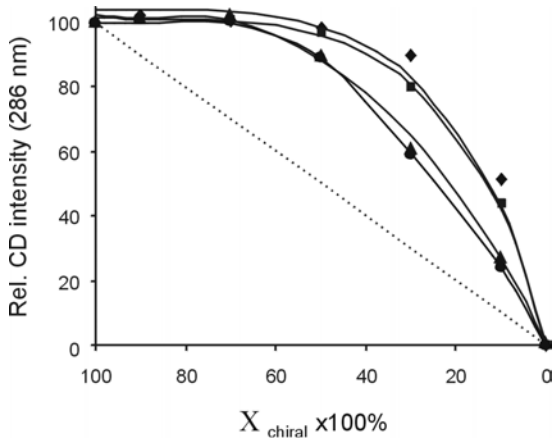

Figure 4.10. Plot of the relative CD-intensities at the thermodynamic equilibrium for different mole ratios of chiral component (**1a**: *exchange method*: ■, *direct method*: ♦; **1b**: *direct method*: ▲, *exchange method*: ●). The solid lines represent the calculated best fit using the thermodynamic model previously described. The dotted line represents the expected CD-intensity in absence of amplification of chirality.

Table 4.2: Difference in free energy between the (*P*)- and (*M*)-diastereomers of assemblies $\mathbf{1x}_3$•((*R*)-MePheCYA)$_{12}$ as a result of the presence of chiral centers in the assembly calculated using the thermodynamic model.[a]

1x	Method	$\Delta G^o_{M/P}$ (kJ mol^{-1})[b]	ΔG^o_{tot} (kJ mol^{-1})[c]
1a	direct	119.4	1432.8
1a	exchange	119.4	1432.8
1b	direct	2.8	33.6
1b	exchange	2.7	32.4

[a] [(*P*)-$\mathbf{1x}_3$•((*R*)-MePheCYA)$_{12}$] = [$\mathbf{1x}_3$•(BuCYA)$_{12}$] = 1.0 mM, 343 K, benzene. [b] Difference of free energy per chiral centre. [c] Total free energy difference between (*P*)- and (*M*)-diastereomers of assemblies $\mathbf{1x}_3$•((*R*)-MePheCYA)$_{12}$.

The analysis of the data obtained using the thermodynamic model clearly shows that the introduction of a rigid spacer (*m*-xylene) in the tetramelamine building block decreases the amplification of chirality in tetrarosette assemblies. The decrease in $\Delta G^o_{M/P}$ is probably due to the introduction of geometrical constrains in the assemblies bearing the rigid *m*-xylene spacer. Previous studies have shown that the formation of assemblies with the tetramelamine **1b** (rigid spacer) displays negative cooperativity[22] between the two double rosette layers,[12] while assemblies with tetramelamine **1a** display positive cooperativity between the two double rosette layers. Therefore, to obtain high degrees of chiral amplification, the tetrarosette assemblies should be formed with tetramelamine building blocks connected via a flexible spacer allowing the cooperative formation of the assembly.

4.3. Conclusions

In this chapter, the amplification of chirality in tetrarosette assemblies under thermodynamically controlled conditions has been described. The degree of chiral amplification is not influenced by the method of formation of the system, *i.e. direct method* or *exchange method*. The difference in free energy between the *M*- and *P*-diastereomers of the tetrarosettes introduced by a chiral center is 40 times higher than in the case of double rosette assemblies. This difference in the extent of chiral amplification

is due to a decrease in the dissociation rate constant of the tetramelamine building blocks. Thus, it is possible to control the amplification of chirality in the rosette systems increasing the number of layers in the assemblies, obtaining extremely high chiral amplification for noncovalent systems, similar to chiral amplification obtained with covalent polymeric structures. Moreover, the substitution of the bisureido spacer by the more rigid *m*-xylene spacer results in a considerable decrease in the amplification of chirality, probably due to geometric/steric contrains introduced in the system by the rigid spacer.

4.4. Experimental section

Synthesis. The synthesis of tetramelamines **1a**[13] and **1b**,[12] and cyanurate derivatives BuCYA and (*R*)-MePheCYA have been reported previously.[23]

Assembly formation. *Direct method*: Assemblies were formed by dissolving the calix[4]arene tetramelamines **1** and the corresponding cyanurate (BuCYA/(*R*)-MePheCYA) in a 1:4 molar ratio in tolune, after which the solution was heated up for one week at 100 ^{o}C. After being dried under high vacuum, the assemblies were ready for use. In a standard example, 7.08 mg (0.003 mmol) of tetramelamine **1a** and 2.22 mg (0.012 mmol) of BuCYA were dissolved in toluene and the resultant solution was heated at 100 ^{o}C for one week. After evaporation of the solvent, the assemblies were ready to use.
Exchange method: Assemblies **1x**$_3$•(BuCYA/(*R*)-MePheCYA)$_{12}$ (**x** = **a**, **b**) were prepared from **1x**$_3$•(DEB)$_{12}$ by exchange of DEB with BuCYA/(*R*)-MePheCYA. In a typical example, 9.30 mg (0.001 mmol) of assembly **1a**$_3$•(DEB)$_{12}$ was dissolved in 1 ml of $CDCl_3$, and 1 equivalent (with respect to DEB) of BuCYA (2.22 mg, 0.012 mmol) were added. The solution was stirred for 30 minutes. After this time, the assembly **2**$_3$•(BuCYA)$_{12}$ was ready to use.

CD titration studies. Assembly solution (1.0 mM) of the homomeric assemblies were mixed in ratios 90:10 to 10:90 at room temperature and introduced in a thermostated

bath at 100 ^{o}C immediately after mixing. The CD intensities were monitored in time at constant temperature. The resulting plots were treated as described in the text.

Thermodynamic model. The model was implemented in MicroMath® Scientist® for Windows, Version 2.01. Text file of the model is provided in the appendix.

4.5. References and notes

[1] Feringa, B. L.; van Delden, R. A. *Angew. Chem. Int. Ed.* **1999**, *38*, 3418-3438.

[2] Avalos, M.; Babiano, R.; Cintas, P.; Jiménez, J. L.; Palacios, J. C. *Chem. Commun.* **2000**, 887-892.

[3] Green, M. M.; Rediy, M. P.; Johnson, R. J.; Darling, G.; O'Leary, D. J.; Wilson, G. J. *J. Am. Chem. Soc.* **1989**, *111*, 6452-6454.

[4] Green, M. M.; Peterson, N. C.; Sato, T.; Teramoto, A.; Cook, R.; Lifson, S. *Science* **1995**, *268*, 1860-1866.

[5] van Gestel, J.; van der Schoot, P.; Michels, M. A. J. *Macromolecules* **2003**, *36*, 6668-6673.

[6] Green, M. M.; Garetz, B. A.; Munoz, B.; Chang, H.; Hoke, S.; Cooks, R. G. *J. Am. Chem. Soc.* **1995**, *117*, 4181-4182.

[7] van Gestel, J. *Macromolecules* **2004**, *37*, 3894-3898.

[8] For examples of amplification of chirality in covalent polymers: a) Green, M. M.; Park, J.-W.; Sato, T.; Teramoto, A.; Lifson, S.; Selinger, R. L.; Selinger, J. W. *Angew. Chem. Int. Ed.* **1999**, *38*, 3138-3154; b) Green, M. M.; Cheon, K.-S.; Yang, S.-Y.; Park, J.-W.; Swansburg, S.; Liu, W. *Acc. Chem. Res.* **2001**, *34*, 672-680.

[9] For examples of amplification of chirality in noncovalent polymers: a) Palmans, A. R. A.; Vekemans, J. A. J. M.; Havinga, E. E.; Meijer, E. W. *Angew. Chem. Int. Ed. Engl.* **1997**, *36*, 2648-2651; b) Brunsveld, L.; Schenning, A. P. H. J.; Broeren, M. A. C.; Janssen, H. M.; Vekemans, J. A. J. M.; Meijer, E. W. *Chem. Lett.* **2000**, 292-293; c) Brunsveld, L.; Lohmeijer, B. G. G.; Vekemans, J. A. J. M.; Meijer, E. W. *Chem. Commun.* **2000**, 2305-2306; d) Schenning, A. P. H. J.; Jonkheijm, P.; Peeters, E.; Meijer,

E. W. *J. Am. Chem. Soc.* **2001**, *123*, 409-416; e) Brunsveld, L.; Meijer, E. W.; Prince, R. B.; Moore, J. S. *J. Am. Chem. Soc.* **2001**, *123*, 7978-7984.

[10] a) Yashima, E.; Maeda, K.; Nishimura, T. *Chem. Eur. J.* **2004**, *10*, 42-51; b) Fenniri, H.; Deng, B.-L.; Ribbe, A. E. *J. Am. Chem. Soc.* **2002**, *124*, 11064-11072; c) Mizuno, Y.; Aida, T. *Chem. Commun.* **2003**, 20-21; d) Link, D. R.; Natale, G.; Saho, R.; Maclennan, J. E.; Clark, N. A.; Körblova, E.; Walba, D. M. *Science* **1997**, *278*, 1924-1927; e) Ishi-i, T.; Crego-Calama, M.; Timmerman, P.; Reinhoudt, D. N.; Shinkai, S. *J. Am. Chem. Soc.* **2002**, *124*, 14631-14641.

[11] Prins, L. J.; Timmerman, P.; Reinhoudt, D. N. *J. Am. Chem. Soc.* **2001**, *123*, 10153-10163.

[12] Jolliffe, K. A.; Timmerman, P.; Reinhoudt, D. N. *Angew. Chem. Int. Ed.* **1999**, *38*, 933-937.

[13] Prins, L. J.; Neuteboom, E. E.; Paraschiv, V.; Crego-Calama, M.; Timmerman, P.; Reinhoudt, D. N. *J. Org. Chem.* **2002**, *67*, 4808-4820.

[14] a) Jolliffe, K.; Crego-Calama, M.; Fokkens, R.; Nibbering, N. M. M.; Timmerman, P.; Reinhoudt, D. N. *Angew. Chem. Int. Ed.* **1998**, *37*, 1247-1251; b) Timmerman, P.; Jolliffe, K. A.; Crego-Calama, M.; Weidmann, J.-L.; Prins, L. J.; Cardullo, F.; Snellink-Ruël, B. H. M.; Fokkens, R.; Nibbering, N. M. M.; Shinkai, S.; Reinhoudt, D. N.; *Chem. Eur. J.* **2000**, *6*, 4104-4115.

[15] 5-Ethyl-5-phenylbarbituric acid (EPB) was used instead of DEB because of the lack of a binding site for the Ag^+ ion in the assemblies with DEB.

[16] Paraschiv, V.; Crego-Calama, M.; Ishi-i, T.; Padberg, C. J.; Timmerman, P.; Reinhoudt, D. N. *J. Am. Chem. Soc.* **2002**, *124*, 7638-7639.

[17] Prins, L. J.; de Jong, F.; Timmerman, P.; Reinhoudt, D. N. *Nature* **2000**, *408*, 181-184.

[18] Bielejewska, A.; Marjo, C.; Prins, L. J.; Timmerman, P.; de Jong, F.; Reinhoudt, D. N. *J. Am. Chem. Soc.* **2001**, *123*, 7518-7533.

[19] Assembly (*P*)-**1a**$_3$•(BuCYA)$_{12}$ which is formed using an enantioselective process (substitution of a chiral barbiturate derivative for the nonchiral BuCYA)[13,17] has a slightly lower $\Delta\varepsilon$ than assembly (*P*)-**1a**$_3$•((*R*)-MePheCYA)$_{12}$. For this reason, the relative CD intensities were related to the ratio (*P*)-**1a**$_3$•((*R*)-MePheCYA)$_{12}$/(*P*)-**1a**$_3$•(BuCYA)$_{12}$.

[20] When the chiral centers are in the cyanurate building blocks, a center with (*R*)-stereochemistry induces generally the formation of assemblies with (*P*)-helicity. Thus, when (*R*)-MePheCYA is present the formation of the (*M*)-diastereomer is unfavorable.
[21] The kinetic model was implemented in MicroMath® Scientist® for Windows, version 2.01. However, an internal error of the software precluded the possibility to use this software and therefore the model.
[22] Negative cooperativity in assemblies formed with tetramelamine **1b** means that formation of the first double rosette disfavors formation of the second double rosette, while positive cooperativity in assemblies formed with tetramelamine **1a** means that formation of the first double rosette favors the formation of the whole assembly.
[23] Prins, L. J.; Hulst, R.; Timmerman, P.; Reinhoudt, D. N. *Chem. Eur. J.* **2002**, *8*, 2288-2301.

APPENDIX TO CHAPTER 4

This model is implemented in MicroMath® Scientis® for Windows, Version 2.01.

Thermodynamic Model

// MicroMath Scientist Model File
IndVars: RTOT
DepVars: S, R, B, PR12, MR12, PR11B1, MR11B1, PR10B2, MR10B2, PR9B3, MR9B3, PR8B4, MR8B4
DepVars: PR7B5, MR7B5, PR6B6, MR6B6, PR5B7, MR5B7, PR4B8, MR4B8, PR3B9, MR3B9
DepVars: PR2B10, MR2B10, PR1B11, MR1B11, PB12, MB12
Params: SF, KROS, fm
PR12=KROS*R^12
MR12=KROS*fm^12*R^12
PR11B1=12*KROS*R^11*B
MR11B1=12*fm^11*KROS*R^11*B
PR10B2=66*KROS*R^110*B^12
MR10B2=66*fm^10*KROS*R^10*B^2
PR9B3=220*KROS*R^9*B^3
MR9B3=220*fm^9*KROS*R^9*B^3
PR8B4=495*KROS*R^8*B^4
MR8B4=495*fm^8*KROS*R^8*B^4
PR7B5=792*KROS*R^7*B^5
MR7B5=792*fm^7*KROS*R^7*B^5
PR6B6=924*KROS*R^6*B^6
MR6B6=924*fm^6*KROS*R^6*B^6
PR5B7=792*KROS*R^5*B^7
MR5B7=792*fm^5*KROS*R^5*B^7
PR4B8=495*KROS*R^4*B^8

MR4B8=495*fm^4*R^4*B^8

PR3B9=220*KROS*R^3*B^9

MR3B9=220*fm^3*KROS*R^3*B^9

PR2B10=66*KROS*R^2*B^10

MR2B10=66*fm^2*KROS*R^2*B^10

PR1B11=12*KROS*R*B^11

MR1B11=12*fm*KROS*R*B^11

PB12=KROS*B^12

MB12=KROS*B^12

A1=12*PR12+11*PR11B1+10*PR10B2+9*PR9B3+8*PR8B4+7*PR7B5+6*PR6B6+5*PR5B7+4*PR4B8

A2=3*PR3B9+2*PR2B10+PR1B11+12*MR12+11*MR11B1+10*MR10B2+9*MR9B3+8*MR8B4

A3=7*MR7B5+6*MR6B6+5*MR5B7+4*MR4B8+3*MR3B9+2*MR2B10+MR1B11

RROS=A1+A2+A3

R=RTOT-RROS

C1=12*PB12+11*PR1B11+10*PR2B10+9*PR3B9+8*PR4B8+7*PR5B7+6*PR6B6+5*PR7B5+4*PR8B4

C2=3*PR9B3+2*PR10B2+PR11B1+12*MB12+11*MR1B11+10*MR2B10+9*MR3B9+8*MR4B8

C3=7*MR5B7+6*MR6B6+5*MR7B5+4*MR8B4*3*MR9B3+2*MR10B2+MR11B1

BROS=C1+C2+C3

B=12-RTOT-BROS

P1=PR12+PR11B1+PR10B2+PR9B3+PR8B4+PR7B5+PR6B6+PR5B7+PR4B8+PR3B9+PR2B10

P2=PR1B11+PB12

P=P1+P2

M1=MR12+MR11B1+MR10B2+MR9B3+MR8B4+MR7B5+MR6B6+MR5B7+MR4B8+MR3B9+MR2B10

M2=MR1B11+MB12

M=M1+M2

S=SF*((P-M)/(P+M))

0.0<R<1

0.0<B<1

***

With RTOT = total concentration of chiral cyanurate ***CYA**; S = CD-intensity;
R = concentration of ***CYA**; B = concentration of **CYA**; SF = scaling factor;
$f_m = \exp -((\Delta G_{P/M}^0)/RT)$; KROS = 10^{10}. In this model the composition of the assemblies is given by the letters R and B (R for ***CYA** and B for **CYA**) and the chirality of the assembly by the letter M or P.

Chapter 5

Hydrogen-bonded receptors for stereoselective recognition of saccharides*

In this chapter the stereoselective recognition of saccharides by a noncovalent hydrogen-bonded tetrarosette receptor is described. The tetrarosette $\mathbf{1}_3$•$(DEB)_{12}$*, which is present as a racemic mixture of M- and P-helices, recognizes a saccharide molecule leading to the amplification of one of the enantiomeric receptors. This stereoselective process is studied by* ^1H *NMR and CD-spectroscopy.*

* This work has been published: Ishi-i, T.; Mateos-Timoneda, M. A.; Timmerman, P.; Crego-Calama, M.; Reinhoudt, D. N.; Shinkai, S. *Angew. Chem. Int. Ed.* **2003**, *42*, 2300-2305.

5.1. Introduction

The design of new synthetic receptors is a fast-growing area of supramolecular chemistry,[1] with the aim to understand and use intermolecular forces to produce devices such as catalysts and sensors. One important feature for the development of such devices is the control over the chirality of the molecular recognition process. Important guidelines for efficient chiral recognition are (a) a high degree of preorganization of the receptor and (b) oriented host-guest interactions such as H-bonding, both of which are essential for the selective complexation of one enantiomeric guest over the other.[2]

Saccharide recognition is very important for many processes occurring in nature, such as cell-cell interaction, carbohydrate transportation, and carbohydrate metabolism.[3,4] X-ray crystallographic analysis of saccharide-protein complexes has revealed that neutral and charged functionalities are preorganized in the three dimensional binding pocket that recognizes saccharide molecules via hydrogen-bonding interactions.[5] This has provided valuable information for the design of artificial saccharide receptors.[6-13] Generally, these receptors have a covalent scaffold decorated with neutral[6-12] and charged functionalites.[13] Moreover, several covalent receptors display enantioselectivity in the recognition of the saccharide guests.[8,14]

Recently, noncovalent synthesis[15] has led to new types of artificial receptors that self-assembled via multiple noncovalent interactions such as hydrogen-bonding[16] or metal-ligand interactions,[17] with the advantage of using dynamic combinatorial chemistry to generate large numbers of receptors in a easy way, and thus, increasing the chances to find better receptors for the target guest.[18,19] In this chapter, the carbohydrate recognition by hydrogen-bonded tetrarosette assemblies is described.

5.2. Results and discussion

5.2.1. Formation of tetrarosette assemblies $\mathbf{1}_3$•(BA/CYA)$_{12}$ and $\mathbf{4}_3$•(BA/CYA)$_{12}$

Hydrogen-bonded tetrarosette assemblies $\mathbf{1}_3$•(BA/CYA)$_{12}$ and $\mathbf{4}_3$•(BA/CYA)$_{12}$ are formed from 15 components, three calix[4]arene tetramelamine **1** or **4** and twelve barbituric acid (BA) or cyanuric acid (CYA) derivatives (Chart 5.1).[20-22]

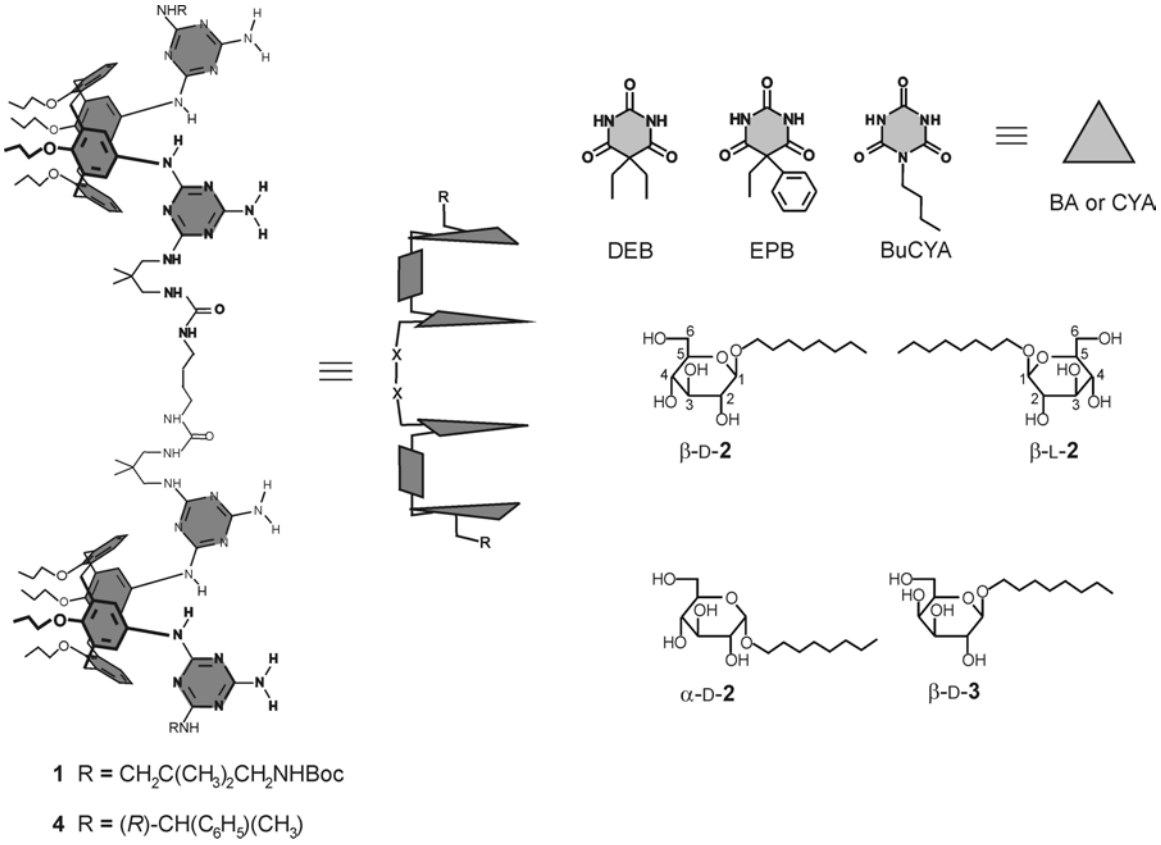

Chart 5.1. Chemical and schematic representation of the tetramelamines **1** and **4**, cyanurate/barbiturate derivatives, and saccharide guest molecules. Boc = *tert*-butyloxycarbonyl.

A total of 72 cooperative hydrogen bonds hold the building blocks together to form a fully assembled tetrarosette structure, each 'floor' of the assembly corresponding to one rosette motif (Figure 5.1). Tetramelamines **1** and **4** consist of two calix[4]arene units, which are covalently connected via two urea moieties. By the self-assembly of the tetrarosette receptor, a total of six urea functionalities are positioned in the central cavity, formed between the two double rosette motifs, for saccharide recognition. In the absence

of any source of chirality, the tetrarosette assembly is present as a racemic mixture of *P*- and *M*-enantiomers ((*P*)-**1**$_3$•(BA/CYA)$_{12}$ and (*M*)-**1**$_3$•(BA/CYA)$_{12}$) (Figure 5.1a), while the introduction of chiral centers (*R*)- or (*S*)- in the tetramelamine moieties of the assembly leads to the formation of exclusively one of the two possible diastereomers (Figure 5.1b).[23]

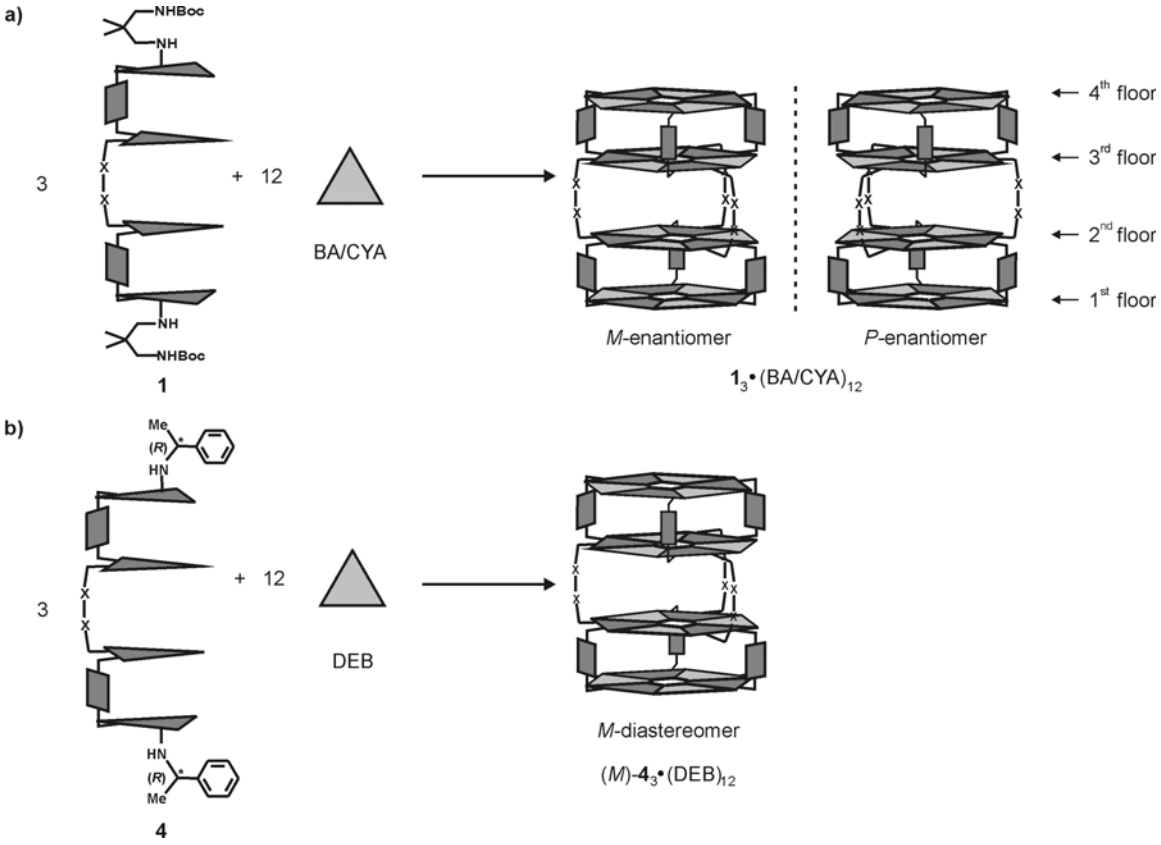

Figure 5.1. Schematic representation of the formation of the tetrarosette assembly from a) achiral and b) chiral tetramelamine.

5.2.2. Recognition of saccharides by a racemic mixture of receptors

Recognition of *n*-octyl β-D-glucopyranoside (β-D-**2**) by **1**$_3$•(DEB)$_{12}$ (DEB = 5,5-diethyl barbituric acid) is reflected in shifts and splitting of the ^{1}H NMR signals in $CDCl_3$ (Figure 5.2). As expected, in addition to the original NH^A signal of the urea, a new signal (NH$^{A'}$) corresponding to the complex between one of the isomers (*P*- or *M*-) of **1**$_3$•(DEB)$_{12}$ and β-D-**2** is observed at lower magnetic field (Δδ 0.05 ppm, 10 equivalents

of β-D-**2**). Possibly, the downfield shift is due to the formation of one hydrogen-bond between the urea carbonyl group of $\mathbf{1}_3$•$(DEB)_{12}$ and one hydroxyl group of β-D-**2**. More importantly, similar shifts and splittings upon guest binding are observed for H^{a2} and H^{c2} signals on the second and third rosette floors, whereas the corresponding signals on the first and fourth floors show no splitting.[24] The intensities of the new signals ($H^{a2'}$ and $H^{c2'}$) slightly increase with the amount of β-D-**2** added, whereas the original signals decrease. This means that from the racemic mixture of the *P*- and *M*-isomers of $\mathbf{1}_3$•$(DEB)_{12}$,[20] one of the two enantiomers recognizes the chiral guest stereoselectively, resulting in the formation of one diastereomeric complex.

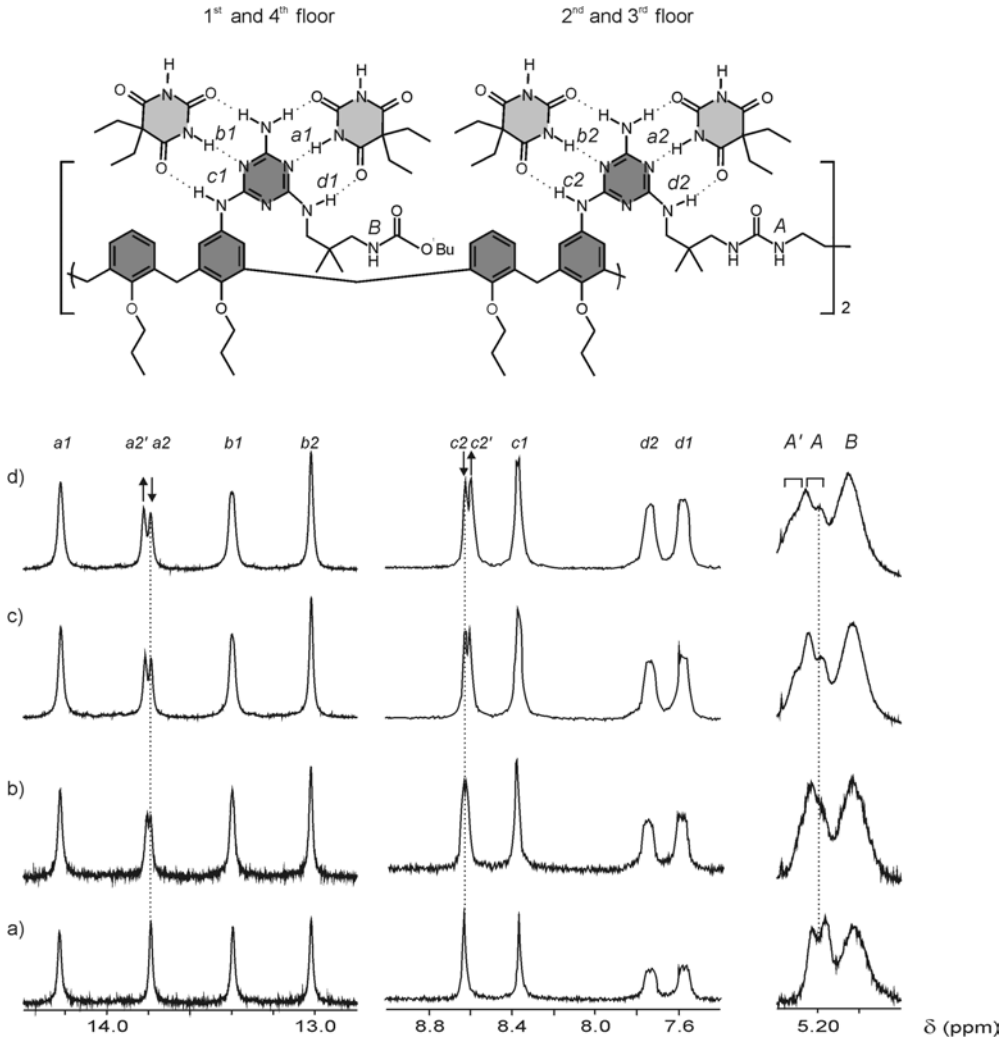

Figure 5.2. Parts of the ^{1}H NMR spectra of $\mathbf{1}_3$•$(DEB)_{12}$ (1 mM) in $CDCl_3$ at 20°C in the presence of a) 0, b) 3, c) 5, and d) 10 equivalents of β-D-**2**.

This conclusion is supported by the induced signal in the Circular Dichroism (CD) spectrum. The racemic mixture of (*M*)-**1**$_3$•(DEB)$_{12}$ and (*P*)-**1**$_3$•(DEB)$_{12}$ is CD silent. The addition of β-D-**2** to this mixture induces a negative Cotton effect around 290-310 nm, a clear evidence for the formation of the *P*-rosette assembly (Figure 5.3).[23]

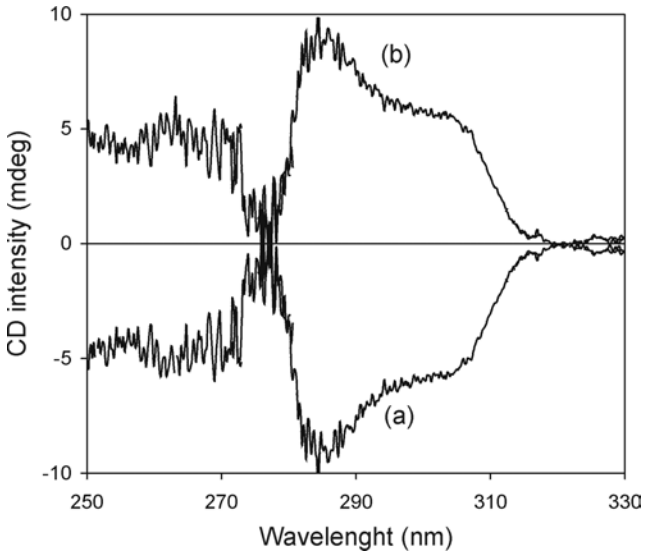

Figure 5.3. CD spectra of **1**$_3$•(DEB)$_{12}$ (1 mM) in the presence of 10 equivalents of (a) β-D-**2** and (b) β-L-**2** in $CDCl_3$ (in 0.01 cm width cell at 20 ^oC).

Thus, as a result of the chiral recognition, the *P*-enantiomer, which binds β-D-**2** more strongly, is amplified in the mixture as both enantiomers (*P*- and *M*-) are in dynamic equilibrium (Figure 5.4).[25] Subsequently, a ^1H NMR titration was performed with *n*-octyl β-L-glucopyranoside (β-L-**2**). Also the chiral recognition of β-L-**2** by (*M*)-**1**$_3$•(DEB)$_{12}$ is reflected in shifts and splittings of the ^1H NMR signals in $CDCl_3$. As expected, the appearance of a positive Cotton effect around 290-310 nm in the CD spectrum was observed, indicating the amplification of the *M*-rosette assembly.

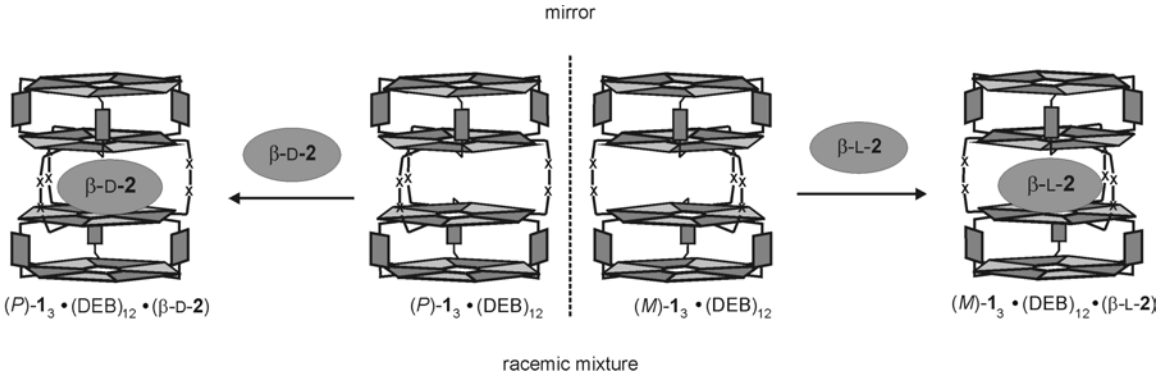

Figure 5.4. Schematic representation of the enantioselective recognition of saccharides by a racemic mixture of assemblies.

On the basis of CD-data, binding constants K_P for the complexation **1**$_3$•(DEB)$_{12}$ with β-D-**2** and β-L-**2** can be obtained according to equations (Eq. 5.1-5.5, see below). In this chiral complexation, it is assumed that the binding constant (K_P) of β-D-**2** with (*P*)-**1**$_3$•(DEB)$_{12}$ is much larger than that (K_M) with (*M*)-**1**$_3$•(DEB)$_{12}$.

$$K_P = \frac{[(P)\text{-}\mathbf{1}_3\cdot(\mathrm{DEB})_{12}\cdot(\beta\text{-}\mathrm{D}\text{-}\mathbf{2})]}{[(P)\text{-}\mathbf{1}_3\cdot(\mathrm{DEB})_{12}][(\beta\text{-}\mathrm{D}\text{-}\mathbf{2})]} \qquad \text{(Eq. 5.1)}$$

$$[(P)\text{-}\mathbf{1}_3\cdot(\mathrm{DEB})_{12}] = [(M)\text{-}\mathbf{1}_3\cdot(\mathrm{DEB})_{12}] = \left(1-\frac{\frac{d.e.}{100}}{2}\right)\times[\mathbf{1}_3\cdot(\mathrm{DEB})_{12}]_0 \qquad \text{(Eq. 5.2)}$$

$$[\beta\text{-}\mathrm{D}\text{-}\mathbf{2}] = [\beta\text{-}\mathrm{D}\text{-}\mathbf{2}]_0 - \left(\frac{d.e.}{100}\times[\mathbf{1}_3\cdot(\mathrm{DEB})_{12}]_0\right) \qquad \text{(Eq. 5.3)}$$

$$[(P)\text{-}\mathbf{1}_3\cdot(\mathrm{DEB})_{12}\cdot(\beta\text{-}\mathrm{D}\text{-}\mathbf{2})] = \frac{d.e.}{100}\times[\mathbf{1}_3\cdot(\mathrm{DEB})_{12}]_0 \qquad \text{(Eq. 5.4)}$$

$$d.e.(\%) = \left(\frac{\mathrm{CD_{obs}}}{\mathrm{CD}_{100\%d.e.}}\right)\times 100 \qquad \text{(Eq. 5.5)}$$

in which, [(*P*)-**1**$_3$•(DEB)$_{12}$•(β-D-**2**)], [(*M*)-**1**$_3$•(DEB)$_{12}$], [(*P*)-**1**$_3$•(DEB)$_{12}$], and [β-D-**2**] are the concentrations of the corresponding species, [**1**$_3$•(DEB)$_{12}$]$_0$ and [β-D-**2**]$_0$ are initial concentrations of host and guest, and *d.e.* (%) is the diastereomeric excess of *P*-assemblies that is obtained from the ratio of observed and standard CD intensities (CD_{obs}

and $CD_{100\%\ d.e.}$). The CD intensity (67 mdeg) at 300 nm of the diastereomer (*M*)-**4**$_3$•$(DEB)_{12}$ is used as reference ($CD_{100\%\ d.e.}$), because the CD spectral shape of (*M*)-**4**$_3$•$(DEB)_{12}$ is similar to that of **1**$_3$•$(DEB)_{12}$•(β-D-**2**) complex. Under the conditions ([**1**$_3$•$(DEB)_{12}$]$_0$ = 1 mM, [β-D-**2**]$_0$ = 10 mM, $CD_{obs\ 300\ nm}$ = 6 mdeg, *d.e.* = 9%), a K_p value of 20 M^{-1} can be estimated.

The 1:1 stoichiometry of the complexes (*P*)-**1**$_3$•$(DEB)_{12}$•(β-D-**2**) and (*M*)-**1**$_3$•$(DEB)_{12}$•(β-L-**2**) was determined from a Job plot (Figure 5.5).[26,27]

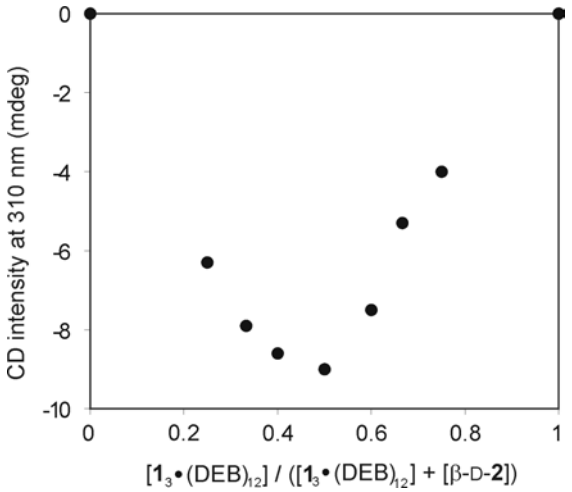

Figure 5.5. Job plot for the complexation of **1**$_3$·$(DEB)_{12}$ with β-D-**2**: the sum of [**1**$_3$·$(DEB)_{12}$] and [β-D-**2**] was maintained constant (10 mM) in $CDCl_3$.

While similar chiral recognition of β-D-**2** using different barbiturate-based assembly **1**$_3$•$(EPB)_{12}$ (EPB = 5-ethyl-5-phenyl barbituric acid) was observed by ^{1}H NMR and CD spectroscopy, the cyanuric acid-based assembly **1**$_3$•$(BuCYA)_{12}$ did not show any shift or splitting in the ^{1}H NMR spectrum. Furthermore, for this assembly the CD spectrum upon addition of β-D-**2** remained unchanged,[28] indicating no complexation of the saccharide by the receptor **1**$_3$•$(BuCYA)_{12}$. Most certainly, the different orbital electron distribution for BA and CYA is the reason for the distinct behavior.[29]

Computational studies (gas phase MM calculation, Quanta 97/CHARMm 24.0) confirmed the observed enantioselectivity. In the complex with (*P*)-**1**$_3$•$(DEB)_{12}$, β-D-**2** is located in the cavity without any steric hindrance (Figure 5.6). A urea carbonyl group in the receptor forms a hydrogen bond with the hydroxyl group at the 4-position of β-D-**2**

(see chart 5.1 for numerical assigment). In contrast, for the 'mismatching' complex (*P*)-**1**$_3$•(DEB)$_{12}$•(β-L-**2**), the modeling shows that the alkyl chain of β-L-**2** breaks the hydrogen bonding network on the second rosette floor.

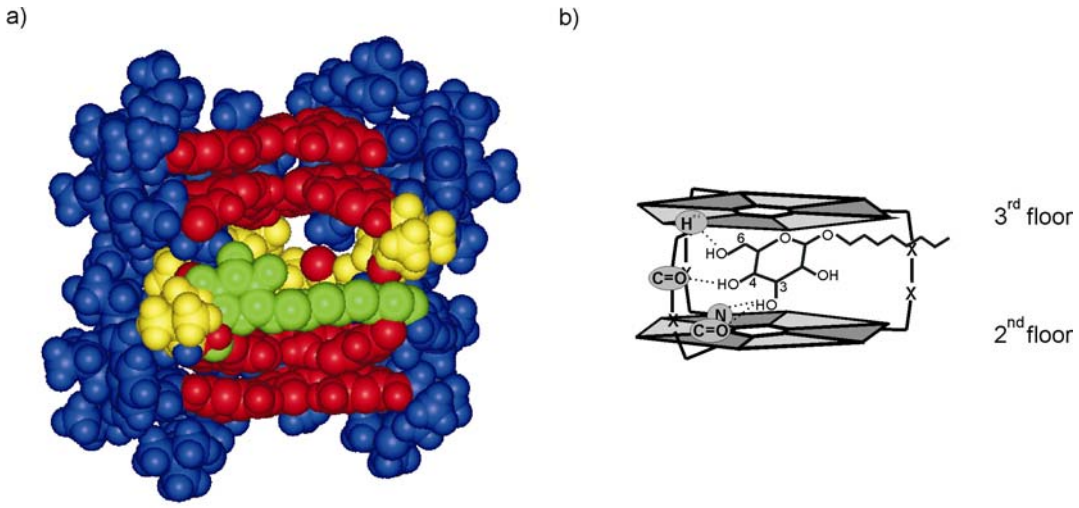

Figure 5.6. a) Computer simulated structure of (*P*)-**1**$_3$•(DEB)$_{12}$•(β-D-**2**) (a cross-sectional view of the assembly is depicted to show the environment inside the cavity occupied by the sugar) (blue = calix[4]arene, red = rosette floors, green = saccharide, and yellow = urea groups). b) Schematic representation of (*P*)-**1**$_3$•(DEB)$_{12}$•(β-D-**2**) (for clarity only the second and third floors of the tetrarosette assembly are shown).

In contrast to β-D-**2**, its α-isomer, *n*-octyl α-D-glucopyranoside (α-D-**2**), and epimer, *n*-octyl β-D-galactopyranoside (β-D-**3**) (see Chart 5.1 for chemical structures), were not recognized by **1**$_3$•(DEB)$_{12}$ as indicated by no shifting or splitting of the ^{1}H NMR signals and no presence of CD-signal. This trend in the complexation can be rationalized by the strength of the intramolecular hydrogen-bonds in the pyranosides.[8-10] The intramolecular hydrogen bonds that would be affected by the complexation (Figure 5.7) become stronger upon changing from α-D-**2** to β-D-**3**. This analysis suggests that pyranosides in which weaker intramolecular hydrogen bonds are disrupted during the recognition process bind more strongly to the receptor.

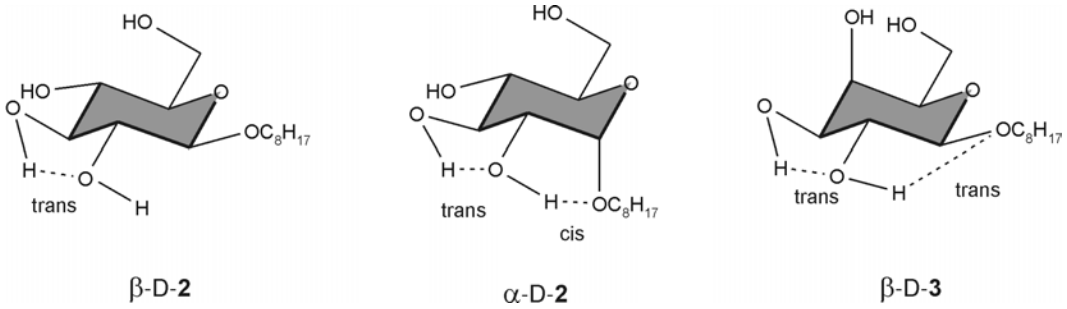

Figure 5.7. Intramolecular hydrogen bonds in compound β-D-**2**, α-D-**2**, and β-D-**3** that compete with hydrogen bonding in the complexation process.

5.2.3. Saccharide recognition by chiral receptors

To further probe the stereoselectivity of the recognition of saccharide by the tetrarosette assemblies, complexation experiments using chiral receptor (*M*)-**4**$_3$•(DEB)$_{12}$ were performed. In this case, instead of the racemic mixture of receptors (*P*)-**1**$_3$•(DEB)$_{12}$ and (*M*)-**1**$_3$•(DEB)$_{12}$, the diastereomeric assembly (*M*)-**4**$_3$•(DEB)$_{12}$ is used as receptor.

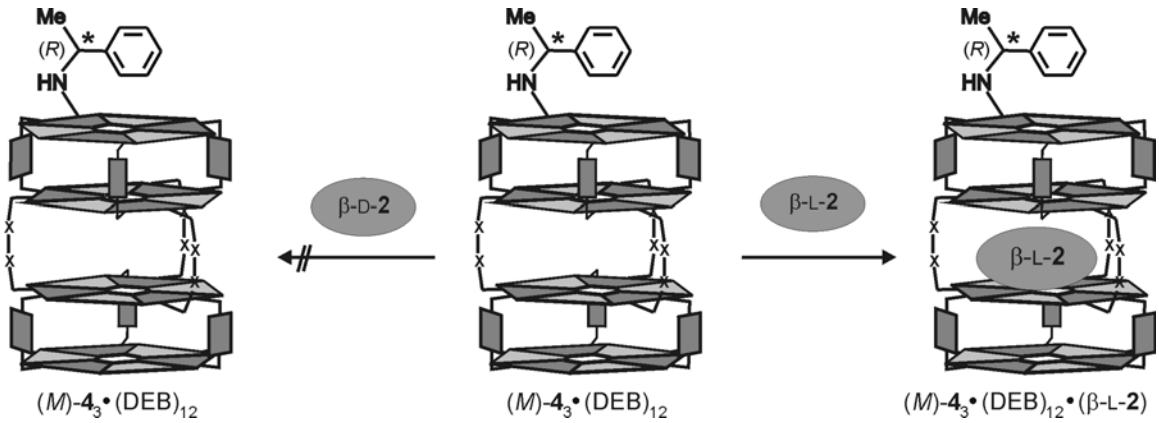

Figure 5.8. Schematic representation of the enantioselective recognition of saccharides by a chiral tetrarosette.

The 'mismatch' combination of receptor (*M*)-**4**$_3$•(DEB)$_{12}$ and β-D-**2** (Figure 5.8) does not show any changes in the ^{1}H NMR spectrum. In contrast, the recognition of *n*-octyl-β-L-glucopyranoside (β-L-**2**) by (*M*)-**4**$_3$•(DEB)$_{12}$ (matching pair) is reflected in the corresponding shifts in the ^{1}H NMR spectra in $CDCl_3$ (Figure 5.9). Similarly as observed for assembly **1**$_3$•(DEB)$_{12}$, the urea proton NH^A shifts to lower magnetic field (Δδ 0.10

ppm, 10 equivalents of β-L-**2**) together with shifts for H^{a2} and H^{c2} on the second and third rosette floors were observed, whereas the corresponding signals (H^{a1} and H^{c1}) on the first and fourth floors remained unchanged.

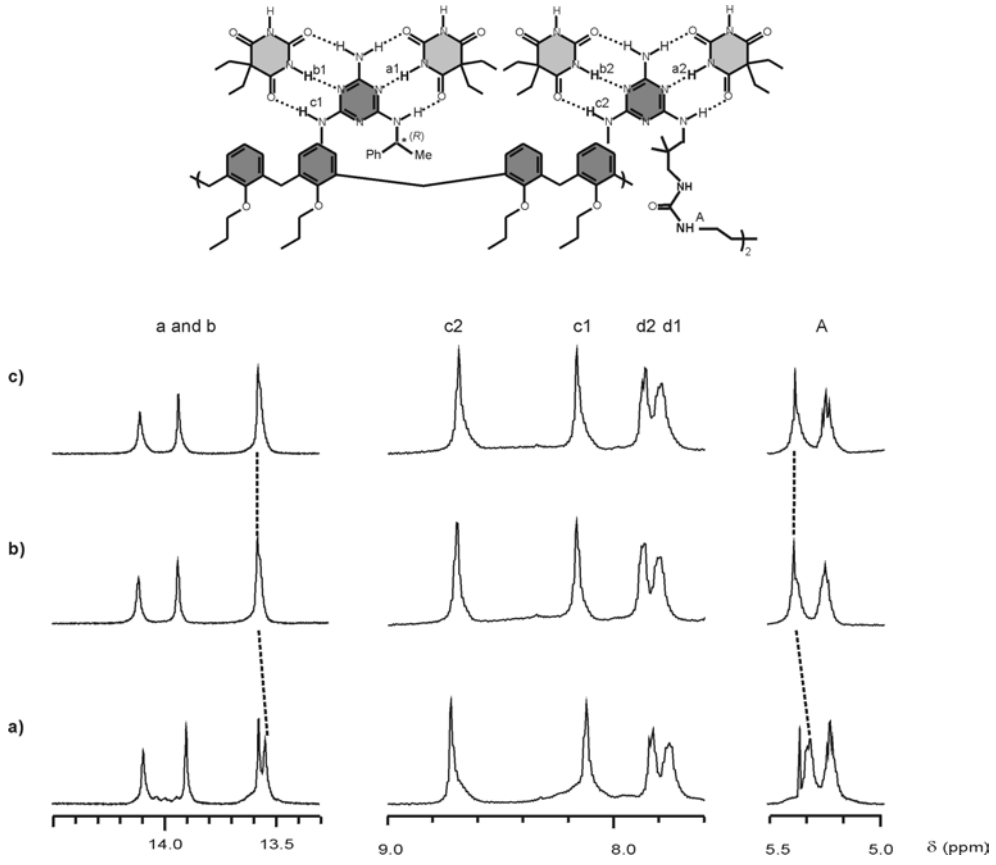

Figure 5.9. ^{1}H NMR spectra of $\mathbf{4}_3\cdot(DEB)_{12}$ (1mM) in $CDCl_3$ at 20 °C in the presence of a) 0, b) 5, and c) 10 equivalents of β-L-**2**.

In contrast to what occurred in the complexation studies with the racemic mixture (*M*/*P*)-$\mathbf{1}_3$•$(DEB)_{12}$, the addition of β-L-**2** to the chiral assembly (*M*)-$\mathbf{4}_3$•$(DEB)_{12}$ does not result in measurable changes in the CD spectra (Figure 5.10). Assembly (*M*)-$\mathbf{4}_3$•$(DEB)_{12}$ is already diastereomerically pure thus the complexation of the guest saccharide is not accompanied by an increase in the concentration of the best receptor, resulting in the absence of changes in the CD-spectrum.

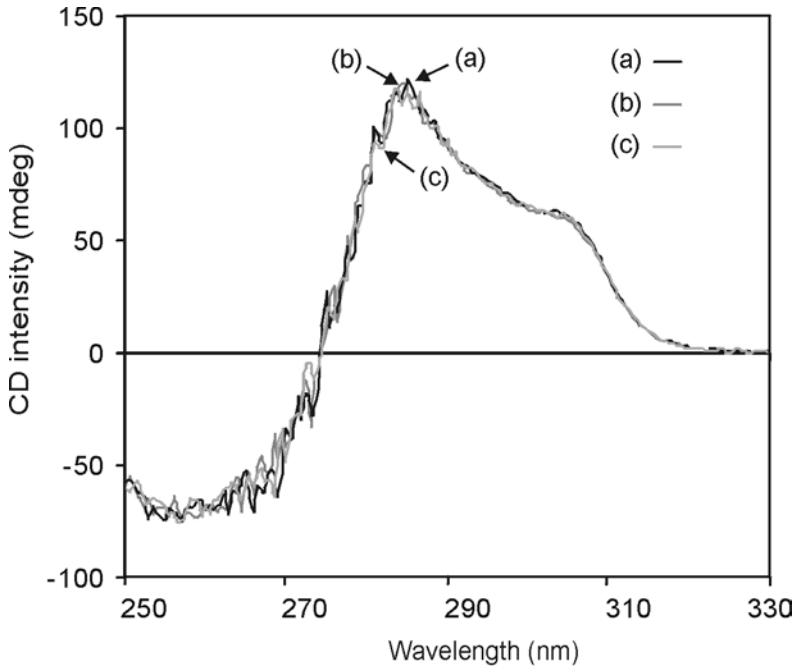

Figure 5.10. CD spectrum of $\mathbf{4}_3$·$(DEB)_{12}$ (1mM) in $CDCl_3$ in the presence of (a) 0 (black line), (b) 5 (grey line), and (c) 10 equivalents (light grey line) of β-L-**2**.

5.3. Conclusions

In conclusion, the results showed in this chapter demonstrate for the first time the recognition of saccharides by a hydrogen-bonded assembly. More important, the recognition of the monosaccharide guest molecules occurs enantioselectively and displays selectivity against different saccharides. Futhermore, the addition of an enantiomeric saccharide to the racemic mixture of the enantiomeric receptors leads to the complexation of the chiral guest only by one of the enantiomeric receptors, resulting in the amplification of the best receptor. This enantioselective recognition of saccharide molecules was also demonstrated using a diastereomeric assembly. This diastereomeric receptor is only capable to complex one enantiomer of the guest.

Previous studies in our group have shown that the tetrarosette assemblies are quite stable even in polar media (at least up to 60% methanol/$CDCl_3$). Thus, the saccharide recognition with similar assemblies in polar environment is feasible.

5.4. Experimental section

^{1}H NMR spectra were recorded on a Varian Inova 300 spectrometer or on a Varian Unity 400 WB spectrometer. Residual solvent protons were used as an internal standard and chemical shifts are given relative to tetramethylsilane (TMS) or to the residual solvent signal. Laser desorption ionization mass spectrometry was performed using a modified MALDI-TOF instrument (Voyager RP-DE, Perseptive Biosystems/Applied Biosystems, Framingham, MA, USA), equipped with delayed extraction. A 337 nm UV nitrogen laser producing 2 ns pulses and the mass spectra were obtained in the linear mode. No organic acid matrix could be used during the experiments due to instability of the assemblies. An 8-10 μl of the sample of a known concentration was deposited on the (cold) spot-well, adding a 0.5 μl of a 10-6 molar solution of $AgOOCCF_3$. The samples were covered by a non-acidic liquid polymer-film, not interacting or mixing with the samples. To avoid crystallization of the samples, the pressure in the ion source was reduced drastically, keeping the pressure in the time-of-flight region under relatively high vacuum. The samples were introduced via a sample-plate insertion system at near atmosphere pressure. Threshold laser energies were used in order to avoid fragmentation due to high-energy laser power. After each experiment internal calibrations were performed using a mixture of a known proteins (ACTH 1-36, Bovine Insulin B oxidized, Bovine Insulin, Myoglobin (horse heart) and Cytochrome C (horse heart)) of the selected mass range. CD spectra were measured on a JASCO J-715 spectropolarimeter in a 0.01 cm width cell. Compounds **1**,[22] **4**,[22] BuCYA,[30] and β-L-**2**[31] were synthesized according to methods described previously. All the remaining compounds and reagents were purchased from Aldrich, Fluka, or Acros and used without further purification.

Molecular mechanics calculations. Initial structures, created by manual modification of the X-ray structure of a double rosette assembly,[30] and by observed NOE connectivities used as distance constraints, as well as visualizations were carried out with Quanta 97.[32] The MD calculations were run with CHARMm, version 24.0.[33] Parameters were taken from Quanta 97, and point charges were assigned with the charge template

option in Quanta/CHARMm; excess charge was smoothened, rendering overall neutral residues. A distance-dependent dielectric constant was applied with ε = 1. No cut-offs on the nonbonded interactions were used. Energy-minimized were performed with the Steepest Descent and Adopted Basis Newton-Raphson methods until the root mean square of the energy gradient was <0.001 kcal mol^{-1} $Å^{-1}$.

5.5. References and notes

[1] Webb, T. H.; Wilcox, C. S. *Chem. Soc. Rev.* **1993**, *22*, 383-395.

[2] Alcazar, V.; Diederich, F. *Angew. Chem. Int. Ed. Engl.* **1992**, *31*, 1521-1523.

[3] Davis, A. P.; Wareham, R. S. *Angew. Chem. Int. Ed.* **1999**, *38*, 2978-2996.

[4] a) James, T. D.; Sandanayake, K. R. A. S.; Shinkai, S. *Angew. Chem. Int. Ed. Engl.* **1996**, *35*, 1910-1922; b) James, T. D.; Linnane, P.; Shinkai, S. *Chem. Commun.* **1996**, 281-288.

[5] a) Lemieux, R. U. *Chem. Soc. Rev.* **1989**, *18*, 347-374; b) Quiocho, F. A. *Pure Appl. Chem.* **1989**, *61*, 1293-1306; c) Weis, W. I.; Drickhamer, K. *Annu. Rev. Biochem.* **1996**, *65*, 441-473; d) Spurlino, S. P.; Lu, G.-Y.; Quiocho, F. A. *J. Biol. Chem.* **1991**, *266*, 5202-5219.

[6] a) Bonar-Law, R. P.; Davis, A. P.; Murray, B. A. *Angew. Chem. Int. Ed. Engl.* **1990**, *29*, 1407-1408; b) Davis, A. P.; Menzer, S.; Walsh, J. J.; Williams, D. J. *Chem. Commun.* **1996**, 453-455; c) Mizutani, T.; Kurahashi, T.; Murakami, T.; Matsumi, N.; Ogoshi, H. *J. Am. Chem. Soc.* **1997**, *119*, 8991-9001; d) Bhattarai, K. M.; Davis, A. P.; Perry, J. J.; Walter, C. J. *J. Org. Chem.* **1997**, *62*, 8463-8473; e) Inoue, M.; Chiba, J.; Nakazumi, H. *J. Org. Chem.* **1999**, *64*, 8170-8176; f) Mazik, M.; Bandmann, H.; Sicking, W. *Angew. Chem. Int. Ed.* **2000**, *39*, 551-554; g) Mazik, M.; Sicking, W. *Chem. Eur. J.* **2001**, *7*, 664-670; h) Benito, J. M.; Gómez-García, M.; Blanco, J. L. J.; Mellet, C. O.; Fernández, J. M. G. *J. Org. Chem.* **2001**, *66*, 1366-1372.

[7] Kikuchi, Y.; Tanaka, Y.; Sutarto, S.; Kobayashi, K.; Toi, H.; Aoyama, Y. *J. Am. Chem. Soc.* **1992**, *114*, 10302-10306.

[8] Bonar-Law, R. P.; Sanders, J. K. M. *J. Am. Chem. Soc.* **1995**, *117*, 259-271.

[9] Huang, C.-Y.; Cabell, L. A.; Anslyn, E. V. *J. Am. Chem. Soc.* **1994**, *116*, 2778-2792.

[10] Cuntze, J.; Owens, L.; Alcázar, V.; Seiler, P.; Diederich, F. *Helv. Chim. Acta* **1995**, *78*, 367-390.

[11] a) Bhattarai, K. M.; Bonar-Law, R. P.; Davis, A. P.; Murray, B. A. *J. Chem. Soc., Chem. Commun.* **1992**, 752-754; b) Liu, R.; Still, W. C. *Tetrahedron Lett.* **1993**, *34*, 2573-2576; c) Anderson, S.; Neidlein, U.; Gramlich, V.; Diederich, F. *Angew. Chem. Int. Ed. Engl.* **1995**, *34*, 1596-1600; d) Smith, D. K.; Diederich, F. *Chem. Commun.* **1998**, 2501-2502; e) Bähr, A.; Droz, A. S.; Püntener, M.; Neidlein, U.; Anderson, S.; Seiler, P.; Diederich, F. *Helv. Chim. Acta* **1998**, *81*, 1931-1963; f) Kim, H.-J.; Kim, Y.-H.; Hong, J.-I. *Tetrahedron Lett.* **2001**, *42*, 5049-5052.

[12] a) Davis, A. P.; Wareham, R. S. *Angew. Chem. Int. Ed.* **1998**, *37*, 2270-2273; b) Rusin, O.; Král, V. *Chem. Commun.* **1999**, 2367-2368; c) Rusin, O.; Král, V. *Tetrahedron Lett.* **2001**, *42*, 4235-4238; d) Rusin, O.; Lang, K.; Král, V. *Chem. Eur. J.* **2002**, *8*, 655-663.

[13] a) Das, G.; Hamilton, A. D. *J. Am. Chem. Soc.* **1994**, *116*, 11139-11140; b) Neidlein, U.; Diederich, F. *Chem. Commun.* **1996**, 1493-1494; c) Das, G.; Hamilton, A. D. *Tetrahedron Lett.* **1997**, *38*, 3675-3678; d) Droz, A. S.; Diederich, F. *J. Chem. Soc., Perkin Trans. 1* **2000**, 4224-4226; e) Král, V.; Rusin, O.; Charvátová, J.; Anzenbacher, J. Jr.; Fogl, J. *Tetrahedron Lett.* **2000**, *41*, 10147-10151; f) Král, V.; Rusin, O.; Schimdtchen, F. P. *Org. Lett.* **2001**, *3*, 873-876; g) Bitta, J.; Kubik, S. *Org. Lett.* **2001**, *3*, 2637-2640; h) Tamaru, S.; Yamamoto, M.; Shinkai, S.; Khasanov, A. B.; Bell, T. W. *Chem. Eur. J.* **2001**, *7*, 5270-5276; i) Tamaru, S.; Shinkai, S.; Khasanov, A. B.; Bell, T. W. *Proc. Natl. Acad. Sci. USA* **2002**, *99*, 4972-4976.

[14] a) Bhattarai, K. M.; Bonar-Law, R. P.; Davis, A. P.; Murray, B. A. *J. Chem. Soc., Chem. Commun.* **1992**, 752-754; b) Hong, J.-I.; Namgoong, S. K.; Bernardi, A.; Still, W. C. *J. Am. Chem. Soc.* **1991**, *113*, 5111-5112; c) Still, W. C. *Acc. Chem. Res.* **1996**, *29*, 155-163; d) Striegel, S. *Curr. Org. Chem.* **2003**, *7*, 81-102.

[15] Reinhoudt, D. N.; Crego-Calama, M. *Science* **2002**, *295*, 2403-2407.

[16] a) Conn, M. M.; Rebek, J. Jr. *Chem. Rev.* **1997**, *97*, 1647-1668; b) Rebek, J. Jr. *Acc. Chem. Res.* **1999**, *32*, 278-286; c) Rebek, J. Jr. *Chem. Commun.* **2000**, 637-643; d) Prins, L. J.; Timmerman, P.; Reinhoudt, D. N. *Angew. Chem. Int. Ed.* **2001**, *40*, 2383-2426.

[17] a) Linton, B.; Hamilton, A. D. *Chem. Rev.* **1997**, *97*, 1669-1680; b) Fujita, M. *Chem. Soc. Rev.* **1998**, *27*, 417-425; c) Caulder, D. L.; Raymond, K. N. *Acc. Chem. Res.* **1999**, *32*, 975-982; d) Caulder, D. L.; Raymond, K. N. *J. Chem. Soc.; Dalton Trans.* **1999**, 1185-1200; e) Fujita, M.; Umemoto, K.; Yoshizawa, M.; Fujita, N.; Kusukawa, T.; Biradha, K. *Chem. Commun.* **2001**, 509-518.

[18] Goodman, M. S.; Jubian, V.; Linton, B.; Hamilton, A. D. *J. Am. Chem. Soc.* **1995**, *117*, 11610-11611.

[19] a) Crego-Calama, M.; Hulst, R.; Fokkens, R.; Nibbering, N. M. M.; Timmerman, P.; Reinhoudt, D. N. *Chem. Commun.* **1998**, 1021-1022; b) Crego-Calama, M.; Timmerman, P.; Reinhoudt, D. N. *Angew. Chem. Int. Ed.* **2000**, *39*, 755-758.

[20] Jolliffe, K. A.; Timmerman, P.; Reinhoudt, D. N. *Angew. Chem. Int. Ed.* **1999**, *38*, 933-937.

[21] Paraschiv, V.; Crego-Calama, M.; Ishi-i, T.; Padberg, C. J.; Timmerman, P.; Reinhoudt, D. N. *J. Am. Chem. Soc.* **2002**, *124*, 7638-7639.

[22] Prins, L. J.; Neuteboom, E. E.; Paraschiv, V.; Crego-Calama, M.; Timmerman, P.; Reinhoudt, D. N. *J. Org. Chem.* **2002**, *67*, 4808-4820.

[23] Prins, L. J.; Huskens, J.; de Jong, F.; Timmerman, P.; Reinhoudt, D. N. *Nature* **1999**, *398*, 498-502.

[24] The signal of H^c of the 1st and 4th floor of the receptor suffers a very small splitting. However, this split might be due to small conformational changes of the assembly during the recognition of the saccharide molecules.

[25] a) Ishi-i, T.; Crego-Calama, M.; Timmerman, P.; Reinhoudt, D. N.; Shinkai, S. *Angew. Chem. Int. Ed.* **2002**, *41*, 1924-1929; b) Ishi-i, T.; Crego-Calama, M.; Timmerman, P.; Reinhoudt, D. N.; Shinkai, S. *J. Am. Chem. Soc.* **2002**, *124*, 14631-14641.

[26] Job, A. *Justus Liebigs Ann. Chem.* **1928**, *9*, 113-134.

[27] MALDI-TOF mass spectrometry by using Ag^+-labeling technique to detect the complex was also used. However, only the ion peak of the parent assembly was observed at m/z = 9978.0 (calcd for $C_{528}H_{684}N_{114}O_{78}Ag$, 9976.2). For MALDI-TOF mass spectrometry using Ag^+-labeling technique see: Timmerman, P.; Jolliffe, K. A.; Crego-Calama, M.; Weindmann, J.-L.; Prins, L. J.; Cardullo, F.; Snellink-Ruel, B. H. M.;

Fokkens, R.; Nibbering, N. M. M.; Shinkai, S.; Reinhoudt, D. N. *Chem. Eur. J.* **2000**, *6*, 4104-4115.

[28] $\mathbf{1}_3$•$(BuCYA)_{12}$ was obtained by two different methods:[20] (i) from $\mathbf{1}_3$•$(DEB)_{12}$ upon exchange of DEB for BuCYA and (ii) the direct mixing of **1** and BuCYA in toluene and subsequent heating (100 °C) and evaporation. Neither case showed complexation with β-D-**2** even after 2 weeks or higher temperature (55 °C).

[29] The three dimensional structure of DEB, which is arising from sp^3-carbon in a 6-membered ring, is better suited for guest encapsulation, while the flatter structure of BuCYA is less favored because the complexed guest could be expelled out more easily.

[30] Timmerman, P.; Vreekamp, R. H.; Hulst, R.; Verboom, W.; Reinhoudt, D. N.; Rissanen, K.; Udachin, K. A.; Ripmeester, J. *Chem. Eur. J.* **1997**, *3*, 1823-1832.

[31] Vill, V.; Böcker, T.; Thiem, J.; Fischer, F. *Liq. Crystals* **1989**, *6*, 349-356.

[32] Quanta97, *Molecular Simulations*, Waltham, MA, **1997**.

[33] a) Brooks, B. R.; Bruccoleri, R. E.; Olafsen, B. D.; States, D. J.; Swaminathan, S.; Karplus, M. *J. Comput. Chem*. **1983**, *4*, 187-217; b) Momany, F. A.; Klimkowski, V. J.; Schäfer, L. *J. Comput. Chem*. **1990**, *11*, 654-662; c) Momany, F. A.; Rone, R.; Kunz, H.; Frey, R. F.; Newton, S. Q.; Schäfer, L. *J. Mol. Struct*. **1993**, *286*, 1-18.

Chapter 6

Ditopic complexation and selective release of neutral molecules by hydrogen-bonded receptors*

In this chapter the simultaneous complexation of different neutral guest molecules by noncovalent hydrogen-bonded receptors is described. The double rosette assembly $\mathbf{1}_3$•$(DEB)_6$ *is able to encapsulate selectively a neutral noncovalent trimer in the pocket situated between the two subdomains (floors) of the receptor (endo-complexation) while simultaneously complexing different neutral guest molecules at the periphery of the assembly (exo-complexation). The tetrarosette assembly* $\mathbf{2}_3$•$(DEB)_{12}$ *is able to encapsulate, in a similar manner, a noncovalent trimer in each of the pockets of the individual double rosettes (endo-complexation) while simultaneously other neutral guest molecules are encapsulated in the internal cavity situated between the two double rosette subdomains (endo-complexation). Moreover, the two types of receptors are able to selectively release the guest molecules upon the addition of the appropriate external stimuli.*

* Part of this work has been accepted for publication: Mateos-Timoneda, M. A.; Kerckhoffs, J. M. C. A.; Crego-Calama, M.; Reinhoudt, D. N. *Angew. Chem. Int. Ed.* **2005**.

6.1. Introduction

Molecular recognition is one of the key phenomena in nature that determines the function of the biomolecules. It is best expressed in the specific binding of one or several substrates to an enzyme. An extreme example of this process is the replication of DNA, in which one DNA strand is specifically recognized due to the formation of specific patterns of hydrogen bonds. The understanding of the mechanism of (bio)molecular recognition is crucial for example in the development of new drugs with activity against different diseases and to mimic the activity of these biosystems.[1-3] The 'lock-and-key' theory explains the selectivity and (stereo)specificity found in biomolecular recognition,[4] where the correct positions of the substrates arises from the formation of multiple noncovalent bonds (π–π interactions, hydrogen bonds, metal-π interactions, etc) between the different discrete binding sites of the host (lock) and the different sites for binding of the guest molecule (key).[5-7] These principles of biomolecular recognition[8] have successfully lead to synthetic receptors[9] able to bind a guest species such as cations,[10] anions,[11] or small neutral molecules.[12]

Further control of the molecular recognition process can be achieved through the formation of multiple interactions at different areas of the host molecule, as observed at the antibody-antigen interface,[13] as well as by the interaction of a host with two or more different guest molecules.[14] The knowledge of the higher hierarchy of the molecular recognition is also important for the understanding in the recognition of a variety of biomolecular processes. For example, at the active site of the enzymes, specific recognition of the transition state by the enzyme is required (selective *endo*-recognition), whereas the initial protein-protein recognition can be more loose and flexible (non-selective *exo*-recognition).

Numerous efforts have been realized in order to obtain synthetic receptors capable to complex two different types of guest molecules, usually cations and anions.[15] The simultaneous complexation of two (or more) neutral guest molecules is not common for synthetic molecular receptors and has been only achieved in the interior of capsule-like assemblies (*endo*-receptors).[16]

Previous studies in our group have shown the ability of hydrogen bonded assemblies to act as *endo*-receptor (encapsulating three guest molecules)[17] or as *exo*-receptor (complexing up to six guest molecules).[18] In this chapter the first examples of noncovalent receptors able to act simultaneously as an *endo-exo* or *endo-endo-endo* receptor for neutral molecules are described. The hydrogen-bonded *endo-exo* receptor is based on the double rosette scaffold. This receptor is able to selectively encapsulate a neutral noncovalent trimer in the pocket situated in between two subdomains (floors) of the double rosette (*endo*-complexation) while simultaneously complexing different neutral guest molecules at the periphery of the assembly (*exo*-complexation) (Figure 6.1a), resembling the hierarchy of molecular biorecognition. The hydrogen-bonded *endo-endo-endo* receptor is based on the tetrarosette scaffold. This receptor is able to encapsulate two noncovalent trimers in each of the individual double rosette of the tetrarosette while simultaneously encapsulating different neutral guest molecules in the internal cavity formed between the two double rosettes (Figure 6.1b). In addition, as in many biological systems, the receptors have the ability to selectively release guest molecules complexed in the internal cavities when the appropriate external stimuli is given while the other guest molecules, complexed at the periphery or in the cavity of the double and tetrarosette, respectively, remain complexed to the receptor.

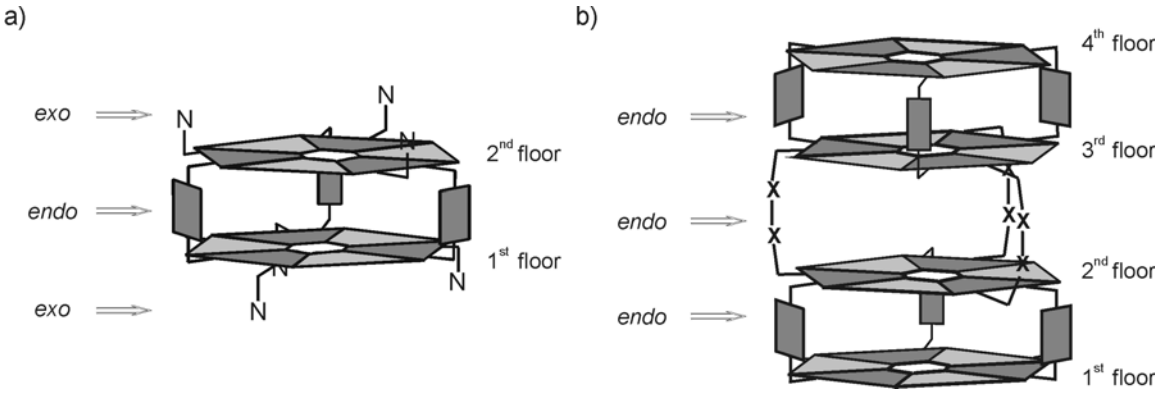

Figure 6.1. Schematic representation of a) double rosette and b) tetrarosette receptors showing the "*endo-exo*" and "*endo-endo-endo*" sites for recognition, respectively.

6.2. Results and discussion

The *endo-exo* receptor $\mathbf{1}_3$•$(DEB)_6$ consists of three calix[4]arene dimelamines **1** and six barbiturate or cyanurate molecules held together through the formation of 36 cooperative hydrogen bonds (Chart 6.1).[19] The periphery of the self-assembled double rosette is decorated with six pyridyl groups able to complex a variety of dicarboxylic acids **4a-c** (a *nonselective* recognition process) in a 1:3 fashion. Simultaneously, they are able to encapsulate a noncovalent trimer of alizarin (**3a)** (a *selective* recognition process). The *endo-endo-endo* $\mathbf{2}_3$•$(DEB)_{12}$ receptor consists of three calix[4]arene tetramelamines **2** and twelve barbiturate or cyanurate molecules held together through 72 cooperative hydrogen bonds (Chart 6.1).[20] In this tetrarosette receptor a total of six urea functionalities are positioned in the central cavity formed between the two double rosette motifs. The urea groups are able to complex several guest molecules, such as nitrophenol derivatives **5** and the saccharide β-L-**6**. Additionally the tetrarosette receptor can encapsulate two noncovalent trimers of alizarin (**3a**). Each of these trimers is complexed between the two floors of each double rosette.

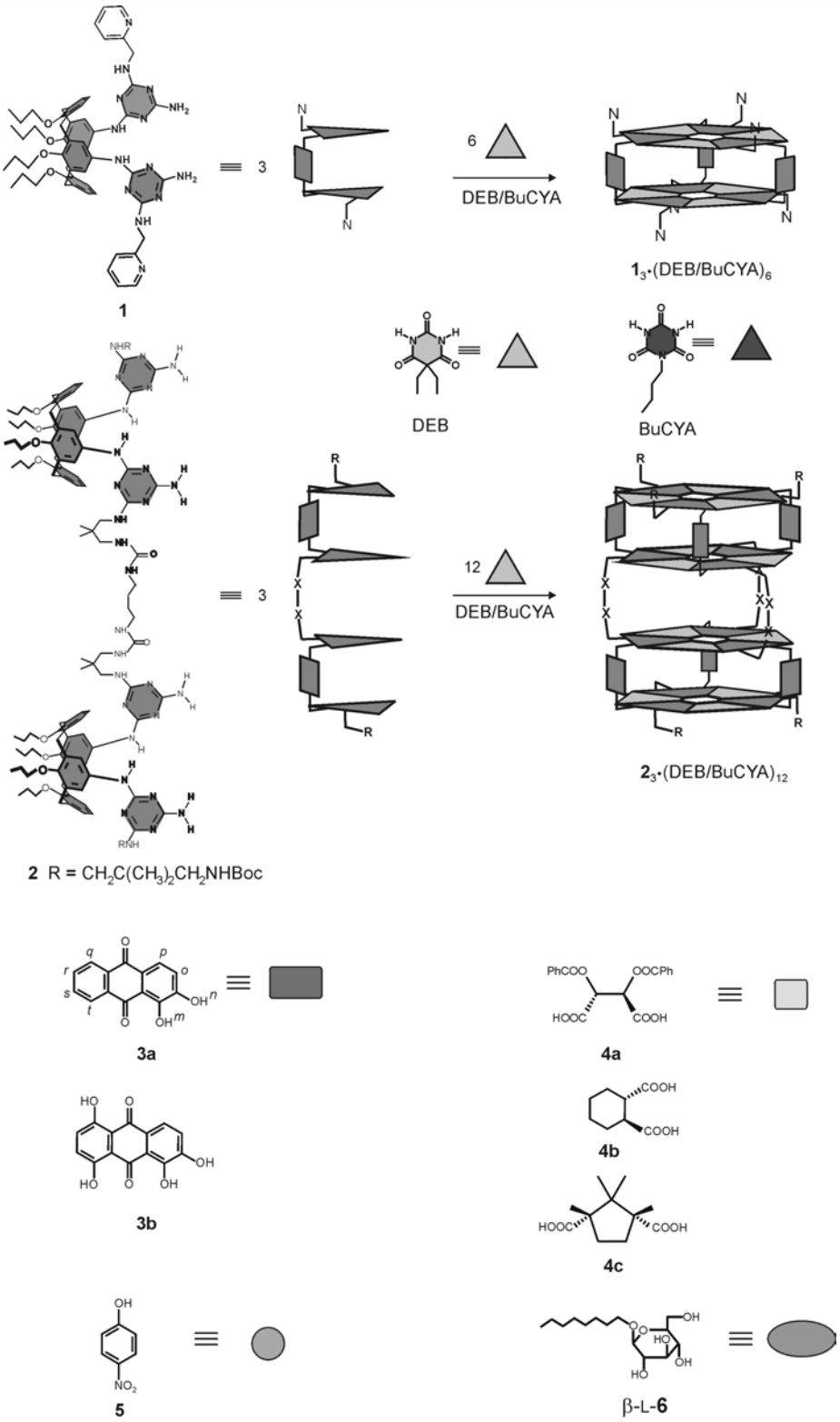

Chart 6.1. Chemical and schematic representation of the dimelamine **1** and tetramelamine **2**, cyanurate/barbiturate derivatives, and the corresponding hydrogen-bonded assemblies $\mathbf{1}_3$•(DEB/BuCYA)$_6$ and $\mathbf{2}_3$•(DEB/BuCYA)$_{12}$ and guest molecules **3a,b**, **4a-c, 5**, and β-L-**6**. Boc = *tert*-butyloxycarbonyl.

6.2.1. Complexation studies and selective release with the *endo-exo receptor* $\mathbf{1}_3$•*(DEB)*$_6$

Previous studies in our group[17a] have described the encapsulation of alizarin **3** (*endo*-complexation) within the two rosette layers of an assembly similar to $\mathbf{1}_3$•$(DEB)_6$ but with different substituents in the dimelamine fragment. The noncovalent trimer ($\mathbf{3a}_3$) is formed through intermolecular formation of hydrogen bonds between one of the two carbonyl groups of one alizarin and one of the two hydroxyl groups of the adjacent alizarin molecule. The encapsulation is accompanied by a change in the symmetry of the host assembly, from D_3- to C_{3h}-symmetry (Figure 6.2).[17a,21] In order to introduce *exo* binding sites in the double rosettes, pyridyl groups were introduced in the calix[4]arene dimelamine **1**, allowing the complexation of different diacids as guest molecules.

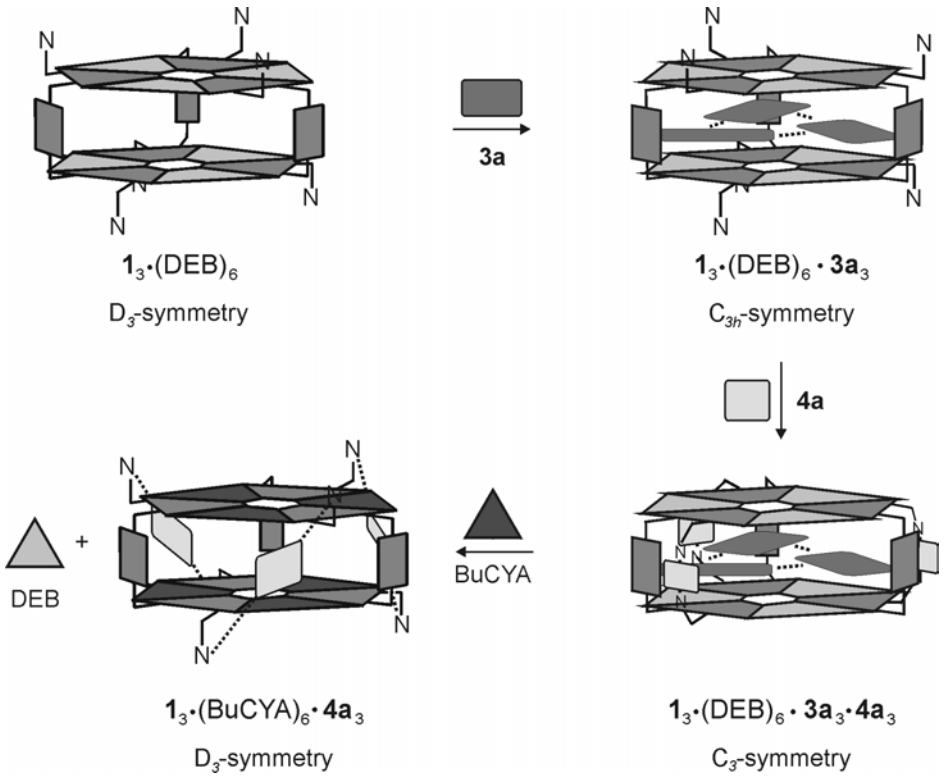

Figure 6.2. Schematic representation of the recognition and release of guests **3a** and **4a** by receptors $\mathbf{1}_3$•$(DEB)_6$/$\mathbf{1}_3$•$(BuCYA)_6$. The corresponding symmetry of the assemblies is also given: assemblies with D_3-symmetry ($\mathbf{1}_3$•$(DEB)_6$ and $\mathbf{1}_3$•$(BuCYA)_6$•$\mathbf{4a}_3$) have the two melamine rings in each calix[4]arene in a staggered orientation while assemblies with C_{3h} and C_3-symmetry ($\mathbf{1}_3$•$(DEB)_6$•$\mathbf{3a}_3$ and $\mathbf{1}_3$•$(DEB)_6$•$\mathbf{3a}_3$•$\mathbf{4a}_3$, respectively) have these rings in an eclipsed orientation.

Upon addition of 3 equivalents of alizarin (**3a**) to a 1.0 mM solution of the hydrogen-bonded receptor $\mathbf{1}_3$•$(DEB)_6$ in toluene-d_8, the ^{1}H NMR spectrum shows shifts of nearly all the signals, both for the host assembly and for the guest (Figure 6.3b). For example, the signals of the NH_{DEB}-protons involved in the hydrogen bonding array, H^a and H^b, shift upfield from 14.85 and 14.08 to 14.43 and 13.81 ppm, respectively. Similarly, proton H^i of the 2-methylpyridine substituents of the melamine rings undergoes an upfield shift of ~ 0.5 ppm upon the addition of alizarin. Molecular simulation studies (Quanta 97, CHARMm 24.0) suggest that H^i is pointing to the center of the receptor, resulting in the observed upfield shift in the ^{1}H NMR spectrum. Large upfield shifts were also observed for the aromatic protons of the guest molecules **3a** (> 3.0 ppm), indicating their encapsulation in the interior of the assembly. Moreover, the downfield shift observed for alizarin hydroxyl OH^n proton ($\Delta\delta$ ~ 3.6 ppm) indicates the formation of intermolecular hydrogen bonds between the carbonyl and hydroxyl groups of adjacent guest molecules. Thus, the ^{1}H NMR spectrum confirms the encapsulation (*endo*-complexation) of **3a** as a noncovalent trimer by receptor $\mathbf{1}_3$•$(DEB)_6$ resulting in the complex $\mathbf{1}_3$•$(DEB)_6$•$\mathbf{3a}_3$. The encapsulation of alizarin is very selective and sensitive to small structural changes. For example, when protons H^q and H^t of alizarin **3a** are replaced by hydroxyl groups in 1,2,5,8-anthraquinone (**3b**) no encapsulation was observed.[22]

The encapsulation of the alizarin trimer breaks the D_3 symmetry of the receptor $\mathbf{1}_3$•$(DEB)_6$, leading to the formation of the complex $\mathbf{1}_3$•$(DEB)_6$•$\mathbf{3a}_3$ with C_{3h} symmetry (Figure 6.2). This change in symmetry implies a conversion of the two melamine rings of each calix[4]arene from the staggered conformation in the empty receptor to an eclipsed conformation in the complex.

Once the encapsulation of **3a** in $\mathbf{1}_3$•$(DEB)_6$ was achieved (*endo*-complexation), the simultaneous role of $\mathbf{1}_3$•$(DEB)_6$ as an *exo*-receptor was studied. Addition of 3 equivalents of dibenzoyl-D-tartaric acid (**4a**) to the complex $\mathbf{1}_3$•$(DEB)_6$•$\mathbf{3a}_3$ resulted in upfield shifts of the signals H^a and H^b from 14.43 and 13.81 to 14.38 and 13.76 ppm, respectively (Figure 6.3c). The signal for proton H^i shifts downfield ~ 0.1 ppm. The signal of H^i at 5.40 ppm is indicative for the formation of hydrogen bonds between the 2-methylpyridyl substituents of the calix[4]arene dimelamine and the diacid **4a**.[18b] The stoichiometry of the complexation of **4a** by $\mathbf{1}_3$•DEB_6•$\mathbf{3a}_3$ is not clear from these ^{1}H NMR

studies. But circular dichroism (CD) studies (data not shown) on the complexation of **3a** by receptor $\mathbf{1}_3$•$(BuCYA)_6$ clearly showed the formation of a complex with 1:2 stoichiometry as major species, even though the complexes with 1:1 and 1:3 stoichiometries are also present as minor species, probably due to steric effects or allosteric conformational changes.[23] The acids interact with the receptor via two-point interactions. These interactions are only possible '*sideways*', *i.e.* each diacid interacts with both floors of the double rosette, where one carboxylic acid of the guest is hydrogen-bonded to the pyridyl of the calix[4]arene dimelamine of the first floor while the other acid group of the same guest interacts with the other pyridyl group of the same calix[4]arene dimelamine.

The *exo*-complexation is not very substrate selective, because other diacids with different chemical structure, such as (1*R*,2*R*)-cyclohexane-1,2-dicarboxylic acid **4b** and (1*S*,3*R*)-camphoric acid **4c**, are also complexed in a similar fashion (data not shown).

Thus, the data show the complexation of six guest molecules of two different types of neutral guest molecules (alizarin **3a** and diacid **4a**). Hydrogen-bonded trimer $\mathbf{3a}_3$ is encapsulated in the internal cavity of the receptor $\mathbf{1}_3$•$(DEB)_6$ while three molecules of guest **4a** are complexed at the periphery of the host assembly through formation of hydrogen bonds between the pyridyl groups of the dimelamine moieties and the carboxylic groups of the guest molecules. Furthermore, as it occurs with biomolecules, the receptor shows two different degrees of selectivity in the molecular recognition process; *i.e.* the *endo*-recognition is very selective and sensitive to the structure of the guest while the *exo*-recognition is not structurally very demanding.

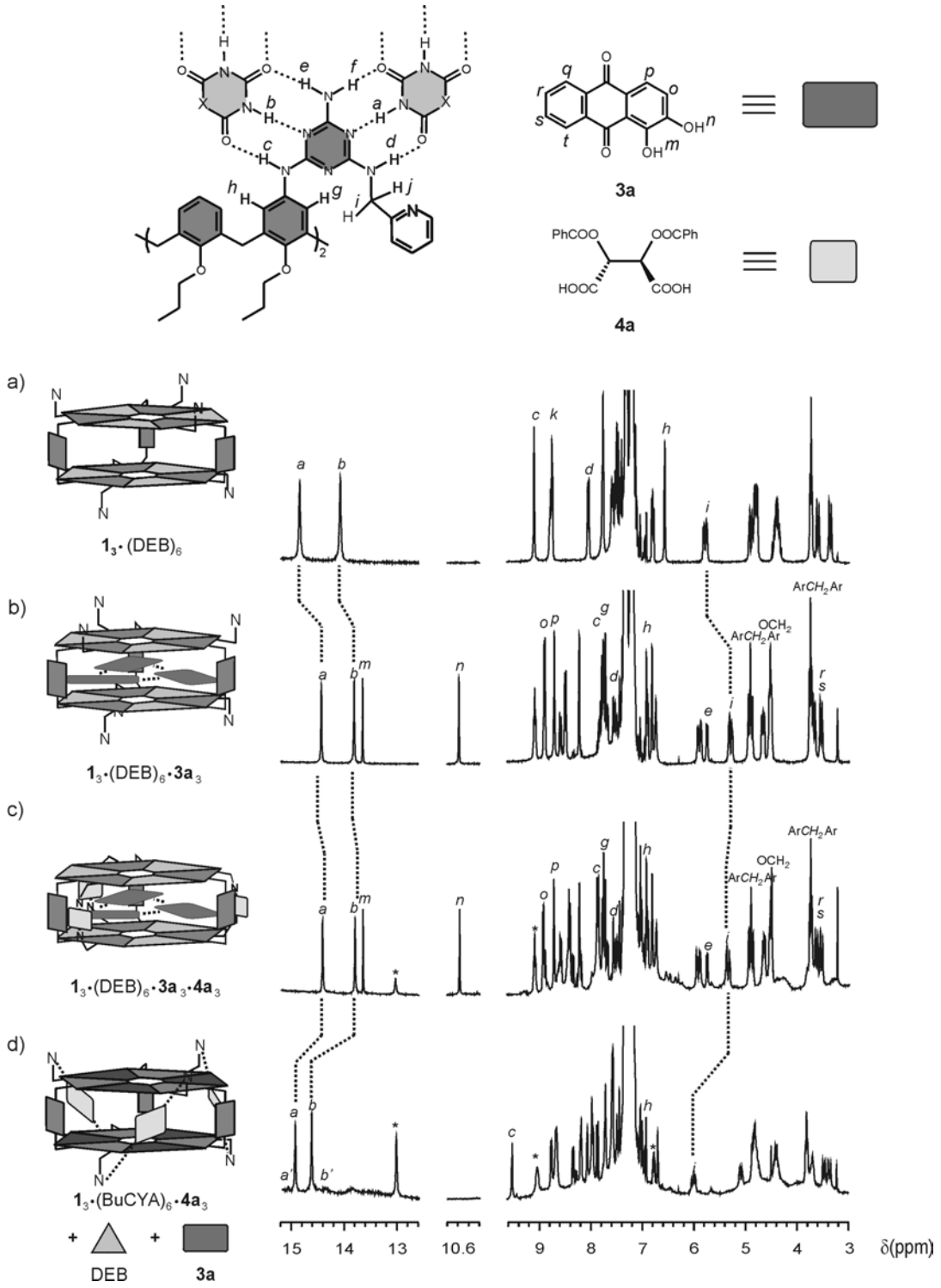

Figure 6.3. Part of the ^{1}H NMR spectra (300 MHz) of a) assembly $\mathbf{1}_3$•$(DEB)_6$ (1 mM), b) $\mathbf{1}_3$•$(DEB)_6$ + 3 equiv. **3a**, c) $\mathbf{1}_3$•$(DEB)_6$•$\mathbf{3a}_3$ + 3 equiv. **4a**, and d) $\mathbf{1}_3$•(DEB_6)•$\mathbf{3a}_3$•$\mathbf{4a}_3$ + 6 equiv. BuCYA. Signals marked with * belong to the free **3a**. All spectra were recorded at 298 K in toluene-d_8.

The controlled release of the different guest molecules from the hydrogen-bonded assembly was also studied.[24] Cyanurates form stronger hydrogen bonds with melamines than barbiturates, allowing the exchange of DEB for BuCYA.[25] Previously, the release of the trimer $\mathbf{3a}_3$ from a similar receptor upon addition of BuCYA was proven by ^{1}H NMR spectroscopy. [17a] Also the addition of the BuCYA to complex $\mathbf{1}_3$•(DEB)$_6$•$\mathbf{3a}_3$•$\mathbf{4a}_3$ showed the controlled release of the hydrogen bonded trimer $\mathbf{3a}_3$, while the guest molecules at the periphery still stay complexed resulting in the assembly $\mathbf{1}_3$•(BuCYA)$_6$•$\mathbf{4a}_3$. The release of the three guest molecules **3a** is achieved because cyanurate based assemblies are not able to encapsulate **3a** due to geometrical differences between barbiturate and cyanurate-based assemblies.[17a] The release was proven by means of ^{1}H NMR and circular dichroism (CD) spectroscopy (Figures 6.3d and 6.4, respectively). Addition of 6 equivalents of BuCYA (with respect to complex $\mathbf{1}_3$•(DEB)$_6$•$\mathbf{3a}_3$•$\mathbf{4a}_3$) to a solution of the complex $\mathbf{1}_3$•(DEB)$_6$•$\mathbf{3a}_3$•$\mathbf{4a}_3$ in toluene-d_8 showed a ^{1}H NMR spectrum where the signals for protons H^a and H^b are splitted and shifted downfield from 14.38 and 13.76 ppm to 14.95 and 14.64 ppm, respectively (Figure 6.3d). The spliting of the signals is the result of the transfer of chirality from the chiral guest (**4a**) to the assembly.[18c] This induction of chirality is not complete, therefore the two possible diastereomers are formed.[26] Furthermore, proton H^i showed a downfield shift of ~ 0.6 ppm. The release of the guest trimer $\mathbf{3a}_3$ is also clearly supported by the disappearance of the signal at 10.58 ppm (this signal corresponds to the OH^n when it forms intermolecular hydrogen bonds between the different molecules of **3**). Moreover, all the signals of $\mathbf{1}_3$•(DEB)$_6$•$\mathbf{3a}_3$•$\mathbf{4a}_3$ have disappeared and only signals corresponding to complex $\mathbf{1}_3$•(BuCYA)$_6$•$\mathbf{4a}_3$ and free **3a** and DEB can be seen. The ^{1}H NMR spectrum of the receptor complexing both $\mathbf{3a}_3$ and $\mathbf{4a}_3$ after the addition of BuCYA is similar to the ^{1}H NMR spectrum of $\mathbf{1}_3$•(BuCYA)$_6$•$\mathbf{4a}_3$ formed by direct mixing of assembly $\mathbf{1}_3$•(BuCYA)$_6$ and 3 equivalents of **4a** (data not shown).[18b]

Additional proof for the complexation and selective release of guest molecules **3a** and **4a** from $\mathbf{1}_3$•(DEB)$_6$•$\mathbf{3a}_3$•$\mathbf{4a}_3$ was obtained from CD-spectroscopy (Figure 6.4). Receptor $\mathbf{1}_3$•(DEB)$_6$ exists as a racemic mixture of (*P*)- and (*M*)-enantiomers[18b] and is therefore CD inactive. As it has been mentioned earlier, addition of alizarin **3a** to the receptor $\mathbf{1}_3$•(DEB)$_6$ results in the formation of the complex $\mathbf{1}_3$•(DEB)$_6$•$\mathbf{3a}_3$ which is

accompanied by a change in symmetry of the hydrogen bonded receptor from D_3 to C_{3h}. In the C_{3h}-symmetry, the orientation of the two melamine moieties adopts an eclipsed conformation, resulting in an achiral complex. Addition of **4a** to $\mathbf{1}_3$•$(DEB)_6$•$\mathbf{3a}_3$ results in the appearance of a CD signal (Figure 6.4) due to the complexation and transfer of chirality from **4a** to $\mathbf{1}_3$•$(DEB)_6$•$\mathbf{3a}_3$ which results in a change in the symmetry of the complex $\mathbf{1}_3$•$(DEB)_6$•$\mathbf{3a}_3$ from C_{3h} to C_3 for $\mathbf{1}_3$•$(DEB)_6$•$\mathbf{3a}_3$•$\mathbf{4a}_3$.[27] Moreover, addition of BuCYA to $\mathbf{1}_3$•$(DEB)_6$•$\mathbf{3a}_3$•$\mathbf{4a}_3$ leads to a new signal in the CD spectrum. This signal is very similar to the CD spectrum of $\mathbf{1}_3$•$(BuCYA)_6$•$\mathbf{4a}_3$ formed by direct mixing of assembly $\mathbf{1}_3$•$(BuCYA)_6$ and 3 equivalents of **4a**.[18b] Thus, addition of BuCYA to $\mathbf{1}_3$•$(DEB)_6$•$\mathbf{3a}_3$•$\mathbf{4a}_3$ leads to the release of the trimeric $\mathbf{3a}_3$ and change of symmetry from C_3 back to D_3. In the assembly $\mathbf{1}_3$•$(BuCYA)_6$•$\mathbf{4}_3$, the chirality of **4a** is transferred to the complex, resulting in the predominant formation (*d.e.* 90%) of one of the two possible diastereomeric assemblies, (*P*)- $\mathbf{1}_3$•$(DEB)_6$•$\mathbf{4a}_3$, and therefore exhibiting a signal in the CD spectrum.[18b,c]

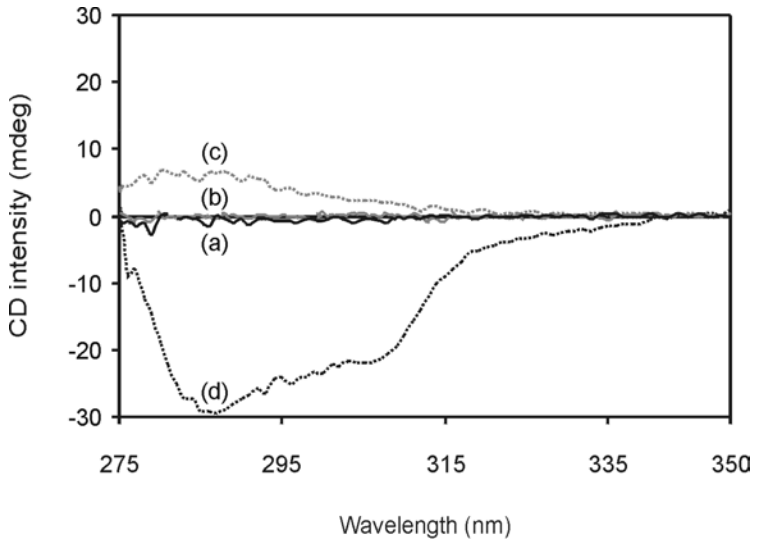

Figure 6.4. CD spectra (1.0 mM solution) (a) $\mathbf{1}_3$•$(DEB)_6$ (black line), (b) $\mathbf{1}_3$•$(DEB)_6$ + 3 equivalents of **3a**, (c) $\mathbf{1}_3$•$(DEB)_6$•$\mathbf{3a}_3$ + 3 equivalents of **4a**, and (d) $\mathbf{1}_3$•$(DEB)_6$•$\mathbf{3a}_3$•$\mathbf{4a}_3$ + 1 equivalent of BuCYA (with respect to DEB). The spectra were recorded at 298 K in toluene-d_8.

Interestingly, a large influence in the complexation and encapsulation behavior is observed when the order of addition of the guest molecules **3a** and **4a** was reversed.

Addition of 3 equivalents of **4a** directly to a solution of assembly $\mathbf{1}_3$•$(DEB)_6$ in toluene-d_8 resulted in almost complete disassembly of the double rosette as reflected in the disappearance of the signals for protons H^a and H^b in the ^1H NMR spectrum. Based on the integration of the appropriate signals in the ^1H NMR spectrum (Figure 6.5a,b), only 8% of the hydrogen-bonded receptor remains intact. Due to the higher acidity of the diacid **4a** compared to DEB,[28] it is possible that **4a** forms stronger hydrogen bonds with the calix[4]arene dimelamine building blocks **1**, leading to the destruction of the assembly. However, after subsequent addition of 3 equivalents of **3a** to this solution, the resulting ^1H NMR spectrum is identical to the ^1H NMR spectrum obtained previously when the guest molecules **4a** are added after formation of the complex $\mathbf{1}_3$•$(DEB)_6$•$\mathbf{3a}_3$ (see Figures 6.3c and 6.5c). Thus, the host assembly $\mathbf{1}_3$•$(DEB)_6$ is reassembled upon addition of the alizarin **3a** even in the presence of diacids **4a**. Moreover, the encapsulation of **3a** allows also the complexation of the guest **4a**, thus resulting in the quantitative formation of $\mathbf{1}_3$•$(DEB)_6$•$\mathbf{3a}_3$•$\mathbf{4a}_3$ (Figure 6.5c). The reassembly of the host receptor is probably due to the stabilizing effect of the π–π interactions between the guest **3a** and the calix[4]arene and dimelamine rings of **1**. Addition of 6 equivalents of BuCYA to $\mathbf{1}_3$•$(DEB)_6$•$\mathbf{3a}_3$•$\mathbf{4a}_3$ leads to the exchange of DEB for BuCYA and release of **3a** (Figure 6.5d). The presence of $\mathbf{1}_3$•$(BuCYA)_6$•$\mathbf{4a}_3$ after the exchange of DEB by BuCYA was also proven by CD-spectroscopy.

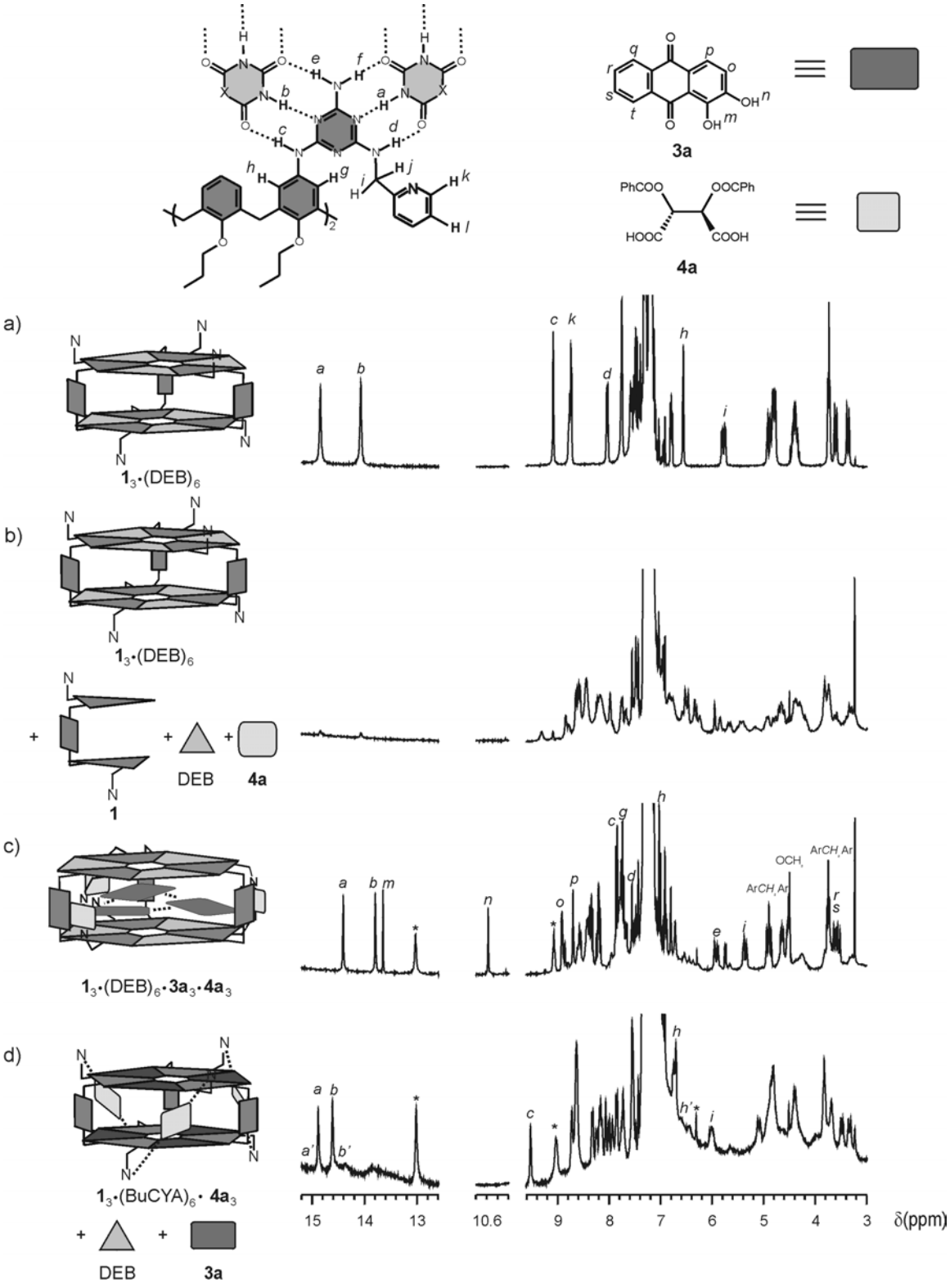

Figure 6.5. Part of the ^{1}H NMR spectra (300 MHz) of a) assembly $\mathbf{1}_3$•(DEB)$_6$ (1 mM), b) $\mathbf{1}_3$•(DEB)$_6$ + 3 equiv. **4a**, c) $\mathbf{1}_3$•(DEB)$_6$ + 3 equiv. **4a** + 3 equiv. **3a**, and d) $\mathbf{1}_3$•(DEB)$_6$•$\mathbf{3a}_3$•$\mathbf{4a}_3$ + 6 equiv. BuCYA. Signals marked with * belong to the free guest **3a**. All spectra were recorded at 298 K in toluene-d_8.

6.2.2. Complexation and release with the endo-endo-endo receptor $\mathbf{2}_3$•(DEB)$_{12}$

6.2.2.a. Exchange of guest molecules in the endo-receptor $\mathbf{2}_3$•(DEB)$_{12}$

Phenol derivatives[17c] and saccharide guest molecules[17b] (see Chapter 5) can be encapsulated in the cavity formed between double rosette motifs of assembly $\mathbf{2}_3$•(DEB)$_{12}$ through the formation of hydrogen bonds between the ureido groups of the tetramelamine moieties and the hydroxyl groups of the guest molecules **5** and β-L-**6** (Figure 6.6). Stoichiometries of 1:1 and 1:4 for the complexes with β-L-**6** and **5**, respectively, were calculated from Job plots with binding constants of 20 and 286 M^{-1}, respectively. The complexation of the guest molecules does not lead to a change in the symmetry of the receptor, which exist exclusively as the SSS-isomer.[29]

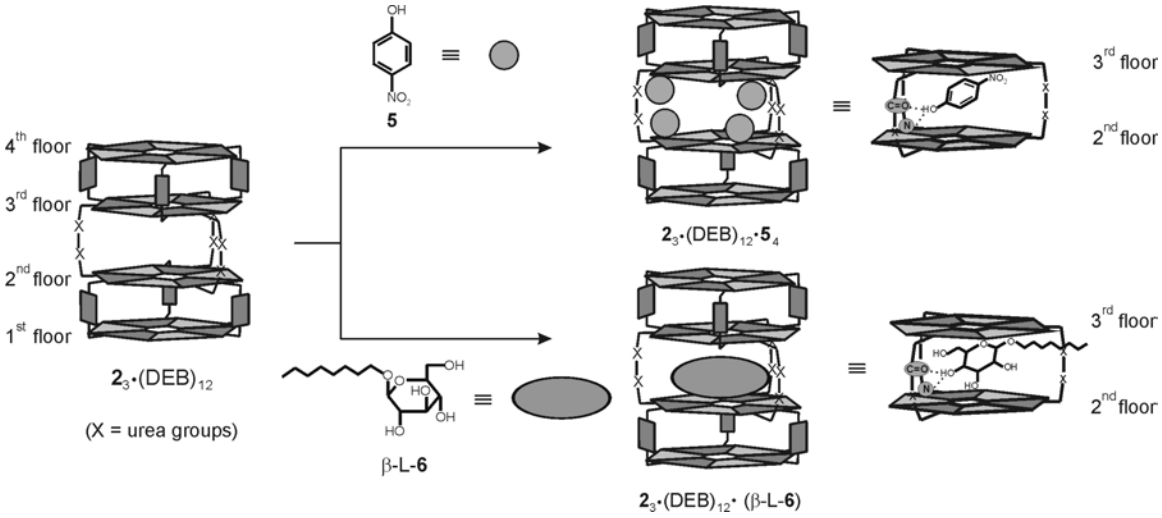

Figure 6.6. Schematic representation of the complexation of guest **5** and β-L-**6** by receptor $\mathbf{2}_3$•(DEB)$_{12}$. The hydrogen bonds formed between the guest and receptor are also shown (for clarity only the 2nd and 3rd floors of the assembly are depicted). In the complexation of guest **5** by the receptor $\mathbf{2}_3$•(DEB)$_{12}$ only one molecule of guest, of the four that are complexed, is depicted.

Addition of 10 equivalents of β-L-**6** to a 1.0 mM solution $\mathbf{2}_3$•(DEB)$_{12}$ in $CDCl_3$ leads to changes in the ^{1}H NMR spectra (see Chapter 5), such as the splitting of the signal of H^{a2} and H^{c2} as well as the splitting of the NH^A signal of the urea, indicating the

complexation of the saccharide guest in the cavity formed in between the two double rosette motifs (Figure 6.7b).

Addition of 10 equivalents of 4-nitrophenol (**5**) to $\mathbf{2}_3$•$(DEB)_{12}$•(β-L-**6**) (1.0 mM solution in $CDCl_3$) resulted in downfield shift of the signals for proton NH^A ($\Delta\delta \sim 0.43$ ppm) while the proton of the terminal carbamate moiety NH^B remained unshifted, indicating that the guest **5** is interacting with the ureido carbonyl groups that are positioned in the cavity formed by $\mathbf{2}_3$•$(DEB)_{12}$. Upfield shifts for the signals of protons NH^{a2} ($\Delta\delta \sim 0.1$ ppm) and NH^{b2} ($\Delta\delta \sim 0.05$ ppm) of the second and third floor of the tetrarosette were also observed (Figure 6.7c). The ^{1}H NMR spectrum of $\mathbf{2}_3$•$(DEB)_{12}$•(β-L-**6**) after the addition of **5** was similar to the ^{1}H NMR spectrum of $\mathbf{2}_3$•$(DEB)_{12}$•$\mathbf{5}_4$ formed by direct mixing of $\mathbf{2}_3$•$(DEB)_{12}$ and 10 equivalents of **5**.[17c] These results clearly indicate that the guest β-L-**6** is expelled from the receptor $\mathbf{2}_3$•$(DEB)_{12}$ upon addition of 4-nitrophenol **5**. The replacement of β-L-**6** by **5** must be the result of the larger association constant of the nitrophenol derivative **5** with receptor $\mathbf{2}_3$•$(DEB)_{12}$. Previously our group has reported that the complexation of phenols is related to the acidity of the phenolic group.[17c]

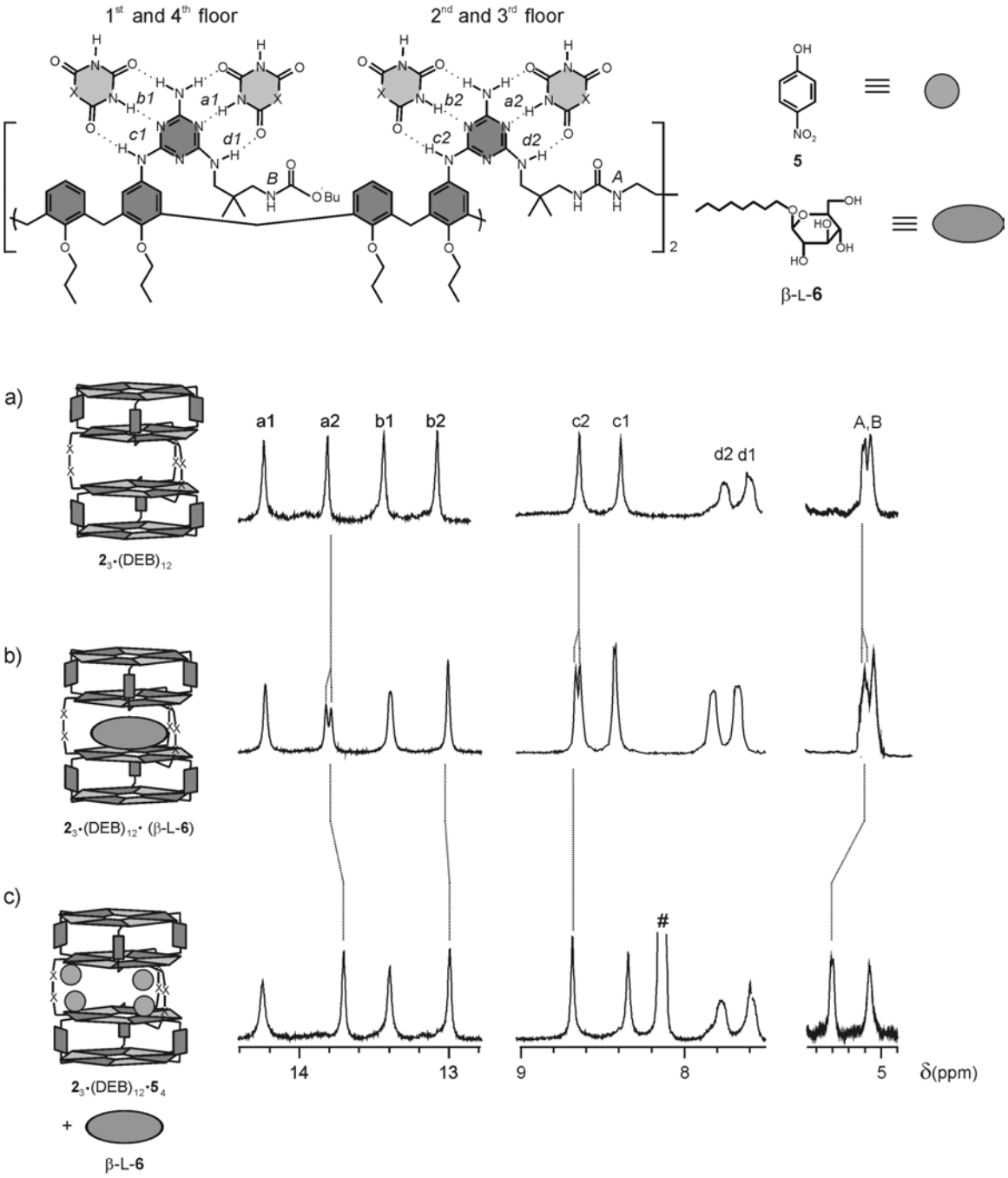

Figure 6.7. Part of the ^{1}H NMR spectra (300 MHz) of a) assembly $\mathbf{2}_3$•$(DEB)_{12}$ (1 mM), b) $\mathbf{2}_3$•$(DEB)_{12}$ + 10 equiv. β-L-**6**, and c) $\mathbf{2}_3$•$(DEB)_{12}$•(β-L-**6**) + 10 equiv. **5**. Signal marked with # corresponds to guest molecule **5**. All spectra were recorded at 298 K in $CDCl_3$.

The exchange of the guest molecules is also corroborated by CD-spectroscopy. Addition of 10 equivalents of β-L-**6** to the receptor $\mathbf{2}_3$•$(DEB)_{12}$ (1.0 mM in $CDCl_3$)

resulted in the appearance of a positive signal around 290-310 nm in the CD-spectrum due to the formation of (*M*)-$\mathbf{2}_3$•$(DEB)_{12}$•(β-L-**6**) (see Chapter 5). As result of the chiral recognition, the *M*-enantiomer, which binds β-L-**6** more strongly, is amplified in the mixture as both enantiomers are in dynamic equilibrium, thus inducing a Cotton effect. Addition of 10 equivalents guest **5** to (*M*)-$\mathbf{2}_3$•$(DEB)_{12}$•(β-L-**6**) resulted in the disappearance of the CD signal, indicating the exchange of the guest molecules. Addition of guest molecule **5** to $\mathbf{2}_3$•$(DEB)_{12}$ did not induce a Cotton effect in the CD spectrum, since both enantiomers (*P*- and *M*-) of $\mathbf{2}_3$•$(DEB)_{12}$ will bind the achiral guest **5** with the same strength.

6.2.2.b. Complexation studies and selective release with the endo-endo-endo receptor $\mathbf{2}_3$•$(DEB)_{12}$

In the previous section, the *endo*-complexation of saccharide molecules in the interior cavity of the receptor $\mathbf{2}_3$•$(DEB)_{12}$ and the replacement of this guest by addition of nitrophenol **5** have been explained in detail. It has also been shown that the exchange of the guest molecules is possible due to the larger association constant of the nitrophenol derivative with the self-assembled receptor.

Furthermore, to increase the complexity of the molecular recognition process and to test the ability of the receptor to act also as an *endo-endo-endo* receptor, the possible encapsulation of alizarin in each of the double rosette motifs of the tetrarosette receptor was studied (Figure 6.8).

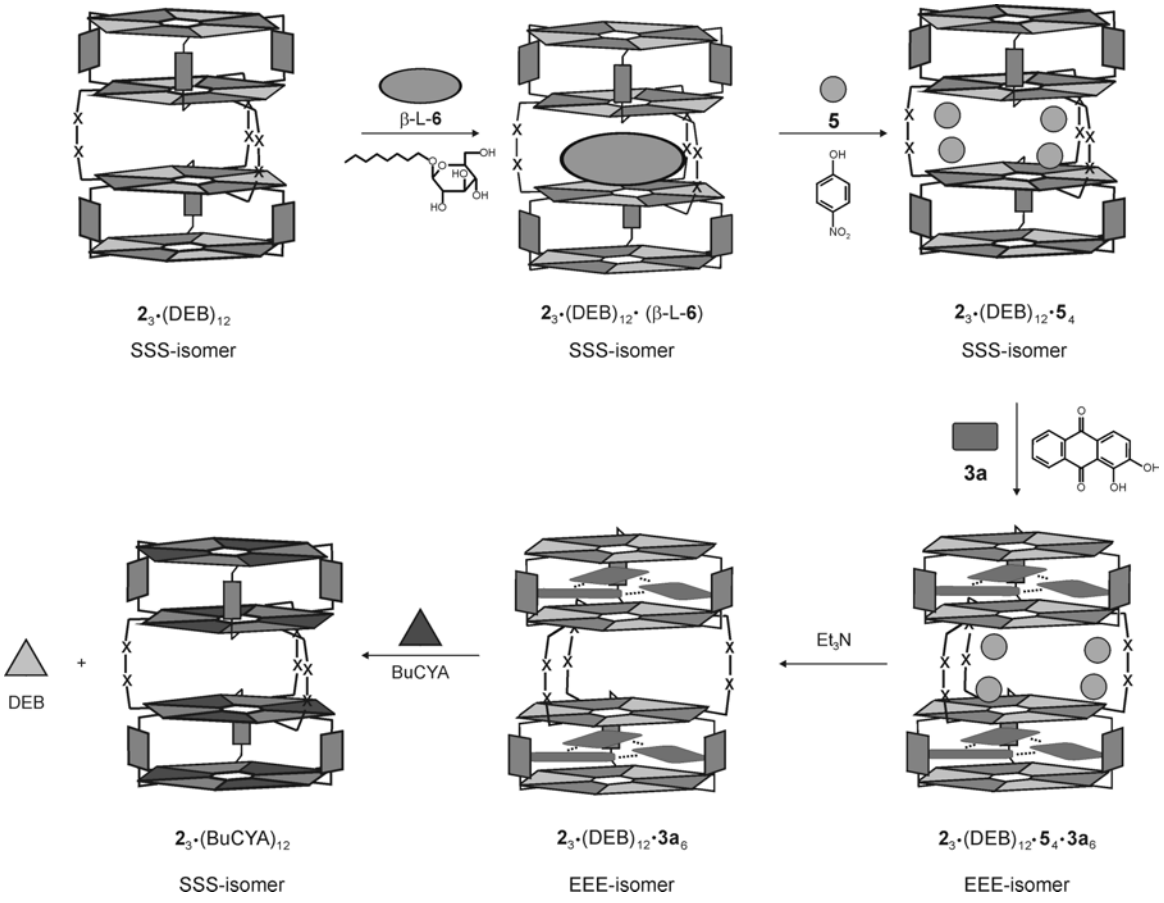

Figure 6.8. Schematic representation of the recognition and release of guests **3a**, **5**, and β-L-**6** by $\mathbf{2}_3$•$(DEB)_{12}$/$\mathbf{2}_3$•$(BuCYA)_{12}$.

Addition of 6 equivalents of alizarin **3a** to the complex $\mathbf{2}_3$•$(DEB)_{12}$•$\mathbf{5}_4$ (obtained after replacement of guest β-L-**6**) showed remarkable shifts of most of the signals in the ^{1}H NMR spectrum (Figure 6.9b). The NH_{DEB}-protons (H^a and H^b) showed upfield shifts from 14.25, 13.69, 13.38, and 12.97 ppm to 13.13, 12.94, 12.91, and 12.60 ppm, respectively. The OH^n of alizarin **3a** was shifted downfield from 6.24 ppm for the free **3a** to 9.63 ppm in the complex $\mathbf{2}_3$•$(DEB)_{12}$•$\mathbf{5}_4$•$\mathbf{3a}_6$ ($\Delta\delta$ 3.39 ppm), which indicated the formation of a hydrogen bond of this proton with the carbonyl of the adjacent **3a** molecule. The aromatic protons H^r, H^s, and H^t of **3a** are shifted 3.30 ppm upfield (from 8.15-7.81 ppm for the free guest **3a** to 4.85-4.51 ppm in the complex), indicating that they are partially included in the calix[4]arene. The integration of the appropriate ^{1}H NMR signals yielded a 6:1 ratio for the complexation (**3a** : $\mathbf{2}_3$•$(DEB)_{12}$•$\mathbf{5}_4$). Thus, two trimers of **3a** are encapsulated in the tetrarosette receptor, one between the 1st and 2nd

rosette floors and one in between the 3rd and 4th rosette floors (Figure 6.8), while the four guest molecules **5** are encapsulated in the cavity between the two double rosette motifs. Similar to the complexation of alizarin **3a** in double rosette assemblies (see section 6.2.1), the complexation of alizarin **3a** by receptor $\mathbf{2}_3$•$(DEB)_{12}$ is accompanied by a change in the symmetry of the receptor from the SSS-isomer to the EEE-isomer.[30] Thus, the addition of alizarin **3a** to complex $\mathbf{2}_3$•$(DEB)_{12}$•$\mathbf{5}_4$ leads to the formation of complex $\mathbf{2}_3$•$(DEB)_{12}$•$\mathbf{5}_4$•$\mathbf{3a}_6$ in which ten molecules of neutral guest molecules are complexed through a combination of different noncovalent interactions such as hydrogen bonds and π–π interactions, in different internal cavities of the self-assembled receptor, which is formed from fifteen components through the formation of 72 cooperative hydrogen bonds. This means that through spontaneous noncovalent synthesis, a discrete assembly is formed by four different molecules in a ratio 3:12:6:4 with a total of 25 individual molecules! The assembly is held together by 84 H-bonds.

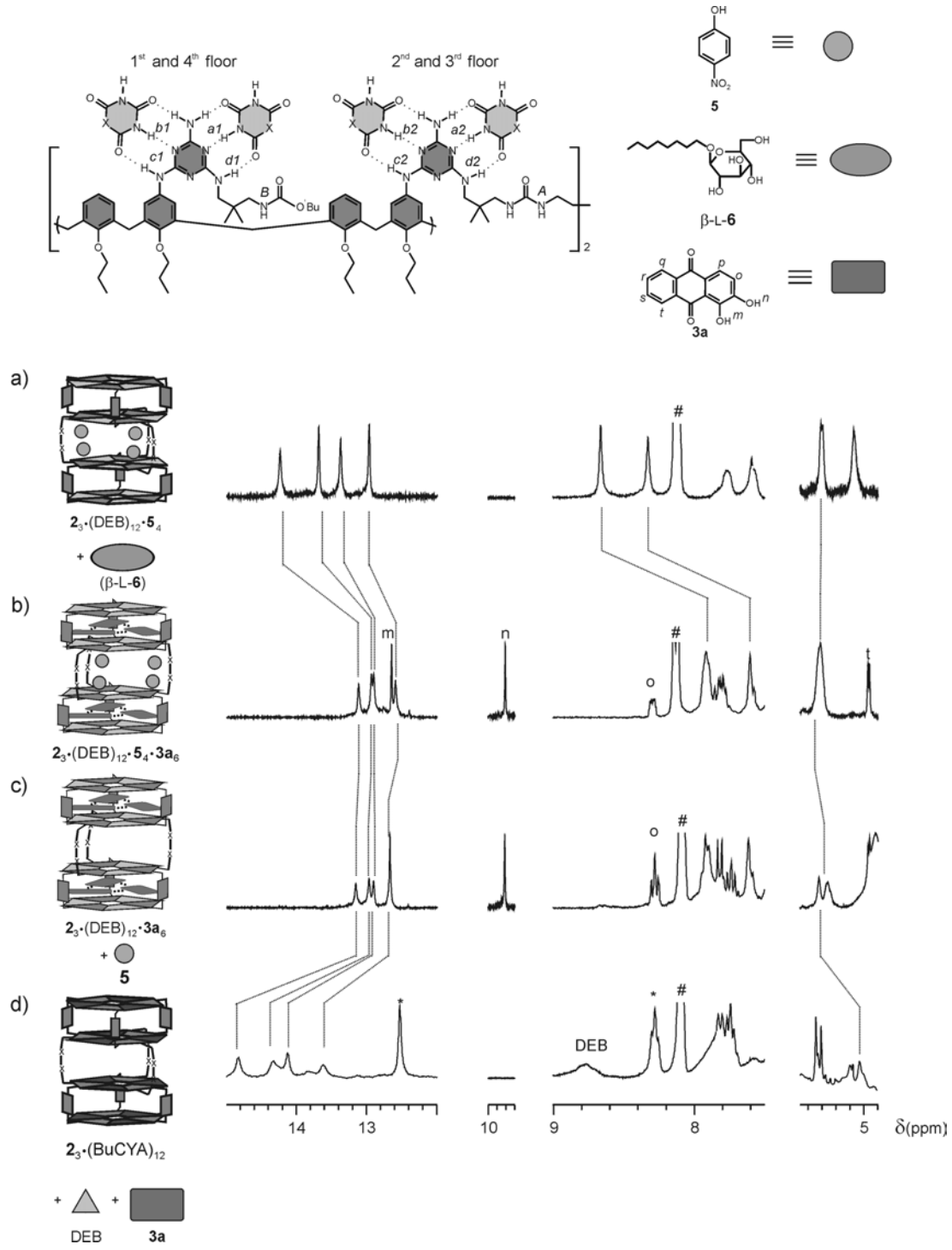

Figure 6.9. Part of the ^{1}H NMR spectra of a) $\mathbf{2}_3$•(DEB)$_{12}$• (β-L-**6**) + 10 equivalents of **5**, b) $\mathbf{2}_3$•(DEB)$_{12}$•$\mathbf{5}_4$ + 6 equivalents of **3**, c) $\mathbf{2}_3$•(DEB)$_{12}$•$\mathbf{5}_4$•$\mathbf{3a}_6$ + 10 µl of Et_3N (1.0 M solution in $CDCl_3$), and d) $\mathbf{2}_3$•(DEB)$_{12}$•$\mathbf{3a}_6$ + 1 equivalent of BuCYA (with respect to DEB). All signals marked with * correspond to free guest **3a** and signals marked with # correspond to guest **5**. All spectra were recorded at 298 K in $CDCl_3$.

Also with the *endo-endo-endo* receptor $\mathbf{2}_3$•$(DEB)_{12}$ release experiments were performed to compare the release behavior with the *exo-endo* receptor $\mathbf{1}_3$•$(DEB)_6$.

Addition of 10 µl of Et_3N (1.0 M in $CDCl_3$) to a solution of the complex $\mathbf{2}_3$•$(DEB)_{12}$•$\mathbf{5}_4$•$\mathbf{3a}_6$ in $CDCl_3$ showed a ^{1}H NMR spectrum in which the signal for the proton H^{b2} (2^{nd} and 3^{rd} floor of the receptor) is shifted downfield (from 12.60 to 12.68 ppm) (Figure 6.9c). This shift indicates that proton H^{b2} is not anymore in the shielding cone of the phenyl group of the guest **5** (anisotropic effect) and therefore, proving the release of 4-nitrophenol (**5**) from the internal cavity of complex $\mathbf{2}_3$•$(DEB)_{12}$•$\mathbf{5}_4$•$\mathbf{3a}_6$. Furthermore, also the upfield shift of 0.12 ppm of the NH^A proton indicates the release of **5.** This shift is the result of the rupture of the hydrogen-bond between **5** and the ureido groups of the host $\mathbf{2}_3$•$(DEB)_{12}$. On the other hand, the presence of the signal at 9.63 ppm corresponding to the intramolecular hydrogen bonding array of the trimer $\mathbf{3a}_3$ together with the other characteristic ^{1}H NMR signals for the encapsulation of **3a,** indicate that the two trimers $\mathbf{3a}_3$ still remain encapsulated in the host assembly $\mathbf{2}_3$•$(DEB)_{12}$. Moreover, the ^{1}H NMR spectrum obtained after the addition of Et_3N to $\mathbf{2}_3$•$(DEB)_{12}$•$\mathbf{5}_4$•$\mathbf{3a}_6$ is similar to the ^{1}H NMR spectrum of $\mathbf{2}_3$•$(DEB)_{12}$•$\mathbf{3a}_6$ obtained by direct mixing of receptor $\mathbf{2}_3$•$(DEB)_{12}$ and 6 equivalents of guest **3a** (plus, of course, the signal of free **5**).

In Section 6.2.1, it was shown that the addition of BuCYA to double rosette $\mathbf{1}_3$•$(DEB)_6$•$\mathbf{3a}_3$•$\mathbf{4a}_3$ allows the controlled release of the hydrogen bonded trimer $\mathbf{3a}_3$ due to the exchange of DEB by BuCYA and the inability of the cyanurate based receptor $\mathbf{1}_3$•$(BuCYA)_6$ to encapsulate the trimer $\mathbf{3a}_3$. Similarly, the addition of BuCYA to the tetrarosette $\mathbf{2}_3$•$(DEB)_{12}$•$\mathbf{3a}_6$ (obtained by previous release of guest **5** from $\mathbf{2}_3$•$(DEB)_{12}$•$\mathbf{5}_4$•$\mathbf{3a}_6$ upon addition of Et_3N) results in the release of the two trimers of **3a**. The addition of BuCYA (1 equivalent with respect to DEB) results in a ^{1}H NMR spectrum where the signals for proton $H^{a1\text{-}2}$ and $H^{b1\text{-}2}$ are shifted downfield (from 13.17, 12.98, 12.91, and 12.68 ppm to 14.55, 14.15, 13.97, and 13.54 ppm, respectively) indicating that the exchange of DEB by BuCYA has taken place (Figure 6.9d). Furthermore, the disappearance of the signal OH^n at 9.64 ppm (indicative of the intramolecular hydrogen bond array between the **3a** molecules) clearly confirms the release of the two hydrogen bonded trimers $\mathbf{3a}_3$ from the receptor $\mathbf{2}_3$•$(DEB)_{12}$. The ^{1}H NMR spectrum after the addition of BuCYA to $\mathbf{2}_3$•$(DEB)_{12}$•$\mathbf{3a}_6$ is similar to the ^{1}H NMR

spectrum of the assembly $\mathbf{2}_3$•$(BuCYA)_{12}$ formed by the exchange of DEB by BuCYA in $\mathbf{2}_3$•$(DEB)_{12}$.[20b]

These data clearly demonstrate the successive complexation and selective release of different neutral guest molecules by the hydrogen bonded receptor $\mathbf{2}_3$•$(DEB)_{12}$.

6.3. Conclusions

In this chapter the complexation and encapsulation of two different types of neutral guest molecules has been demonstrated showing perfect control over the molecular recognition process at two different levels. The noncovalent host molecules $\mathbf{1}_3$•$(DEB)_6$ display two different modes of complexation, *i.e.* as an *exo*-receptor for three molecules of carboxylic acid **4a** at the periphery of the assembly and as an *endo*-receptor templating the formation of a noncovalent hydrogen-bonded trimer of alizarin **3a** in the interior cavity of the assembly. Moreover, the addition of BuCYA leads to the release of the guest molecules **3a**, while the guest molecules **4a** remain complexed. It has also been demonstrated that the order of addition of the different guest molecules is important for the encapsulation and complexation processes. The initial addition of dicarboxylic acid molecules **4a** destroys the parent host assembly $\mathbf{1}_3$•$(DEB)_6$. However, the addition of the alizarin **3a** leads to the quantitative reassembly of the host $\mathbf{1}_3$•$(DEB)_6$ and complexation/encapsulation of the two different guest molecules resulting in the formation of $\mathbf{1}_3$•$(DEB)_6$•$\mathbf{3a}_3$•$\mathbf{4a}_3$.

On the other hand, the noncovalent host $\mathbf{2}_3$•$(DEB)_{12}$ can act as an *endo-endo-endo* receptor, *i.e.* by templating the formation of two noncovalent hydrogen-bonded trimers of alizarin **3a** (one trimer in each of the individual double rosettes) and by encapsulating four molecules of 4-nitrophenol **5** in the interior cavity formed in between the two double rosette motifs. This leads to the formation of complex $\mathbf{1a}_3$•$(DEB)_6$•$\mathbf{5}_4$•$\mathbf{3a}_6$ in which ten molecules of two different guest types are encapsulated in the three different cavities of the assembly $\mathbf{2}_3$•$(DEB)_{12}$. The addition of Et_3N to the complex $\mathbf{2}_3$•$(DEB)_{12}$•$\mathbf{5}_4$•$\mathbf{3a}_6$ results in the selective release of the guest molecules **5** from the internal cavity of the receptor, while the two alizarin trimers $\mathbf{3a}_3$ remain complexed. Addition of BuCYA to the resulting

complex $\mathbf{2}_3$•$(DEB)_{12}$•$\mathbf{3a}_6$ allows the exchange of the DEB for BuCYA, and the release of the guest **3a** from receptor $\mathbf{2}_3$•$(DEB)_{12}$.

Thus, the building up of supramolecular complexity, both in the self-assembly of the receptor and in the recognition processes of the different guests, through the control of different noncovalent interactions, such as hydrogen bonds and π–π interactions, has been achieved. This allows to bring together, with total control over molecular recognition, a large number of individual neutral molecules, both for the double and tetrarosette receptors (comprising nine and fifteen building blocks, respectively), and guest molecules (six and ten guest molecules, respectively). The control over the molecular recognition is an important goal in the supramolecular chemistry field due to the possible application of these concepts in nanotechnology, where the control over the formation and spatial arrangement on the systems is an important requirement for the *bottom-up* approach to the fabrication of nanosize structures. Moreover, further control over the self-assembly process is also achieved by the stepwise and selective release and exchange of guest molecules.

6.4. Experimental section

^{1}H NMR spectra were recorded on a Varian Inova 300 spectrometer or on a Varian Unity 400 spectrometer. Residual solvent protons were used as an internal standard and chemical shifts are given relative to tetramethylsilane (TMS). CD spectra were measured on a JASCO J-715 spectropolarimeter in a 0.01 cm width cell. Compounds **1**,[18b] **2**,[20c] and BuCYA[31] were prepared according to methods described previously.

Formation of assemblies $\mathbf{1}_3$•$(DEB)_6$/$(BuCYA)_6$ and $\mathbf{2}_3$•$(DEB)_{12}$/$(BuCYA)_{12}$. Hydrogen bonded assemblies $\mathbf{1}_3$•$(DEB)_6$ and $\mathbf{2}_3$•$(DEB)_{12}$ were prepared by mixing calix[4]arene dimelamine **1** or calix[4]arene tetramelamine **2** with 2 or 4 equivalents of DEB, respectively, in $CDCl_3$ for 15 minutes. For example, 3.06 mg (0.003 mmol) of **1** and 1.10 mg (0.006 mmol) of DEB were dissolved in 5 ml of $CDCl_3$, and stirred until all the compounds were dissolved. After evaporation of the solvent under high-vacuum, the

assembly is ready to use. Similarly, assembly $\mathbf{1}_3$•$(BuCYA)_6$ was prepared by mixing calix[4]arene dimelamine **1** with 2 equivalents of BuCYA in $CDCl_3$. Assembly $\mathbf{2}_3$•$(BuCYA)_{12}$ was prepared from $\mathbf{2}_3$•$(DEB)_{12}$ by exchange of DEB with BuCYA. In a typical example, 9.30 mg (0.001 mmol) of assembly $\mathbf{2}_3$•$(DEB)_{12}$ was dissolved in 1 ml of $CDCl_3$, and 1 equivalent (with respect to DEB) of BuCYA (2.22 mg, 0.012 mmol) was added. The solution was stirred for 30 minutes. After this time, the assembly $\mathbf{2}_3$•$(BuCYA)_{12}$ was ready to use.

6.5. References and notes

[1] Meyer, E. A.; Castellano, R. K.; Diederich, F. *Angew. Chem. Int. Ed.* **2003**, *42*, 1210-1250.

[2] Fiammengo, R.; Crego-Calama, M.; Reinhoudt, D. N. *Curr. Opin. Chem. Biol.* **2001**, *5*, 660-673.

[3] J. Ohkanda, J.; Lockman, J. W.; Kothare, M. A.; Qian, Y.; Blaskovich, M.; Sebti, S.; Hamilton, A. D. *J. Med. Chem.* **2002**, *45*, 177-188.

[4] *The Lock and Key Principle: The state of the art - 100 Years on*, Ed: Behr, J. P, Wiley, Chichester, **1994**.

[5] Reinhoudt, D. N.; Crego-Calama, M. *Science* **2002**, *295*, 2403-2407.

[6] a) Goodsell, D. S.; Olson, A. J. *Annu. Rev. Biophys. Biomol. Struct.* **2000**, *29*, 105-153; b) Zhang, Z., Merrit, E. A.; Ahn, M.; Roach, C.; Hou, Z.; Verlinde, C. L. M. J.; Hol, W. G. J.; Fan; E. *J. Am. Chem. Soc.* **2002**, *124*, 12991-12998.

[7] Cooke, G.; Rotello, V. M. *Chem. Soc. Rev.* **2002**, *31*, 275-286.

[8] *Principles of Molecular Recognition*, Eds: Buckingham, A. D.; Legon, A. C.; Roberts, S. M. Blackie, London, **1993**.

[9]Harley, J. H.; James, T. D.; Ward, C. J. *J. Chem. Soc., Perkin Trans. 1* **2000**, 3155-3184.

[10] a) Cram, D. J.; Kaneda, T.; Helgeson, R. C.; Brown, B.; Knobler, C. B.; Meverick, E.; Trueblood, K. N. *J. Am. Chem. Soc.* **1985**, *107*, 3645-3657; b) Fabbrizzi, L.; Poggi, A. *Chem. Soc. Rev.* **1995**, *24*, 197-202; c) Bell, T. W.; Khasanov, A. B.; Drew, M. G. B.; Filikov, A.; James, T. L. *Angew. Chem. Int. Ed.* **1999**, *38*, 2543-2547.

[11] a) Tobey, S. L.; Anslyn, E. V. *J. Am. Chem. Soc.* **2003**, *125*, 10963-10970; b) Gale, P. A. *Coord. Chem. Rev.* **2001**, *213*, 79-128; c) Suksai, C.; Tuntulani, T. *Chem. Soc. Rev.* **2003**, *32*, 192-202; d) Sessler, J. L.; Camiolo, S.; Gale, P. A. *Coord. Chem. Rev.* **2003**, *240*, 17-55; e) Linares, J. M.; Powell, D.; Bowman-James, K. *Coord. Chem. Rev.* **2003**, *240*, 57-75; f) Choi, K. H.; Hamilton, A. D. *Coord. Chem. Rev.* **2003**, *240*, 101-110; g) Fabbrizzi, L.; Liccheli, M.; Rabaioli, G.; Taglietti, A. *Coord. Chem. Rev.* **2000**, *205*, 85-108.

[12] a) Middel, O.; Verboom, W.; Reinhoudt, D. N. *Eur. J. Org. Chem.* **2002**, *16*, 2587-2597; b) Droz, A. S.; Diederich, F. *J. Chem. Soc. Perkin Trans. 1*, **2000**, 4224-4226; c) Tamaru, S.; Shinkai, S.; Khasanov, A. B.; Bell, T. W. *Proc. Nat. Acad. Sci. USA* **2002**, *99*, 4972-4976; d) Orner, B. P.; Salvatella, X.; Quesada, J. S.; de Mendoza, J.; Giralt, E.; Hamilton, A. D. *Angew. Chem. Int. Ed.* **2002**, *41*, 117-119; e) Almaraz, M.; Raposo, C.; Martín, M.; Caballero, M. C.; Moran, J. R. *J. Am. Chem. Soc.* **1998**, *120*, 3516-3517.

[13] a) Amit, A. G.; Marinzza, R. A.; Phillips, S. E. V.; Poljak, R. J. *Science* **1986**, *233*, 747-753; b) Lerner, R. A.; Benkovic, S. J.; Schultz, P. G. *Science* **1991**, *252*, 659-667 , and references therein.

[14] a) Mammen, M.; Choi, S.-K.; Whitesides, G. M. *Angew. Chem. Int. Ed.* **1998**, *37*, 2754-2794; b) Huskens, J.; Mulder, A.; Auletta, T.; Nijhuis, C. A.; Ludden, M. J. W.; Reinhoudt, D. N. *J. Am. Chem. Soc.* **2004**, *126*, 6784-6797.

[15] a) Shi, X. D.; Mullaugh, K. M.; Fettinger, J. C.; Jiang, Y.; Hofstadler, S. A.; Davis, J. T. *J. Am. Chem. Soc.* **2003**, *125*, 10830-10841; b) Casnati, A.; Massera, C.; Pelizzi, N.; Stibor, I.; Pinkassik, E.; Ugozzoli, F.; Ungaro, R. *Tetrahedron Lett.* **2002**, *43*, 7311-7314; c) Chrisstoffels, L. A. J.; de Jong, F.; Reinhoudt, D. N.; Sivelli, S.; Gazzola, L.; Casnati, A.; Ungaro, R. *J. Am. Chem. Soc.* **1999**, *121*, 10142-10151; d) Pelizzi, N.; Casnati, A.; Friggeri, A.; Ungaro, R. *J. Chem. Soc., Perkin Trans. 2* **1998**, 1307-1311; e) Hilmey, D. G.; Paquete, L. A. *J. Org. Chem.* **2004**, *69*, 3262-3270.

[16] a) Ebbing, M. H. K.; Villa, M.-J.; Valpuesta, J.-M.; Prados, P.; de Mendoza, J. *Proc. Nat. Acad. Sci. USA* **2002**, *99*, 4962-4966; b) Barbour, L. J.; Caira, M. R.; le Roex, T.; Nassimbeni, L. R. *J. Chem. Soc., Perkin Trans. 2* **2002**, 1973-1979; c) Heinz, T.; Rudkevich, D. M.; Rebek, J. Jr. *Nature* **1998**, *394*, 764-766; d) Körner, S. K.; Tucci, F. C.; Rudkevich, D. M.; Heinz, T.; Rebek, J. Jr. *Chem. Eur. J.* **2000**, *6*, 187-195; e)

Shivanyuk, A.; Rebek, J. Jr. *J. Am. Chem. Soc.* **2002**, *124*, 12074-12075; f) Chen, J.; Rebek, J. Jr. *Org. Lett.* **2002**, *4*, 327-329; g) Starnes, S. D.; Rudkevich, D. M.; Rebek, J. Jr. *J. Am. Chem. Soc.* **2001**, *123*, 4659-4669.

[17] Hydrogen-bonded assemblies acting as *endo*-receptors: a) Kerckhoffs, J. M. C. A.; van Leeuwen, F. W. B.; Spek, A. L.; Kooijman, H.; Crego-Calama, M.; Reinhoudt, D. N. *Angew. Chem. Int. Ed.* **2003**, *42*, 5717-5722; b) Ishi-i, T.; Mateos-Timoneda, M. A.; Timmerman, P.; Crego-Calama, M.; Reinhoudt, D. N.; Shinkai, S. *Angew. Chem. Int. Ed.* **2003**, *42*, 2300-2305; c) Kerckhoffs, J. M. C. A.; Ishi-i, T.; Paraschiv, V.; Timmerman, P.; Crego-Calama, M.; Shinkai, S.; Reinhoudt, D. N. *Org. Biomol. Chem.* **2003**, *1*, 1-9.

[18] Hydrogen bonded assemblies acting as *exo*-receptors: a) Crego-Calama, M.; Timmerman, P.; Reinhoudt, D. N. *Angew. Chem. Int. Ed.* **2000**, *39*, 755-758; b) Ishi-i, T.; Crego-Calama, M.; Timmerman, P.; Reinhoudt, D. N.; Shinkai, S. *J. Am. Chem. Soc.* **2002**, *124*, 14631-14641; c) Ishi-i, T.; Crego-Calama, M.; Timmerman, P.; Reinhoudt, D. N.; Shinkai, S. *Angew. Chem. Int. Ed.* **2002**, *41*, 1924-1929.

[19] a) Vreekamp, R. H.; van Duynhoven, J. P. M.; Hubert, M.; Verboom, W.; Reinhoudt, D. N. *Angew. Chem. Int. Ed. Engl.* **1996**, *35*, 1215-1218; b) Timmerman, P.; Vreekamp, R. H.; Hulst, R.; Verboom, W.; Reinhoudt, D. N.; Rissanen, K.; Udachin, K. A.; Ripmeester, J. *Chem. Eur. J.* **1997**, *3*, 1823-1832.

[20] a) Jolliffe, K. A.; Timmerman, P.; Reinhoudt, D. N. *Angew. Chem. Int. Ed.* **1999**, *38*, 933-937; b) Paraschiv, V.; Crego-Calama, M.; Ishi-i, T.; Padberg, C. J.; Timmerman, P.; Reinhoudt, D. N. *J. Am. Chem. Soc.* **2002**, *124*, 7638-7639; c) Prins, L. J.; Neuteboom, E. E.; Paraschiv, V.; Crego-Calama, M.; Timmerman, P.; Reinhoudt, D. N. *J. Org. Chem.* **2002**, *67*, 4808-4820.

[21] Prins, L. J.; Jolliffe, K. A.; Hulst, R.; Timmerman, P.; Reinhoudt, D. N. *J. Am. Chem. Soc.* **2000**, *122*, 3617-3627.

[22] Kerckhoffs, J. M. C. A.; ten Cate, M. G. J.; Mateos-Timoneda, M. A.; van Leeuwen, F. W. B.; Snellink-Ruël, B.; Spek, A. L.; Kooijman, H.; Crego-Calama, M.; Reinhoudt, D. N. submitted for publication.

[23] Shinkai, S.; Ikeda, M.; Sugasaki, A.; Takeuchi, M. *Acc. Chem. Res.* **2001**, *34*, 494-503.

[24] a) Park, K. *Controlled Drug Delivery: Challenges and Strategies*, American Chemical Society, Washington, DC, **1997**; b) Douglas, T.; Young, M. *Nature* **1998**, *393*, 152-155; c) Mal, N. K.; Fujiwara, M.; Tanaka, Y. *Nature* **2003**, *421*, 350-353.

[25] Bielejewska, A. G.; Marjo, C. E.; Prins, L. J.; Timmerman, P.; de Jong, F.; Reinhoudt, D. N. *J. Am. Chem. Soc.* **2001**, *123*, 7518-7533.

[26] In the absence of chiral auxiliary, the receptor is presented as a racemic mixture of the *P*- and *M*-enantiomers and therefore only two signals (~ 13-15 ppm) are expected for the NH protons of the barbiturate/cyanurate components in the ^{1}H NMR spectrum. However, the addition of chiral diacids (D- or L-) leads to the formation of diastereomeric ((*P*)-D or (*M*)-L) assemblies (chirality induction), and therefore four signals are expected, two signals for each diastereomeric receptor, if the induction of chirality is not quantitative.

[27] The encapsulation of alizarin by assemblies bearing chiral groups leads to a change of symmetry from D_3 to C_3.[22] The CD spectrum of the complex formed by the chiral assemblies resembles the one obtained from complex $\mathbf{1}_3$•(DEB)$_6$•$\mathbf{3a}_3$•$\mathbf{4a}_3$.

[28] The pK_a value of DEB is 7.4 and of guest **4a** is 2.99 (see: a) Dawson, R. M. C. *Data for biochemical research*, Oxford, Clarendon Press, **1959**; b) Chidambaram, N.; Burgess, D. J. *AAPS Pharmsci.* **2000**, *2*, 1-11.)

[29] The isomers are coded with 3 letters (S for staggered; E for eclipsed), which represent the relative orientation of the melamine fragments between the rosette layers 1st and 2nd, 2nd and 3rd, and 3rd and 4th floors, respectively. The presence of only four signals for the NH_{DEB} protons in the ^{1}H NMR spectrum indicate that the assembly can only exist as SSS, SES, and EEE-isomer. Previous studies have demonstrated that only the SSS-isomer is present.[20]

[30] If the same behaviour is expected for the change in orientation of the melamine rings upon encapsulation of **3a**, only the EEE and ESE-isomers can be formed. Based on symmetry, the four signals observed in the ^{1}H NMR spectrum upon complexation of **3a** indicates that assembly $\mathbf{2}_3$•(DEB)$_{12}$•$\mathbf{3a}_3$ is the EEE-isomer (eight signals would be expected for the ESE-isomer).

[31] Prins, L. J.; Hulst, R.; Timmerman, P.; Reinhoudt, D. N. *Chem. Eur. J.* **2002**, *8*, 2288-2301.

Chapter 7

Catalytic chaperone effect in tetrarosette assembly formation

In this chapter, the role of barbiturate derivatives as catalytic chaperones in the formation of (chiral) cyanurate-based tetrarosette assemblies is studied. This type of supramolecular catalyst for the self-assembly of supramolecules (catalytic chaperone) is applied also to the enantioselective noncovalent synthesis of tetrarosettes leading to enantiopure assemblies with half-life time to racemization at room temperature of 42 days!

7.1. Introduction

Self-assembly is nature's favorite way to generate the complexity required to promote energetically demanding biological processes.[1] It denotes the spontaneous connection of a few (or many) components into discrete and well-defined structures.[2] The main advantage of self-assembly is that noncovalent bonds are formed spontaneously and reversibly under conditions of thermodynamic equilibrium, with the possibility of error corrections ('*self-healing*') and without undesired side-products.[3] Due to the implications for nanotechnology, one of the main goals of noncovalent synthesis (and specially of self-assembly as its main tool) is the construction of nanometer size structures, with absolute control over the spatial disposition of the molecular components.[4] However, for the formation of noncovalent structures with size $\geq$ 3nm, with a large number of weak interactions, it is expected that the kinetics of formation will be no longer fast at the time scale of their formation.[5,6]

To direct synthesis to the desired product, chemists have made use of "helpers" or of "templates" in noncovalent synthesis of supramolecular assemblies, specially after discovering that the replication of DNA involves a templated synthesis.[7] In general, a template organizes an assembly of atoms with respect to one or more geometric loci, in order to achieve a particular linking of atoms.[8,9] This strategy, also known as template assisted synthesis, has lead to the guest-templated formation of covalent and noncovalent systems,[10,11] self-replicating systems,[12] and molecular imprinted polymers,[13] as well as the selection of the best receptor in dynamic combinatorial libraries.[14] In many cases, nature also needs the assistance in the folding of polypeptides to obtain the conformation that gives the polypeptide its biological properties.[15] The use of the so-called "chaperones" provides a solution to the problem. Chaperones have been defined as a family of proteins that mediate the correct assembly of other polypeptides, inhibiting incorrect molecular interactions that will generate nonfunctional structures, but are not themselves components of the final functional structure.[15,16] Surprisingly, the use of molecular chaperones has hardly been exploited for the synthesis of (non)covalent assemblies,[5] probably due to the 'popular believe' that noncovalent synthesis of self-assembled aggregates always takes place under thermodynamic equilibrium conditions.

Generally speaking, the main difference between the template and the chaperone is that while the template has to be (usually noncovalently) attached during the whole process (synthesis) to direct the formation of the desired product, the chaperon only stabilizes metastable conformations of the protein and it is not always attached to it during the whole folding process.[15] The only example found in literature of the use of synthetic chaperones has been recently published by our group.[5] In this example an equimolar amount of chaperone promoted the noncovalent synthesis of a hydrogen-bonded assembly which formation was unattainable without the chaperone. Ideally one would like chaperones to be catalytic rather than stoichiometric.

Supramolecular catalysts (or artificial enzymes)[17] have been designed to reproduce features of natural enzymes, such as astonishing selectivities and catalytic efficiencies, in the outcome of chemical reactions such as Diels-Alder, S_N2, etc.[17,18] The requirements for these type of supramolecular catalysts include binding to the substrate(s), reaction with it (with a given rate, selectivity, and turnover), and release of the products, thus regenerating the catalyst for a new cycle. However, all supramolecular catalysts described until now are designed to influence the result of a chemical reaction, not the self-assembly process of supramolecules.

In this chapter, the first example of a synthetic catalytic chaperone is presented. A barbiturate derivative acts as catalytic chaperone in the noncovalent synthesis of cyanurate based tetrarosette assemblies. The barbiturate derivative inhibits the formation of kinetically stable ill-defined assemblies and allows the formation of the tetrarosette assembly. Furthermore, the barbituric chaperone is able to accelerate the overall reaction time for the noncovalent synthesis of the tetrarosette without being modified, allowing its reuse. More importantly, this catalytic chaperone not only facilitates the formation of a self-assembled aggregate, but is also used for the enantioselective noncovalent synthesis of assemblies. The chiral chaperone leads to the quantitative noncovalent synthesis of enantiopure assemblies with half-lives of racemization of 42 days!

7.2. Results and Discussion

7.2.1. Synthesis

Tetramelamines **1**, 5-((*R*)-2-phenylproply)-5'-ethylbarbiturate (R-BAR), BuCYA and (*R*)-MePheCYA (Chart 7.1) have been synthesized following methods previously described.[19,20]

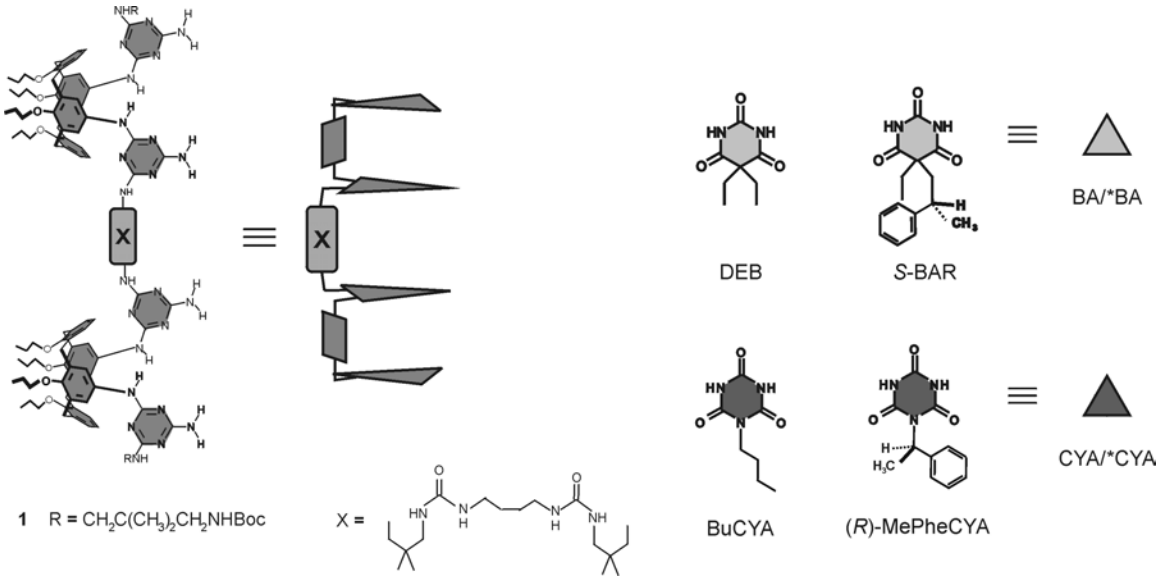

Chart 7.1. Chemical and schematic representation of tetramelamine **1** and barbiturate (BA/*BA)/cyanurate (CYA/*CYA) building components.

7.2.2. Assembly studies of cyanurate-based tetrarosette assemblies

In Chapter 4 it is shown that the formation of cyanurate-based tetrarosette assemblies is a kinetically controlled self-assembly process. Mixing tetramelamine **1** with BuCYA (1:4 ratio) in chloroform at room temperature did not result in the expected tetrarosette assembly $\mathbf{1}_3$•$(BuCYA)_{12}$. The characteristic four signals in the region δ = 15-13 ppm in the ^{1}H NMR spectrum expected for the formation of hydrogen bonds between the NH protons of the cyanurate and the melamine rings of **1** in $\mathbf{1}_3$•$(BuCYA)_{12}$ were not present (Figure 7.1). Instead, the mixing process leads to the formation of nondefined

structures which display high kinetic stability. Only after heating at 100 °C for one week, the ^{1}H NMR shows the formation of the assembly $\mathbf{1}_3$•(BuCYA)$_{12}$ (Figure 7.1b).

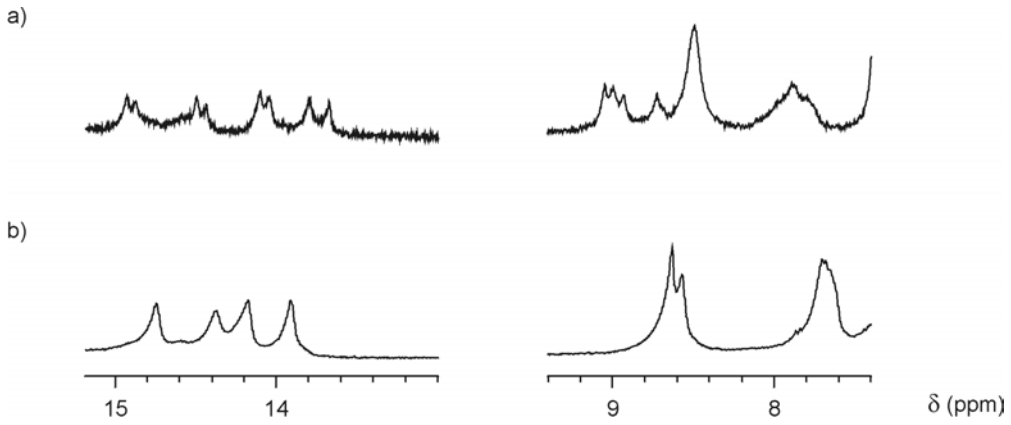

Figure 7.1. Parts of the ^{1}H NMR spectra of tetramelamine **1** and BuCYA (1:4 ratio) a) immediately after mixing, and b) after ome week at 100 °C. The spectra were recorded in $CDCl_3$ at room temperature.

The high kinetic stability of these ill-defined assemblies was confirmed by CD spectroscopy (Figure 7.2). Mixing tetramelamine **1** and chiral cyanurate (*R*)-MePheCYA resulted in the appearance of a signal in the CD spectrum (Figure 7.2a). The close resemblance with the CD-spectra of double rosette assemblies strongly suggests the presence of double rosette subdomains in the ill-defined structures. After heating the mixture for one week at 100 °C, the shape of the CD signal had changed to the shape of the CD spectrum of chiral tetrarosette assemblies with the maximum CD intensity located at 286 nm (Figure 7.2b).

Gel permeation chromatography (GPC) also confirmed the conversion of the ill-defined assemblies in the well-defined tetrarosette assembly. Analysis of the 1:4 mixture of **1** and BuCYA directly after mixing showed the elution of structures with a broad molecular weight (M_W) distribution, while after heating of the mixture at 100 °C for one week, the chromatogram showed the elution of only one fraction with defined M_W corresponding to assembly $\mathbf{1}_3$•(BuCYA)$_{12}$.

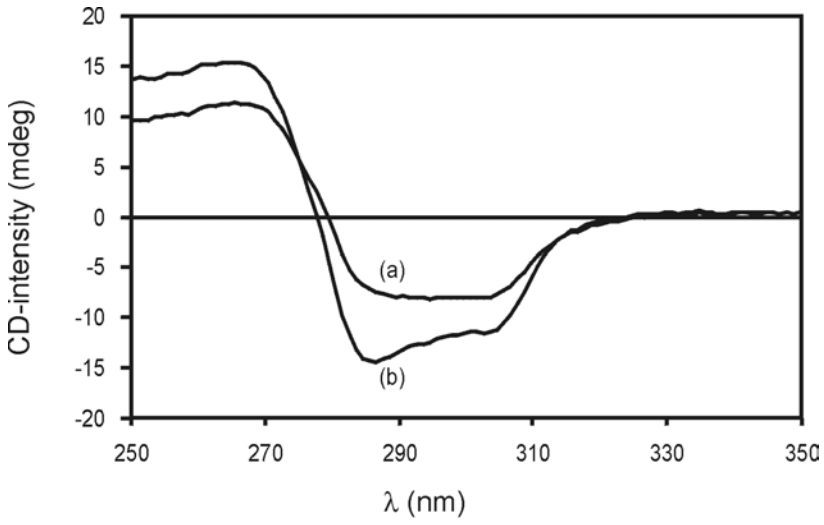

Figure 7.2. CD spectra of a 1:4 mixture of tetramelamine **1** and (*R*)-MePheCYA (1:4 ratio) a) immediately after mixing, and b) after one week at 100 ^{o}C. The spectra were recorded in $CDCl_3$ at room temperature.

7.2.3. Achiral barbiturate derivatives as catalytic chaperone in the noncovalent synthesis of tetrarosettes

One possible way to overcome the problem of formation of kinetically stable ill-defined assemblies is the use of molecular chaperones (Figure 7.3). This strategy is widely used in nature for the correct folding of proteins. In Chapter 4, the role of DEB as chaperon in the formation cyanurate-based tetrarosette assemblies was briefly discussed.[5] The 'chaperone' strategy involves the formation of the assembly using a barbiturate derivative (1:4 ratio tetramelamine:barbiturate) and subsequent exchange by cyanuric acid derivatives (1:1 ratio DEB:cyanuric acid) in the correct self-assembled tetrarosette (see Chapter 4, *exchange* method). This exchange is possible due to the formation of stronger hydrogen-bonds between the pair melamine:cyanurate than between the pair melamine:barbiturate.[21]

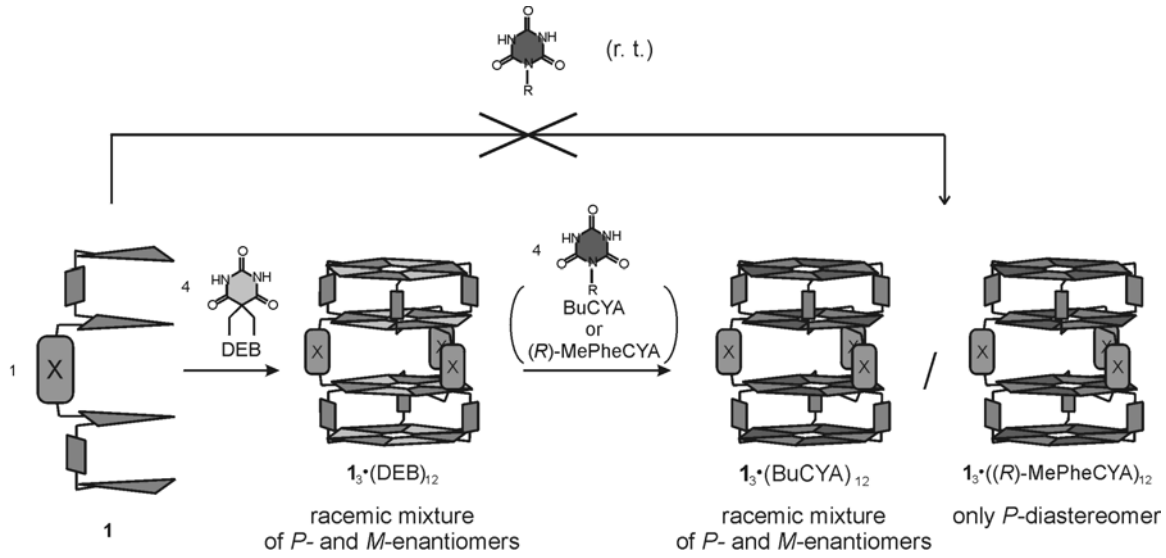

Figure 7.3. 'Chaperoned' formation of cyanurate-based tetrarosette assemblies.

The use of catalytic amounts (1:1 ratio of tetramelamine **1**:DEB instead of the stoichiometric 1:4 ratio) of DEB as chaperone was studied using ^{1}H NMR and circular dichroism (CD) spectroscopy. The catalytic function of DEB in the self-assembly of superstructures is depicted in Figure 7.4. Moreover, the turn-over of the DEB was also studied.

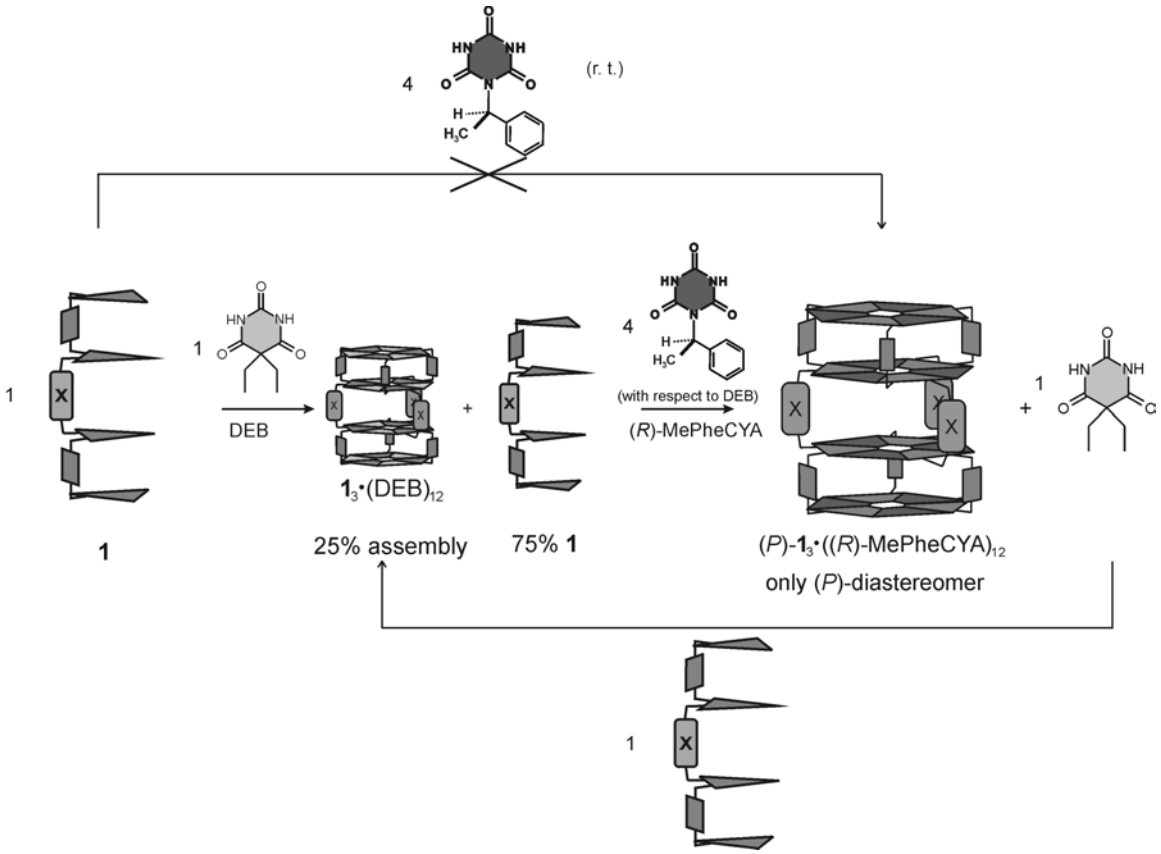

Figure 7.4. Schematic representation of the formation of cyanurate-based tetrarosette assemblies showing the catalytic chaperone effect of the DEB molecules.

The first step for the formation of cyanurate-based tetrarosette was the mixing of the tetramelamine **1** and DEB in a 1:1 ratio. The ^{1}H NMR spectrum of this mixture (1.0 mM in $CDCl_3$) shows four sharp signals in the region between δ = 15-13 ppm, characteristic of the formation of tetrarosette assemblies (Figure 7.5a) plus the signal of the free tetramelamine **1**. Integration of the appropriate signals indicates that only 25% of the assembly $\mathbf{1}_3$•(DEB)$_{12}$ is formed and 75% of tetramelamine **1** is present in the reaction mixture. Thus, the self-assembly process of tetramelamine **1** and DEB shows positive cooperativity, *i.e.* the formation of the first double rosette in $\mathbf{1}_3$•(DEB)$_{12}$ strongly preorganizes the second set of dimelamines such that only free **1** and fully assembled tetrarosette are observed. The second step is the addition of 4 equivalents of cyanurate derivative ((*R*)-MePheCYA) (1:4 DEB:cyanurate) to the mixture, resulting in the almost quantitative formation of (*P*)-$\mathbf{1}_3$•((*R*)-MePheCYA)$_{12}$ (+ free DEB). The ^{1}H NMR

spectrum of the assembly (0.3 mM in $CDCl_3$) shows the disappearance of the signals of assembly $\mathbf{1}_3$•$(DEB)_{12}$ and free **1** and the appearance of four new signals at lower field and a new broad signal at ~ 8.4 ppm corresponding to free DEB (Figure 7.5b). Thus, the ^{1}H NMR spectroscopy clearly indicates the exchange of DEB by the cyanurate derivatives and the formation of the assembly $\mathbf{1}_3$•$((R)$-MePheCYA$)_{12}$.[5] The replacement of the barbiturate by cyanurate derivatives is due to the formation of stronger hydrogen bonds between the melamine-cyanurate than between melamine-barbiturate because of the higher acidity of the cyanurate derivative.[21]

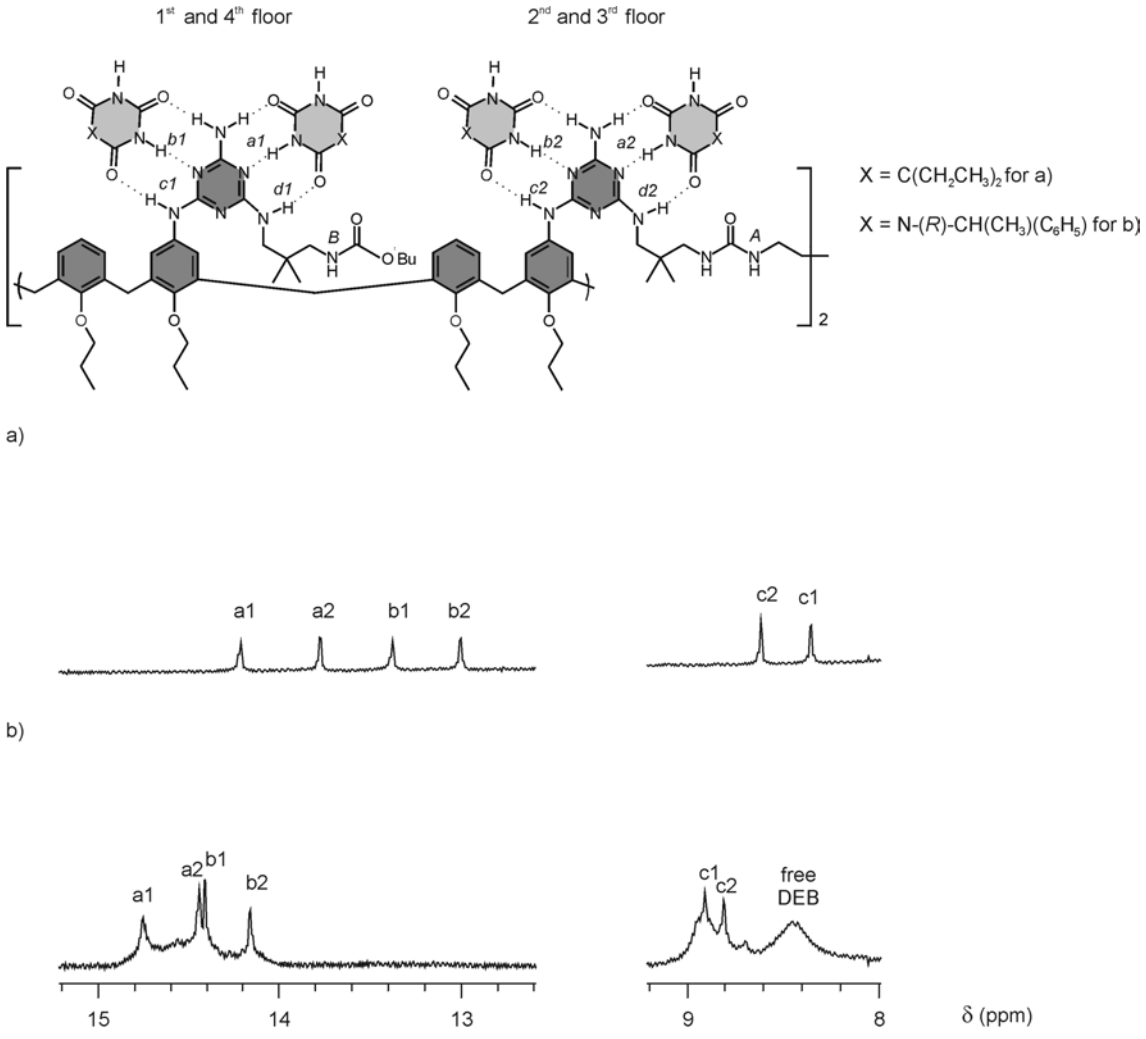

Figure 7.5. Parts of the ^{1}H NMR spectra of a) mixture 1:1 of tetramelamine **1** and DEB, and b) after the addition of 4 equivalents (1:4 DEB:cyanurate) of (*R*)-MePheCYA. All ^{1}H NMR spectra were recorded in $CDCl_3$ (1.0 mM) at room temperature (400 MHz).

Additional proof for the formation of $\mathbf{1}_3$•((*R*)-MePheCYA)$_{12}$ is obtained from CD-spectroscopy (Figure 7.6). The mixture of tetramelamine **1** and DEB (1.0 mM in $CDCl_3$) is CD inactive, because both components are not chiral and the assembly that is formed (25%) is present as a racemic mixture of both *P*- and *M*-enantiomers (Figure 7.6a).[22] However, after addition of (*R*)-MePheCYA (1:4 ratio DEB:(*R*)-MePheCYA), the appearance of a signal in the CD-spectrum, similar in shape to a typical CD-spectra of tetrarosette assemblies with a maximum at 286 nm, indicates the formation (100%) of $\mathbf{1}_3$•((*R*)-MePheCYA)$_{12}$ (Figure 7.6b). The formation of assembly $\mathbf{1}_3$•((*R*)-MePheCYA)$_{12}$ is quantitative because the CD intensity is similar to the CD intensity of a chiral tetrarosette assembly (concentration 0.33 mM).[23] Thus, also the presence of catalytic amounts of DEB allows the quantitative formation of cyanurate-based tetrarosette assemblies. Furthermore, the use of a chiral cyanurate in the last step of the 'chaperoned' reaction leads to the diastereoselective formation of the assembly, *i.e.* the presence of chiral centers with (*R*)-stereochemistry in the cyanurate derivative induces the exclusive formation of the (*P*)-assembly. Thus, the chirality in the assembly is introduced in the exchange process using a chiral cyanurate not by using a chiral catalytic chaperone (see below). However, to be a true catalyst, in its strict sense, it should display turn-over. Therefore, the possible turn-over (and the recycling) of the expelled DEB molecules from the hydrogen-bonded assembly was also studied. Addition of tetramelamine **1** (1 equivalent respect to free DEB) to the mixture of assembly $\mathbf{1}_3$•((*R*)-MePheCYA)$_{12}$ and free DEB and subsequent addition of (*R*)-MePheCYA (4 equivalents with respect to tetramelamine **1**) led to a CD signal in which the maximum CD intensity has been doubled, indicating that the concentration of the assembly was double in the mixture (from 0.33 mM to 0.66 mM) (Figure 7.6c).

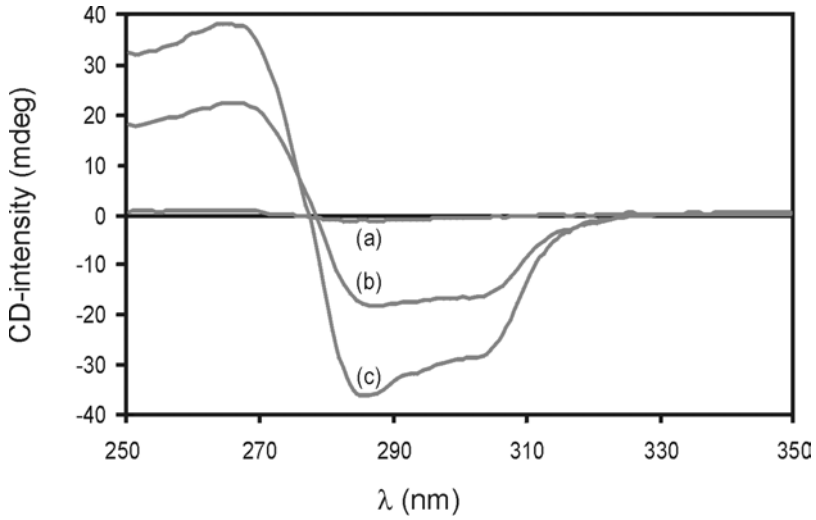

Figure 7.6. CD spectra of a 1:1 mixture of tetramelamine **1** and DEB before (a) and after (b) the addition of 4 equivalents of (*R*)-MePheCYA, and (c) after subsequent addition of 1 equivalent of tetramelamine **1** and 4 equivalents of (*R*)-MePheCYA. The number of equivalents is related to DEB. All the spectra were recorded in $CDCl_3$ at room temperature.

The DEB displays the characteristics of a catalyst, *i.e.* it is not part of the product, it is not modified during the reaction (thus, allowing turnover), and more important, increases the rate of the reaction (100 ^{o}C to room temperature and one week to a few minutes). In strict sense, a 'traditional' catalyst accelerates a step of the reaction by lowering the activation energy of a single transition state (Scheme 7.1a). However, the mechanism of the actuation of the catalytic chaperon is not clear. Two options are plausible:[15] i) the chaperon accelerates one of the reaction steps in the formation of the correct assembly or ii) the chaperon inhibits the formation of the kinetically stable ill-defined assemblies (Scheme 7.1c).

Given the complexity of the system containing both the well-defined tetrarosette as well as the ill-defined aggregates all in dynamic equilibrium, it is impossible to identify a single assembly event that is catalyzed. Therefore, it is only possible to talk about the overall effect of the catalytic chaperone.

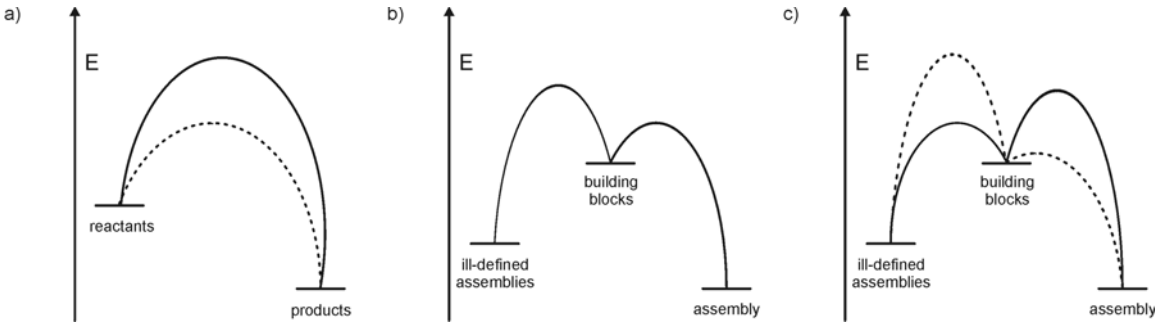

Scheme 7.1. Graphical representation of the energetic effects of catalysts and chaperones. In example a) the addition of a catalyst to a reaction mixture lowers the activation energy of the reaction (dotted line). b) the formation of the correct assembly is favored both kinetically and thermodynamically; this is a case of strict self-assembly where chaperones are not required. c) the formation of an incorrect structure is favored kinetically; the addition of a chaperone, indicated by the dotted lines, could either block the misassembly pathway, or lower the activation energy of the correct pathway.

7.2.4. Chiral barbiturate derivatives as catalytic chaperone in the noncovalent synthesis of enantiopure tetrarosette assemblies

The development of enantiopure structures is important in the development of new applications of self-assembled systems in the fields of nanotechnology and material sciences. It was envisioned that one of the possible ways to fabricate them is to make use of enantioselective catalysts. For this reason, the chaperone effect of a chiral barbiturate derivative was studied in the enantioselective formation of tetrarosette assemblies (Figure 7.7).

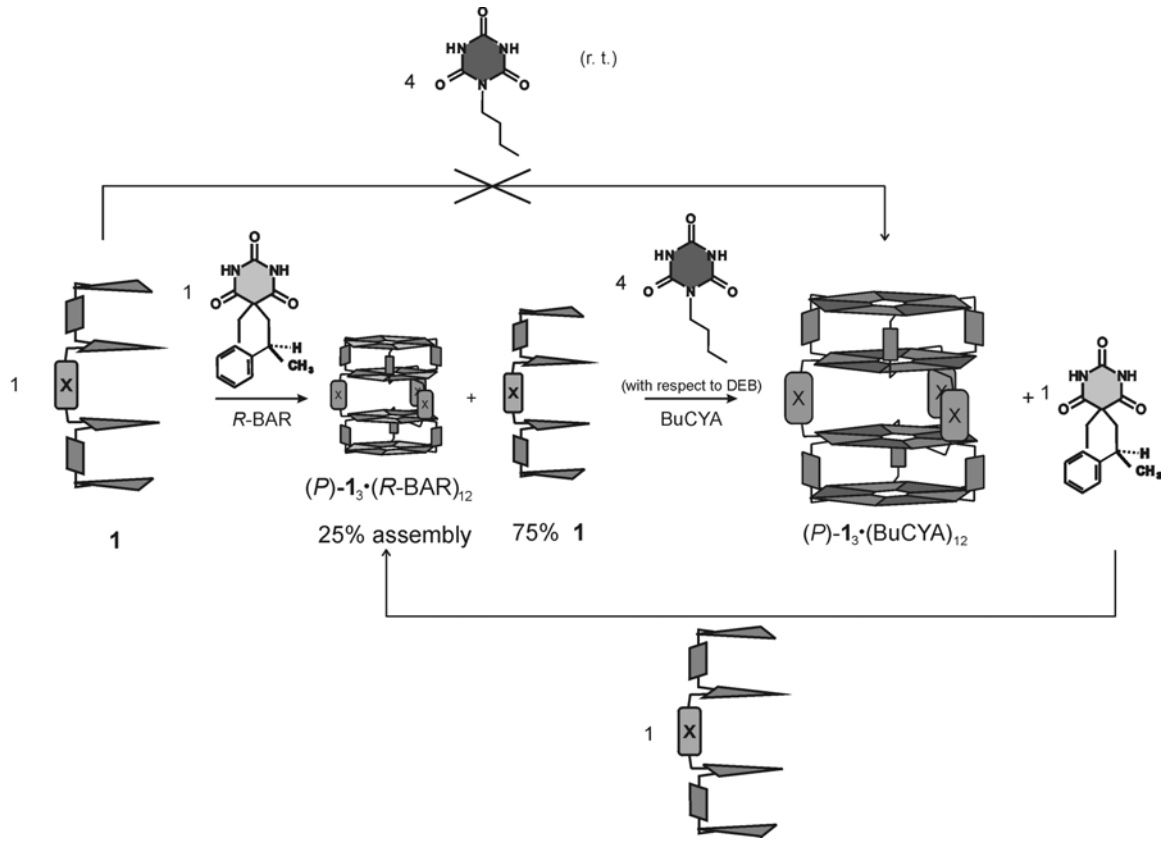

Figure 7.7. Schematic representation of the enantioselective formation of cyanurate-based tetrarosette assemblies showing the catalytic chaperone effect of the chiral *R*-BAR molecules.

Similar to the use of achiral barbiturate derivatives as catalytic chaperones, the ^{1}H NMR spectrum of a mixture 1:1 of tetramelamine **1** and *R*-BAR in $CDCl_3$ (1.0 mM) shows the formation of 25% of the (diastereomerically) pure assembly (*P*)-**1**$_3$•(*R*-BAR)$_{12}$.

The ^{1}H NMR of this mixture shows a complicated set of signals in the region δ = 15-13 ppm (Figure 7.8a) because of the different orientations of the *R*-BAR within the assembly (*P*)-**1**$_3$•(*R*-BAR)$_{12}$.[24] Further addition of 4 equivalents (with respect to *R*-BAR) of BuCYA resulted in the formation of the assembly (*P*)-**1**$_3$•(BuCYA)$_{12}$ as can be judged by the disappearance of the signals of assembly (*P*)-**1**$_3$•(*R*-BAR)$_{12}$ and free **1** and the appearance of four new signals in the region δ = 15-13 ppm (and the signal of free *R*-BAR). Integration of the appropriate signals in the ^{1}H NMR spectrum shows the almost quantitative formation of assembly (*P*)-**1**$_3$•(BuCYA)$_{12}$ (Figure 7.8b).[25]

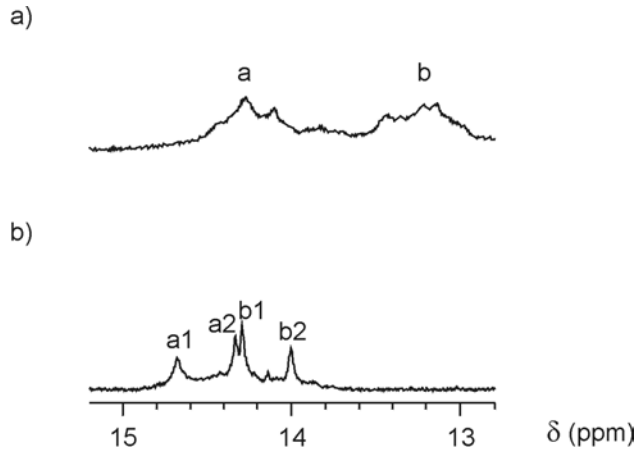

Figure 7.8. Part of the ^{1}H NMR spectra of a mixture 1:1 of tetramelamine **1** and *R*-BAR, a) before and b) after the addition of 4 equivalents (with respect to *R*-BAR) of BuCYA. All ^{1}H NMR spectra were recorded in $CDCl_3$ at room temperature (400 MHz).

Previous studies in the noncovalent enantioselective synthesis of double rosette assemblies have shown that the replacement of a chiral barbiturate by cyanurate derivatives occurs with complete memory of the chirality,[26] that is to say that the exchange process occurs quantitatively and without loss of the handedness of the assembly. The crucial question is whether the chiral barbiturate acts as chaperone with conservation of chirality, *i.e.* is the chirality imprinted by the catalytic chiral barbiturate in the 1:1 mixture of tetramelamine **1** and *R*-BAR is transferred upon exchange by BuCYA to the assembly $\mathbf{1}_3$•$(BuCYA)_{12}$, therefore leading to the enantiopure assembly (*P*)-$\mathbf{1}_3$•$(BuCYA)_{12}$? The CD spectrum of the mixture of tetramelamine **1** and *R*-BAR in a 1:1 ratio (1.0 mM) shows a signal due to the formation of the 25% of assembly (*P*)-$\mathbf{1}_3$•$(R\text{-}BAR)_{12}$ (Figure 7.9a). Addition of BuCYA leads to a stronger signal in the CD spectrum (Figure 7.9b), despite the fact that the assembly (*P*)-$\mathbf{1}_3$•$(BuCYA)_{12}$ no longer contains any chiral center. It can be concluded that the process leads to the quantitative enantioselective formation of assembly (*P*)-$\mathbf{1}_3$•$(BuCYA)_{12}$ (0.33 mM).

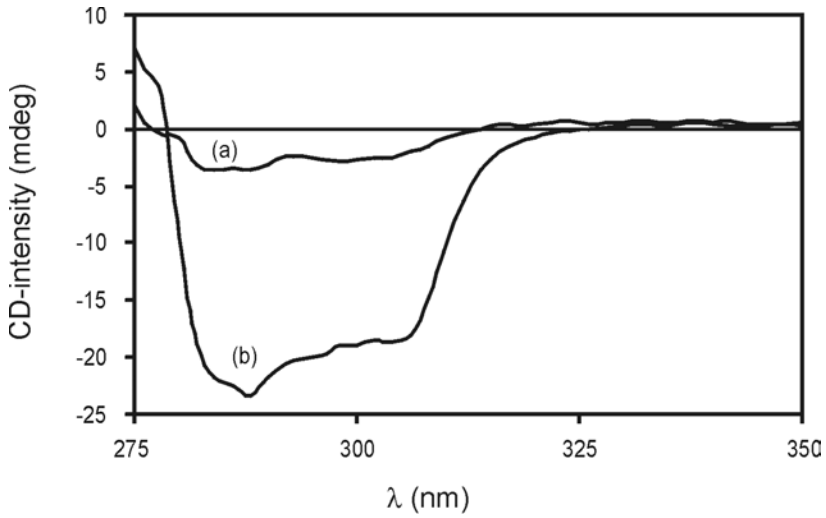

Figure 7.9. CD spectra of 1:1 mixture of tetramelamine **1** and *R*-BAR (1.0 mM), a) before, and b) after the addition of BuCYA. All spectra were recorded in toluene-d_8 at room temperature.

Thus, it is possible to synthesize enantiopure assemblies ((*P*)-$\mathbf{1}_3$•$(BuCYA)_{12}$) using a chiral catalytic chaperon (*R*-BAR). Similar to achiral barbiturate molecules (DEB), the *R*-BAR molecules display both the typical features of a catalyst and a chaperon, *i.e.* accelerates the formation of the assembly inhibiting the incorrect interactions between tetramelamines and cyanurate derivatives, it is not part of the product and it is not consumed or modified during the reaction. Moreover, the process displays the "chiral memory" effect, resulting in the formation of enantiopure assemblies.

7.2.5. Racemization studies with enantiopure assemblies formed using the chaperone effect of chiral barbiturates

To obtain a better understanding of the enantioselective formation of tetrarosette assemblies (*P*)-$\mathbf{1}_3$•$(BuCYA)_{12}$ using the catalytic chaperone, racemization studies were carried out.

As a result of racemization, assembly (*P*)-$\mathbf{1}_3$•$(BuCYA)_{12}$ will be converted in time to a racemic mixture of the (*P*)- and (*M*)-enantiomers. To determine the activation energy for the racemization process, the racemization rate was measured by monitoring the decrease of the CD intensity in time at different temperatures (Figure 7.10a).

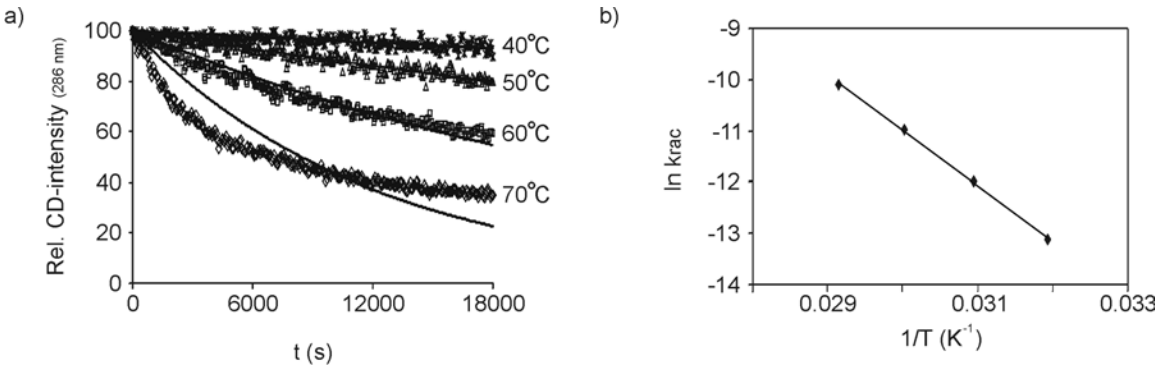

Figure 7.10. a) Racemization of assembly (*P*)-**1**$_3$•(BuCYA)$_{12}$ monitored by the decrease of the CD intensity in time at different temperatures. The time-dependent measurements were started immediately after the addition of 4 equivalents of BuCYA (relative to *R*-BAR) to a 1.0 mM solution of a 1:1 mixture of **1** and *R*-BAR in toluene at room temperature. The solid lines are the best fits to the racemization model described in the text. b) Arrenhius' plot of lnk_{rac} versus 1/T.

The resulting curves were fitted to the racemization model as depicted in equation 7.1.

$$(P)\text{-}\mathbf{1}_3\bullet(\text{BuCYA})_{12} \underset{k_{rac}}{\overset{k_{rac}}{\rightleftharpoons}} (M)\text{-}\mathbf{1}_3\bullet(\text{BuCYA})_{12} \qquad (\text{Eq. 7.1})$$

In equation 7.1, k_{rac} [s^{-1}] is the rate constant for racemization. Linear regression analysis gave the values for k_{rac} as reported in Table 7.1.

Table 7.1. Racemization rate constants of assembly (*P*)-**1**$_3$•(BuCYA)$_{12}$ formed using the catalytic and stoichiometric chaperone as function of temperature.

	Catalytic chaperone	Stoichiometric Chaperone
T (^{o}C)	k_{rac} (x 10^{-6} s^{-1})	k_{rac} (x 10^{-6} s^{-1})
70	41.3	50.8
60	16.8	17.8
50	6.2	9.69
40	2.0	2.13

Subsequent analysis of these data using Arrenhius' equation, *i.e.* $k_{rac} = A \cdot e^{\frac{-E_{act}}{RT}}$, gave an activation energy for racemization of 89.8±2.6 kJ mol^{-1} (Figure 7.10b). The calculated half-life times for racemization of assembly (*P*)-**1**$_3$•(BuCYA)$_{12}$ in the presence of 1 equivalent of free *R*-BAR (with respect to tetramelamine **1**) at 20 ^{o}C is approximately 42 days! When similar racemization studies with enantiopure tetrarosette assembly (*P*)-**1**$_3$•(BuCYA)$_{12}$ formed using *R*-BAR as chaperone (in a 1:4 ratio with respect to tetramelamine **1**, stoichiometric chaperone) are performed (see Table 7.1), an activation energy for racemization of 87.6±3.4 kJ mol^{-1} and a half-life time of 22 days in toluene at 20 ^{o}C were found. Previous studies have shown that the expelled free barbiturate *R*-BAR catalyzes the racemization of enantiopure double rosette assemblies.[26] Comparison of the results obtained for the racemization of enantiopure tetrarosette assemblies using the stoichiometric chaperone and catalytic chaperone shows that the free molecules of barbiturate plays an active role in the racemization process of the assemblies. It is important to notice the two different roles of the barbiturate molecules as catalyst in the self-assembly of the tetrarosette assemblies and as catalyst in the racemization process of the enantiopure assemblies. Nevertheless, it is not certain that the mechanism of actuation is the same.

Based on this observation, the following model is proposed for the racemization of assembly (*P*)-**1**$_3$•(BuCYA)$_{12}$:

$$(P)\text{-}\mathbf{1}_3\bullet(\text{BuCYA})_{12} \underset{k_{uncat}}{\overset{k_{uncat}}{\rightleftharpoons}} (M)\text{-}\mathbf{1}_3\bullet(\text{BuCYA})_{12} \qquad \text{(Eq. 7.2)}$$

$$(P)\text{-}\mathbf{1}_3\bullet(\text{BuCYA})_{12} + R\text{-BAR} \underset{k_{cat}}{\overset{k_{cat}}{\rightleftharpoons}} (M)\text{-}\mathbf{1}_3\bullet(\text{BuCYA})_{12} + R\text{-BAR} \qquad \text{(Eq. 7.3)}$$

which results in the following rate equation

$$R_{t=0} = \frac{d([(P)\text{-}\mathbf{1}_3 \bullet (\text{BuCYA})_{12}])}{dt} = k_{uncat}[(P)\text{-}\mathbf{1}_3 \bullet (\text{BuCYA})_{12}]_0 + k_{cat}[R\text{-BAR}][(P)\text{-}\mathbf{1}_3 \bullet (\text{BuCYA})_{12}]_0$$

In order to obtain the values of the k_{uncat} and k_{cat}, racemization studies at a constant initial concentration of (*P*)-**1**$_3$•(BuCYA)$_{12}$ in the presence of additional amounts

of *R*-BAR were carried out and the racemization rate constants were plotted versus the concentration of *R*-BAR (Figure 7.11).

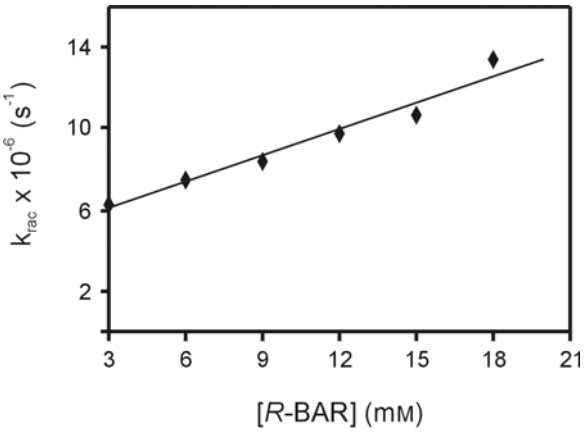

Figure 7.11. Determination of k_{cat} and k_{uncat} from a plot of k_{rac} versus [*R*-BAR].

Fitting of the data resulted in k_{uncat}= 5 x 10^{-6} s^{-1} and k_{cat} = 4 x 10^{-7} s^{-1} (at 50 °C). The value for k_{uncat} was determined from extrapolation of k_{rac} to [*R*-BAR] = 0 mM. Because only a relatively small concentration range of [*R*-BAR] was studied (3-18 mM), the k_{uncat} value has a relatively large error.

From the k_{cat} and k_{uncat} values it can be calculated that racemization of a 1.0 mM solution of (*P*)-**1**$_3$•(BuCYA)$_{12}$ (and consequently 3.0 mM *R*-BAR) occurs for 80% via the uncatalyzed pathway and only 20% via the catalyzed pathway. However, this ratio is strongly concentration dependent.

7.3. Conclusions

Strategies used in nature for the correct folding of proteins (chaperon effect) and in covalent synthesis (catalysis) are exploited here in the noncovalent synthesis of hydrogen-bonded assemblies. The use of barbiturate derivatives in the formation of cyanurate-based teterarosette assemblies inhibits incorrect interactions between the building blocks (chaperon) and exhibits characteristic features of a catalyst. This process

leads to the formation of tetrarosette assemblies in quantitative yield with absolute control over the stereochemistry of the assembly.

Moreover, the 'chaperoned' catalytic process displays enantioselectivity when the barbiturate derivative is chiral. The use of a chiral barbiturate as a chaperone leads to the enantioselective noncovalent synthesis of tetrarosettes assemblies (*P*)-**1**$_3$•(BuCYA)$_{12}$ with half-life time to racemization of 42 days when the chiral *R*-BAR is still present!

7.4. Experimental section

Tetramelamines **1**, 5-((*R*)-2-phenylproply)-5'-ethylbarbiturate (*R*-BAR), BuCYA and (*R*)-MePheCYA (Chart 7.1) have been synthesized following methods previously described.[19,20]

Barbiturate-cyanurate exchange experiments. Typically, 4 equivalents of cyanurate derivative (BuCYA or (*R*)-MePheCYA) were added (as a solid) to 1 ml of a 1.0 mM solution of a 1:1 mixture of tetramelamine **1** and barbiturate (*R*-BAR or DEB) in $CDCl_3$ or toluene-d_8. CD and ^{1}H NMR measurements were started as soon as possible after mixing at variable temperatures.

7.5. References and notes

[1] Fiammengo, R.; Crego-Calama, M.; Reinhoudt, D. N. *Curr. Opin. Chem. Biol.* **2001**, *5*, 660-673.

[2] a) Whitesides, G. M.; Grzybowski, B. *Science* **2002**, *295*, 2418-2421; b) Lehn, J.-M. *Supramolecular Chemistry: Concepts and Perspectives*, VCH, Weinheim, **1995**.

[3] Reinhoudt, D. N.; Crego-Calama, M. *Science* **2002**, *295*, 2403-2407.

[4] a) Jackman, R.; Wilbur, J.; Whitesides, G. M. *Science* **1995**, *269*, 664-666; b) Xia, Y. N.; Whitesides, G. M. *Annu. Rev. Mater. Sci.* **1998**, *28*, 153-184; c) Bushey, M. L.; Nguyen, T. Q.; Zhang, W.; Horoszewski, D.; Nuckolls, C. *Angew. Chem. Int. Ed.* **2004**, *43*, 5446-5453.

[5] Paraschiv, V.; Crego-Calama, M.; Ishi-i, T.; Padberg, C. J.; Timmerman, P.; Reinhoudt, D. N. *J. Am. Chem. Soc.* **2002**, *124*, 7638-7639.

[6] Davis, J. T.; Kaucher, M. S.; Kotch, F. W.; Iezzi, M.; Clover, B. C.; Mullaugh, K. M. *Org. Lett.* **2004**, *6*, 4265-4268, and references cited therein.

[7] Watson, J. D.; Crick, F. H. C. *Nature* **1953**, *171*, 737-738.

[8] a) Anderson, S.; Anderson, H. L.; Sanders, J. K. M. *Acc. Chem. Res.* **1993**, *26*, 469-475; b) Thompson, M. C.; Busch, D. H. *J. Am. Chem. Soc.* **1964**, *86*, 213-217.

[9] Steed, J. W.; Atwood, J. L. *Supramolecular Chemistry*, Wiley, West Sussex, **2000**.

[10] Tokunaga, Y.; Ridkevich, D. M.; Santamaria, J.; Hilmersson, G.; Rebek, J. Jr. *Chem. Eur. J.* **1998**, *4*, 1449-1457.

[11] Anderson, H. L.; Sanders, J. K. M. *Angew. Chem. Int. Ed. Engl.* **1990**, *29*, 1400-1440.

[12] a) Vilar R. *Supramolecular Assembly via Hydrogen Bonds II*, Structure and Bonding ed.; Mingos, D. M. P., Springer, Berlin, **2004**, *vol. 111*, pp 85-137; b) Lee, D. H.; Granja, J. R.; Martinez, J. A.; Severin, K.; Ghadiri, M. R. *Nature* **1996**, *382*, 525-528; c) Hof, F.; Craig, S. L.; Nuckolls, C.; Rebek, J. Jr. *Angew. Chem. Int. Ed.* **2002**, *41*, 1488-1508; d) Luther, A.; Brandsch, R.; von Kiedrowski, G. *Nature* **1998**, *396*, 245-248; e) Conn, M. M.; Wintner, E. A.; Rebek, J. Jr. *Angew. Chem. Int. Ed. Engl.* **1994**, *33*, 1577-1579.

[13] Davidson, L.; Hayes, W. *Curr. Org. Chem.* **2002**, *6*, 265-281.

[14] a) Crego-Calama, M.; Timmerman, P.; Reinhoudt, D. N. *Angew. Chem. Int. Ed.* **2000**, *39*, 755-758; b) Furlan, R. L. E.; Otto, S.; Sanders, J. K. M. *Proc. Natl. Acad. Sci. USA* **2002**, *99*, 4801-4804.

[15] Ellis, R. J.; van der Vies, S. M. *Annu. Rev. Biochem.* **1991**, *60*, 321-347.

[16] Ellis, R. J. *Phil. Trans. R. Soc. Lond. B* **1993**, *339*, 257-261.

[17] a) Kirby, A. J. *Angew. Chem. Int. Ed. Engl.* **1996**, *35*, 707-724; b) Sanders, J. K. M. *Chem. Eur. J.* **1998**, *4*, 1378-1383.

[18] a) Hof, F.; Rebek, J. Jr. *Proc. Natl. Acad. Sci. USA* **2002**, *99*, 4775-4777; b) Davis, A. V.; Yeh, R. M.; Raymond, K. N. *Proc. Natl. Acad. Sci. USA* **2002**, *99*, 4793-4796.

[19] Prins, L. J.; Neuteboom, E. E.; Paraschiv, V.; Crego-Calama, M.; Timmerman, P.; Reinhoudt, D. N. *J. Org. Chem.* **2002**, *67*, 4808-4820.

[20] Prins, L. J.; Hulst, R.; Timmerman, P.; Reinhoudt, D. N. *Chem. Eur. J.* **2002**, *8*, 2288-2301.

[21] Bielejewska, A.; Marjo, C.; Prins, L. J.; Timmerman, P.; de Jong, F.; Reinhoudt, D. N. *J. Am. Chem. Soc.* **2001**, *123*, 7518-7533.

[22] Prins, L. J.; Huskens, J.; de Jong, F.; Timmerman, P.; Reinhoudt, D. N. *Nature* **1999**, *398*, 498-502.

[23] The chiral assembly was formed mixing in a 1:4 ratio tetramelamine **1** and (*R*)-MePheCYA in toluene and heating the resulting solution at 100 ^{o}C for one week.

[24] Due to the asymmetry of the substituents of the *R*-BAR building blocks, the phenyl groups can adopt different orientations going up or down of the rosette plane in the different floors of the assembly, leading to the observed complicated set of signals (instead of the expected 4 signals) in the ^{1}H NMR spectrum of the 1:1 mixture of tetramelamine **1** and *R*-BAR.

[25] Surprisingly when the studies were carried out in toluene-d_8, the ^{1}H NMR spectrum of the 1:1 mixture of tetramelamine **1** and *R*-BAR shows four sharp signals for the hydrogen-bonded NH protons of the barbiturate, indicating that all the *R*-BAR are oriented in a similar way, probably to maximize the interactions with the solvent molecules.

[26] Prins, L. J.; de Jong, F.; Timmerman, P.; Reinhoudt, D. N. *Nature* **2000**, *408*, 181-184.

Summary

In this thesis different aspects of functional hydrogen-bonded (double and tetrarosette) assemblies are described. The functions were inspired by naturally occurring mechanisms such as molecular recognition, supramolecular chirality and its origin, and biostrategies for the correct folding of proteins. The studies presented in this thesis are focused on the different 'social' roles of these (chiral) assemblies: As hosts able to accommodate simultaneously different (chiral) guest molecules, as molecular sergeants whose (chiral) orders are followed by molecular soldiers, and as molecular chaperones inhibiting incorrect interactions in the formation of the assemblies.

Double and tetrarosette assemblies are formed upon mixing calix[4]arene dimelamines and calix[4]arene tetramelamines, in apolar solvents such as chloroform and benzene, with barbiturate derivatives in a 1:2 and 1:4 ratio, respectively. The assembly process is driven by the formation of 36 (double rosette) or 72 (tetrarosette) hydrogen bonds between the complementary hydrogen bonding arrays of the different building blocks, leading to assemblies with high thermodynamic stability.

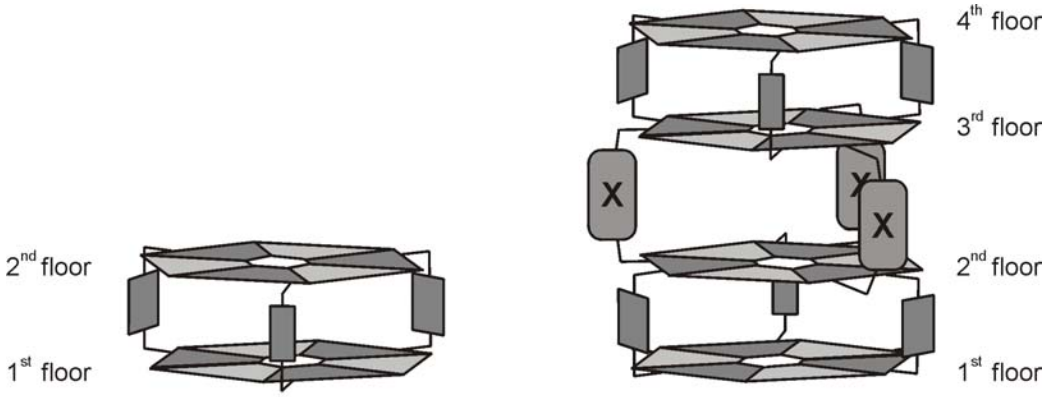

Chapter 1 provides a general introduction to the field of noncovalent synthesis of supramolecular assemblies. In Chapter 2 an overview of the supramolecular chirality

expressed by noncovalent assemblies is given. The concepts and principles that have emerged in this field during the past decade have been discussed and illustrated with selected examples.

In Chapter 3 it has been shown by 'sergeants-and-soldiers' experiments under thermodynamically controlled conditions that the amplification of chirality in hydrogen-bonded double rosette assemblies can be modulated via the substituents in the different building blocks of the assemblies. Different substitutions were incorporated at various positions on the calix[4]arene dimelamine and the chiral cyanurate components. The introduction of bulky groups in the dimelamine moiety leads to a decrease in the free energy between the *P*- and *M*-diastereomers of the assembly from 21.0 to 8.4 kJ mol^{-1}. The introduction of different functionalities on the calix[4]arene skeleton also alters the extent of the chiral amplification. Furthermore, the bulkiness and position of the chiral group of the cyanurate building blocks play an important role in the amplification of chirality.

Chapter 4 describes the amplification of chirality of tetrarosette hydrogen-bonded assemblies. The use of tetrarosette assemblies leads to differences in free energy between the *P*- and *M*-diastereomers of the assembly up to 40 times higher than for double rosette assemblies. 'Sergeants-and-soldiers' experiments in the amplification of chirality have also shown that the difference in free energy between the *P*- and *M*-diastereomers of the tetrarosette assemblies only depends on the structure of the calix[4]arene tetramelamine building blocks and is independent of the methodology used for the formation of the assemblies. It has also been demonstrated that the introduction of rigid spacers to link covalently two calix[4]arene dimelamines, leads to a decrease of the extent of the chiral amplification.

In Chapter 5 the stereoselective recognition of saccharide derivatives by tetrarosette assemblies is described. The recognition process occurs in the cavity formed between the 2nd and 3rd floor of the assembly with a binding constant of 20 M^{-1} and a 1:1 stoichiometry as determined by CD spectrometry. When a racemic tetrarosette receptor is used, the complexation of the sugar derivative leads to the amplification of one of the enantiomeric receptors. For example, complexation of a β-D-sugar leads to the amplification of the *P*-enantiomer from the racemic mixture of receptors while the *M*-

enantiomer is amplified upon complexation of a β-L-saccharide derivative. The use of a diastereomerically pure assembly leads to the complexation of only one of the two enantiomeric sugar derivatives. For example, the M-diastereomer is only able to encapsulate the β-L-derivative.

Chapter 6 describes the simultaneous complexation of different neutral guest molecules by double and tetrarosette hydrogen-bonded receptors. The double rosette assemblies act as *endo*-*exo* receptors. Anthraquinone derivatives are encapsulated in the interior of the assembly (*endo*-receptor) and carboxylic diacids are complexed at the exterior of the receptor (*exo*-receptor) leading to an assembly with 15 different neutral molecules. The *endo*-recognition is very sensitive to structural changes of the guest molecule, while the *exo*-complexation is not very substrate selective. Moreover, the order of addition of the different guest molecules is very important for the outcome of the recognition and assembly processes. Tetrarosette assemblies are *endo*-*endo*-*endo* receptors. Two noncovalent trimers of anthraquinone derivatives are encapsulated in the two double rosette submotifs of the assembly (*endo*-*endo*-complexation) while simultaneously one sugar molecule or four phenol derivatives are encapsulated in the internal cavity situated between the two double rosette subdomains (*endo*-complexation). Moreover, the correct external stimuli lead to the selective release of the different guest molecules in a controlled fashion.

In Chapter 7 the use of biological concepts (chaperone) to overcome the problem of kinetic traps in the formation of cyanurate-based tetrarosette assemblies is described. The barbiturate building blocks act as chaperones inhibiting the formation of kinetically stable ill-defined assemblies and furthermore, this molecular chaperone accelerates the overall speed of the assembly formation, thus acting as catalyst of the self-assembly process. Moreover, chiral barbiturate derivatives lead to the "chaperoned" enantioselective synthesis of tetrarosette assemblies with half-life time to racemization of 42 days!

Samenvatting

In dit proefschrift worden verschillende aspecten van functionele waterstofgebrugde (dubbele en tetrarozet) assemblages beschreven. De functies zijn geïnspireerd door in de natuur voorkomende mechanismen zoals moleculaire herkenning, supramoleculaire chiraliteit en zijn oorsprong, en bio-geinspireerde strategieën voor de correcte vouwing van eiwitten. De studies die in dit proefschrift gepresenteerd worden zijn meer gefocust op verschillende "sociale" rollen van deze (chirale) assemblages. Als gastheren die tegelijkertijd verschillende (chirale) gastmoleculen kunnen complexeren, als moleculaire sergeanten wiens (chirale) orders worden opgevolgd door soldaten en als moleculaire chaperonnes die verkeerde interacties in de vorming van assemblages kunnen te voorkomen of repareren.

Dubbele en tetra-rozetassemblages worden gevormd door calix[4]areen dimelamines en calix[4]areen tetramelamines te mengen in apolaire oplosmiddelen zoals chloroform en benzeen met barbituraatderivaten in respectievelijk een 1:2 en een 1:4 verhouding. Het assemblageproces wordt gedreven door de vorming van 36 (dubbele rozet) en 72 (tetrarozet) waterstofbruggen tussen de complementaire waterstofbrugvormende groepen van de verschillende bouwstenen, leidend tot assemblages met een hoge thermodynamische stabiliteit.

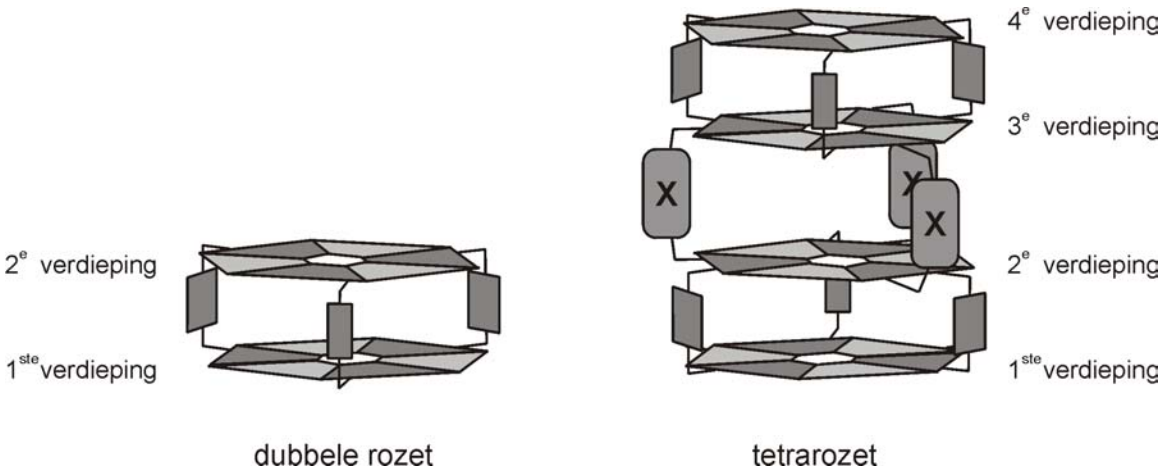

dubbele rozet tetrarozet

Hoofdstuk 1 geeft een algemene introductie tot het veld van de niet-covalente synthese van supramoleculaire assemblages. In Hoofdstuk 2 wordt een overzicht gepresenteerd van supramoleculaire chiraliteit van niet-covalente assemblages. De concepten en principes die gedurende het laatste decennium uit dit veld zijn gekomen worden bediscussieerd aan de hand van enkele geselecteerde voorbeelden.

In Hoofdstuk 3 wordt, aan de hand van "sergeant en soldaten" experimenten onder thermodynamisch gecontroleerde omstandigheden, aangetoond dat de versterking van chiraliteit in waterstofgebrugde dubbele rozetassemblages kan worden gemoduleerd met de substituënten in de verschillende bouwstenen van de assemblages. Verschillende substituënten werden op diverse posities van de calix[4]areendimelamines en de chirale cyanuraten ingevoerd. De introductie van volumineuze groepen in de dimelamines leidt tot een afname van het vrije energie verschil tussen de *P*- and *M*-diastereoisomeren van 21.0 tot 8.4 kJ mol^{-1}. Ook de introductie van verschillende functionaliteiten in het calix[4]areen skelet verandert de mate van chirale versterking. Verder speelt de grootte en positie van de chirale groep in het cyanuraat een belangrijke rol in de versterking van chiraliteit.

Hoofdstuk 4 beschrijft de chirale versterking van waterstofgebrugde tetrarozet assemblages. Het gebruik van de tetrarozetassemblages leidt tot verschillen in vrije energie tussen de *P*- and *M*-diastereoisomeren van de assemblage die wel 40 maal hoger zijn dan voor de dubbele rozet assemblages. "Sergeant en soldaten" experimenten in de versterking van chiraliteit laten ook zien dat het verschil in vrije energie tussen de *P*- and *M*-diastereoisomeren van de tetrarozetassemblages alleen afhangt van de structuur van de calix[4]areentetramelamine bouwstenen, en onafhankelijk is van de methodologie gebruikt voor de vorming van de assemblages. Er is ook aangetoend dat meer rigide spacergroepen die de twee calix[4]areendimelamines covalent binden, leidt tot een afname in de chirale versterking.

In Hoofdstuk 5 wordt de stereoselectieve herkenning van saccharidederivaten door tetrarozetassemblages beschreven. Het herkenningsproces vindt plaats in de holte gevormd tussen de tweede en de derde vloer van de assemblage met een bindingsconstante van 20 M^{-1} en een 1:1 stoichiometrie, zoals vastgesteld met CD spectrometrie. Wanneer een racemische tetrarozetreceptor wordt gebruikt, leidt de

complexering van suiker-derivaten tot een toename van één van de enantiomere receptoren. Complexering van een β-D-suiker leidt bijvoorbeeld tot de versterking van het *P*-enantiomeer uit het racemische mengsel van receptoren terwijl het *M*-enantiomeer toenaamt na complexering van een β-L-saccharide derivaat. Het gebruik van een diastereomeer zuiver assemblage leidt tot de complexering van slechts één van de twee enantiomere suikerderivaten. Het *M*-diastereomer kan bijvoorbeeld alleen het β-L-derivaat complexeren.

Hoofdstuk 6 beschrijft de gelijktijdige complexering van verschillende neutrale gastmoleculen door dubbele en tetrarozet waterstofgebrugde receptoren. De dubbele rozetassemblages doen dienst als *endo-exo* receptoren. Antrachinonderivaten worden gecomplexeerd binnenin het assemblage (*endo*-receptor) en dicarbonzuren worden gecomplexeerd aan de buitenkant van de receptor (*exo*-receptor), wat leidt tot de assemblage van 15 verschillende neutrale moleculen. De *endo*-herkenning is zeer gevoelig voor structuurveranderingen van het gastmolecuul, terwijl de *exo*-complexering niet erg substraatselectief is. Verder is de volgorde van toevoeging van de verschillende gastmoleculen erg belangrijk voor de uitkomst van de herkennings- en assemblageprocessen. Tetrarozetassemblages zijn *endo-endo-endo* receptoren. Twee, niet-covalente, antrachinon trimeren worden gecomplexeerd in de twee dubbele rozetmotieven van de assemblage (*endo-endo*-complexering) terwijl tegelijkertijd één suikermolecuul of vier fenol derivaten worden gecomplexeerd in de holte tussen de twee dubbele rozet sub-domeinen (*endo*-complexering). Verder leiden externe stimuli tot de selectieve vrijlating van de verschillende gastmoleculen in een gecontroleerde manier.

In Hoofdstuk 7 wordt het gebruik, van biologische concepten (chaperone) om het probleem van de “kinetische val” in de vorming van cyanuraat-gebaseerde tetrarozetassemblages op te lossen. De barbituraat bouwstenen doen dienst als chaperonnes die de formatie van kinetisch stabiele, slecht-gedefinieerde assemblages voorkomen en verder versnelt deze moleculaire chaperonne de snelheid van de assemblagevorming, en dient zo als katalysator voor het zelf-assemblage proces. Ook leiden chirale barbituraat derivaten tot de “gechaperonneerde”: enantioselectieve synthese van tetrarozetassemblages met halfwaardetijden van racemisatie van 42 dagen!

Acknowledgments

Finally, after four years, the time to thank a lot of people that made of this time a wonderful experience has arrived, both professionally and personally. I hope that I do not forget anybody, but if I do, please forgive me and for the ones that I remember, keep on mind that it is difficult to find the words to express what I really feel.

First I would like to thank my promotor Professor David N. Reinhoudt for the privilege and opportunity he has given to me to work in his group. David, you gave me all the freedom that I ever desired to make my own choices over the project while at the same time, the right amount of criticism to bring the research to a higher level. Bedankt voor alles.

I want to thank my supervisor Mercedes Crego Calama for guiding me through the whole necessary process to get this thesis, having her office's door always open for me, even when she was really busy with other stuff. Dear Merce, we had our good and bad moments, but I think that that makes you a great supervisor. Merce, de verdad no tengo palabras para agradecerte todo lo que has hecho por mi, tanto en el trabajo, como personalmente, con esos cafés mañaneros, alguna que otra cerveza (o era vodka?) por los bares de Enschede y muchas conversaciones que siempre recordaré (la noche me confunde!!!). Gracias de corazón y espero que tú me recuerdes a mi igual que yo lo haré contigo.

I would also like to thank many people that helped me during these four years with my research. First, I would like to thank Tsutomu Ishi-i for the collaboration in the enantioselective complexation of saccharide derivatives (Chapter 5) and for (even) considering putting my name to his first son. I thank Jessica Kerckhoffs for our collaboration in the multiple complexation of different guests (Chapter 6). I want to thank Aldrik Velders and Clemens Padberg for their help with the NMR and GPC in the determination the chaperone effect of the barbiturate molecules in the formation of the tetrarosette assemblies (Chapter 7). My appreciation also goes to Leonard Prins, who found time during the writing of his thesis to explain me how to create models using Scientist® (Chapters 3 and 4). I want also thank Jurriaan Huskens, who always had (or

found, more accurately) time to answer my many questions, with whom I had really nice discussions about the origin of life and many physical (and not so physical) laws. I thank Juan José García and Mattijs ten Cate for our discussions about the wonderful world of the rosette assemblies, usually smoking a cigarette and drinking a coffee. Tieme Stevens en Annermarie Montanaro ben ik erkentelijk voor de analyse van niuewe verbindingen (niet zo veel, he?) I want to thank Marcel de Bruine, for having always a smile when I was arriving to his office with a request of chemicals and glassware, and Richard Egberink, for the things related with computers and laptops (Richard, the mail is not working…). I thank Carla Weber and Izabel Katalanc for helping me (with a smile) any time I needed some administration paperwork. I want to thank all the present and former people of the SMCT, that made the lab a wonderful place to work, while at the same time, have fun!!

I want to thank Aldrik Velders, Marina Giannotti, and Socorro Vazquez for reading and correcting my concept thesis, and I hope that they did it with a smile.

También es el tiempo de agradecer a mucha gente que ha hecho que estar en Enschede no haya sido el "infierno" que parecía al principio. Primero quiero dar las gracias a Claudia Jansen, que me trató genial cuando vine a hacer la entrevista allá por octubre de 2000. Juanjo, que te voy a decir a ti, solo darte las gracias por esos maravillosos ratos que pasamos en tu casa jugando al Quake 2 (this also applies to Leon Woldering: Ik heb vandaag niet geslapen) y bebiendo algún que otro "sabor a rayos" y haciendo el bandido por el "CHINCHIN". Mattijs (of Matias) "the cowboy", dank je voor luisteren naar mij met mijn stomme dingentjes en voor de gezellig tijd in Berlijn en Enschede, je bent altijd welkom in mijn huis. Alart, de meester van de SMCT, the perfect guy to have a nice "dialogo de besugos" about everything. Fijs, dank je wel voor de tijd dat we samen schreen onze proefschriften en luisterden naar de radio (en zongen!!!) en voor de leuke tijd met jouw familie (Lieke, Sven and Zoë). I want to thank the "squash team" (Fernando, Emiel, Monica, Aldrik, Marina, Lourdes and Alessio) for the nice time every Wednesday's night, and guys, keep trying, someday we will defeat Aldrik… Another important day in my life in Enschede was Thursday's night in "De Beiaard": beers, vegaburgers, gewoon burgers, spare ribs,… we didn't need to look at the menu, we know it by heart!!! These people deserve special thanks, they have made my life much

nicer in Enschede. Emiel (or was it Emilio?), the 'italian' guy (crazy about the soccer, eats lots of pasta, likes more wine than beer…) who married a 'dutch' girl Monica (Pipbrio) (loves bitterbollen, speaks dutch, supports Zwolle F.C…). Another important couple these Thurdays' nights was Bas (this wine is fighting me!) and Barbara (don't be nasty), always nice to have them around. There were always much more people there, and I thank all of them for being there with the "incondicionales" (Emiel, Monica, Barbara, Bas, Alessio, Olga, Fernando, Lourdes, Marina, and of course, Dennis y el chicho).

Y por fin, el turno de la gente que es muy especial para mi. I want to thank my two paranimfen and their support guys for everything they have done for me. Olga (Orga o Olja?) y Alessio (there is a coffee in the pot), Lourdes (I have a handicap!) y Fernando ("El Matador"): Gracias por este tiempo que hemos pasado juntos, aguantándome mi mal humor y frustraciones cuando las cosas no iban como quería, especialmente tú, Olga, los cianuratos de esta tesis te lo agradecen, y también todos los momentos divertidos (que han sido más que los malos), tanto dentro como fuera del laboratorio. Este experiencia no hubiera sido la misma sino hubierais estado vosotros cuatro conmigo. No encuentro las palabras para agradeceros todo lo que habéis hecho por mí: Gracias, Grazie, Merci.

Marina, gracias por todo lo que has hecho por mí. Me has dado apoyo cuando más lo necesitaba para acabar esta tesis y devolverme la alegría que había perdido.

Quique y Eva, gracias por todo el apoyo que me habéis dado (vía email) y cada vez que he ido a España, hacerme sentir como si nunca me hubiera ido de allí.

Quiero dar las gracias a las dos personas más especiales en mi vida, mis padres. Sin vosotros dos no habría logrado acabar aquí. Me habéis dado todo el apoyo que necesitaba, incluso cuando el apoyo tenía que darlo yo a vosotros. Me duele muchísimo que no podáis estar aquí (físicamente) el día de mi promotion, pero seguro que estaréis en mi corazón.

Miguel Angel Mateos Timoneda

About the Author

Miguel Angel Mateos Timoneda was born in Almería, Spain, on December 26, 1976. He studied chemistry at the University of Salamanca in Salamanca from 1994 till 1999. During this period he stayed for three months at Sidenor S.A. (Reinosa, Cantabria, Spain). From September 1999 till June 2000 he did his undergraduate research in the group of Prof. Dr. Francisco Bermejo González on the subject "Condensation reactions between α-angelicalactone and aldehydes. Regio- and Stereoselectivity".

In March 2001 he joined the Supramolecular Chemistry and Technology group of Prof. Dr. Ir. David N. Reinhoudt at the University of Twente, the Netherlands, as a Ph.D. student. The results of his research are described in this thesis.